VRIJE UNIVERSITEIT

Simulating discharge and sediment yield characteristics in the Meuse basin during the late Holocene and 21st Century

ACADEMISCH PROEFSCHRIFT

ter verkrijging van de graad Doctor aan
de Vrije Universiteit Amsterdam,
op gezag van de rector magnificus
prof.dr. L.M. Bouter,
in het openbaar te verdedigen
ten overstaan van de promotiecommissie
van de faculteit der Aard- en Levenswetenschappen
op vrijdag 23 januari 2009 om 13.45 uur
in de aula van de universiteit,
De Boelelaan 1105

door

Philip James Ward

geboren te Wakefield, Verenigd Koninkrijk

promotor:	prof.dr. J.F. Vandenberghe
copromotoren:	dr. H. Renssen
	prof.dr. J.C.J.H. Aerts
	dr. R.T. van Balen

reading committee: prof.dr. B. van den Hurk
dr. C. Kasse
dr. H. Middelkoop
prof.dr. G. Verstraeten
dr. M.J.M. de Wit

This research was carried out at:

VU University Amsterdam
Faculty of Earth and Life Sciences
Department of Palaeoclimatology and Geomorphology
De Boelelaan 1085
1081 HV Amsterdam
The Netherlands

This research was carried out in the framework of the Dutch National Research Project 'Climate changes Spatial Planning' (www.klimaatvoorruimte.nl).

ISBN: 978-90-813595-1-1
NUR code: 935

Simulating discharge and sediment yield characteristics in the Meuse basin during the late Holocene and 21st Century

In Dutch: Simulatie van de afvoer en sedimentlast van het Maasbekken tijdens het late Holoceen en de 21e eeuw

Author: P.J. Ward

Copyright © P.J. Ward, 2008

Cover photo: Water drop. © Pdiaz, Dreamstime.com

Printed by: PrintPartners Ipskamp, Enschede, The Netherlands

Contents

Acknowledgements 9

Samenvatting / Dutch summary 13

Chapter 1 25
Introduction

Chapter 2 35
Verification of a coupled climate-hydrological model against Holocene palaeohydrological records
Global and Planetary Change, 57(3-4), 283-300

Chapter 3 59
Strong increases in flood frequency and discharge of the River Meuse over the late Holocene: impacts of long-term anthropogenic land use change and climate variability
Hydrology and Earth System Sciences, 12, 159-175

Chapter 4 85
Sensitivity of discharge and flood frequency to 21st Century and late Holocene changes in climate and land use (River Meuse, northwest Europe)
Submitted to Climatic Change

Chapter 5 107
River Meuse suspended sediment yield: a new estimate and past estimates revisited
Netherlands Journal of Geosciences, 87(2), 189-193

Chapter 6 115
The impact of land use and climate change on late Holocene and future suspended sediment yield of the Meuse catchment
Geomorphology, in press, doi:10.1016/j.geomorph.2008.07.006

Chapter 7 139
Synthesis

References 151

Appendices 167

Acknowledgements

At the start of 2005 I visited Jeroen Aerts at the IVM to discuss a possible research project for my Master's dissertation. Little did I know that this would result in a 3 year contract at the VU to write this book. Minutes later Jeroen introduced me to Hans Renssen, and I had a job description in my hand and was being encouraged to apply for a Ph.D. position at the Department of Palaeoclimatology and Geomorphology. First, then, many thanks to Hans and Jeroen for introducing me to this study and for being my co-promotors, and to my promotor Jef Vandenberghe and co-promoter Ronald van Balen. Whilst the thought of having four supervisors with different specialisations first seemed fairly daunting, it proved to be a great help, and the monthly discussions were always rewarding. Thanks to Jef for making sure the project stayed on track and for allowing me to take the research in the directions I wanted. As my daily supervisor, many thanks to Hans for all the advice over the last 3 years, and for always finding the time to critically read articles and reports even when snowed under yourself. Many thanks also to Jeroen, whose enthusiasm always provided new research ideas and whose pragmatism helped keep me on focus. I'm looking forward to working together on many more projects at the IVM. Thanks to Ronald, especially for all the help with the erosion and sedimentation part of the research, and for the programming help which certainly helped to speed up the data processing!

Many thanks are also due to the members of the reading committee, Bart van den Hurk, Kees Kasse, Hans Middelkoop, Gert Verstraeten, and Marcel de Wit, for the attention and suggestions that they have given to my thesis. I also thank the various reviewers of my papers, David Labat, Michel van der Meulen, Marcel van der Perk, Murugesu Sivapalan, and numerous anonymous reviewers, for their critical reading and suggestions.

Special thanks are due to Marcel de Wit, who has shown so much interest in my project from the start, and has critically read earlier versions of several papers. Many thanks for the interesting and stimulating discussions during my visits to Arnhem, and for the enthusiasm you have shown in my work. Also, of course, many thanks for the numerous datasets, articles, and contacts that you provided; without these the research certainly wouldn't have been finished within the 3 years.

A couple of times during the last few years I've had the pleasure of making short visits to the K.U. Leuven. I'd like to thank Gert Verstraeten for all the help and advice you gave on using WATEM/SEDEM, for co-authoring Chapter 6, and for the useful feedback on Chapter 5. Also thanks to Anton van Rompaey, whose land use convertor proved invaluable in producing land use maps for Chapter 6, and Bastiaan Notebaert for providing me with a number of Belgian datasets and articles, and for the powerful Belgian beers during his visit to Amsterdam!

At Utrecht University I'd like to thank Hans Middelkoop; the discussion at the start of the soil erosion and sedimentation module was very useful. Also, many thanks to Gilles Erkens for his interest and enthusiasm in my research; our exchange of ideas and results has been very rewarding. At Wageningen University I'd like to thank Peter Verburg for providing the future land use data, for co-authoring Chapter 4, and for the useful discussions and comments. Also thanks to Martha Bakker for the interesting discussion and ideas. Thanks to Frans Bunnik (TNO) for the useful discussions on past land cover. Also many thanks to Julia Pongratz (Max Planck Institute for Meteorology) for the data on past land use changes and for the interesting email exchanges; it was good to finally meet in Vienna.

Of course, special thanks are due to all my colleagues and friends at the Department of Palaeoclimatology and Geomorphology, and at the rest of the Institute of Earth Sciences, for the *gezellige* lunches, coffee-breaks, and borrels. Luckily my new work is just up the stairs, so I'm looking forward to many more *Donderdorsts* (*Donderdorsten*?) in the future! Special thanks to my (ex-)roommates Cedric and Didier for all the help; I'll miss the Beach Boys on Friday afternoon! Also thanks to Ane for the help with InDesign, and Geert-Jan, with whom many an hour has been spent puzzling over the peculiarities of a certain GIS program.

Numerous people at the IVM have helped out with this project. Many thanks to Hans de Moel and Laurens Bouwer for their advice on the STREAM model, especially during the first few months. Also, the GIS advice from Alfred Wagtendonk and Nancy Omtzigt spared me many a frustrating afternoon; thanks for all the help. Also, many thanks to everyone at the IVM for making me feel so welcome since I started working there in August.

Luckily, the last 3 years have not just been spent writing this book! Many thanks to all my friends, in the Netherlands and in the U.K., for all the good times in the last few years. A special thanks to my family for their support, not only with this thesis, but over the last 30 years in general! Thanks to my *paranimfen*, Stijn Brouwer and Cedric van Meerbeeck, for all the help preparing for the big day, but more importantly for the friendship over the last three years.

Last, but definitely not least, a huge thanks to Dieuwke, who I met just a month after starting work on this thesis. You've always been there to listen to my Ph.D. frustrations; your advice and suggestions are always greatly appreciated, even if I don't always admit it! Over the last three years your help with Dutch manuscripts, press releases, and Dutch summaries has made my life much easier; thanks for all the (many!) corrections. But more importantly, thanks for all the interest, support, and encouragement, especially during the final months. Dieuwke, tige tank!

Samenvatting / Dutch summary

Achtergrond

De verwachting is dat toekomstige klimaatverandering grote gevolgen zal hebben voor stroombekkens over de hele wereld, waaronder veranderingen in gemiddelde afvoer en overstromingsfrequentie van rivieren (Kundzewicz et al., 2007) en veranderingen in de intensiteit van bodemerosie en het transporteren van sedimenten naar rivieren (e.g. Houben et al., 2006; Toy et al., 2002). De resultaten van recente met computermodellen uitgevoerde simulaties laten zien dat de gevolgen van toekomstige klimaatverandering relatief groot zouden kunnen zijn in Europa (Giorgi, 2006), met in Noordwest-Europa tijdens de winter een toename van neerslag van tussen de 5% en de 20% (Giorgi en Coppola, 2007). Veranderingen in de hydrologie van een stroombekken zijn echter niet alleen afhankelijk van het klimaat, maar ook van landgebruik. Landgebruikveranderingen zijn het gevolg van complexe interacties tussen fysische, socio-economische en politieke processen (Van Rompaey et al., 2002; Verburg, 2006), inclusief klimaatverandering. Het is tegenwoordig algemeen aanvaard dat afnames in het areaal bos in het verleden hebben geleid tot significante toenames van rivierafvoer en bodemerosie op meerdere plekken ter wereld (e.g. Andréassian, 2004; Bork en Lang, 2003; Bosch en Hewlett, 1982; Calder, 1993; Hornbeck et al., 1993; Sahin en Hall, 1996; Van Rompaey et al., 2002).

In Nederland wordt het belang van onderzoek naar de invloed van klimaatverandering op de hydrologie al sinds de late jaren tachtig erkend (e.g. De Boer en Groot, 1990). In het Maasbekken is het belang van dergelijk onderzoek alleen maar toegenomen sinds de grote overstromingen van 1993 en 1995. In die jaren trad de Maas buiten haar oevers wat leidde tot grootschalige overstromingsschade in de aangrenzende landen. Om een voorbeeld te noemen: de directe financiële schade als gevolg van de overstromingen van 1993 kwam alleen al in Nederland uit boven de €100 miljoen (Wind et al., 1999). Sindsdien zijn tal van studies uitgevoerd om de veranderingen in de hydrologie van het Maasbekken gedurende de laatste eeuw te onderzoeken. Deze studies laten zien dat, hoewel de jaargemiddelde afvoer van de Maas redelijk stabiel is gebleven tijdens de 20^{e} eeuw (De Wit et al., 2001; Tu, 2006; WL, 1994a), de grootte van de maximale afvoer per jaar significant hoger is sinds halverwege de jaren tachtig (Pfister et al., 2000; Tu, 2006). Daarnaast zijn meerdere hydrologische modellen gebruikt om de gevolgen van toekomstige klimaatverandering op de hydrologie van de Maas te onderzoeken (e.g. Booij, 2005; Bultot et al., 1988; De Wit et al., 2001, 2007a; Gellens en Roulin, 1998; Middelkoop en Parmet, 1998; Van Deursen, 2000). De resultaten van deze studies laten, als gevolg van de verandering in het klimaat, een toename zien in de overstromingsfrequentie in de 21^{e} eeuw, vooral in het winter halfjaar (november t/m april). De resultaten van Booij (2005) laten bijvoorbeeld een toename zien in de grootte van hoge afvoeren met een herhalingstijd van 100 jaar van ca. 9% tot 13% tussen het einde van de

20e en het einde van de 21e eeuw.

Tot nu toe is relatief weinig onderzoek uitgevoerd naar de gevolgen van landgebruikveranderingen in het Maasbekken, mede doordat het areaal bos relatief stabiel gebleven is in de laatste eeuw (DGRNE, 2000; Knol et al., 2004; Tu, 2006). Ashagrie et al. (2006) en Tu (2006) vonden geen aanwijzingen dat landgebruikveranderingen tijdens de 20e eeuw hebben geleid tot significante veranderingen in de afvoer van de Maas.

Zowel in het Maasbekken als in andere middelgrote en grote bekkens is weinig onderzoek verricht met betrekking tot de invloed van klimaat- en landgebruikveranderingen op bodemerosie en het transport van geërodeerde sedimenten naar rivieren op de schaal van het gehele stroomgebied. Deze processen zijn echter wel belangrijk op de politieke agenda op lokaal, landelijk en Europees niveau (Van Rompaey et al., 2005). Bovendien kunnen deze processen tal van milieuproblemen veroorzaken. Bodemerosie op agrarisch land heeft meerdere nadelige on-site gevolgen, zoals op de korte termijn het verlies van de bovenlaag en afnemende oogsten, en op de lange termijn afnemende productiviteit (Verstraeten et al., 2002). Het verplaatsen van geërodeerd bodemmateriaal naar rivieren vormt ook een grote bron van nutriënten, pesticiden en zware metalen (Boers, 1996; De Wit en Behrendt, 1999; Verstraeten en Poesen, 2002), wat nadelig kan zijn voor de waterkwaliteit in rivieren en estuaria. Tevens kan het transporteren van geërodeerde sedimenten grote gevolgen hebben voor de morfologie van rivierbeddingen (e.g. Asselman en Middelkoop, 1995; De Moor et al., 2008) en het ecologisch functioneren van overstromingsvlaktes (Richards et al., 2002). Veranderingen in bodemerosie en het transporteren van geërodeerde sedimenten naar rivieren kunnen worden onderzocht door het analyseren van veranderingen in sedimentlast (de hoeveelheid sediment dat in een bepaalde tijdsperiode langs een bepaald punt van een rivier stroomt).

Tot op heden hebben studies naar de veranderingen van Maasafvoer en sedimentlast (op de schaal van het gehele bekken) ofwel gekeken naar afvoerreeksen van de laatste eeuw, ofwel gebruik gemaakt van hydrologische modellen die gekalibreerd zijn op metingen van die periode om veranderingen in de 21e eeuw te simuleren. Dit levert echter problemen op voor het bestuderen van veranderingen op de lange termijn (bijv. perioden van honderd tot duizend jaar). Ten eerste zijn nauwkeurige metingen van de dagelijkse Maasafvoer pas sinds 1911 beschikbaar en voor sedimentlast pas sinds 1995. Deze meetreeksen zijn te kort om de invloed van klimaatveranderingen op de lange termijn te bestuderen (Alcamo et al., 2000; Ely et al., 1993; Knox, 1984; Meybeck, 2003). Ten tweede zijn de resultaten van deze modellen niet gevalideerd tegen perioden waarin de leefomgeving anders was dan die van de laatste eeuw. Daarnaast is het bosareaal van het Maasbekken relatief stabiel gebleven gedurende de laatste eeuw, waardoor het moeilijk is om de gevolgen van grootschalige landgebruik-verandering te bestuderen.

Een manier om de veranderingen op de lange termijn wel te onderzoeken is het bestuderen van veranderingen in het hydrologische systeem tijdens een periode voordat metingen verricht zijn. Dit vakgebied heet paleohydrologie, waarvan het belang nog is verwoord in het meest recente rapport van de 'Intergovernmental Panel on Climate Change' (IPCC, 2007). De resultaten van paleohydrologische studies kunnen een dataset opleveren waartegen modelresultaten gevalideerd kunnen worden op duizendjarige tijdschalen (Lang en Bork, 2006). Het simuleren van paleoafvoeren maakt het ook mogelijk om de gevolgen van lange termijn klimaatveranderingen op rivierafvoer te analyseren, evenals de gevolgen van meer omvangrijke veranderingen in klimaat en landgebruik dan die van de laatste eeuw. Bovendien, door afvoeren en sedimentlast te simuleren voor perioden waarin de invloed van de mens op de leefomgeving gering was, is het mogelijk de gevolgen van menselijke activiteiten te bestuderen ten opzichte van de natuurlijke situatie. Het modelleren van afvoeren en sedimentlast tijdens het Holoceen op de schaal van gehele stroombekkens is echter nog niet goed ontwikkeld. Bogaart et al. (2003) maakten gebruik van een numeriek model om veranderingen in de afvoer van de Maas gedurende lange perioden (>100 jaar per tijdstap) tijdens de laatste Glaciaal-Interglaciaal transitie te bestuderen. Voor zover mij bekend zijn echter nog voor geen enkele stroombekken ter wereld simulaties uitgevoerd met een ruimtelijke verdeling op hoge resolutie voor perioden tijdens het late Holoceen. Het ontwikkelen van zulke modellen is een interessante uitdaging, en zou kunnen leiden tot een beter inzicht in de relatieve invloed van klimaat- en landgebruikveranderingen op rivierafvoeren.

Onderzoeksdoel en onderzoeksvragen

Om in te spelen op de bovengenoemde vraagstukken, zijn de belangrijkste doelen van deze Ph.D. studie om lange termijn trends en veranderingen in de afvoer, overstromingsfrequentie en sedimentlast van de Maas te bestuderen tijdens het late Holoceen en de 21e eeuw, als gevolg van natuurlijke en antropogene veranderingen in klimaat en landgebruik, én om de relatieve invloed van deze factoren ten opzichte van elkaar te analyseren. Om deze doelen te verwezenlijken zijn de volgende onderzoeksvragen opgesteld:

1. Kunnen we een gekoppelde klimaat-hydrologische modelleringaanpak ontwikkelen om lange termijn veranderingen in paleoafvoeren te simuleren? In hoeverre kunnen geologische en geomorfologische gegevens (zgn. proxy data) gebruikt worden om de bruikbaarheid van dergelijke modellen te analyseren als gereedschap voor het reconstrueren van paleoafvoeren?
2. Hoe is de afvoer en de overstromingsfrequentie van de Maas veranderd tussen een periode waarin de natuurlijke klimaatforceringen vergelijkbaar waren met die van vandaag en de invloed van de mens op landgebruik minimaal was (4000-3000 BP, 'before present', d.w.z. de jaren voor 1950 na Chr.), en een periode die beïnvloed is door antropogene veranderingen in landgebruik (1000-2000 na Chr.) en de menselijke uitstoot van broeikasgassen en sulfaataërosolen (postindustriële revolutie)? Welke factoren veroorzaken deze veranderingen?

3. Wat zijn de relatieve invloeden van de te verwachten klimaat- en landgebruikveranderingen op de afvoer en overstromingsfrequentie van de Maas tijdens de 21e eeuw? Hoe vergelijken deze veranderingen zich met de natuurlijke en antropogene veranderingen op de lange termijn in het late Holoceen?
4. Wat voor gevolgen hebben klimaat- en landgebruikveranderingen gehad op bodemerosie en sedimentlast in het Maasbekken tijdens het late Holoceen? Wat voor gevolgen kunnen we verwachten in de 21e eeuw?

Antwoorden op de onderzoeksvragen

Het gebruik van een gekoppeld klimaat-hydrologisch model om paleoafvoer te analyseren

Voor zover mij bekend zijn voorafgaand aan deze studie geen onderzoeken uitgevoerd om paleoafvoeren te simuleren voor het Holoceen met gebruik van een ruimtelijk verdeeld hydrologisch model. Voordat een gedetailleerd model kon worden opgezet voor de Maas, was daarom de eerste stap in dit promotieonderzoek (Hoofdstuk 2; Ward et al., 2007) een model met een lage ruimtelijke resolutie (0.5° x 0.5°) en een maandelijkse tijdstap op te zetten om de paleoafvoeren van 19 rivieren te simuleren (Amazone, Donau, Ganges, Kongo, Krishna, Lena, Maas, Mackenzie, Mekong, Mississippi, Murray-Darling, Nijl, Oder, Rijn, Sacramento-San Joaquin, Syr Darja, Volta, Wolga, Zambezi). Dit is uitgevoerd als pilotstudy om de bruikbaarheid van deze aanpak te bestuderen met betrekking tot het evalueren van lange termijn veranderingen in paleoafvoeren. Het klimaatmodel ECBilt-CLIO-VECODE (Brovkin et al., 2002; Goosse en Fichefet, 1999; Opsteegh et al., 1998) is offline gekoppeld met het hydrologische model STREAM (Aerts et al., 1999) om de afvoer van deze rivieren te simuleren tijdens drie perioden, namelijk Vroeg Holoceen (9000-8650 BP), Mid Holoceen (6200-5850 BP) en Recent (1750-2000 na Chr.). De resultaten van de simulaties zijn vervolgens vergeleken met schattingen van paleoafvoeren op basis van multi-proxy data beschikbaar in de literatuur (bijv. geologisch, geomorfologisch, etc.), om te bepalen in hoeverre de modelresultaten hiermee overeen kwamen. Voor elk stroombekken zijn de proxy data geclassificeerd als *goed*, *redelijk* of *slecht*. De classificatie heeft betrekking op de betrouwbaarheid van de data om de feitelijke veranderingen in de paleoafvoeren in de bovengenoemde stroombekkens en perioden weer te geven. Voor de simulaties waarvoor de proxy data als *goed* of *redelijk* werden geclassificeerd, kwamen de modelresultaten in 72% van de gevallen volledig overeen met de proxy data. Bovendien kwamen de resultaten van 92% van die simulaties redelijk overeen met de proxy data. De overeenkomsten waren vooral sterk in het geval van Europese bekkens beïnvloed door maritieme klimaten, en in het geval van subtropische bekkens beïnvloed door de moessons van het noordelijke halfrond.

Omdat het gekoppelde klimaat-hydrologische model succesvol is toegepast voor het simuleren van de paleoafvoeren van deze rivieren, is het vervolgens toegespitst op de Maas (Hoofdstuk 3; Ward et al., 2008a). De spatiale resolutie is verhoogd tot 2' x 2' (ongeveer 2.4 km x 3.7 km) en een dagelijkse tijdstap is gebruikt om veranderingen in overstromingsfrequentie te kunnen simuleren. Ten opzichte van het mondiale model, waarin enkel natuurlijke veranderingen in landgebruik als gevolg van klimaatveranderingen zijn voorgeschreven, is voor het Maasmodel aandacht besteed aan de antropogene veranderingen in landgebruik tussen 4000 BP en het heden. De gesimuleerde veranderingen in afvoer en overstromingsfrequentie uit het hogere resolutie Maasmodel komen overeen met kwalitatieve resultaten uit multi-proxy data.

Deze toepassingen van het gekoppelde model laten zien dat de methode een bruikbaar gereedschap kan vormen om lange termijn veranderingen in paleoafvoer te analyseren. Geologische en geomorfologische reconstructies van paleoafvoer maken het mogelijk om de resultaten van hydrologische modellen te verifiëren voor perioden waarin de leefomgeving anders was dan tegenwoordig. Daarmee is de betrouwbaarheid van deze modellen verhoogd met betrekking tot hun geschiktheid voor het simuleren van de effecten van toekomstige klimaat- en landgebruikveranderingen.

Late Holoceen afvoer en overstromingsfrequentie van de Maas: gevolgen van klimaat- en landgebruikverandering

Het gekoppelde klimaat-hydrologische model is gebruikt om de dagelijkse afvoer van de Maas te simuleren voor twee perioden: 4000-3000 BP en 1000-2000 na Chr. (Hoofdstuk 3; Ward et al., 2008a). De periode 4000-3000 BP is gebruikt als 'natuurlijk' referentiekader. In deze periode was menselijke activiteit in het bekken gering. De natuurlijke klimaatforceringen waren vergelijkbaar met die van vandaag (Goudie, 1992) en het gebied was nog (bijna) volledig bebost (Bunnik, 1995; Gotjé et al., 1990; RWS Limburg/IWACO, 2000). De periode 1000-2000 na Chr. kenmerkt zich door veranderingen in het hydrologische systeem door landgebruikveranderingen (ontbossing, herbebossing, veenontginning, ruralisatie, verstedelijking), en als gevolg van menselijke uitstoot sinds het industriële tijdperk ook een toename van het gehalte aan broeikasgassen en sulfaataërosolen in de atmosfeer. Door de afvoeren en overstromingsfrequenties van deze twee perioden te vergelijken is het dus mogelijk om de invloed van menselijke veranderingen in landgebruik en klimaat te analyseren.

Uit de resultaten van deze studie blijkt dat zowel de gemiddelde afvoer als de overstromingsfrequentie van de Maas significant zijn toegenomen in de periode tussen het natuurlijke referentiekader 4000-3000 BP en het laatste millennium. De gemiddelde afvoer is toegenomen met 6.6% tussen 4000-3000 BP (244.8 $m^3 s^{-1}$) en 1000-2000 na Chr. (260.9 $m^3 s^{-1}$); de sterkste toename vond plaats in het zomer halfjaar (mei t/m oktober) (+21.6%). De herhalingstijd van afvoeren groter dan 3000 $m^3 s^{-1}$ (vergelijkbaar met die tijdens de overstromingen van 1926 en 1993)

nam af van 77 jaar in de periode 4000-3000 BP tot 65 jaar in de periode 1000-2000 na Chr. Op deze tijdschaal zijn de toenames in afvoer en overstromingsfrequentie bijna volledig het resultaat van veranderingen in landgebruik, met name door het afnemen van de evapotranspiratie als gevolg van de opgetreden ontbossingen. Op deze duizendjarige tijdschaal hebben klimaatveranderingen geen significante invloed gehad op de afvoer van de Maas. Tussen de 19^{e} en 20^{e} eeuw heeft de invloed van klimaatverandering de invloed van landgebruikveranderingen echter overweldigd. Hoewel evapotranspiratie hoger lag in de 20^{e} eeuw dan in de 19^{e} eeuw (als gevolg van herbebossing en de toename van de temperatuur), was de gemiddelde afvoer in de 20^{e} eeuw hoger (270 m^3 s^{-1}) dan in alle voorafgaande eeuwen, en zelfs 2.5% hoger dan tijdens de 19^{e} eeuw. Bovendien kwamen hoge afvoeren van minstens 3000 m^3 s^{-1} bijna twee keer zo vaak voor tijdens de 20^{e} eeuw dan tijdens het natuurlijke referentiekader 4000-3000 BP. De versterkte toenames in afvoer en overstromingsfrequentie tussen de 19^{e} en 20^{e} eeuw zijn bijna volledig het gevolg van een aan het versterkte broeikaseffect gerelateerde stijging van het jaarlijkse (en vooral winterse) neerslagtotaal.

De resultaten van Maasafvoer uit het mondiale model (Hoofdstuk 2; Ward et al., 2007) laten zien dat lange termijn veranderingen in orbitale parameters (de baan van de aarde rond de zon) hebben geleid tot weinig verandering in afvoer tussen de perioden 9000-8650 BP, 6200-5850 BP en 1750-2000 na Chr. De resultaten van het gedetailleerde Maasmodel (Hoofdstuk 3; Ward et al., 2008a) laten ook zien dat de natuurlijke veranderingen in het klimaat tussen de perioden 4000-3000 BP en 1000-2000 na Chr. weinig invloed hadden op de afvoer van de Maas. Doordat antropogene landgebruikverandering niet werd meegenomen in het mondiale model, zijn de gevolgen hiervan niet gesimuleerd tussen het Mid Holoceen en recente tijdsperioden in laatstgenoemde model configuratie.

Verandering in de afvoer en frequentie van hoge afvoeren van de Maas tijdens de 21^{e} eeuw

De dagelijkse afvoer van de Maas is gesimuleerd voor de 21^{e} eeuw (Hoofdstuk 4; Ward et al., 2008b). De forceringen gebruikt in het klimaatmodel waren gebaseerd op de ‘Special Report on Emission Scenarios’ (SRES) van het ‘Intergovernmental Panel on Climate Change’ (IPCC, 2000). SRES scenario’s A2 en B1 zijn gebruikt omdat dit respectievelijk een van de meest extreme en een van de minst extreme scenario’s zijn (wat betreft de concentratie CO_2 in de atmosfeer tegen 2100 na Chr.). Ze kunnen daarom gebruikt worden om de gevolgen van klimaatverandering te analyseren onder een grote range mogelijke veranderingen. Voor landgebruik in de 21^{e} eeuw is gebruik gemaakt van twee scenario’s uit het EURURALIS 2.0 project (WUR/MNP, 2007); de ‘Continental Market’ en ‘Global Cooperation’ scenario’s. De mogelijke socio-economische ontwikkelingen waarop deze scenario’s zijn gebaseerd (de zogenaamde concept storylines) corresponderen respectievelijk met die van de A2 en B1 scenario’s van de SRES (en zijn dus zo genoemd in dit proefschrift), hoewel de concept storylines breder getrokken zijn om specifiek rekening te houden met landgebruik vraagstukken en Europees

agrarisch beleid (Westhoek et al., 2006). Deze scenario's laten relatief weinig verandering in landgebruik zien tussen de 20e en 21e eeuw. De meest significante verandering, vergeleken met de 20e eeuw, is een toename van het areaal bos met 2% onder scenario B1 (en daarmee samen een afname in het areaal agrarisch land van ca. 2%).

De resultaten voor de 21e eeuw vertonen een toename van de jaarlijkse temperatuur, neerslag en afvoer tot waarden ver boven de waarden die gesimuleerd zijn voor de perioden 4000-3000 BP en 1000-2000 na Chr. De toenames in jaargemiddelde afvoer tussen de perioden 1950-2000 na Chr. en 2050-2100 na Chr. (+16.6% voor A2 en +12.7% voor B1) zijn groter dan de toename in jaargemiddelde afvoer over de hele periode 4000-3000 BP tot 1950-2000 na Chr. (+10.0%). Bovendien is de herhalingstijd van hoge afvoeren groter dan 3000 m^3 s^{-1} (wat vergelijkbaar is met de afvoer tijdens de overstromingen van 1926 en 1993) toegenomen van eens per 40 jaar tijdens de 20e eeuw tot eens per 20 jaar in de 21e eeuw onder scenario A2, en eens per 25 jaar onder scenario B1. De gesimuleerde toenames in jaargemiddelde afvoer en overstromingsfrequentie zijn significant groter onder scenario A2 dan onder scenario B1. Desalniettemin zijn de toenames tussen de 20e en 21e eeuw onder het meer optimistische B1 scenario groot en statistisch significant. Op deze tijdschaal is de invloed van de gematigde landgebruikverandering, gesimuleerd voor de 21e eeuw, klein. De toenames in afvoer en overstromingsfrequentie zijn bijna volledig het resultaat van de gesimuleerde veranderingen in het klimaat. Tussen de periode 4000-3000 BP en de 20e eeuw is weinig verandering waargenomen in de herhalingstijd van extreme afvoeren (herhalingstijd 1250 jaar), waarbij de grootschalige ontbossing van het bekken slechts een geringe invloed had op dergelijke gebeurtenissen. Voor de 21e eeuw worden echter, vooral als resultaat van de toename van neerslag tijdens de winter, toenames verwacht onder beide scenario's.

De sedimentlast van het Maasbekken: de invloed van klimaat- en landgebruikverandering in het late Holoceen en de 21e eeuw

Om de invloed van lange termijn veranderingen in klimaat en landgebruik op de sedimentlast van de Maas te bestuderen is gebruik gemaakt van het hellingerosie- en sedimentatie model WATEM/SEDEM (Van Oost et al., 2000; Van Rompaey et al., 2001a; Verstraeten et al., 2002). Hiermee is de sedimentlast berekend per periode van 50 jaar (Hoofdstuk 6; Ward et al., 2008c). Veranderingen in het klimaat (namelijk de erosiviteit van de neerslag) zijn berekend aan de hand van de resultaten uit het klimaatmodel ECBilt-CLIO-VECODE (Brovkin et al., 2002; Goosse en Fichefet, 1999; Opsteegh et al., 1998), en veranderingen in landgebruik zijn gebaseerd op historische documenten en projecties voor de 21e eeuw uit het EURURALIS project (WUR/MNP, 2007). De sedimentlast van de Maas is significant toegenomen gedurende het late Holoceen. Tijdens het natuurlijke referentiekader 4000-3000 BP bleef de gemiddelde 50-jr sedimentlast redelijk constant (gemiddeld ca. 92,000 Mg a^{-1}). De gemiddelde sedimentlast in het laatste millennium (306,000 Mg a^{-1}) is meer dan het drievoud van dat van

4000-3000 BP. De 50-jr sedimentlast is verre van constant geweest gedurende de laatste 1000 jaar en laat een significant opwaartse trend zien tussen de 11^{e} en 19^{e} eeuw tot een piek van ca. 388,000 Mg a^{-1} in de 19^{e} eeuw. Deze resultaten laten hetzelfde patroon zien als het beperkte aantal geomorfologische studies die uitgevoerd zijn in de regio. Op een duizendjarige tijdschaal is het overgrote deel van deze toename het gevolg van menselijke veranderingen in landgebruik, vooral het vervangen van bos met akkerland. In de 20^{e} eeuw resulteerden herbebossing en urbanisatie in een afname in gesimuleerde sedimentlast tot ca. 281,000 Mg a^{-1}. Dit resultaat is in tegenspraak met twee eerder uitgevoerde studies (Close-Lecocq et al., 1982; Lemin et al., 1987), die stellen dat de sedimentlast toenam tussen de late 19^{e} en late 20^{e} eeuw. In Hoofdstuk 5 (Ward, 2008a) laat ik zien dat de toename, opgetekend in laatstgenoemde studies, net zo goed het gevolg kan zijn van jaarlijkse variabiliteit of de methoden gebruikt in die studies en geen bewijs vormt voor een structurele toename in sedimentlast. Het is echter wel mogelijk, zoals voorgesteld door Lemin et al. (1987), dat de bedijking van de Maas tussen Namen en Luik tijdens de 20^{e} eeuw wel geleid heeft tot een toename van de sedimentlast in die periode. Om te onderzoeken wat voor invloed de bedijking heeft gehad op de sedimentlast zou het nuttig zijn om gedetailleerde geomorfologische analyses uit te voeren die kijken hoe de sedimentatie van de overstromingsvlakte is veranderd tijdens de laatste eeuw.

De resultaten voor de 21^{e} eeuw zijn sterk afhankelijk van de gebruikte scenario's (klimaat en landgebruik). Relatief sterke toenames in de erosiviteit van de neerslag, gesimuleerd voor de 21^{e} eeuw onder scenario's A2 en B1, leiden tot toenames in sedimentlast vergeleken met de 20^{e} eeuw van respectievelijk 12% en 8%. De gebruikte landgebruikscenario's leiden echter tot een afname in sedimentlast van respectievelijk 26% en 46%, vooral als gevolg van het vervangen van akkerland door weide en grasland. Het netto effect in de 21^{e} eeuw is dus een toename van de sedimentlast in vergelijking met de sedimentlast van de 20^{e} eeuw.

De resultaten van een gevoeligheidsanalyse laten zien dat, hoewel landgebruikverandering de grootste invloed heeft op lange termijn veranderingen in sedimentlast, de gevoeligheid van sedimentlast voor veranderingen in het klimaat toeneemt naarmate het areaal ontboste land toeneemt.

Slotconclusies

Veranderingen in landgebruik en klimaat hebben beiden een grote invloed op de afvoer, overstromingsfrequentie en sedimentlast van de Maas. In de laatste 4000 jaar heeft het grootschalig ontbossen van het bekken geleid tot substantiële toenames in deze drie parameters, terwijl op een duizendjarige tijdschaal (natuurlijke) veranderingen in het klimaat slechts een secundaire rol hebben gespeeld. Terwijl ontbossingen hebben geleid tot een toename in de frequentie van hoge afvoeren in het late Holoceen, hebben ze geringe invloed gehad op de meest extreme afvoeren (bijv. hoge afvoeren met een herhalingstijd van 1250 jaar en langer). In de 21^{e} eeuw nemen de gesimuleerde waarden voor de jaarlijkse

temperatuur en neerslag toe tot waarden ver boven die van de laatste 4000 jaar. Als gevolg hiervan worden verdere toenames verwacht in afvoer en de frequentie van hoge afvoeren, zelfs voor de meest extreme overstromingen. De gevolgen van de verwachte landgebruikveranderingen hierop zijn gering. Landgebruik blijft echter een dominante rol spelen in bodemerosie en sedimentlast. Ondanks een relatief grote toename in de neerslagerosiviteit in de 21e eeuw ten opzichte van de 20e eeuw, laat ons model een afname zien in de sedimentlast van de Maas. Dit komt omdat de verwachte toenames als gevolg van een toename in neerslagerosiviteit kleiner zijn dan de verwachte afnames als gevolg van de gesimuleerde veranderingen in landgebruik (vooral het vervangen van akkerland door weide en grasland). Zelfs kleine modificaties in landgebruik kunnen grote veranderingen in sedimentlast veroorzaken. Bovendien neemt de gevoeligheid van sedimentlast voor veranderingen in het klimaat toe naarmate het areaal beboste land afneemt.

Implicaties voor het waterbeheer

Grootschalige veranderingen in het areaal bos in een stroombekken kunnen grote gevolgen hebben voor afvoer, overstromingsfrequentie, bodemerosie en sedimentlast. Grootschalige herbebossing van het Maasbekken in de 21e eeuw wordt echter niet verwacht (WUR/MNP, 2007) omdat de economische vraag naar land groot is en er veel aandacht wordt besteed aan het behouden van cultuurhistorische landschappen. Hoewel het potentiële gebruik van herbebossing als maatregel tegen overstromingen beperkt is in het Maasbekken, kan het vervangen van slechts enkele percentages van het totaaloppervlak akkerland door bos grote voordelen opleveren voor bodemerosie en sedimentlast. De invloed van herbebossing op de timing van piekafvoeren (als gevolg van het vertragen van afvoersnelheden) is niet onderzocht in dit proefschrift.

Hoewel de invloed van de verwachte landgebruikveranderingen voor de 21e eeuw op de frequentie van hoge afvoeren klein is, is dit niet per se het geval voor het overstromingsrisico. Analyses van overstromingsrisico's moeten ook de potentiële schade als gevolg van eventuele overstromingen in beschouwing nemen. Dit kan sterk afhankelijk zijn van veranderingen in landgebruik, en dan met name urbanisatie. Het is daarom van belang dat er, naast de frequentie van hoge afvoeren, ook studies worden uitgevoerd om de invloed van veranderingen in landgebruik (en klimaat) op overstromingsrisico's te berekenen.

Veranderingen in afvoer, overstromingsfrequentie en sedimentlast in de 21e eeuw zijn allemaal afhankelijk van het gebruikte klimaatscenario. Zelfs onder het relatief optimistische B1 scenario zijn de gesimuleerde toenames in afvoer en overstromingsfrequentie groot voor de komende eeuw. Daaruit volgt dat deze toenames mogelijk onvermijdelijk zijn, zelfs wanneer een gecoördineerde en onmiddellijke actie op mondiale schaal zou worden ondernomen om de uitstoot van broeikasgassen te mitigeren. Dit onderstreept de noodzaak van aanpassingsmaatregelen om de kans op overstromingen in de toekomst te

verminderen. Dergelijke strategieën moeten robuust zijn met betrekking tot hun flexibiliteit in de toekomst, moeten expliciet kunnen omgaan met onzekerheden en moeten voordelen opleveren onder verschillende scenario's van de toekomst. Multifunctionele landgebruiksplanning, waarbij het landgebruik in overstromingsrisicogebieden in overeenstemming is met tijdelijke inundaties, kan hierin een sleutelrol spelen. Een voorbeeld hiervan is de Grensmaas waar momenteel grindwinning plaatsvindt in een gebied van ca. 1100 ha. om het rivierbed te verbreden en een meer esthetisch landschap te creëren. Behalve de voordelen voor natuurbehoud en toerisme, zal dit leiden tot minder kans op wateroverlast door een vergroting van de afvoercapaciteit van de rivier en extra gebieden voor waterretentie tijdens hoge afvoeren.

De gesimuleerde afname van de sedimentlast van de Maas in de 21^{e} eeuw (in vergelijking met de 20^{e} eeuw) zou voordelig kunnen zijn voor een aantal reeds lopende en geplande overstromingsmaatregelen. In een internationaal actieplan tegen overstromingen dat in 1998 door de aangrenzende landen is opgesteld zijn bijvoorbeeld maatregelen opgenomen om de kwetsbaarheid van het bekken voor overstromingen te verminderen, inclusief de constructie van retentiebekkens, de constructie of het herstel van overstromingsvlaktes, en het vergroten van de afvoercapaciteit door het verbreden van het rivierbed en overstromingsvlaktes. Een gevolg van een afname van de sedimentlast van de Maas zou kunnen zijn dat minder baggerwerkzaamheden nodig zijn om deze maatregelen in stand te houden.

Volgens de huidige regelgeving in Nederland moeten de waterkeringen een bepaalde waterstand kunnen weren, de zogenaamde maatgevende waterstand. De maatgevende waterstand is een waterstand met een bepaalde herhalingstijd (in jaren). Deze herhalingstijd is op dit moment eens per 1250 jaar voor het bedijkte deel van de Maas, en eens per 250 jaar voor het onbedijkte deel (Ministry of Transport, Public Works and Water Management, 2005, 2006). Sinds de introductie van de Wet op de Waterkeringen in 1995 moet de maatgevende waterstand elke vijf jaar opnieuw beoordeeld worden. Momenteel gebeurt dit aan de hand van de maatgevende afvoer (d.w.z. de afvoer bij Borgharen met een herhalingstijd van eens per 1250 jaar) en wordt geschat op basis van de statistische extrapolatie van gemeten afvoerreeksen. De resultaten van deze studie laten echter zien dat de afvoer geassocieerd met deze herhalingstijd in de toekomst zal stijgen, waardoor schattingen gebaseerd op gemeten afvoerreeksen te laag zullen zijn. Het gebruik van multi-ensemble simulaties van afvoer, zoals gedaan is in deze studie, zou dit mogelijk kunnen ondervangen en gebruikt kunnen worden om de maatgevende afvoer te schatten onder verschillende scenario's van toekomstige klimaat- en landgebruikveranderingen.

De implicaties die voortvloeien uit deze studie zijn niet alleen van belang voor het Maasbekken, maar ook voor stroombekkens over de gehele wereld waar grote veranderingen in de afvoer worden verwacht. Aerts et al. (2006), bijvoorbeeld,

simuleerden de afvoer van 15 rivieren verspreid over de wereld (gebruik makend van het model beschreven in Hoofdstuk 2; Ward et al., 2007). De resultaten hiervan lieten zien dat voor de meerderheid van deze rivieren de te verwachten verandering in de afvoer tussen de 20e en 21e eeuw minstens zo groot (of groter) is dan de verandering gesimuleerd tussen de perioden 9000-8650 BP en 1750-2000 na Chr.

Eén van de grote voordelen van het gebruik van gekoppelde modellen om afvoer, overstromingsfrequentie en sedimentlast te simuleren op duizendjarige tijdschalen is dat het mogelijk is om de relatieve invloed van klimaat- en landgebruikverandering uit te splitsen. Deze methode staat toe om de invloed van menselijke activiteiten te analyseren tegen een natuurlijk referentiekader. Dit is niet mogelijk wanneer alleen naar gemeten en/of gesimuleerde reeksen van de laatste of huidige eeuw wordt gekeken. Bovendien kunnen de resultaten van de modellen worden geverifieerd tegen bewijzen uit geomorfologische en geologische bronnen voor perioden waarin de leefomgeving anders was dan die van tegenwoordig. Om deze redenen is deze aanpak een goede methode om de invloed van veranderingen in klimaat- en landgebruik op afvoer, overstromingsfrequentie, en sedimentlast te bestuderen.

Chapter 1

Introduction

1.1 Background and problem definition

Future climate change is expected to have major impacts on river systems around the world, and could cause changes in discharge and flood frequency (Kundzewicz et al., 2007), and soil erosion and the delivery of sediments to river channels (e.g. Houben et al., 2006; Toy et al., 2002). An analysis of a recent set of global climate change simulations shows that Europe is amongst the Earth's most sensitive regions to future climate change (Giorgi, 2006), with model projections of increased winter precipitation in north-west Europe of between 5% and 20% (Giorgi and Coppola, 2007). Changes in basin hydrology, however, depend not only on climate but also on land use. Changes in land use are the result of complex interactions between physical, socio-economic, and political processes (Van Rompaey et al., 2002; Verburg, 2006), including climatic change. It is now widely acknowledged that past decreases in forest cover have caused significant increases in discharge and soil erosion around the globe (e.g. Andréassian, 2004; Bork and Lang, 2003; Bosch and Hewlett, 1982; Calder, 1993; Hornbeck et al., 1993; Sahin and Hall, 1996; Van Rompaey et al., 2002).

In the Netherlands, the importance of research into the effects of climate change on hydrology has been recognised since at least the late 1980s (e.g. Boer and De Groot, 1990). For the Meuse basin (Fig. 1.1), this was given added impetus by the major floods of 1993 and 1995. In those years the Meuse overflowed its banks, leading to extensive flood damage in the riparian states. For example, the direct financial losses associated with the floods of 1993 were estimated to be above €100 million for the Netherlands alone (Wind et al., 1999). Since then, numerous studies have been carried out to examine hydrological changes in the catchment over the last century. These studies show that whilst mean annual and monthly discharge have remained fairly stable over the course of the 20th Century (De Wit et al., 2001; Tu, 2006; WL, 1994a), annual and winter maximum daily discharge have been significantly higher since the mid-1980s than during the rest of the 20th Century (Pfister et al., 2000; Tu, 2006). Numerous hydrological models have also been used to assess the impacts of climate change on Meuse hydrology in the future (e.g. Booij, 2005; Bultot et al., 1988; De Wit et al., 2001, 2007a; Gellens and Roulin, 1998; Middelkoop and Parmet, 1998; Van Deursen, 2000). These studies suggest that the anticipated climate change of the 21st Century will lead to an increase in flood frequency, especially in the winter half-year (November-April). For example, Booij (2005) simulated an increase in the magnitude of flood events with a return period of 100 years of ca. 9 to 13% between the end of the 20th and 21st Centuries.

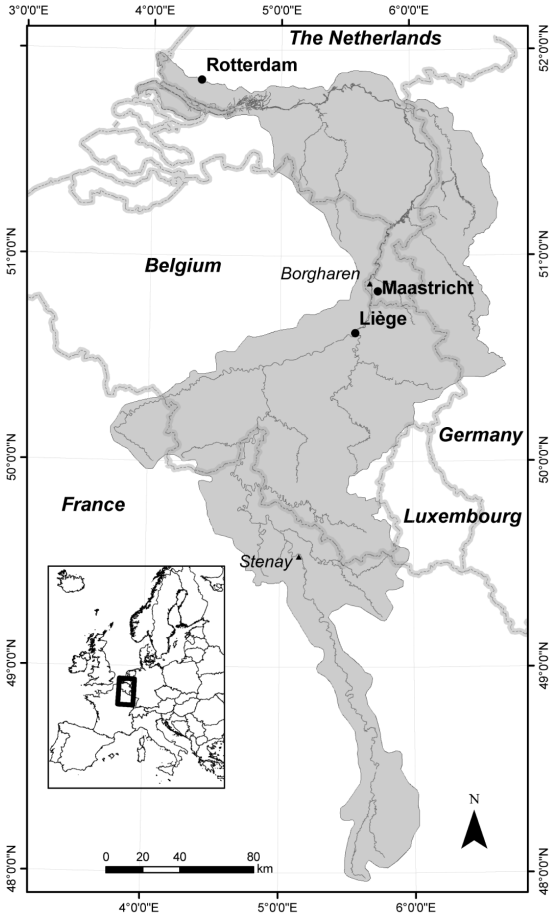

Fig. 1.1: Map showing the location of the Meuse Basin (after RWS Limburg/IWACO, 2000). The basin has an area of ca. 33,000 km^2, and covers parts of France, Luxembourg, Belgium, Germany, and the Netherlands. The inset shows the location of the Meuse basin in Europe.

Much less research has been carried out to examine the effects of changes in forest cover in the Meuse basin because the forested area has remained relatively stable at the basin scale over the course of the last century (DGRNE, 2000; Knol et al., 2004; Tu, 2006). Neither Ashagrie et al. (2006) nor Tu (2006) found evidence in observed discharge records to suggest that land use changes in the 20th Century had a significant effect on Meuse discharge.

In the Meuse basin, as in many medium to large catchments, research into the effects of climate and land use change on soil erosion and sediment delivery at the basin scale are lacking. This is despite the fact that these processes now have an important position on the political agendas of local, national, and European policy makers, can lead to a plethora of environmental problems, and can pose

substantial financial burdens on society (Van Rompaey et al., 2005). Soil erosion on arable land has numerous detrimental on-site impacts, including the loss of topsoil and fertilisers, decreased crop yield and accessibility (due to the formation of gullies) in the short-term, and decreased soil productivity in the long-term (Verstraeten et al., 2002). The delivery of sediments eroded from agricultural areas is also responsible for the supply of nutrients, pesticides, and heavy metal contaminants to river channels (e.g. Boers, 1996; De Wit and Behrendt, 1999; Stam, 1999; Verstraeten and Poesen, 2002), which can have an impact on the water quality of rivers and coastal areas. Sediment delivery also impacts on channel and floodplain morphology (e.g. Asselman and Middelkoop, 1995; De Moor et al., 2008); the ecological functioning of floodplains (Richards et al., 2002); and sediment deposition rates in reservoirs and ponds (Verstraeten and Poesen, 1999). Changes in soil erosion and sediment delivery can be assessed by analysing the sediment yield of rivers (i.e. the amount of sediment passing a certain position in the river channel over a given period of time).

To date, studies which have been carried out to examine changes in Meuse discharge and sediment yield at the basin scale have either been based on observed records of the last century, or have used models calibrated against observations for that period to simulate changes in the 21st Century. However, when studying long-term changes (centennial to millennial) this is problematic. Firstly, accurate daily measurements of Meuse discharge have only been made since 1911, and since 1995 for sediment yield. These records are too short to evaluate the effects of long-term climatic changes (Alcamo et al., 2000; Ely et al., 1993; Knox, 1984; Meybeck, 2003). Secondly, the performances of these models have not been validated for periods in which environmental conditions were different to those during the last century. Thirdly, at a basin scale the forested area has been relatively stable over the last century, so it is difficult to assess the effects of large-scale changes in land use.

A useful way to address the lack of long-term observed measurements is to examine the hydrological response to environmental changes prior to the period in which instrumental measurements were taken. This field of study is known as palaeohydrology, and can be defined as:

> "*…the science of the waters of the earth, their composition, distribution and movement on ancient landscapes from the beginning of the first rainfall to the beginning of continuous hydrological records*" (in Gregory, 1996).

The relevance of data from the period prior to instrumental records in the study of global change is recognised in the Fourth Assessment Report of the Intergovernmental Panel on Climate Change (IPCC, 2007).

Studies of palaeohydrology provide a dataset for the validation of model response on millennial timescales (Lang and Bork, 2006). They also enable us to simulate

the response of discharge and sediment yield to changes in climate over longer timescales, to greater amplitudes of climatic change, and to more extensive changes in land use. Furthermore, the use of millennial timescales allows for a more realistic investigation of extreme events with low return frequencies. Moreover, by simulating discharge and sediment yield during time-periods in which human influence on the environment was negligible, the effects of anthropogenic activities can be assessed in relation to natural reference conditions. However, the modelling of Holocene discharge and sediment yield at the basin scale is in its infancy. Bogaart et al. (2003) used a process-based numerical model to simulate long-term (> 100 year) changes in mean Meuse discharge during the last Glacial-Interglacial transition, but simulations at a higher temporal resolution, or for periods in the more recent Holocene period, remain elusive, not only for the Meuse but also for rivers around the globe. As with simulations of discharge, simulations of Meuse sediment yield during the Holocene are also currently lacking. The development and application of such models therefore forms an interesting challenge, and one from which much information on the effects of long-term changes in climate and land use could be derived.

1.2 Objectives and research questions

In order to respond to the issues raised in Section 1.1, the main objectives of this Ph.D. study are to assess the long-term trends and changes in discharge, flood frequency, and sediment yield of the River Meuse during the late Holocene and the 21st Century in response to natural and anthropogenic changes in climate and land use, and to compare the relative impacts of these factors on different timescales. Assessments of this nature are of great importance for the Meuse basin, since the damages associated with flooding and soil erosion are high. Moreover, relatively long records of climate and discharge provide reliable datasets for the calibration of models. In order to address these objectives, the following key research questions have been formulated:

1. Can we develop a coupled climate-hydrological modelling approach to simulate long-term changes in palaeodischarge? To what extent can multi-proxy data be used to test the performance of such models as tools for palaeodischarge assessment?
2. How has the discharge and flood frequency of the River Meuse changed between a natural reference period when the natural climate forcings were similar to those of today and human influence on land use was minimal (4000-3000 BP), and a period influenced by anthropogenic changes in land use (1000-2000 AD) and greenhouse gas and sulphate aerosol emissions (post industrial revolution)? What mechanisms caused these changes in discharge and flood frequency?
3. What are the relative effects of climate change and land use change on the discharge and flood frequency of the Meuse during the 21st Century? How do these compare to the effects of long-term natural and anthropogenic change over the late Holocene?

4. What effects have changes in land use and climate had on soil erosion and sediment yield in the Meuse basin during the late Holocene? What effects can be expected in the 21st Century?

1.3 General research strategy

In this section I describe the basic approach used to address these research questions. The descriptions of the methods and models are general; more detailed descriptions can be found in the relevant chapters of the thesis, as described in Section 1.5. The general research approach is shown schematically in Fig. 1.2.

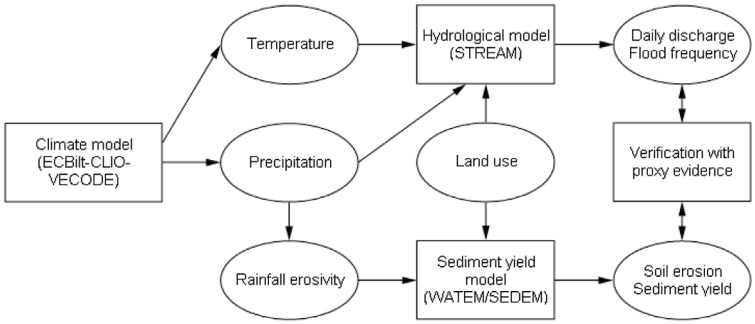

Fig. 1.2: Flow diagram illustrating the general research approach used in this thesis. The climate model, hydrological model, and sediment yield model, were all run for the periods 4000-3000 BP (natural reference period), and 1000-2100 AD.

In order to examine the effects of long-term changes in land use and climate change on discharge, flood frequency, and sediment yield over the late Holocene, computer models were used to simulate these changes for two time-periods: 4000-3000 BP and 1000-2100 AD. The period 4000-3000 BP was selected as it represents the most recent time-period in which the natural orbital forcings on climate were broadly similar to those of today (Goudie, 1992), whilst human influence on land use was minimal (Bunnik, 1995; Gotjé et al., 1990; RWS Limburg/IWACO, 2000). The period 1000-2100 AD was heavily influenced by human activities, namely changes in land use throughout the period, and anthropogenic emissions of greenhouse gases and sulphate aerosols since the industrial revolution. By comparing changes in discharge, flood frequency, and sediment yield between these two periods, it is therefore possible to examine and delineate the effects of changes in climate and land use. The results of the computer simulations were compared with evidence of past environmental changes based on observations and geomorphological records. Throughout this thesis, dates indicated as BP (Before Present, where present is defined as 1950) are given in calendar years (cal. yrs.) unless otherwise stated.

Changes in discharge and flood frequency were examined by coupling a climate model with a hydrological model. For this purpose the climate model ECBilt-

CLIO-VECODE (Brovkin et al., 2002; Goosse and Fichefet, 1999; Opsteegh et al., 1998) and the hydrological model STREAM (Spatial Tools for River basins and Environment and Analysis of Management options) were used (Aerts et al., 1999). ECBilt-CLIO-VECODE is a three-dimensional coupled climate model consisting of three components describing the atmosphere, ocean, and vegetation. The model was forced by annually varying orbital parameters, atmospheric volcanic aerosol content, fluctuations in solar activity, and atmospheric greenhouse gas and sulphate aerosol concentrations. STREAM is a grid-based spatially distributed water balance model that describes the hydrological cycle as a series of storage compartments and flows. As well as climate data, the main inputs for STREAM are a digital elevation model (DEM), land use maps, and maps of soil water holding capacity. The maps of land use and soil water holding capacity used in this study were based on observations for the present day, simulations for the future, and reconstructions for the late Holocene based on historical sources and pollen analyses.

The effects of changes in land use and climate change on the sediment yield of the Meuse river were examined by coupling the same climate model (ECBilt-CLIO-VECODE) with a spatially distributed soil erosion and sediment delivery model (WATEM/SEDEM) (Van Oost et al., 2000; Van Rompaey et al., 2001a; Verstraeten et al., 2002). WATEM/SEDEM is a grid-based model that uses GIS raster layers as input. Soil erosion is calculated based on the Revised Universal Soil Loss Equation (RUSLE) (Renard et al., 1991), and eroded sediment is either routed through the basin to a permanent river channel, or redeposited on the slopes, based on transport capacities of overland flow per grid cell.

1.4 Framework of the research project

This project was carried out in the framework of the Dutch National Research Programme ‘Climate changes Spatial Planning’ (www.klimaatvoorruimte.nl). The programme is co-funded under the Dutch decree on subsidies for investments in the knowledge infrastructure (BSIK, formerly ICES-KIS-3). The research programme was developed in close collaboration with a wide range of stakeholders, including a number of Dutch governmental ministries, regional and local governmental agencies, the private sector, and non-governmental organisations (NGOs). The consortium partners include numerous nationally and internationally recognised institutes. The main objectives of the programme are:

- to offer the Dutch government, the private sector, and other stakeholders a clustered, high-quality, and accessible knowledge infrastructure on the interface of climate change and spatial planning;
- to engage a dialogue between stakeholders and scientists in order to support the development of spatially explicit adaptation and mitigation strategies that anticipate for climate change and contribute to a safe, sustainable, and resilient socio-economic infrastructure in the Netherlands.

The programme is subdivided into five themes: (a) climate scenarios, (b) mitigation, (c) adaptation, (d) integration, and (e) communication. This project is carried out under the theme Climate Scenarios (CS), the main aims of which are:

1. uncovering the role of vital atmospheric processes in shaping our climate and improvement of measurements of vital climate parameters;
2. production of climate scenarios and time-series relevant for spatial planning;
3. assessing the future by mining the past climate (palaeoclimatology);
4. tailoring climate information for end users in a participatory way.

This study mainly addresses sub-theme (3), and has been carried out under project CS9, entitled 'Modelling and reconstructing precipitation and flood frequency in the Meuse catchment during the late Holocene'.

1.5 Thesis outline

This thesis contains seven chapters. Chapters 2 to 6 are based on five papers which have either been published, or accepted or submitted for publication, in international peer-reviewed scientific journals. Next to these papers, the work carried out during this Ph.D. project has so far contributed to two further scientific papers, a technical report, and a number of publications in the professional media. For a full list of these publications please refer to Section 1.6.

Chapter 1 provides an introduction and background to the research, and sets out the main objectives and research questions.

Chapter 2 contains a description of the set-up, calibration, and validation of a coupled climate-hydrological model for simulating Holocene palaeodischarge in 19 rivers around the globe (Amazon, Congo, Danube, Ganges, Krishna, Lena, Mackenzie, Mekong, Meuse, Mississippi, Murray-Darling, Nile, Oder, Rhine, Sacramento-San Joaquin, Syr Darya, Volga, Volta, Zambezi). The simulations are carried out with a monthly time-step and a relatively low spatial resolution (0.5° x 0.5°). The model results are compared to palaeodischarge estimates from multi-proxy records, based on an extensive review of published literature. Since such a coupled climate-hydrological model has not previously been applied to studies of palaeodischarge during the late Holocene, this part of the thesis forms a pilot-study of the general research approach. This pilot study therefore provides an evaluation of the usefulness of the methodology in palaeodischarge retrodiction, prior to its application to the Meuse basin, and is based on Ward et al. (2007).

The modelling approach tested in Chapter 2 is then applied to the Meuse basin in Chapter 3. The spatial resolution of the model is increased greatly, and a daily time-step is used. As well as mean discharge, the use of a daily time-step facilitates the examination of flood frequencies. I examine the effects of changes in climate and land use on Meuse discharge and flood frequency in the periods 4000-3000 BP and 1000-2000 AD. This chapter is based on Ward et al. (2008a).

In Chapter 4 (based on Ward et al., 2008b) the model described in Chapter 3 is then used to simulate the potential effects of changes in land use and climate on discharge and flood frequency in the 21st Century. These changes are compared to the millennial scale changes and trends discussed in Chapter 3.

Chapters 5 and 6 deal with the sediment yield of the Meuse basin. In Chapter 5, observed records of Meuse discharge and suspended sediment concentration are used to estimate the annual sediment yield over the period 1995-2005. The findings are then compared to those made by other authors at various times over the last 125 years. In Chapter 6, changes in the sediment yield over a much longer time-scale are discussed. A soil erosion and sediment delivery model is used to examine the effects of changes in climate and land use change on sediment yield over the periods 4000-3000 BP and 1000-2000 AD. Chapter 5 is based on Ward (2008a), and Chapter 6 is based on Ward et al. (2008c).

Finally, in Chapter 7, I present a synthesis of the results discussed in the preceding chapters, and discuss the findings in the context of the original key research questions. There is also a discussion of some of the implications of the research findings for water management and spatial planning. Finally, a number of recommendations for future research are made.

1.6 Publications related to this thesis

- Aerts, J.C.J.H., Renssen, H., Ward, P.J., De Moel, H., Odada, E., Bouwer, L.M., Goosse, H., 2006. Sensitivity of global river discharges under Holocene and future climate conditions. Geophysical Research Letters, 33, L19401, doi:10.1029/2006GL027493.

- Renssen, H., Lougheed, B.C., Aerts, J.C.J.H., De Moel, H., Ward, P.J., Kwadijk, J.C.J., 2007. Simulating long-term Caspian Sea level changes: The impact of Holocene and future climate conditions. Earth and Planetary Science Letters, 261, 685-693, doi:10.1016/j.epsl.2007.07.037.

- Ward, P.J., 2007a. A coupled climate-hydrological model for Meuse palaeodischarge modelling: set-up and calibration. Technical Report: July 2007, VU University Amsterdam, Amsterdam, The Netherlands, 41 pp.

- Ward, P.J., 2007b. Grote toename in de overstromingsfrequentie van de Maas door grootschalige ontbossingen. Climate changes Spatial Planning Newsletter, 9, p.6, www.klimaatvoorruimte.nl.

- Ward, P.J., 2008a. River Meuse suspended sediment yield: a new estimate and past estimates revisited. Netherlands Journal of Geosciences, 89(2), 189-193.

- Ward, P.J., 2008b. Zicht op Maasafvoer door de eeuwen heen. Land en Water, 8, 30-31.

- Ward, P.J., Aerts, J.C.J.H., De Moel, H., Renssen, H., 2007. Verification of a coupled climate-hydrological model against Holocene palaeohydrological records. Global and Planetary Change, 57(3-4), 283-300, doi:10.1016/j.gloplacha.2006.12.002.

- Ward, P.J., Renssen, H., Aerts, J.C.J.H., Van Balen, R.T., Vandenberghe, J., 2008a. Strong increases in flood frequency and discharge of the River Meuse over the late Holocene: impacts of long-term anthropogenic land use change and climate variability. Hydrology and Earth System Sciences, 12, 159-175, www.hydrol-earth-syst-sci-net/12/159/2008.

- Ward, P.J., Renssen, H., Aerts, J.C.J.H., Verburg, P.H., 2008b. Sensitivity of discharge and flood frequency to 21st Century changes in climate and land use (River Meuse, northwest Europe). Submitted to Climatic Change.

- Ward, P.J., Van Balen, R.T., Verstraeten, G., Renssen, H., Vandenberghe, J., 2008c. The impact of land use and climate change on late Holocene and future suspended sediment yield of the Meuse catchment. Geomorphology, *in press*, doi:10.1016/j.geomorph.2008.07.006.

Chapter 2

Verification of a coupled climate-hydrological model against Holocene palaeohydrological records

Abstract

We have coupled a climate model (ECBilt-CLIO-VECODE) and a hydrological model (STREAM) offline to simulate the palaeodischarge of 19 rivers (Amazon, Congo, Danube, Ganges, Krishna, Lena, Mackenzie, Mekong, Meuse, Mississippi, Murray-Darling, Nile, Oder, Rhine, Sacramento-San Joaquin, Syr Darya, Volga, Volta, Zambezi) for three time-slices: Early Holocene (9000-8650 BP), Mid Holocene (6200-5850 BP), and recent (1750-2000 AD). To evaluate the model's skill in retrodicting broad changes in mean palaeodischarge we have compared the model results with palaeodischarge estimates from multi-proxy records. We have compared the general trends inferred from the proxy data with statistical differences in modelled discharge between the three periods, thereby developing a technique to assess the level of agreement between the model and proxy data. The quality of the proxy data for each basin has been classed as *good*, *reasonable*, or *low*. Of the model runs for which the proxy data were *good* or *reasonable*, 72% were in *good* agreement with the proxy data, and 92% were in at least *reasonable* agreement. We conclude that the coupled climate-hydrological model performs well in simulating mean discharge in the time-slices studied. The discharge trends inferred from the proxy and model data closely follow latitudinal and seasonal variations in insolation over the Holocene. For a number of basins for which agreement was not *good* we have identified specific mechanisms which could be responsible for the discrepancy, primarily the absence of the Laurentide ice sheet in our model. In order to use the model in an operational sense within water management studies, it would be useful to use a higher spatial resolution and a daily time-step.

This chapter is based on the paper: Ward, P.J., Aerts, J.C.J.H., De Moel, H., Renssen, H., 2007. Verification of a coupled climate-hydrological model against Holocene palaeohydrological records. Global and Planetary Change, 57(3-4), 283-300, doi:10.1016/j.gloplacha.2006.12.002.

2.1 Introduction

Climate is one of the principal driving forces of hydrological systems and even modest climate changes have the potential to cause significant changes in hydrological processes (Knox, 2000, 2003), including changes in the volume and temporal distribution of river discharge (Van Deursen, 1995). An understanding of these changes is of utmost importance since future climate change may alter both flood and drought characteristics of river systems (Meybeck, 2003).

In order to plan for these changes, quantitative data are required on both long-term average discharge and the changes in frequency and intensity of peak and low flows (Aerts and Droogers, 2004). To provide these estimates, simulated future climate data can be used as input for hydrological models, which can then be utilised to project future changes in discharge regimes. Numerous attempts have been made to develop such models at the global scale (e.g. Alcamo et al., 2003; Arnell, 1999; Döll et al., 2003; Klepper and Van Drecht, 1998; Vörösmarty et al., 1998; Yates, 1997), and at the individual basin level (see e.g. Arnell et al., 2001, p. 203, and references therein). To provide projections of future discharge, such models are validated by comparing their output to observed data on past discharge from gauging stations. However, even the longest instrumental records are too short to adequately evaluate long-term and large ranges of potential climatic variations (Chatters and Hoover, 1986; Ely et al., 1993; Knox, 2000).

Studies of palaeodischarge provide a means to overcome this lack of long-term observed data by providing a dataset for the validation of model response over periods of thousands of years. To date, few studies have been carried out to model palaeodischarge based on palaeoclimatic data. Coe and Harrison (2002) used runoff fields derived directly from a GCM (General Circulation Model) in combination with a river routing algorithm to simulate lake level changes in northern Africa at ca. 6 ka. BP. At the basin scale the use of runoff data derived directly from GCMs has the disadvantage that runoff fields are less well resolved than climatic fields. Research using climatic output from climate models, coupled with hydrological models, to specifically simulate Holocene river discharge, remains elusive.

The main goal of this study is to develop a coupled climate-hydrological model for simulating Holocene discharge. The study involves the offline coupling of the climate model ECBilt-CLIO-VECODE and the hydrological model STREAM. This is achieved through the following means:

- set up and calibrate the model for the recent period for 19 rivers;
- model the discharge of these rivers during three time-slices in the Holocene;
- identify independent proxy data on Holocene discharge for these rivers;
- evaluate the model's ability to simulate the main trends in changes of palaeodischarge magnitude.

2.2 Methods

In this study we compare simulated river discharges to proxy records of palaeodischarge for three time-slices in the Holocene, namely 9000-8650 BP (Early Holocene), 6200-5850 BP (Mid Holocene), and 1750-2000 AD (recent). The abbreviations EH, MH, and RT are used respectively to refer to these time-slices. The period 9000-8650 BP was selected since it represents the time-period in which seasonal and latitudinal anomalies in insolation values compared to present were near the Holocene maximum (Berger, 1978). The period 6200-5850 BP represents a period with seasonal differences in insolation between those of 9000-8650 BP and present. Furthermore, the latter period is used as a standard reference period for comparing model and proxy data, e.g. The Project for Intercomparison of Land-Surface Parameterization Schemes (PILPS: Henderson-Sellers et al., 1996). The research approach is shown schematically in Fig. 2.1.

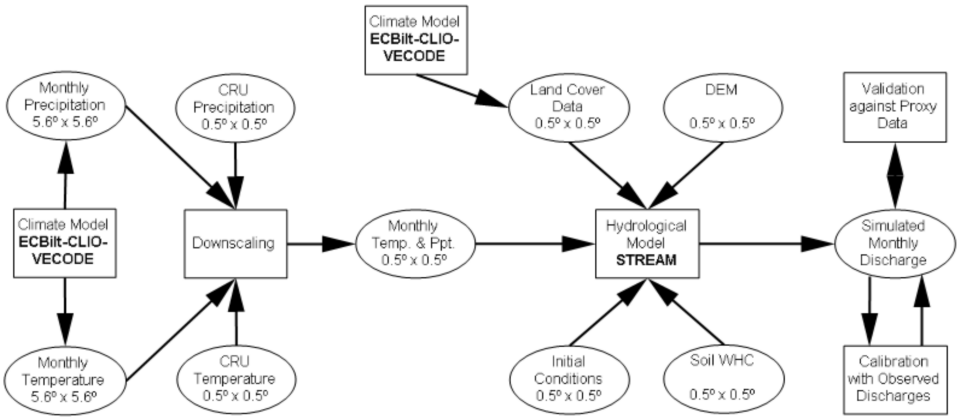

Fig. 2.1: Flowchart of the research approach and methodology used in this study.

The climate data used as input in the hydrological model were derived from a 9000 year experiment using ECBilt-CLIO-VECODE (Renssen et al., 2005a). As the hydrological model, STREAM (Aerts et al, 1999), was run at a finer spatial resolution than ECBilt-CLIO-VECODE, a downscaling step was implemented. Nineteen basins were selected for modelling (Fig. 2.2), based on their geographical distribution and on the availability of palaeodischarge proxy data. Given the resolution of the hydrological model (0.5° x 0.5°), only medium or large basins were modelled, with the exception of the Meuse (ca. 33,000 km^2 (Pfister et al., 2004)). Whilst this basin is relatively small compared to the other basins studied, it forms the core of the rest of this thesis, and hence it was included in this study.

2.2.1 Climate model and Holocene climate experiment

ECBilt-CLIO-VECODE is a three-dimensional coupled climate model consisting of three components describing the atmosphere, ocean, and vegetation. The atmospheric component is ECBilt (Opsteegh et al., 1998), and the ocean-sea-

Fig. 2.2: World map showing the rivers modelled in this study. The GIS map was constructed by Renssen & Knoop (2000) and was used in the hydrological model to set the boundaries of the modelled basins.

ice component is CLIO (Goosse and Fichefet, 1999). The final component is VECODE, a dynamic vegetation model which simulates the dynamics of two main terrestrial plant types (forest and grasses) as well as bare soil, in response to climatic fluctuations (Brovkin et al., 2002). In ECBilt-CLIO-VECODE the simulated vegetation covers only affect the land-surface albedo, but do not influence other processes such as soil hydrology (Goosse et al., 2005). ECBilt is an Earth System Model of Intermediate Complexity (EMIC) (see Claussen et al., 2002), and runs two orders of magnitude faster than most Comprehensive General Circulation Models (Opsteegh et al., 1998). It was therefore possible to model the Holocene in a transient run, allowing for states of non-equilibrium in the climate (Renssen et al., 2005a).

The output of ECBilt-CLIO-VECODE used in this study were derived from a 9000 year long experiment forced by annually varying orbital parameters, and atmospheric greenhouse gas and sulphate aerosol concentrations (Renssen et al., 2005a). Besides these external forcings, several internal feedback mechanisms play an important role, especially albedo feedbacks. However, the deglaciation of the Laurentide ice sheet in the early Holocene was not considered. In the experiment used here (Renssen et al., 2005a), a number of important shorter term forcing mechanisms are not included, especially fluctuations in solar activity and volcanic aerosol content. Thus the forcing parameters effect long-term (millennial) climatic fluctuations; as a result short-term discharge fluctuations will be difficult to detect. However, as the aim of this study is to assess the model's ability to retrodict broad changes in palaeodischarge magnitude, the long-term signal is of particular use. The atmospheric component of ECBilt-CLIO-VECODE has a spatial resolution of ca. 5.6° x 5.6° and a monthly output interval. Due to this low spatial resolution, and the relatively simple atmospheric physics, the model is unable to capture El Niño Southern Oscillation (ENSO) variability, which may have been different during the Holocene than today (Moy et al., 2002). However,

since we are examining the mean long-term discharge trends over 250-350 year time-slices, decadal variations in discharge are not analysed. Given the quasi-geostrophic nature of the model, climates in tropical regions are generally less well resolved than those in other areas (Goosse et al., 2005).

2.2.2 Hydrological model

STREAM (Spatial Tools for River basins and Environment and Analysis of Management options) is a grid-based spatially distributed water balance model that describes the hydrological cycle of a drainage basin as a series of storage compartments and flows (Aerts et al., 1999). It is based on the RHINEFLOW model of Kwadijk (1991, 1993). STREAM calculates the water balance per grid cell using the Thornthwaite equations for potential evapotranspiration (Thornthwaite, 1948) and the Thornthwaite and Mather equations for actual evapotranspiration (Thornthwaite and Mather, 1957). The main flows and storage compartments used to calculate water availability per grid cell are shown in Fig. 2.3. The direction of water flow between grid cells is based on a digital elevation model (DEM). STREAM or RHINEFLOW have been successfully applied to numerous basins of varying size and in different regions. There exists a large number of hydrological models, all of which have various advantages and disadvantages depending on their application. In Appendix 1 the main concepts involved in hydrological modelling are discussed, as well as the reasons for using the STREAM model in this thesis.

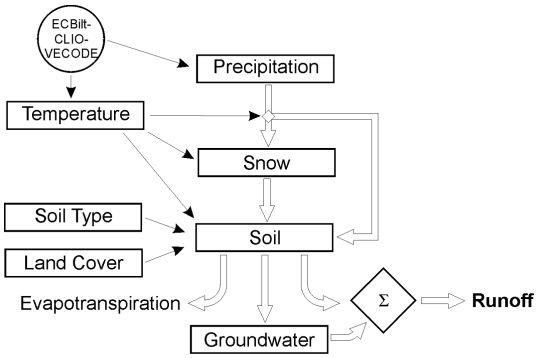

Fig. 2.3: Water balance storage compartments and flows in the STREAM model (adapted from Aerts et al., 1999).

In this pilot study, STREAM was run at a spatial resolution of 0.5° x 0.5° using a monthly time-step. This resolution was selected for a number of reasons. As one of the objectives of our study is to assess the model's ability to simulate the main trends in changes of palaeodischarge magnitude, a daily time-step was deemed inappropriate as the palaeodischarge proxy data do not give indications of daily flows. Furthermore, running the model on a global scale with a daily time-step would be computationally too demanding. The choice of the spatial resolution

was based on similar considerations. Moreover, the Climate Research Unit (CRU) of the University of East Anglia has created a gridded-set of observed climate variables for the globe at a 0.5° x 0.5° resolution (CRU TS 2.0) (Mitchell et al., 2003), which has been found to be useful for the downscaling of climate model data to regional resolutions (Bouwer et al., 2004).

2.2.3 STREAM input data

We created a raster GIS database with all maps digitised to a 0.5° x 0.5° resolution. In this section a summary of the input data sources is given.

2.2.3.1 Climate data

The climate data (mean monthly temperature and precipitation) were derived from ECBilt-CLIO-VECODE, and were subsequently downscaled to the resolution of the STREAM model. The first step was a spatial downscaling procedure (Bouwer et al., 2004), whereby the values from the ca. 5.6° x 5.6° climate model grid were resampled onto a 0.5° x 0.5° grid. The spatially downscaled climate maps have a resolution of 0.5° x 0.5°, but only reflect spatial variability at the scale of the climate model (5.6° x 5.6°), which is too coarse for direct use in (regional) hydrological studies (Arnell et al., 1996; Bouwer et al., 2004; Kleinn et al., 2005; Wood et al., 2002, 2004). Therefore a second downscaling step was required to introduce a more realistic and greater degree of spatial variability. There are two main approaches to downscaling climate model data: statistical methods (e.g. Bouwer et al., 2004; Wilby and Wigley, 1997; Wilby et al., 1998; Wood et al., 2002) and dynamical approaches using regional circulation models (RCMs) nested within the coarser climate model (e.g. Cocke and LaRow, 2000; Kim et al., 2000; Murphy, 2000; Wood et al., 2002; Yarnal et al., 2000). The results of these two approaches have been found to have similar levels of skill (e.g. Wilby et al., 2000; Wood et al., 2004), but dynamical methods are computationally far more demanding (Bouwer et al., 2004). The scale of our study renders this approach prohibitive, since the global spread of basins would necessitate the nesting of several RCMs into ECBilt-CLIO-VECODE.

Statistical downscaling involves the use of correction factors (for temperature additive and for precipitation multiplicative) which are applied to the low resolution modelled data so as to preserve the statistical properties of a higher resolution observed climate dataset (Bouwer et al., 2004). In our study this approach was problematic because in some areas very large correction values would have been necessary. This would have been the case especially in arid areas where very high correction factors based on current precipitation patterns would have been transferred to other periods in the Holocene. For instance, it is known that the Sahel received more precipitation than today during parts of the Holocene, and at times would have been covered by grasses (Renssen et al., 2003; Roberts, 2002). Using a very high correction factor (based on current arid Sahel conditions) to downscale EH precipitation data would result in arid conditions whilst this was not the case.

Therefore, we devised a new redistribution technique. Observed monthly temperature and precipitation data at a 0.5° x 0.5° resolution were obtained for the baseline period 1961-1990 from the CRU TS 2.0 dataset (Mitchell et al., 2003). The mean observed temperature and precipitation values were upscaled to the resolution of ECBilt-CLIO-VECODE simply by calculating the mean values of all high-resolution cells belonging to the corresponding 5.6° x 5.6° grid cell. The differences between the observed temperature and precipitation values at the lower and the higher resolution were then calculated, thereby creating correction factors on a 0.5° x 0.5° grid. Subsequently these correction factors were applied to the spatially downscaled ECBilt-CLIO-VECODE data. Using this approach the total precipitation and average temperature simulated by ECBilt-CLIO-VECODE are redistributed over the higher resolution grid cells according to the present day spatial distribution, whilst the absolute values at the resolution of ECBilt-CLIO-VECODE remain unchanged. Hence, temperature and precipitation gradients resulting from differences in relief and distance from the oceans are better represented in the climate data. This approach assumes that the present day regional distribution of temperature and precipitation was the same during the Holocene time-slices studied. In reality this is not the case since climatic patterns change (IPCC, 2001). However, as Kleinn et al. (2005) indicate, for catchments of several thousand square-kilometres and for runoff evolution on a monthly timescale, catchment mean precipitation is the most important factor for river discharge whilst the finer scale distribution within the catchment is less important.

2.2.3.2 Soils and hydrography

A crop factor (*CropF*) map is used in STREAM for the calculation of potential evapotranspiration based on the Thornthwaite (1948) equations. The crop factor map used in this study for 1750-2000 AD was based on a map of land cover characteristics from the WARibaS project (Klepper and Van Drecht, 1998), and was reclassed to crop factors based on land use coefficients listed in Kwadijk (1993), and Aerts and Bouwer (2002). For the EH and MH, the anomalies between the VECODE output for those time-slices and the VECODE output for the recent time-slice were calculated, and then reclassed to crop factor anomalies. These anomalies were then reconciled with the modern crop factor map to create crop factor maps for the palaeo time-slices. As such, only land cover changes resulting from natural climatic change were used to force the hydrological model. The simulated change in basin averaged crop factor between the time-slices is very low in most cases. A change in basin-wide palaeo crop factor of more than 5% (compared to RT) was only registered for the following basins and time-slices: Krishna, EH (+6.6%); Nile, MH (+6.5%), EH (+13.0%); Syr Darya, EH (+6.0%). Hence, for the majority of basins studied the simulated effects of land cover changes on evapotranspiration were low.

A map showing the water holding capacity (*WHC*) of the soil is used by STREAM in the calculation of evapotranspiration, direct runoff, groundwater seepage,

and baseflow. In this study the *WHC* map was taken from the WARibaS project (Klepper and Van Drecht, 1998), and was used for all three time-slices. Changes in soil types during the Holocene are therefore not included in this study.

The flow direction map of Renssen and Knoop (2000) was used to determine the direction of water flow between grid cells in STREAM. This map was constructed by determining water flow direction based on the TerrainBase DEM of the National Geophysical Data Center (NGDC, 1997). The resulting map was compared with data on the location of major river basins from the ArcWorld database (ESRI, 1992); the similarity was good (Renssen and Knoop, 2000).

To obtain realistic initial conditions for soil water storage, groundwater storage, snow cover, and accumulated potential water loss (*init* maps) we adopted a *perpetual simulation* technique (Kleinn et al., 2005). Prior to commencing model calibration the *init* maps were assigned dummy values (the results of previous test runs). The model was then run for a period of 50 years (i.e. 600 iterations), and the output maps for these parameters after the final iteration were used as input *init* maps.

2.2.3.3 Discharge data

Data for the Nile were taken from Hurst et al. (1946), as cited in Hipel and McLeod (1994). TU Delft provided observed data for the Zambezi. The discharge data for the other rivers were taken from the RivDis database (Vörösmarty et al., 1998), except for those for the Congo, which were taken from the SAGE river discharge database (http://www.sage.wisc.edu/riverdata/).The gauging station locations and the periods for which calibration was carried out can be found in Table 2.1.

2.2.4 Calibration and validation of STREAM

We carried out the calibration of STREAM by varying model parameters with the aim of reproducing annual and monthly discharge characteristics similar to those in the observed record. A similar approach has been successfully employed in numerous studies (e.g. Christensen et al., 2004; Wood et al., 2002). The parameters used for calibration are: *CropF*; *WHC*; *HEAT* (used in the Thornthwaite (1948) equation for calculating potential evapotranspiration); *TOGW* multiplier (determines the proportion of surplus water per grid cell that runs off directly or that seeps to the groundwater); *C* factor (determines the proportion of groundwater that contributes to baseflow); and *MELT* (determines the rate of snowmelt when temperature is above a critical value) (for a more detailed description see Kwadijk (1993)). For all of the basins it was assumed that precipitation would fall as snow below a temperature of 0°C (e.g. Kwadijk, 1993). The only basin where a different value was used was the Syr Darya, where this was set to 2°C to compensate for an overestimation of winter temperatures by ECBilt-CLIO-VECODE in this region.

Table 2.1: Details of the observed discharge datasets used for model calibration, the calibration parameters per basin, and measures of correlation between observed and modelled discharge. [a] total accuracy (the mean annual observed discharge as a percentage of the mean annual modelled discharge); [b] except 1962-63 due to the building of the Red Bluff Diversion Dam.

			Correlation tests			Calibration parameter					
Basin	Period	Gauging station	% [a]	r	N&S	*CropF*	*TOGW*	*C*	*MELT*	*WHC*	*HEAT*
Amazon	1928-83	Obidos	100.1	0.97	0.94	0.285	0.1	4.5	10	1	1
Ganges	1965-75	Paksay	99.0	0.97	0.94	0.83	0.3	1.5	11	1.685	0.1
Krishna	1901-60	Vijayawada	101.3	0.93	0.85	0.39	0.1	1	10	2.5	1
Mekong	1962-87	Nakhon Phanon	99.7	0.99	0.98	1.08	0.4	1.8	12	1.75	0.8
Congo	1971-99	Brazzaville	99.7	0.90	0.55	1.1	0.6	2	1	0.1	0.8
Nile	1901-45	Assiut	100.7	0.99	0.99	12.1	0.6	1.5	10	5	1
Volta	1936-64	Senchi	100.9	0.98	0.96	2.32	0.3	1.7	10	1	1
Zambezi	1979-90	Zumbo	100.3	0.99	0.98	2.16	0.3	1.1	10	1.4	0.5
Murray-Darling	1965-84	Lock 9 Upper	100.5	0.82	0.57	0.9	0.1	1.5	10	3	1
Sacramento-San Joaquin	1948-84[b]	Sacramento	100.7	0.94	0.89	18.5	0.15	2.5	10	5	1
Rhine	1936-84	Rees	100.2	0.87	0.69	0.78	0.1	5	9	0.1	1
Meuse	1911-84	Lith	100.5	0.91	0.81	0.64	0.275	4.5	10	0.1	1
Danube	1921-84	Ceatal Izmail	100.6	0.98	0.95	0.29	0.1	4	10	0.55	1
Oder	1901-86	Gozdowice	100.8	0.96	0.88	0.28	0.19	8	1	0.35	0.5
Mississippi	1965-84	Tarbet Landing	99.9	0.97	0.93	1.46	0.6	2	10	0.1	1
Syr Darya	1930-59	Tyumen Aryk	99.2	0.91	0.82	9.9	0.2	3	60	3.5	1
Volga	1901-35	Volgograd	100.2	0.96	0.91	0.48	0.2	4	9	1	1
Lena	1935-84	Kusur	99.8	0.99	0.98	0.77	0.75	2	40	1	1
Mackenzie	1966-84	Norman Wells	99.7	0.98	0.96	0.98	0.2	2	40	1	1

The downscaled ECBilt-CLIO-VECODE climate data were used as input for the calibration (as opposed to observed climate data) since the palaeodischarge simulations were also carried out using these data. Hence, the discharge series forced by the climate model only reflect discharge trends and not actual monthly or annual discharges (i.e. a wet month in the observed data does not per se correspond to a wet month in ECBilt-CLIO-VECODE). It was therefore only possible to compare the monthly means of discharge over the whole calibration period, and not the paired means of individual months or years. Calibration was carried out for as long a period as possible, the length being primarily determined by the availability of observed discharge data and secondarily by the construction of major dams. No corrections have been made for minor dams, since data on their effects on river discharge are scarce.

A more physically based approach to parameter estimation is of course desirable, but observed data on factors like groundwater storage, proportion of surplus water to runoff, or groundwater seepage are limited. Nevertheless, STREAM does simulate monthly data on changes in soil-water storage, groundwater, and snow cover (results not shown here). Although these results were not compared with independent observed data they did remain in equilibrium over the calibration period.

The agreement between modelled and observed discharge was in the first case assessed by visual inspection of the annual hydrographs. The agreement of the total annual discharge was assessed by expressing the mean annual observed discharge as a percentage of the mean annual modelled discharge (total accuracy, %). The correlation of the paired means of monthly discharge was assessed using the Pearson Product Moment correlation coefficient, r (Legates and McCabe Jr., 1999), and the Nash and Sutcliffe efficiency coefficient (N&S) (Nash and Sutcliffe, 1970). The calibration results and parameters used are listed in Table 2.1. Large differences can be seen for the values of the calibration parameters *CropF* and *WHC* between the different basins. These differences may be related to the relatively low resolution of the land use and soil water holding capacity data, which mask some of the spatial variability of these parameters within each grid cell. Furthermore, some basins may have experienced significant changes in land use over the course of the calibration period, whereas the land use maps on which the spatially distributed *CropF* maps are based refer to a specific moment in time. Also, whilst standard *CropF* values have been used in this study to refer to the different simplified land use types, in reality a much larger variation in these parameters exists. For example, we have used a standard value of *CropF* to refer to the land use ‘forest’, whilst in reality large variations exist in the evapotranspiration characteristics of different forest types around the world.

Hydrographs are presented here for those rivers with the poorest agreement according to the statistical analysis: Congo, Murray-Darling, and Rhine (Fig. 2.4). Whilst there is some discrepancy in the temporal distribution of discharge between

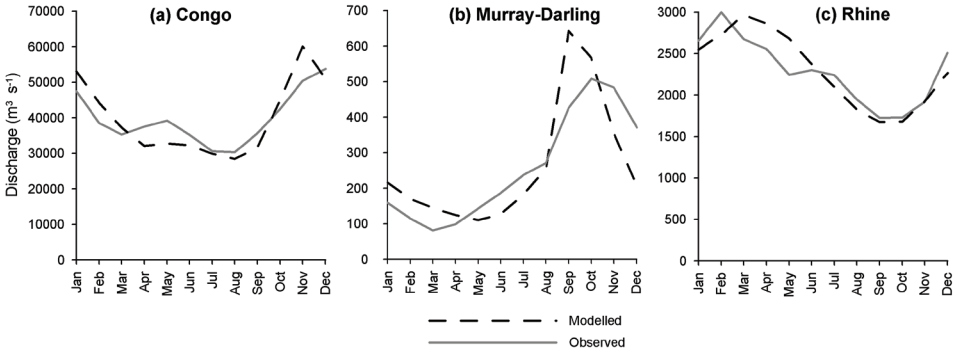

Fig. 2.4: Hydrographs of observed and calibrated model discharge ($m^3 s^{-1}$) for the three basins with the poorest agreement according to the statistical analysis: (a) Congo, (b) Murray-Darling, and (c) Rhine.

modelled and observed data, the general pattern has been preserved. In all three cases the total accuracy of the annual total discharge is very good.

2.2.5 Assessment of agreement between modelled discharges and proxy data

To validate the simulated Holocene discharge results we compared our simulated discharges with multi-proxy records of palaeodischarge obtained through an extensive review of published literature. For each basin we firstly assessed the quality of the proxy data (*good*, *reasonable*, or *low*), in terms of the confidence that they reflect the actual palaeodischarge situation of the river in question during the relevant time-slice. Whilst such an assessment is somewhat subjective, we used three criteria for standardisation:

- Does at least one of the proxy records refer specifically to the basin in question?;
- Does at least one of the proxy records explicitly examine river discharge?;
- Are there multiple proxy records giving the same signal of palaeodischarge?

In principle, where all three of the criteria were met we classed the proxy quality as *good*, where two or more were met as *reasonable*, and otherwise *low*. Thereafter we developed and applied two tests to assess the level of agreement between the modelled and proxy discharge data. Agreement was said to be *good* when both of these tests were passed, *reasonable* when one was passed, and *low* when neither was passed:

Mean Test: This test examines whether the relative change between modelled mean annual discharge in the RT time-slice and the palaeo time-slices is in agreement with the direction of change inferred from the proxy data. Where the proxy data suggest a relative increase or decrease in discharge in relation to the

RT time-slice, the modelled data are in agreement when the latter indicate the same direction of change. For those basins for which the proxy data suggest that palaeodischarge was similar to the RT time-slice, we define similar in the modelled discharge as a relative change between the RT and palaeo time-slices of less than 10%.

Variability test: This test assesses whether the relative change of modelled mean annual palaeodischarge in relation to that of the RT time-slice falls outside the variability around the mean of the latter, and if so whether this change is in agreement with the proxy data. Firstly we calculated whether the modelled mean palaeodischarge fell within or outside 2 standard deviations (2σ) of RT 10-yearly mean annual discharge. We used a 10-yr mean due to the high degree of interannual variability in river discharge. In palaeoclimatic studies it is common to use 30-year means for such assessments, but this was not appropriate here given the relatively short span of the RT time-slice (250 years). Where the proxy data infer a relative increase or decrease of palaeodischarge compared to RT, agreement was conferred where the mean monthly modelled palaeodischarge fell outside 2σ of mean monthly RT modelled discharge. Where the proxy data infer palaeodischarge similar to that of the RT time-slice, agreement was conferred where the mean monthly palaeodischarge fell within 2σ of the mean monthly RT discharge.

2.3 Results

The modelled mean monthly discharges for each basin for the RT time-slice are shown in Table 2.2 (pg. 48). For the EH and MH, modelled discharges are given as percentage changes relative to RT discharge. Similarly, palaeodischarges inferred from the proxy data are indicated as relative changes in direction compared to the RT time-slice (+ / = / -). The specific proxy data used in the model-proxy comparison are discussed in Section 2.4.1. The use of either '+ +' or '- -' indicates that the relative magnitude of change in the EH is greater than that in the MH, according to the proxy data. In the first column of Table 2.2, the basins are grouped according to the quality of the proxy data (*good*, *reasonable*, or *low*). No clear signal was observed for the EH Sacramento-San Joaquin since the proxy records give contradictory evidence. Proxy-model agreement according to the *mean test* is indicated in Table 2.2 by the symbol †, whilst agreement according to the *variability test* is indicated by the symbol *. The *variability test* has not been applied to the Syr Darya, Murray-Darling, or Mekong, since their mean monthly discharges are not normally distributed.

In total, 73% of the palaeodischarge simulations were in *good* agreement with the proxy data, and 89% were in at least *reasonable* agreement. For the basins for which *good* proxy data were available, 77% of the runs simulated discharge in *good* agreement with the proxy data, and all of the runs simulated discharge in *good* or *reasonable* agreement. If we combine the basins for which *good* and *reasonable* proxy data were available, then 72% of the simulated palaeodischarge runs were

in *good* agreement with the proxy data, and 92% were in *good* or *reasonable* agreement.

The proxy records also suggest that the relative magnitude of mean annual discharge was greater in the EH than in the MH for five of the rivers studied: Congo, Ganges, Mekong, Nile, and Volta. For all of these rivers our model simulates lower mean annual discharge in the MH compared to the EH. Hence, the model not only simulates well the relative changes in discharge magnitude between the present day and the palaeo time-slices, but also the relative changes of discharge magnitude between the two palaeo time-slices studied.

2.4 Discussion

2.4.1 Zonal assessment of model and proxy data

For the Holocene time-slices, orbitally-induced variations in insolation are the dominant forcing mechanisms of long-term climatic variability (Kutzbach and Street-Perrot, 1985; Renssen et al., 2005a,b); these variations differ according to both season and latitude. In the Northern Hemisphere (NH), the seasonal contrast in insolation was greater during both the EH and MH than in the RT time-slice. In the NH, more insolation was received during the summer than today in the EH (between +25 and +45 W m^{-2}), and to a lesser extent in the MH (between +10 and +25 W m^{-2}). During the winter, less insolation was received in the NH than today in the EH (0 to -25 W m^{-2}) and the MH (0 to -15 W m^{-2}). For the Southern Hemisphere (SH) the seasonal contrast was smaller in the EH and MH than in the NH (Berger, 1978). Substantial alterations in land cover can significantly affect the discharge regimes of rivers (Andréassian, 2004; Calder, 1993). With respect to land cover changes in our study, VECODE only simulates small land cover anomalies over the time-slices studied, except for in the Krishna, Nile, and Syr Darya basins during the EH, and the Nile basin during the MH, when the crop factors were more than 5% greater compared to those of the RT time-slice. Therefore, the effects of land cover change on simulated discharge will be small for the majority of the basins. If climate is a major driving force of hydrological systems (Knox, 2000), one would expect to see a response to these orbital forcings in the palaeodischarge results. Hence, we present a zonal assessment of the trends indicated by the model and proxy data.

When proxy data are discussed, dates are given using the system found in the original citation, i.e. either cal. yrs. or ^{14}C yrs. are used depending on the system used in the original literature. To simplify comparison between the time-slices, approximate conversions of key dates are shown below, calculated using CalPal Online (http://www.calpal-online.de).

- EH 9000-8650 cal. yr. BP 8100-7850 ^{14}C yr. BP
- MH 6200-5850 cal. yr. BP 5400-5100 ^{14}C yr. BP

Basin	Recent (RT)		Mid Holocene (MH)			Early Holocene (EH)		
Proxy Data Quality	Modelled mean annual discharge ($m^3 s^{-1}$)	2σ of 10-yr mean discharge (%)	Modelled discharge (% change on recent)	Proxy + / = / -	Agreement	Modelled discharge (% change on recent)	Proxy + / = / -	Agreement
Good								
Amazon	152,517	3.5	-0.7 †	-	**Reasonable**	-2.4 †	-	**Reasonable**
Ganges	10,528	8.4	+7.2 † *	= / +	**Good**	+30.2 † *	+ +	**Good**
Congo	36,589	7.1	+11.7 † *	+	**Good**	+12.1 † *	+ +	**Good**
Nile	2554	9.5	+10.9 †*	+	**Good**	+22.1 † *	+ +	**Good**
Sacramento-San Joaquin	658	33.8	-1.0 † *	=	**Good**	+9.1	?	**N/A**
Danube	6557	19.4	+8.1 † *	=	**Good**	+12.5 *	=	**Reasonable**
Lena	16,714	7.6	-0.5 † *	=	**Good**	-3.4 † *	=	**Good**
Reasonable								
Krishna	1714	18.4	+7.8 †	+	**Reasonable**	+26.4 † *	+	**Good**
Volta	1248	13.1	+48.3 † *	+	**Good**	+73.3 † *	+ +	**Good**
Oder	527	15.7	+1.7 † *	=	**Good**	-0.6 † *	=	**Good**
Mississippi	15,617	29.8	+3.1 †	+	**Reasonable**	+5.7	-	**Poor**
Syr Darya	547	N/A	+19.6 †	+	**Good**[1]	+58.0 †	+	**Good**[1]
Mackenzie	8928	9.9	-3.8 † *	=	**Good**	-14.5	+	**Poor**
Low								
Mekong	732	N/A	+12.8 †	+	**Good**[1]	+34.8 †	+ +	**Good**[1]
Zambezi	445	31.4	-44.8	+	**Poor**	-60.7	+	**Poor**
Murray-Darling	221	N/A	+3.5 †	+	**Good**[1]	-20.2 †	-	**Good**[1]
Rhine	2239	8.2	0 † *	=	**Good**	+0.6 † *	=	**Good**
Meuse	319	8.1	+2.6 † *	=	**Good**	+4.5 † *	=	**Good**
Volga	7929	10.3	+8.0 † *	=	**Good**	+6.2 †	+	**Reasonable**

*Table 2.2 (opposite): Comparison of modelled discharge and discharge implied from the proxy data. In the left-hand column the basins are subdivided according to the quality of the proxy data (**good**, **reasonable**, or **low**). The Mid Holocene (MH) and Early Holocene (EH) modelled discharges are expressed as percentage changes in relation to the Recent (RT) time-slice. The proxy data infer a relative change in direction in relation to the RT time-slice. † indicates that the model and proxy data are in agreement according to the mean test; * indicates that the model and proxy data are in agreement according to the variability test. Proxy and model agreement is said to be **good** when both of these tests are passed, **reasonable** when one of the tests is passed, and **poor** when neither is passed. [1] The variability test has not been applied to the Syr Darya, Murray-Darling, or Mekong, since their mean monthly discharge frequencies are not normally distributed. The degree of agreement has been established on the basis of the mean test only (pass = **good** / fail = **poor**).*

2.4.1.1 (Sub)-Tropics

In southern Asia, numerous palaeoclimatic studies record an Asian summer precipitation peak between ca. 9.5-5.5 ^{14}C ka. BP (see Kale et al., 2003), followed by a gradual decrease until present (Overpeck et al., 1996). Regional palaeohydrological reconstructions suggest increased discharges in the EH in response to the strengthened monsoon (Kale et al., 2003). Goodbred and Kuehl (2000) state that the identification of an immense sediment flux to the floodplains and delta plains of the **Ganges** between ca. 11.0-7.0 cal. ka. BP, combined with evidence of floodplain downcutting in two upstream tributaries (Williams and Clarke, 1984), imply that Ganges discharge was much higher in the EH than at present. During the MH, sedimentation rates to the floodplain and delta plain of the Ganges were falling rapidly, but remained higher than in the RT period (Goodbred and Kuehl, 2000). Assuming similar vegetation in the MH and RT time-slices, as suggested by pollen analysis of a peat profile from the Garhwal Himalaya (Phadtare, 2000), this suggests that discharge in the MH was similar to, or slightly higher than, discharge in the RT period. For the **Krishna**, radiocarbon-dated fluvial deposits provide strong evidence of increased incision and terrace formation between ca. 10.0-4.5 ^{14}C ka. BP (Kale and Rajaguru, 1987); the authors relate this to a period of increased river discharge. An investigation of δ^{18}O fluctuations in a sediment core from the South China Sea found a freshwater plume from the Pearl River, representing a runoff extreme that persisted from the early Holocene until ca. 8.3 cal. ka. BP, after which time a salinity maximum ensued (Wang et al., 1999a). This suggests that the EH increase in monsoon precipitation extended to the east of the **Mekong** basin. Furthermore, a multi-proxy analysis of three sediment cores from the western and southern regions of the South China Sea shows a distinct δ^{18}O freshwater signal during the EH, which Wang et al. (1999b) tentatively link to enhanced Mekong discharge.

Proxy records for (sub)-tropical African rivers affected by monsoonal circulation (Congo, Nile, Volta) also suggest a gradual decrease of discharge from an EH peak towards RT. Such a signal is seen in the δ^{18}O compositions of planktonic

foraminifera in **Congo** River Fan sediment cores (Giresse and Lanfranchi, 1984; Preuss, 1990; Uliana et al., 2002). Wirrmann et al. (2001) reconstructed regional environmental conditions based on an analysis of the mineral composition of Lake Ossa sediments (Cameroon), and found evidence of both decreasing discharge and precipitation since at least 5.4 cal. ka. BP. A sapropel unit (ca. 9.0-7.0 cal. ka. BP) in a cyclothem from the eastern Mediterranean reflects a significant increase in the input of less saline water from sources including the **Nile** (Adamson et al., 1980). Stanley (1978) attributes an isotopic change in the same period in core GA32 to an increase in both temperature and freshwater influx. The presence of a calcareous unit (ca. 3.0-0 cal. ka. BP) in the same cyclothem (Adamson et al., 1980) implies aridity in the Nile basin at that time (Stanley and Maldonado, 1977). The $^{87}Sr/^{86}Sr$ ratio of sediments at Manzal Lagoon in the Nile Delta (Krom et al., 2002) suggests that discharge in the MH was higher than in the RT period, but lower than in the EH. Evidence of flooding, and the development of palustrine areas close to the Blue Nile riverbed prior to ca. 8.0 ^{14}C ka. BP, indicates humid conditions and high discharge. Stager et al. (1997) used diatom assemblages to reconstruct Holocene lake level stands of Lake Victoria, regional humidity and, to a certain degree, White Nile discharge. Lake levels were high between ca. 11.4-7.9 cal. ka. BP, and became lower thereafter, culminating in the onset of arid conditions after ca. 2.3 cal. ka. BP. For the EH, Owen et al. (1982) obtained similar results for Lake Turkana, ca. 400 km to the north. No palaeodischarge data specific to the **Volta** were identified, and therefore regional proxy data have been used. Talbot and Delibrias (1980), Talbot and Johannessen (1992), and Talbot et al. (1984) reconstructed palaeo-humidity from sediment cores in Lake Bosumtwi, Ghana, and found that the lake was consistently higher during the EH and MH than in the RT time-slice. An examination of diamondiferous sediments on the Birim River floodplain in Ghana suggests that discharge was high between ca. 9.0-7.5 ^{14}C ka. BP (EH), and somewhat lower thereafter (Hall et al., 1985). Reconstructions based on $\delta^{18}O$ fluctuations in the mouth of the Niger suggest that Niger discharge was also significantly higher in the EH and MH than today (Giresse et al., 1982, cited in Preuss, 1990).

For all of the rivers discussed above, agreement was conferred between proxy and model data; monsoonal climatic and hydrological conditions appear to be well simulated. Noteworthy increases in the crop factors derived from VECODE occurred for the Nile (EH and MH) and Krishna (EH), meaning that the land cover enhanced the potential for evapotranspiration during this period. However, given the large discharge increases in the EH and MH, the increased potential for evapotranspiration (and concomitant decrease in mean discharge) does not appear to have had a dominant influence on discharge. Most of the tropical monsoon basins show slightly higher crop factors during the EH and MH compared to RT, related to greater forest cover. This may have amplified the increase in monsoonal intensity by lowering surface albedo, and consequently enhancing the preferential heating of the continents (Aerts et al., 2006; Kutzbach and Street-Perrot, 1985; Renssen et al., 2005a; Roberts, 2002).

The **Zambezi** lies in an area between two distinct climatic regimes: a generally wet monsoonal climate to the north, and a dry climate to the south. Lakes in tropical eastern Africa were generally higher than present during the MH, and even higher in the EH (Jolly et al., 1998). We infer that this period was wetter than the RT time-slice. A significant increase in mangrove pollen in a core from the Mozambique Channel at ca. 9.0 ^{14}C ka. BP suggests an increase in continental runoff and, more specifically, wetter conditions in the Zambezi Basin. However, the model simulates very large decreases in discharge during both the MH and EH. This discrepancy may be a result of the quasi-geostrophic nature of ECBilt-CLIO-VECODE, which causes a relatively poor simulation of some tropical climates. Furthermore, since the Zambezi lies in an area surrounded by two distinct and different climatic zones, the coarse resolution of ECBilt-CLIO-VECODE may poorly resolve such abrupt geographical changes in climatic regimes.

A continuous reconstruction of **Amazon** Holocene discharge, based on the δ^{18}O composition of planktonic foraminifera in sediment cores from the Amazon fan, suggests that annual discharge in the EH was ca. 93% of RT discharge, and in the MH ca. 90% of RT discharge (Maslin and Burns, 2000). Records of δ^{18}O changes in Lake Junin (Peru) suggest a similar pattern (Seltzer et al., 2000). Van der Hammen et al. (1992) interpret periods of peat layer extension in the EH and MH on the floodplain of the Caquetá basin as periods when river discharge and flood frequency were (slightly) lower than today. Slightly lower simulated discharges for the EH (-2.4%) and MH (-0.7%) are in agreement with these findings, and can be related to fluctuations of insolation at 10°S during the SH summer. This was at a peak in the RT time-slice, almost at a Holocene low during the EH, and between these two values in the MH (Maslin and Burns, 2000). Hence, the RT period is characterised by more intense summer convection over the Amazon basin, resulting in a southward penetration of the Intertropical Convergence Zone (ITCZ), drawing in moist air from the Atlantic Ocean which is deposited over the Amazon Basin as precipitation. During periods of lower insolation at 10°S, atmospheric circulation is thought to be more zonal, preventing the summer penetration of the ITCZ over the Amazon, leading to reduced summer precipitation (Maslin and Burns, 2000). The precipitation anomaly between the time-slices in the ECBilt-CLIO-VECODE data is indeed greatest during the SH summer, lending support to insolation changes as the main causal mechanism.

2.4.1.2 Northern hemisphere mid-latitudes

At NH mid-latitudes the annual distribution of precipitation is more even than at low latitudes, and hence the impact of the positive summer insolation anomaly during the EH and MH on discharge should be smaller, since it is partially offset by the negative insolation anomaly in the winter (Aerts et al., 2006). This inference appears to hold true for European mid-latitude basins with (varying degrees of) maritime influence (Meuse, Rhine, Oder, Danube); proxy data for all of these basins infer similar discharges in the time-slices studied. Rotnicki (1991) applied standard steady uniform flow formulae (*ibid*, p. 439) to the geometric

characteristics of meandering palaeochannels of the Prosna River (a tributary of the **Oder** via the Warta in Poland), and found that discharges in the EH and MH were broadly similar to those in the RT time-slice. Howard et al. (2004) found no evidence of higher or lower discharge than today during the EH or MH in alluvial terrace sequences in the Teleorman Valley, a major **Danube** tributary. Becker and Schirmer (1977) found no periods of major Rannen deposition (subfossilised oak trunk layers) on the Danube or the Main (a **Rhine** tributary) for the three time-slices studied, which may suggest similar discharges. It should be noted that the Main is a pluvial tributary, and therefore its pattern of discharge variation does not necessarily reflect that of the Rhine, which is partly snowmelt fed and partly pluvial (Kwadijk, 1991). Bohncke and Vandenberghe (1991) used palaeobotanical evidence and beetle remains to derive data on Holocene temperature, precipitation, and evapotranspiration in the Mark basin (southern Netherlands), close to the **Meuse** basin. Using these derived variables, discharge estimates were made for the period 14.0-0.5 ^{14}C ka. BP, suggesting that discharge was similar in the EH to the MH. Similar hydrological conditions in northern Belgium during the three time-slices are inferred from palaeobotanical data in combination with data on channel pattern and depositional processes (Vandenberghe et al., 1984). For these basins the simulation results also suggest similar discharges throughout the Holocene, except for the Danube in the EH, where an increase of 12.5% was modelled compared to RT. For the latter basin our model simulated relatively high precipitation depths in the late summer during the EH and MH, perhaps related to the insolation-driven increase in precipitation seasonality as maritime influence diminishes.

In the Eurasian mid-latitude continental basins (Volga, Syr Darya), marked precipitation seasonality exists, and hence the influence of the EH and MH positive summer insolation anomaly assumes a greater importance. Sedimentary records from the **Syr Darya** and Aral Sea suggest relatively low discharge prior to 10.0 cal. ka. BP, with a marked increase from ca. 9.0 cal. ka. BP. Discharge decreased greatly again from ca. 3.5 cal. ka. BP as the climate became drier (Boomer et al., 2000). Climate models estimate that the total annual discharge of all rivers to the Aral Sea in the EH and MH was 153.4 km^3 (Mamedov and Trofimov, 1986), compared to ca. 120 km^3 today (Boomer et al., 2000). Time-continuous data on **Volga** Holocene discharge are not available (Overeem et al., 2003). However, since sea surface temperatures in the Barents Sea have been found to significantly predict long-term variations in CSL (Rodionov, 1994), and there is a strong feedback between Volga discharge and CSL, temperature changes inferred from the δ^{18}O composition of the Greenland Ice Sheet Project 2 (GISP) core have been used to force Volga Holocene discharge (Overeem et al., 2003, based on the work of Tebbens et al., 2000). These simulations suggest that relative to the RT time-slice, EH discharge was higher and MH discharge was similar. These trends are reproduced by our model, and the relative increase in simulated Holocene discharge for the Syr Darya is larger than that for the Volga, again reflecting the increasing influence of the summer insolation anomaly on

discharge with increasing continentality. The increased crop factor of the EH in the Volga basin does not appear to have had a major influence on the discharge regime.

For the mid-latitude North American basins, model-proxy comparison is more complicated. For the MH period, studies of palaeochannel dimensions and particle size analyses of relict flood gravels on a number of Upper **Mississippi** Valley (UMV) tributaries suggest that 1-2 year flood events were larger in the MH than during the RT time-slice (Knox, 1985, 2000). Similar results were obtained by Knox (1985), based on changes in the vertical thickness of point bar sediments. The model simulates the occurrence of very high flows more often in the MH than in the RT time-slice (Fig. 2.5). Therefore, as well as simulating the mean discharge trend in agreement with proxy records, the model has simulated changes in flood frequency during the MH, adding confidence to its retrodictive capabilities. For the EH the same palaeoflood indicators were used to infer reduced discharges of the Mississippi; this is not reflected in the simulation results. The flooding characteristics of the UMV tend to show a strong correlation with continental scale shifts in tropospheric circulation. When the prevailing tropospheric circulation favours strong north-westerly or westerly airflows across the UMV region, air masses of high water-vapour content from the tropics are blocked from reaching the area and large floods are rare (Knox, 2003); this could be the mechanism responsible for reduced floods in the EH. Since ECBilt-CLIO-VECODE simulates some tropical climates relatively poorly, such weather patterns are not well resolved, and this may explain the lack of agreement during the EH. Another explanation is related to the presence of the Laurentide ice sheet in North America during the EH (Knox, 1983, 2000). This would have had a large effect on continental, regional, and local weather patterns in the Upper Mississippi region. As the Laurentide ice sheet is neither modelled by ECBilt-CLIO-VECODE nor STREAM, its effects are not recorded in the simulated discharge results.

Using salinity indicators in sediment cores from the San Francisco Bay estuary, Goman and Wells (2000) found that the discharge of the **Sacramento-San Joaquin** system was broadly comparable to today during the MH. Similar results were obtained by Ingram et al. (1996) based on the $\delta^{18}O$ and $\delta^{13}C$ compositions of fossil molluscs. This also suggests a reduced effect of insolation anomalies on discharge in these latitudes. For the EH, no specific palaeodischarge studies were identified and regional palaeoclimatological reconstructions give greatly different results for sub-regions within the basin (Adam et al., 1981; Davis, 1999; Heusser, 1978; Koehler and Scott Anderson, 1994). Hence, no trend could be identified for the Sacramento-San Joaquin during the EH, and model-proxy comparison was not possible.

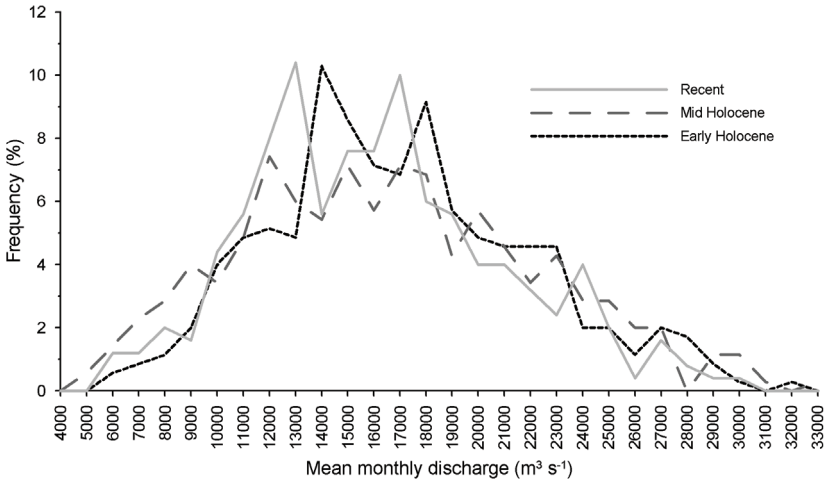

Fig. 2.5: Modelled mean monthly discharge ($m^3 s^{-1}$) frequency distributions for the Mississippi during the Early Holocene, Mid Holocene, and Recent time-slices.

2.4.1.3 Southern hemisphere mid-latitudes

Lake levels in the interior of south-eastern Australia were lower than present during the EH (Harrison and Dodson, 1993). Sediments from Lake Keilambete suggest that the lake was almost dry shortly prior to 10.0 cal. ka. BP, but that its level rose slightly between 10.0-8.0 cal. ka. BP. After ca. 8.0 cal. ka. BP the lake level rose rapidly, and a period of possible overflowing ensued between ca. 6.5-5.5 cal. ka. BP (Bowler, 1981); the simulation results for the **Murray-Darling** agree with these trends. Insolation anomalies during the main rainy season (September to November) were positive for both the EH and MH, and modelled precipitation in this season is higher than RT for both the EH and MH; this is counterintuitive to the discharge results. However, during the SH mid-summer, the insolation anomaly was negative during the Holocene, with a stronger negative signal and lower precipitation for the EH compared to the MH (Berger, 1978). We speculate that this combination of insolation anomalies could explain the changes in discharge trends in the model and proxy records; further research of other time-slices would be necessary to confirm this.

2.4.1.4 Periglacial regions

In response to the NH summer insolation maximum, the EH (and to a lesser extent MH) was relatively warm and wet at northern high latitudes, especially during the summer (Renssen et al., 2005a). In the **Lena** basin these changes have had little impact on mean annual discharge according to both the model and proxy data. Maceral analysis of two Laptev Sea sediment cores suggests that the magnitude of river discharge to the sea remained similar throughout the Holocene (Boucsein et al., 2000). A detailed Holocene environmental reconstruction of the Lena Delta area based on multi-proxy records from Nikolay Lake and a nearby peat sequence

shows no evidence of significant hydrological changes during the time-slices studied (Andreev et al., 2004). A regional review of river channel morphology in East Siberia states that there are no channel morphological indications of large-scale changes in Holocene discharge comparable to those registered for West Siberia and the Russian Plain (Sidorchuk et al., 2003). The ECBilt-CLIO-VECODE climate data for the Lena indicate that whilst summer precipitation was higher in the EH and MH, so too was temperature (and hence evapotranspiration); changes in temperature and precipitation appear to have had a compensatory effect on discharge.

Based on an investigation of the marine mollusc record for glaciated North America and Greenland, Dyke et al. (1996) suggest that large quantities of Laurentide meltwater were still entering the **Mackenzie** during the EH. During this time-slice the Laurentide ice sheet was still in wastage (Dyke and Prest, 1987; Knox, 1983, 2000). Given that the Laurentide ice sheet is neither modelled in the climate model nor the hydrological model, the simulated discharge for the EH was too low, since the huge meltwater component was ignored. The ice sheet would also have affected Mackenzie discharge through its effects on continental, regional, and local weather patterns. According to Maizels' (1995) model of palaeodischarge in polar regions, the discharge of the Mackenzie would have been similar in magnitude to present during the MH, in agreement with the simulation results.

2.4.2 Holocene insolation anomalies and zonal discharge trends

Clear latitudinal patterns of changes in discharge trends have been identified. An examination of the basins studied shows that these changes can be related to latitudinal and seasonal differences in insolation anomalies over the Holocene. The greatest effect is seen in the (sub)-tropical monsoon basins, where higher summer insolation during the EH (and to a lesser extent MH) caused large increases in summer precipitation and discharge. In mid-latitudes the discharge response to variations in insolation are generally less extreme, especially in maritime climates. In northern high latitudes, increased summer precipitation during the EH and MH seems to have been compensated by higher temperatures (and therefore evapotranspiration) during those periods.

In a sensitivity study of 15 rivers, using the same model as described here, Aerts et al. (2006) compared simulated discharge trends of the last 9000 years with simulated trends for the coming century. For most of the rivers studied, the change in mean simulated discharge during the next 100 years compared to present was greater than, or similar to, the change in simulated mean discharge over the last 9000 years. For the coming century, Aerts et al. (2006) suggest that increased atmospheric greenhouse gas concentrations will replace orbitally-induced insolation variations as the dominant forcing mechanism of changes in global river discharge.

2.4.3 Recommendations and applications

Since the model performs well in the majority of the basins for the time-slices studied, it is now possible to apply the approach in an operational sense. The coupled climate-hydrological model can be used to build up references of palaeodischarge over a large range of Holocene climates, or to simulate discharge under future climate change and/or land use scenarios. For water management, one of the most important uses of hydrological models is in peak flow (flood) prediction. In this study the aim was to assess the model's ability to simulate mean discharge, and not specifically flood events. To make predictions of flood magnitude and frequency, modelling should take place at a higher temporal resolution. Nevertheless, the results for the Mississippi give some indication that the current model already appears to simulate changes in flood magnitude and frequency. Furthermore, when using the model to assess flood and low-flow frequencies, a higher spatial resolution should be used, since daily discharge is influenced by the geographical position at which precipitation falls within a basin. The forcing parameters that were used in the climate model effect long-term (millennial) climatic fluctuations. When looking at shorter term discharge fluctuations, other forcing mechanisms should be included, especially solar activity and volcanic aerosol content. In this study, Holocene land cover changes were based on the results of VECODE, which only simulates natural changes in vegetation in response to climatic change. For more detailed discharge assessments at the individual basin level, data on anthropogenic land use changes should be included (e.g. from historical, archaeological, or palynological records).

The absence of the Laurentide ice sheet in our model means that the simulated discharges of North American rivers during the EH are poor. In any future application of the palaeodischarge modelling approach to North American basins it is imperative that the Laurentide ice sheet be included when considering the EH.

2.5 Conclusions

Given the level of agreement between simulated palaeodischarge and palaeodischarge as implied by the proxy records, we conclude that our coupled climate-hydrological model performs well in modelling mean annual discharge over the EH and MH time-slices. On a global scale, orbitally induced variations in insolation are the dominant mechanism responsible for discharge changes in the time-slices studied. Furthermore, the effects of these insolation variations on discharge vary according to latitude, intuitively following latitudinal and seasonal insolation anomalies. In the coming century, increased greenhouse gas concentrations are expected to replace orbitally-induced variations in insolation as the dominant forcing mechanism of global river discharges.

Verification of palaeodischarge models can be carried out for rivers where basin-specific assessments of palaeodischarge exist. For a number of the basins studied here this was not the case. Nevertheless, for those basins for which we

identified *good* or *reasonable* palaeodischarge proxy data, some 72% of the runs were in *good* agreement with the proxy data, and 92% of the runs were in at least *reasonable* agreement. Furthermore, our model was able to simulate relative changes in the magnitude of palaeodischarge between the EH and MH. For those basins for which the model performed well over all three time-slices, considerable confidence is added to the model's skill compared to hydrological models validated only against the period of instrumental records.

Chapter 3

Strong increases in flood frequency and discharge of the River Meuse over the late Holocene: impacts of long-term anthropogenic land use change and climate variability

Abstract

In recent years the frequency of high-flow events on the Meuse (northwest Europe) has been relatively great, and flooding has become a major research theme. To date, research has focused on observed discharge records of the last century and simulations of the coming century. However, it is difficult to delineate changes caused by human activities (land use change, and greenhouse gas and sulphate aerosol emissions) and natural fluctuations on these timescales. To address this problem we coupled a climate model (ECBilt-CLIO-VECODE) and a hydrological model (STREAM) to simulate daily Meuse discharge in two time-slices: 4000-3000 BP (natural situation), and 1000-2000 AD (includes anthropogenic influence). For 4000-3000 BP the basin was assumed to be almost fully forested; for 1000-2000 AD we reconstructed land use based on historical sources. For 1000-2000 AD the simulated mean annual discharge (260.9 $m^3 s^{-1}$) is significantly higher than for 4000-3000 BP (244.8 $m^3 s^{-1}$), and the frequency of large high-flow events (discharge > 3000 $m^3 s^{-1}$) is higher (recurrence time decreases from 77 to 65 years). On a millennial timescale almost all of this increase can be ascribed to land use changes (especially deforestation); the effects of climatic change are insignificant. For the 20th Century, the simulated mean discharge (270.0 $m^3 s^{-1}$) is higher than in any other century studied, and is ca. 2.5% higher than in the 19th Century (despite an increase in evapotranspiration). Furthermore, the recurrence time of large high-flow events is almost twice as short as under natural conditions (recurrence time decreases from 77 to 40 years). On this timescale climate change (strong increase in annual and winter precipitation) overwhelmed land use change as the dominant forcing mechanism.

This chapter is based on the paper: Ward, P.J., Renssen, H., Aerts, J.C.J.H., Van Balen, R.T., Vandenberghe, J., 2008. Strong increases in flood frequency and discharge of the River Meuse over the late Holocene: impacts of long-term anthropogenic land use change and climate variability. Hydrology and Earth System Sciences, 12, 159-175, www.hydrol-earth-syst-sci.net/12/159/2008/.

3.1 Introduction

In recent years the frequency of high-flow events in the Meuse basin (northwest Europe) (Fig. 3.1) has been relatively great compared to the rest of the 20th Century. As a result, flooding and flood mitigation have become major research themes. Hence, numerous studies have been carried out to examine hydrological and climatological changes in the basin.

Observed discharge time-series for the Meuse at Borgharen (Fig. 3.1) show no significant changes in annual or monthly mean discharge over the 20th Century (Tu, 2006). However, increasing trends (albeit statistically insignificant) are detected for annual and winter maximum daily discharge (De Wit et al., 2001). Furthermore, change-point analyses suggest significant increases in annual and winter maximum daily discharge around 1984 (Pfister et al., 2000; Tu, 2006). Similar results are found for numerous Meuse tributaries (Tu, 2006). This increase in the frequency of high-flow events may be related to an increase in annual precipitation totals and the frequency of very wet days in the winter since 1980, due to the fluctuation of large-scale atmospheric circulation (Bouwer et al., 2006) and a strengthened North Atlantic Oscillation (Tu, 2006). Increased precipitation totals and intensity in the second half of the 20th Century, related to variations in atmospheric circulation, have been observed in the Netherlands and Luxembourg (Pfister et al., 2000), and Ntegeka and Willems (2008) found that extreme precipitation became more intense in the winter and spring during the 1990s, based on a statistical examination of 10-minute rainfall intensities at Ukkel (Belgium).

Climate modelling results suggest that average temperatures and winter precipitation depths in the Meuse basin will increase in the 21st Century, whilst summer precipitation will decrease (De Wit et al., 2007a; Kwadijk and Rotmans, 1995; Pfister et al., 2004; Van Deursen, 2000). Based on hydrological modelling, De Wit et al. (2001) suggest that mean annual discharge will remain relatively stable over the 21st Century, whilst Booij (2005) suggests a slight decrease. The seasonal distribution of discharge may change so that winter discharge becomes greater and summer discharge lower (De Wit et al., 2007a). These and other studies, however, suggest that the anticipated climate change of the 21st Century will lead to an increase in flood frequency (Bultot et al., 1988; Gellens and Roulin, 1998; Middelkoop and Parmet, 1998; Van Deursen, 2000).

Discharge, however, depends not only on climate but also on land use. Little research has been carried out to examine the effects of land use change in the basin because the forested area has remained relatively stable at the basin scale over the last century (Knol et al., 2004; Tu, 2006). Ashagrie et al. (2006) and Tu (2006) found no evidence to suggest that land use changes in the 20th Century have had a significant effect on Meuse discharge.

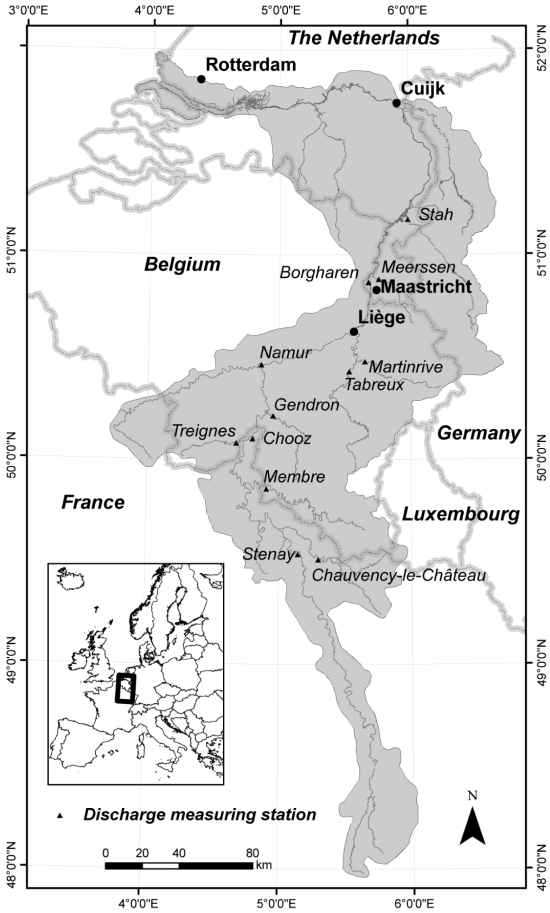

Fig. 3.1: Map showing the location of the Meuse Basin and discharge measuring stations used in this study (after RWS Limburg/IWACO, 2000). The basin has an area of ca. 33,000 km^2, and covers parts of France, Luxembourg, Belgium, Germany, and the Netherlands. The inset shows the location of the Meuse basin in Europe. For this study the model was set up for the area upstream from Borgharen.

The aforementioned studies have examined either the observed discharge record of the last century, or used hydrological models calibrated against observations for that period. However, when studying long-term discharge changes this approach is problematic. Firstly, accurate daily measurements of Meuse discharge have only been made since 1911, which is too short to evaluate long-term climatic changes (Jones, 2000). Secondly, at a basin scale the forested area has been relatively stable over the last century, making it difficult to assess the effects of large-scale changes in land use.

Palaeodischarge modelling provides a means to address the lack of long-term observed data by providing a dataset for the validation of model response on

millennial timescales. This enables us to simulate the response of discharge to changes in climate over longer timescales, and to more extensive changes in land use. However, palaeodischarge modelling is in its infancy. For example, Coe and Harrison (2002) used runoff derived directly from a General Circulation Model (GCM), combined with a river routing algorithm, to simulate lake-level changes in Africa at ca. 6 ka BP. At the basin scale, however, the use of runoff derived directly from GCMs has a disadvantage as runoff output are less well resolved than climatic output. To address this problem, Aerts et al. (2006) and Ward et al. (2007; Chapter 2) coupled a climate model and a hydrological model to simulate the Holocene discharge of rivers around the globe on a monthly time-step; the modelled discharges correspond well with multi-proxy records of palaeodischarge.

The aim of this paper is to examine the sensitivity of Meuse discharge to long-term changes in Holocene climate and land use. This is achieved using the modelling approach of Ward et al. (2007; Chapter 2), but with a daily time-step and higher spatial resolution. Meuse discharge is simulated for two time-slices: 4000-3000 BP and 1000-2000 AD. The period 4000-3000 BP is selected as a natural reference period since the natural climatic forcings were broadly similar to those of today, whilst human influence on land use was minimal (Bunnik, 1995; Gotjé et al., 1990; RWS Limburg/IWACO, 2000). The period 1000-2000 AD was heavily influenced by human activities, namely changes in land use throughout the period, and greenhouse gas and sulphate aerosol emissions since the industrial revolution. By comparing the changes in discharge characteristics between these two situations we can examine the effects of anthropogenic changes in climate and land use.

3.2 Study area

The Meuse is a predominantly rain-fed river with a total length of ca. 875 km. For this study the basin has been modelled upstream from Borgharen (Fig. 3.1). The model was set up upstream from this point for a number of reasons. Firstly, discharge measurements at Borgharen, corrected for canal extractions between Liège and Borgharen, are available since 1911, which is the longest observed discharge time-series in the basin, and allows for model calibration and validation. Secondly, current water management practice in the Netherlands uses daily discharge observations at Borgharen in the estimation of flood return periods. Thirdly, we did not model the basin as far downstream as the current Rhine-Meuse confluence, since its location has changed over the course of the Holocene (Berendsen and Stouthamer, 2001).

Mean annual precipitation over the basin is ca. 950 mm a^{-1}, and is reasonably evenly distributed throughout the year. The spatial distribution of precipitation is to a large extent a reflection of elevation and distance from the coast. Mean temperatures show marked seasonal variations, and annual potential evapotranspiration is much greater in the summer half-year (May-October) than in the winter half-year (November-April) (76% and 24% of the total respectively) (Ashagrie et al., 2006).

The mean annual discharge of the Meuse and its associated canals at the border of Belgium and the Netherlands is ca. 276 $m^3 s^{-1}$; summer and winter half-year mean discharges are 146 $m^3 s^{-1}$ and 406 $m^3 s^{-1}$ respectively (Ashagrie et al., 2006).

3.3 Methods and approach

In this study we couple the climate model ECBilt-CLIO-VECODE (Brovkin et al., 2002; Goosse and Fichefet, 1999; Opsteegh et al., 1998) with the hydrological model STREAM (Aerts et al., 1999) to simulate Meuse palaeodischarge. The hydrological model is run with a daily time-step, and a spatial resolution of 2' x 2' (ca. 2.4 km x 3.7 km). In this section we present the main features of the model.

3.3.1 Models and climate forcing parameters

Traditionally the results of General Circulation Models (GCMs) have been widely employed in hydrological modelling: examples from northwest Europe include the studies of De Wit et al. (2001), Gellens and Roulin (1998), Middelkoop et al. (2001), Pilling and Jones (1999), and Sefton and Boorman (1997). However, since the resolution of these models is typically at least 2.5° x 2.5°, they are rather coarse for direct use in regional hydrological studies (Arnell et al., 1996; Bouwer et al., 2004; Kleinn et al., 2005; Wood et al., 2002, 2004). Hence, numerous recent studies have used the results of higher resolution regional circulation models (RCMs) to force hydrological models (e.g. De Wit et al., 2007a; Kleinn et al., 2005; Shabalova et al., 2003). However, the high computational cost of running GCMs and RCMs makes their use in hydrological studies on millennial timescales unfeasible. Therefore, in this study, ECBilt-CLIO-VECODE (Brovkin et al., 2002; Goosse and Fichefet, 1999; Opsteegh et al., 1998) is used, an Earth System Model of Intermediate Complexity (EMIC). EMICs include the majority of processes described in GCMs, but in a more reduced, or parameterised, form. This simpler nature allows their application to long-term climate simulations over periods of several thousands of years (Claussen et al., 2002).

ECBilt-CLIO-VECODE is a three-dimensional coupled climate model consisting of three components describing the atmosphere, ocean, and vegetation (Brovkin et al., 2002; Goosse and Fichefet, 1999; Opsteegh et al., 1998). The output used in this study are derived from a transient run, forced by annually varying orbital parameters and atmospheric greenhouse gas concentrations following Renssen et al. (2005a), and atmospheric volcanic aerosol content and fluctuations in solar activity following Goosse et al. (2005). The model was run in ensemble mode, with four ensemble members. Each ensemble member represents a single model run. The ensemble members are forced using the same climatic parameters, but with slightly different initial climatic conditions to account for the chaotic behaviour of the atmospheric system. Hence, the difference between the ensemble members gives an idea of the natural variability, whereas an ensemble mean can be used to evaluate long-term trends.

STREAM is a grid-based spatially distributed water balance model that describes the hydrological cycle of a drainage basin as a series of storage compartments and flows (Aerts et al., 1999). It is based on the RHINEFLOW model of Kwadijk (1993), and uses a raster GIS database to calculate the water balance of each grid cell per time-step. The water balance is calculated using the Thornthwaite (1948) equations for potential evapotranspiration and the Thornthwaite and Mather (1957) equations for actual evapotranspiration; these equations use temperature and precipitation as the major input parameters. For each time-step the model generates runoff, groundwater storage (shallow and deep), snow cover, and snow melt. The direction of water flow between cells is based on the steepest descent for the eight surrounding grid cells on a digital elevation model (DEM). The main flows and storage compartments used to calculate water availability per cell are shown in Fig. 3.2. In Appendix 1, a detailed discussion can be found of the considerations behind the selection of the STREAM model.

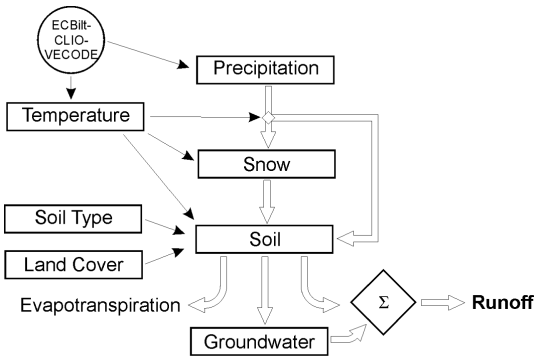

Fig. 3.2: Flowchart showing the main storage compartments and flows of the STREAM palaeodischarge model. STREAM is based on a raster GIS database and calculates the water balance of each grid cell per time-step using the Thornthwaite (1948) equations for potential evapotranspiration and the Thornthwaite and Mather (1957) equations for actual evapotranspiration. For each cell and time-step the model generates runoff, groundwater storage (shallow and deep), snow cover, and snow melt. The direction of water flow between cells is based on the steepest descent for the eight surrounding grid cells on a digital elevation model (DEM).

In this study, STREAM is run at a spatial resolution of 2' x 2'; this is high enough to capture the dominant processes in the basin (Booij, 2002), whilst pragmatic concerns regarding computational time render a higher resolution unfeasible (see Appendix 1). Since we will be running STREAM on a daily time-step, as opposed to the monthly or 10-day time-step used in previous applications, we have added a simple threshold-based direct runoff component to simulate infiltration excess overland flow. When precipitation exceeds a threshold (Ward and Robinson, 1990), excess precipitation runs off regardless of whether the soil is saturated. Runoff is routed through the river network on a daily basis using data on average flow velocities stated in Berger (1992) (see Ward, 2007a). The model was set up

for the catchment upstream from Borgharen (Fig. 3.1), using the USGS GTOPO30 DEM (http://edc.usgs.gov/products/elevation/gtopo30/gtopo30.html).

3.3.2 Input data

3.3.2.1 Climate data

The climate data (daily temperature and precipitation) derived from ECBilt-CLIO-VECODE have a spatial resolution of ca. 5.6° x 5.6°, and therefore need downscaling to the resolution of the STREAM model. The downscaling takes into account the spatial distribution of monthly averages, in accordance with Bouwer et al. (2004), using baseline observed monthly temperature and precipitation data for the period 1901-2000 from the CRU TS 1.2 dataset (Mitchell and Jones, 2005).

The downscaled mean monthly temperature and precipitation data for the period 1901-2000 show good agreement with observed values for all ensemble members (temperature, $r > 0.99$; precipitation, $r > 0.96$). The downscaled daily temperature data were validated against observed values for Maastricht, from the European Climate Assessment & Dataset (ECA&D) (http://eca.knmi.nl) (Klein Tank et al., 2002). The modelled daily temperature data show good agreement with the observations (Mann-Whitney U test (MWU), $\alpha = 0.05$). The number of precipitation-free days at Maastricht (model, 27.5%; observed, 45.7%) is underestimated; this is related to the fact that the original model grid cell represents an area of ca. 5.6° x 5.6°, whilst the observed data refer to a specific point. We found no significant difference between the frequency distributions of observed and simulated daily precipitation for very wet days (10% wettest days) (Kruskal-Wallis (KW) test, $\chi^2 = 1.691$, $p = 0.792$).

Simulated mean annual precipitation for 1000-2000 AD (895.93 mm a^{-1}) is slightly but statistically higher than for 4000-3000 BP (882.56 mm a^{-1}) (t-test, $p < 0.001$) (Fig. 3.3), though there is no statistical difference in variability (F-test, $p = 0.291$). However, whilst mean summer half-year precipitation for 1000-2000 AD (448.22 mm) is significantly higher than for 4000-3000 BP (424.37 mm) (t-test, $p < 0.001$), winter half-year precipitation is lower (1000-2000 AD, 447.71 mm a^{-1}; 4000-3000 BP, 458.19 mm a^{-1}; t-test, $p < 0.001$). The greatest precipitation increase is between July and September. Mean 50-yr precipitation shows neither a significant trend over the period 4000-3000 BP (MK-test, $p = -0.1048$) nor over the last millennium (MK-test, $p = -0.2176$). For the period 1000-2000 AD, mean annual and summer half-year temperatures (9.39°C and 14.66°C respectively) are significantly lower than for 4000-3000 BP (9.65°C and 15.24°C respectively) (t-test, $p < 0.001$). Over the course of the last millennium, mean, summer half-year, and winter half-year 50-yr temperatures show decreasing trends (MK-test, $p < 0.001$, $p < 0.001$, $p = 0.004$ respectively), although clear increases are simulated over the last 150 years (Fig. 3.3). The long-term cooling trend of the late Holocene can be attributed to the biogeophysical effects of deforestation in (northwestern) Europe (Brovkin et al., 2006; Goosse et al., 2006; Matthews et al., 2003). For the 20th Century, mean

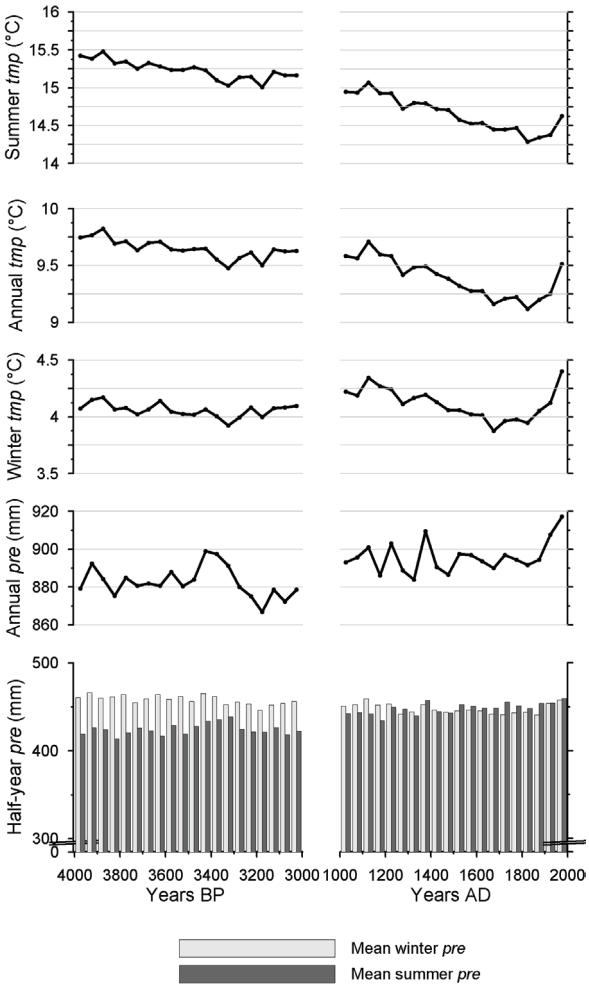

Fig. 3.3: Downscaled ECBilt-CLIO-VECODE climate data for the time-periods 4000-3000 BP and 1000-2000 AD. The means of the four ensemble members are shown for each 50-yr period. The bar charts show summer half-year (May-October) and winter half-year (November-April) precipitation (pre), whilst the lines show long-term changes in mean annual, summer half-year, and winter half-year temperature (tmp), and mean annual precipitation.

simulated annual precipitation is 912.40 mm a^{-1}, and temperature is 9.38°C; both show a relatively large increase in the second half of the 20th Century. Precipitation depths on very wet days (95th and 99th percentiles) are greater during 4000-3000 BP than 1000-2000 AD. Although these precipitation depths increased in the 20th Century compared to the rest of the last millennium, they are still lower than at 4000-3000 BP.

3.3.2.2 Land use data

A crop factor map is used in STREAM to calculate potential evapotranspiration (PE). The crop factor is a dimensionless factor by which the reference PE is multiplied in order to account for the difference in PE over different land use types. In this study we have developed a land use map for each century (Appendix 2). For the period 1000-2000 AD, the temporal pattern of basin-wide land use change is shown in Fig. 3.4. The land use classes have been simplified due to the relative scarcity of detailed historical land use data, and reclassed to crop factor maps based on values in Kwadijk (1993), and Aerts and Bouwer (2002): Urban (0.8); Forests (1.1); Agriculture & Grasslands (0.9); Wetlands (1.1); and Water Bodies (1.5).

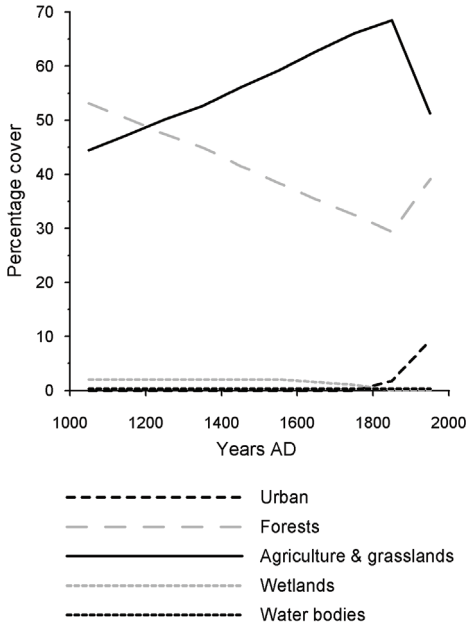

Fig. 3.4: Estimations of Meuse basin land use upstream from Borgharen during the period 1000-2000 AD. Forest cover fell from ca. 53% at the beginning of the last millennium to ca. 29% in the 19th Century, mainly at the expense of agricultural land. Between the 19th and 20th Centuries the percentage cover of forest and urban area increased at the expense of agricultural land.

For the 20th Century, we used the dataset CORINE Land Cover 2000 (CLC2000) 250m version 8/2005 (V2) (© EEA, Copenhagen, 2005), available at http://dataservice.eea.eu.int/dataservice/.

For the 19th Century, data on forest cover and urban area were based on historical census information for Belgium (WL, 1994b), and on historical maps for the Netherlands (Knol et al., 2004). Data on wetlands and peat bogs were based on

the works of Damblon (1992), Petit and Lambin (2002), and RWS Limburg/IWACO (2000). For the French subcatchments census data on forest cover were used, based on the work of Dutoo (1994). For the German and Luxembourg sections of the basin the relative proportions of each land use type were extrapolated based on the values for Dutch Limburg and the Chiers subcatchment respectively. The area under wetlands was estimated based on data from RWS Limburg/IWACO (2000).

A generalised map of land use at ca. 1000 AD was compiled by RWS Limburg/IWACO (2000), as part of a major study to assess the ecological functioning of the Meuse at the basin scale over the last millennium. In this study we used this map to represent land use in the 11th Century, with the land use categories being reclassed to those described above. This map is based mainly on the works of Dornbusch (1997) regarding the extent of forest and important settlements in Europe around 1000 AD, and of Van Es et al. (1988) regarding the distribution of peat bogs and fenlands at that time. The data in the original map are supported by the results of independent studies from other sources (e.g. Blouet et al., 1993; Buisman and Van Engelen, 1995; Dierkens and Plumier-Torfs, 1999). Since the land use map of 1000 AD does not contain any information on water bodies, this class was held constant in our simulations, based on the present-day distribution.

Between the 12th and 18th Centuries inclusive, no quantitative assessments of land use are available and instead the changes were estimated per subcatchment based on qualitative reviews of historical land use change. According to RWS Limburg/IWACO (2000), urbanisation was not a factor of importance until ca. 1850 AD, and hence this class does not occur until the 19th Century. Between the 11th and 18th Centuries, forests were exploited for fuelwood, charcoal, and building materials, and removed to make way for pastures. Later in the period, wood was used as a fuel in the foundries of industrial regions (Froment, 1975; Gotjé et al., 1990; Petit and Lambin, 2002; RWS Limburg/IWACO, 2000; WL, 1994b). Although this forest degradation was concentrated in different parts of the basin during different periods, overall the period 1000-1800 AD was typified by a basin-wide decrease in forest. In the present study a linear reduction in forested area was assumed between the distributions of the 11th and 19th Centuries, as was assumed to be the case for Europe in the period 1000-1700 AD by Brovkin et al. (1999). In reality some centuries will have seen faster/slower rates of deforestation, and the long-term deforestation may at times even have been checked by external influences such as the bubonic plague (e.g. Lang et al., 2003; Ruddiman, 2003). However, since this study aims mainly to assess the long-term trends in discharge, rather than to reconstruct exact estimates of discharge per century, more accurate centennial land use maps are not required. In terms of long-term changes in the areal distribution of wetlands in the basin, fenland destruction commenced in the 16th Century (RWS Limburg/IWACO, 2000), and by the 19th Century almost complete destruction had occurred. Hence, in the present study it was assumed that a linear reduction of area covered by fenlands occurred between these

periods. The destruction of peat bog appears to have commenced in earnest from the end of the 16th Century (RWS Limburg/IWACO, 2000), with a peak around the 18th Century, and the current situation being reached by the late 19th Century. Therefore, in the present study it was assumed that the situation remained stable until the 16th Century inclusive, and that thereafter areal reductions occurred as follows: 17th Century (25% reduction); 18th Century (50% reduction); and 19th Century (100% reduction). An exception to this pattern was in the Peel region (Netherlands), where peat bogs were intact until far into the 19th Century (RWS Limburg/IWACO, 2000).

Although archaeological and pollen evidence suggest that parts of the basin were populated by 4000-3000 BP (Bunnik, 1995; Gotjé et al., 1990; Henrard, 2003), any disturbance in this period was, in our opinion, minor, and too small to have had any significant influence on hydrological processes (see results of sensitivity analysis in Section 3.3.4). Since the natural vegetation of northwest Europe at that time was predominantly deciduous forest (Bunnik, 1995; Gotjé et al., 1990), we have assumed a fully forested basin at 4000-3000 BP, except for those cells referring to 'Water Bodies' (CORINE), and 'Wetlands' (RWS Limburg/IWACO, 2000).

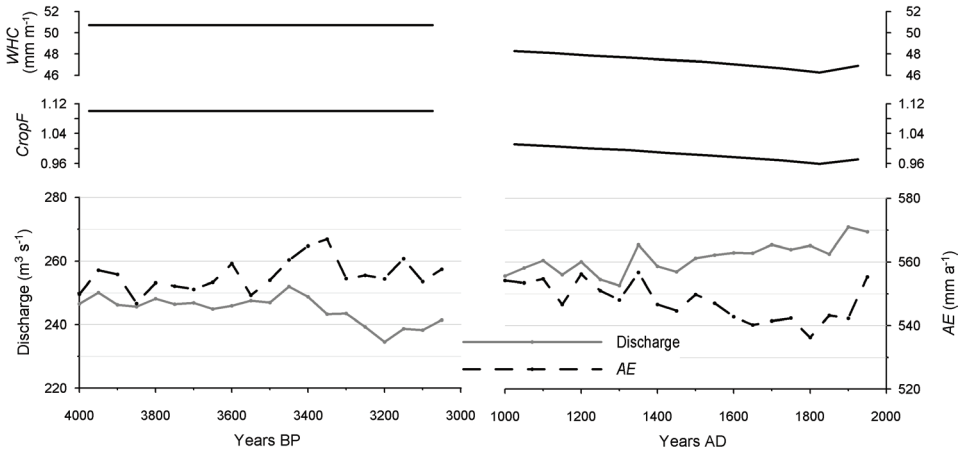

Fig. 3.5: Changes in mean annual discharge at Borgharen, basin-wide mean annual actual evapotranspiration (AE), crop factor (CropF), and soil water holding capacity (WHC). For discharge and AE the mean values of the four ensemble members are shown, and have been lumped into 50-yr periods in order to show the long-term signal. The crop factor reflects changes in basin-averaged land use, and shows a decrease over the last 1000 years due to deforestation, and an increase over the last 100 years, mainly due to reforestation. The changes in WHC are related to changes in land use.

The basin-averaged crop factor (Fig. 3.5) shows a marked reduction between 4000-3000 BP and 1000-2000 AD (conversion of forest to agriculture), and decreases further over the last millennium (deforestation and peat extraction). However, in

the 20th Century the crop factor increases (due to the reforestation of previously cultivated land, although tempered by urbanisation). Changes in land cover (the physical characteristics of the Earth's surface) have shown more change than land use over the last century (e.g. an increase in coniferous forest relative to deciduous forest, and changes in types of agriculture) (Tu, 2006). However, on a millennial timescale the large-scale changes in land use are more important than such changes.

3.3.2.3 Soil water holding capacity

A map showing the maximum water holding capacity (WHC) of the soil (mm) is used in STREAM to calculate evapotranspiration, runoff, groundwater seepage, and baseflow. For the present day we have used the United Nations Food and Agriculture Organization's (FAO) map of WHC (FAO, 2003). Since the FAO dataset has too coarse a resolution to accurately represent the remaining areas of peat-bog in the Meuse basin, we have assigned those areas the modal WHC value for the remaining large intact areas of European peat-bog (FAO, 2003). Changes in land use cause changes in soil textural properties, therefore influencing WHC. The FAO WHC map is based on dominant soil unit, component soil units, texture, soil phase, and relief, but does not explicitly consider vegetation. We found a significant positive correlation between WHC and percentage forest cover between the various soil units, and a significant negative correlation between WHC and percentage cover of agriculture and grasslands (Spearman's rank, $\alpha = 0.05$). Hence, the percentage difference between the mean WHC of soils covered by forests and those covered by agriculture and grasslands was calculated, and the resulting change factors were coupled with the land use anomalies over time, to produce WHC maps for each century, similar to Mahe et al. (2005). For areas covered by rendzinas (shallow humus-rich soils over limestone) the original value of WHC was retained since the WHC of this soil unit is mainly influenced by parent material (FAO, 2003). The estimated change in basin-wide WHC over the late Holocene can be seen in Fig. 3.5. Given the uncertainties in the spatial distribution of land use over the Holocene, the input maps of WHC give only an indication of the situation in each period, but the sign of change at the basin scale is in agreement with the gradual decrease in WHC at the basin scale over the late Holocene (e.g. RWS Limburg/IWACO, 2000).

3.3.3 Calibration and validation

Calibration was carried out for the relatively wet period 1961-2000, and validation for the relatively dry period 1921-1960. The calibration was initially carried out for the main river at Borgharen, using data provided by RWS Waterdienst, pertaining to the 'undivided Meuse'; they are based on discharge measurements at Borgharen, corrected for canal extractions between Liège and Borgharen (De Wit et al., 2007a), and are available since 1911. Further stations on the main river body were obtained for Chooz (Berger, 1992), and Stenay (DIREN Lorraine Bassin Rhin-Meuse). Tributary data were obtained from: Direction Générale des Voies

Hydrauliques Region Wallonne (http://voies-hydrauliques.wallonie.be/opencms/opencms/fr/hydro/annuaires) for the Chiers (Chauvency-le-Château), Semois (Membre), Lesse (Gendron), Amblève (Martinrive), Ourthe (Tabreux), and Viroin (Treignes); Roer and Overmaas Water Board for the Geul (Meerssen) and Roer (Stah); and Berger (1992) for the Sambre (Namur). The calibration was carried out by varying model parameters with the aim of reproducing daily, monthly, and annual discharge characteristics similar to those of the observed records. Where independent measurements exist for output variables other than discharge, these were also used in the calibration; in this case actual evapotranspiration (AE) and the number of snow-cover days.

The parameters used for calibration are: crop factor; WHC; HEAT (used in the Thornthwaite (1948) equation for calculating potential evapotranspiration); TOGW multiplier (determines the proportion of surplus water per grid cell that runs off directly or that seeps to the groundwater); C factor (determines the proportion of groundwater that contributes to baseflow); $SNOW_{tmp}$ (temperature threshold below which precipitation falls as snow and above which snowmelt occurs), and MELT (determines the rate of snowmelt when temperature is above a critical value). The calibration parameters selected for this project were: crop factor, 1.2; HEAT, 0.98; WHC, 0.9; TOGW, 0.6; C, 1.25; $SNOW_{tmp}$, 1.0; and MELT, 7/30. In order to test the sensitivity of the model to changes in these parameters, we carried out a sensitivity analysis, the results of which can be found in Section 3.3.4.

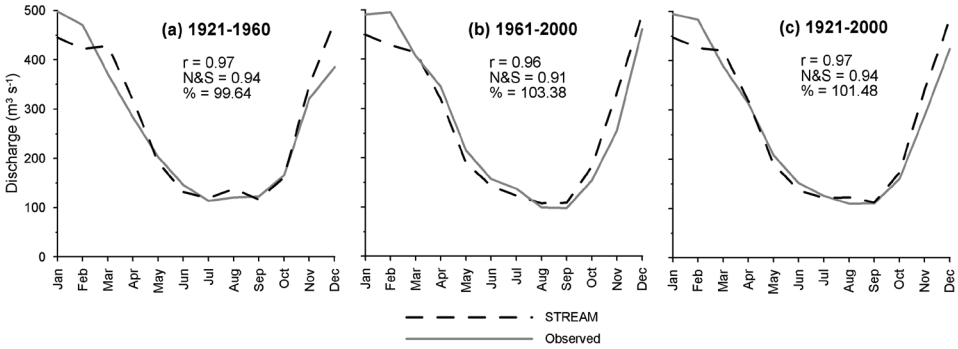

Fig. 3.6: Hydrographs showing the agreement between mean monthly simulated and observed discharge at Borgharen for: (a) the validation period, 1921-1960; (b) the calibration period, 1961-2000; and (c) the entire period 1921-2000. Also shown are the total accuracy (%), Pearson's Product Moment correlation coefficient (r), and Nash & Sutcliffe efficiency coefficient (N&S).

The agreement of total annual discharge was assessed by expressing mean annual modelled discharge as a percentage of mean annual observed discharge (%), and the correlation of the means of monthly discharge was assessed using the correlation coefficient, r, and the Nash and Sutcliffe (N&S) efficiency coefficient (Nash and Sutcliffe, 1970). The annual hydrographs for Borgharen (Fig. 3.6)

show good correlations between mean annual and mean monthly modelled and observed discharges for the calibration and validation periods, as well as for both periods taken together, although the model underestimates mean discharge in the winter. The agreement of total annual discharge was assessed by expressing mean annual modelled discharge as a percentage of mean annual observed discharge (%), and the correlation of the means of monthly discharge was assessed using the correlation coefficient, r, and the Nash and Sutcliffe (N&S) efficiency coefficient (Nash and Sutcliffe, 1970). The modelled and observed daily discharge frequency distributions for 1921-2000 are statistically similar (MWU-test, p = 0.366); this is also the case for the winter half-year. In Table 3.1 the mean annual k^{th} percentiles are given for the calibration and validation runs (k = 1, 25, 50, 75, 90, 95, 99), showing good agreement for low, average, and high-flows. The model slightly overestimates the frequency of summer half-year high-flows (Q_k, k > 97) due to an overestimation of high precipitation events in autumn in ECBilt-CLIO-VECODE. The model simulates the annual, monthly, and daily discharge characteristics of major tributaries well (Ward, 2007a). The underestimation of mean discharge in the winter has implications for the assessment of high-flows as the vast majority of large floods on the Meuse occur during the winter (Berger, 1992). The results should not be taken as exact figures for each period studied, but rather they give an indication of the main trends in changes in flood frequency relative to the simulated results of other periods.

Table 3.1: Magnitudes of mean annual k^{th} percentiles of daily discharge (Q_k, k = 1, 25, 50, 75, 90, 95, 99) at Borgharen for the calibration and validation periods. Bold type indicates that the annual magnitudes are statistically similar to the observed annual discharge magnitudes (t-test, α = 0.05).

	Discharge ($m^3 s^{-1}$)						
Time-period	Q_1	Q_{25}	Q_{50}	Q_{75}	Q_{90}	Q_{95}	Q_{99}
Calibration (1961-2000)	**47.5**	**93.2**	**185.9**	**380.4**	**607.9**	**754.9**	**1096.2**
Validation (1921-1960)	**46.9**	**91.1**	**178.6**	**379.2**	623.1	**774.7**	**1165.7**

For the Meuse basin, no detailed estimates of actual evapotranspiration (AE) are available. The simulated mean annual basin-average potential evapotranspiration (PE) for 1921-2000 (605 mm a^{-1}) is of the same order of magnitude as the estimated PE for the Belgian sub-catchments for 1968-1998 (555 mm a^{-1}) (Leander et al., 2005), although the discrepancy is significant. However, in our model PE is converted into AE using the Thornthwaite and Mather (1957) equations, and whilst a discrepancy exists between modelled and 'observed' PE this is not the case for AE. For the period 1901-2000 we simulate basin-wide precipitation of 912.7 mm a^{-1}, compared to 913.3 mm a^{-1} in the observed (CRU) record; for mean annual discharge at Borgharen for the period 1921-2000 we simulate 268.4 $m^3 s^{-1}$, against 270.4 $m^3 s^{-1}$ in the observed record. Given that the annual values for soil storage, groundwater storage, and snow storage (i.e. the storage compartments of

STREAM) remain constant over these periods, the mean annual AE total must also be correct. The correlation between mean monthly PE totals reflects the annual pattern of changes in PE well (r = 0.92). Another approach to the simulation of evapotranspiration would have been to use PE and AE values from ECBilt-CLIO-VECODE. However, no accurate datasets pertaining to these parameters are available for downscaling the climate model output to the resolution of STREAM.

Data pertaining to the number of days per year on which the ground is covered by snow at Maastricht (Klein Tank et al., 2002, http://eca.knmi.nl), were used in the calibration of parameters pertaining to snowmelt and snowfall. In the model output for 1961-2000, the ground was covered by snow at Maastricht on average 3.6% of days per year, compared to 3.7% of days in the observed record.

3.3.4 Sensitivity analysis

Since the computing time required to run the model rendered a full Bayesian Monte Carlo sensitivity analysis unfeasible, we assessed the model's sensitivity to changes in the calibration parameters by altering the values of individual calibration parameters by ±10% and ±50%. The results of the sensitivity analysis can be found in Table 3.2. The model is sensitive to changes in parameters influencing evapotranspiration (namely crop factor), and fairly insensitive to parameters pertaining to WHC and slope (C). Hence, it is important that the crop factors are reliable, as incorrect crop factors could lead to large errors in the estimation of evapotranspiration. We calculated the present day percentage cover of forest and agriculture for 11 sub-catchments (upstream from the following points): Stenay, Chauvency-le-Château, Membre, Gendron, Martinrive, Meerssen, Chooz, Tabreux, Stah, Namur, Treignes. For each sub-catchment we also calculated the percentage anomaly between annual observed and modelled discharge. We found no correlation between percentage forest cover (which ranges from 20.7% to 57.1%) and model accuracy (Spearman's rank, p = 0.467), which suggests that the accuracy of the model is not biased by the crop factor values used for forest and agriculture. Since the main land use changes of the late Holocene have been between these two land use types, the model should therefore be able to simulate the effects of these land use changes on evapotranspiration.

The basin-wide changes in WHC used in our model (Fig. 3.5) show a maximum change between the periods 4000-3000 BP and 1000-2000 AD of 8.9%. The sensitivity analysis showed that an increase or decrease of WHC of 10% led to a change in mean annual discharge of just ±0.7%, and had little influence on high and low-flows. Hence, our palaeodischarge model is more useful for examining the effects of land use change on evapotranspiration, rather than on soil moisture.

We also tested the sensitivity of the model to changes in land use (and namely the replacement of forest by agriculture) in order to firstly test our assumption that the small-scale presence of humans in the Meuse basin during the period 4000-3000 BP would not have had a significant effect on hydrological processes,

Table 3.2: Results of sensitivity analysis, obtained by running the STREAM model with one climate ensemble member for the period 1961-2000, and adjusting individual calibration parameters by ±10% and ±50%. The correlation between the mean monthly values of each simulation and the observed values is given (Pearson's Product Moment correlation coefficient (r) and Nash and Sutcliffe efficiency coefficient (N&S)). The model is sensitive to changes in crop factor, relatively insensitive to changes in soil water holding capacity (WHC) and slope (C), and very insensitive to changes in other parameters.

Discharge scenario	r	N&S	Q_{ann} ($m^3 s^{-1}$)	Q_{10} ($m^3 s^{-1}$)	Q_{90} ($m^3 s^{-1}$)
Borgharen observed	N/A	N/A	275.1	61.0	625.0
Borgharen simulated	0.97	0.94	274.1	57.9	613.3
Crop factor - 10%	0.96	0.90	300.7	70.0	645.9
Crop factor + 10%	0.97	0.92	251.7	48.7	586.4
WHC - 10%	0.97	0.93	277.0	59.4	618.4
WHC + 10%	0.97	0.95	271.5	56.8	608.7
C - 10%	0.97	0.94	274.1	54.0	617.4
C + 10%	0.97	0.94	274.1	61.4	610.4
Crop factor - 50%	0.89	-0.57	445.2	150.3	812.8
Crop factor + 50%	0.98	0.18	148.9	18.5	406.3
WHC - 50%	0.95	0.88	292.6	68.3	643.0
WHC + 50%	0.99	0.95	253.8	50.4	577.0
C = 1	0.97	0.94	274.1	49.4	622.1
C + 50%	0.95	0.90	274.3	79.4	597.9

and secondly to test the robustness of our generalised maps of land use change. A control run was carried out using the climate data of one ensemble member for the period 4000-3000 BP, assuming the basin to be fully forested (except for those cells pertaining to wetlands). Then, the model was re-run using the same climate data, but replacing the land use maps with new maps showing 5% and 10% deforestation (forest cells were chosen at random and replaced by cells pertaining to agriculture). The results for mean annual and maximum discharge, as well as a number of discharge percentiles, are shown in Table 3.3. The slight increase in mean annual discharge between control and 5% deforestation (+0.8%) is statistically insignificant (t-test, $p = 0.270$), and the effect on high flows is very small. For a deforestation of 10%, the effect on mean discharge (+1.6%) becomes statistically significant (t-test, $p = 0.030$), although it is still minor; the increase in mean annual maximum discharge (+0.4%) is negligible. Further simulations were then carried out whereby 5% and 10% of the forest cells were again replaced by agriculture, but all of the altered cells were concentrated together, thus representing an extreme case scenario of intense deforestation in a particular area. There was no significant difference in discharge between these runs, and the runs in which the deforested cells were distributed randomly (t-test, for 5% deforestation, $p = 0.810$; for 10% deforestation, $p = 0.581$). Given that the effects of a 5% and 10%

deforestation on our mid-Holocene discharge results are minor (even assuming a situation in which this was concentrated in one part of the basin), our assumption that land use at that time can be simulated using a scenario of full forest cover is valid. Furthermore, the results of the sensitivity analysis suggest that our generalised maps of land use change over time are robust, since the model is not oversensitive to small changes, and therefore highly detailed land use maps are not required.

Table 3.3: Sensitivity analysis of the coupled climate-hydrological model to changes in land use from forest to agriculture. The model was run for the period 4000-3000 BP assuming the basin to be fully forested (control), and then re-run assuming scenarios of 5% and 10% deforestation respectively (forest replaced randomly by agriculture). The increases in mean (Q_{ann}) and maximum (Q_{max}) annual discharge as well as various mean annual k^{th} percentiles of daily discharge (Q_k, k = 25, 50, 75, 90, 95) show that a deforestation of 5% has little effect on Meuse discharge.

	Discharge (m^3 s^{-1})						
Scenario	Q_{ann}	Q_{25}	Q_{50}	Q_{75}	Q_{90}	Q_{95}	Q_{max}
Control (Full forest)	241.3	65.8	144.0	342.6	572.1	726.5	1632.4
5% deforestation	243.2	67.0	146.5	345.2	574.5	728.8	1635.7
10% deforestation	245.2	68.3	149.2	347.9	576.8	731.1	1639.0

3.4 Results

In this section we compare the results for 4000-3000 BP with those for 1000-2000 AD. We use the period 4000-3000 BP as a reference period in which the hydrological system was in a natural state. The discharge results for this reference period are compared to those of 1000-2000 AD, during which time the hydrological system was affected by anthropogenic changes in land use and climate.

3.4.1 Mean discharge

The simulated ensemble mean annual discharge shows a statistically significant increase (t-test, $p < 0.001$) of 6.6% between 4000-3000 BP (244.8 m^3 s^{-1}) and 1000-2000 AD (261.0 m^3 s^{-1}) (Fig. 3.5). The variability of mean annual discharge also increased (4000-3000 BP, $\sigma = 39.6$; 1000-2000 AD, $\sigma = 44.8$; F-test, $p < 0.001$). The increase in the winter half-year (+2.3%) was small compared to the increase in the summer half-year (+21.6%) (Fig. 3.7). Reference to Fig. 3.5 shows that discharge in the 20th Century AD (ca. 270.0 m^3 s^{-1}) was higher than in the period 1000-1900 AD, and that mean annual discharge in the period 1000-1900 AD (ca. 260.0 m^3 s^{-1}) was significantly higher than in the period 4000-3000 BP (t-test, $p < 0.001$). The same is not true for the interannual variability, which shows no significant difference between 1000-1900 AD ($\sigma = 44.7$) and the 20th Century ($\sigma = 45.1$) (F-test, $p = 0.544$). During the period 1000-2000 AD, discharge shows an increasing monotonic trend (MK-test, $p < 0.001$) (Fig. 3.5). Surplus water

availability for runoff is in fact dependent on two key components: precipitation and actual evapotranspiration (AE). The long-term changes in discharge cannot be simply related to changes in precipitation over the Holocene. The simulated increase in summer half-year precipitation between 4000-3000 BP and 1000-2000 AD was just 5.6% (compared to a 21.6% increase in summer half-year discharge), whilst winter half-year precipitation depths showed a decrease of 2.3% (compared to a 2.3% increase in winter half-year discharge). Moreover, no monotonic trend of increasing annual precipitation is simulated for the last millennium, in contrast to mean annual discharge. However, simulated AE was significantly higher at 4000-3000 BP than at 1000-2000 AD (t-test, $p < 0.001$). Furthermore, we see a strong decreasing trend in AE over the last 1000 years (MK-test, $p = 0.004$) (Fig. 3.5), mainly as a result of reduced forest cover and hence reduced crop factor, and to a less extent due to reduced temperature.

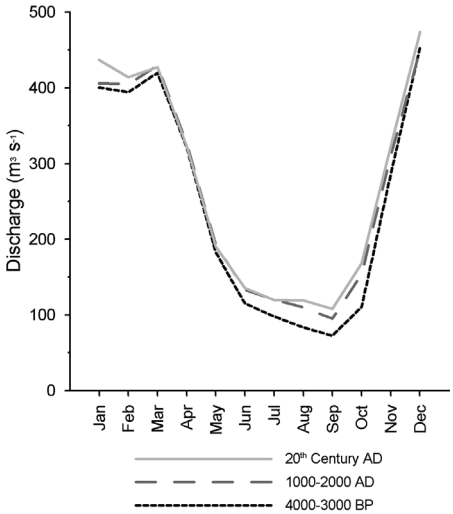

Fig. 3.7: Simulated mean monthly discharge at Borgharen for the periods 4000-3000 BP, 1000-2000 AD, and the 20th Century. The increase in discharge since the period 4000-3000 BP has mainly taken place during the summer half-year (May-October).

We found no simple correlation relating mean annual temperatures to mean discharge or precipitation. Whilst we did simulate a strong positive correlation between 50-yr mean annual discharge and 50-yr summer half-year precipitation totals for the period 1000-2000 AD, no such correlation was noted for 4000-3000 BP. Due to the higher crop factors at 4000-3000 BP, annual PE–AE at that time was almost two times as high as during the last millennium. Hence, more excess precipitation in wet summers could be lost to AE, and therefore fluctuations in summer precipitation had less influence on discharge. This mechanism may also be responsible for the simulated increase in variability of mean annual discharge, since no change in precipitation or temperature variability was simulated between the time-slices.

For the 20th Century we see an increase in mean discharge compared to the 19th Century (Fig. 3.5) (19th Century, 263.5 $m^3 s^{-1}$; 20th Century, 270.0 $m^3 s^{-1}$), despite a significant increase in AE (19th Century, 539.8 mm a^{-1}; 20th Century, 548.8 mm a^{-1}). This increase in discharge is ascribable to a relatively large increase in precipitation in the 20th Century (912.4 mm a^{-1}) compared to the 19th Century (893.1 mm a^{-1}); annual precipitation depths in the former period are thereby greater than in any preceding century.

3.4.2 High-flow events

Between 4000-3000 BP and 1000-2000 AD the frequency of high-flows increased, whilst high-flows occurred even more frequently in the 20th Century than in the rest of the last millennium (Fig. 3.8). The difference between the frequency distributions for the periods 4000-3000 BP and 1000-2000 AD is statistically significant (KS-test, $p < 0.001$), as are the differences between the frequency distributions between the periods 4000-3000 BP and 1000-1900 AD, and 1000-1900 AD and the 20th Century respectively (KS-test, $p < 0.001$).

We examined the changes in the simulated recurrence times of high-flow events of the following magnitudes: Q > 800 $m^3 s^{-1}$, 1300 $m^3 s^{-1}$, 1950 $m^3 s^{-1}$, and 3000 $m^3 s^{-1}$ (Table 3.4). These correspond approximately to the discharge percentiles Q_{95}, Q_{99}, $Q_{99.9}$, and $Q_{99.995}$ in the observed record at Borgharen (1912-2000). Little

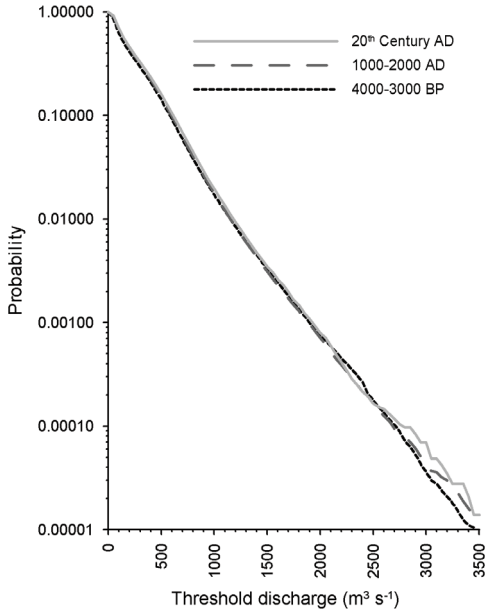

Fig. 3.8: Probability of daily discharge over a threshold. Large high-flow events with discharge in excess of 3000 $m^3 s^{-1}$ (i.e. similar in magnitude to during the floods of 1926 and 1993) are predicted more frequently in the period 1000-2000 AD than in the period 4000-3000 BP. In the 20th Century, the frequency of large high-flow events (Q > 3000 $m^3 s^{-1}$) is greater still.

change is evident in the recurrence times of relatively small to medium high-flows (Q > 800 $m^3 s^{-1}$ and 1300 $m^3 s^{-1}$) between 4000-3000 BP and 1000-2000 AD, although there is a slight but clear increase in frequency with regards to the 20th Century. For large high-flow events with a discharge in excess of Q > 3000 $m^3 s^{-1}$ (similar in magnitude to the floods of 1926 and 1993), a clear increase in recurrence frequency can be seen between 4000-3000 BP and 1000-2000 AD, with a further increase in the 20th Century. The recurrence time of flows of this magnitude is almost twice as short in the 20th Century as in the reference period 4000-3000 BP.

Table 3.4: Simulated recurrence times of daily discharge (Q) in excess of 800, 1300, 1950, and 3000 $m^3 s^{-1}$; these discharge magnitudes correspond approximately to discharge percentiles Q_{95}, Q_{99}, $Q_{99.9}$, and $Q_{99.995}$ respectively, in the observed time-series for Borgharen between 1912-2000 AD. Large high-flow events (Q > 3000 $m^3 s^{-1}$) are simulated almost twice as frequently in the 20th Century as in the natural reference period (4000-3000 BP).

	Discharge ($m^3 s^{-1}$)			
Time-period	> 800	> 1300	> 1950	> 3000
4000-3000 BP	26 days	165 days	3.2 years	77 years
1000-2000 AD	25 days	168 days	3.4 years	65 years
20th Century	22 days	150 days	3.0 years	40 years

To examine whether the simulated number of these large high-flow events (Q > 3000 $m^3 s^{-1}$) for the 20th Century falls within the limits of natural variability, we calculated the number of flow events for which Q > 3000 $m^3 s^{-1}$ for each possible 100-yr period in the simulations. Note that the results of the four ensemble members have been lumped together, and hence each 100-yr period corresponds to 400 years of simulations. Firstly, we filtered out flow events of Q > 3000 $m^3 s^{-1}$ whereby the simulated discharges occurred within 10 days of each other, so as to ensure that independent events were counted, following Tu (2006). For the 20th Century, 10 flow events with Q > 3000 $m^3 s^{-1}$ were simulated in the four ensemble runs. Then we calculated the number of flow events for which Q > 3000 $m^3 s^{-1}$ for every possible 100-yr period in the simulations; 900 possible periods of 100-yr duration exist for each millennial time-slice. During 1000-2000 AD, there were eight periods of 100-yr duration in which this frequency of high-flow events (10 per 100-yr for Q > 3000 $m^3 s^{-1}$) was simulated; for the period 4000-3000 BP it was simulated only one time. Hence, the frequency of large high-flows has been particularly great over the last 100 years, but does not fall outside natural variability.

3.4.3 20th Century trends

We investigated the presence or absence of monotonic trends (Mann-Kendall (MK) test) in the simulated mean annual discharge, precipitation, temperature, and AE time-series over the 20th Century. On this timescale land use is assumed to be constant in our model, so any trend can be ascribed to climatic change. For

mean annual, summer half-year, and winter half-year discharge, as well as for the 75th, 90th, 95th, and 99th percentiles of daily discharge, we found no significant trends. Upward trends were found for mean annual, summer half-year, and winter half-year temperature, which forced significant upward trends in annual and winter half-year AE, although no significant trend in summer half-year AE. For mean annual, summer half-year, and winter half-year precipitation no significant trends were simulated, although these parameters increased weakly. Hence, despite significantly increasing trends in AE over the last 100 years, no significant discharge trend was noted due to the compensatory effect of the weak increasing trend in precipitation.

3.4.4 Relative contributions of climate and land use change to changes in discharge

The results described in Sections. 3.4.1 to 3.4.3 show an increase in mean discharge and flood frequency between the natural reference period (4000-3000 BP) and the last millennium, with a further increase in the 20th Century. Given that the simulated increase in mean discharge mainly took place in the summer half-year, that precipitation shows no trend over the last 1000 years, and that the intensity of large precipitation events was higher in 4000-3000 BP, we attribute the increase in mean discharge and high-flow events to a large extent to changes in land use (lower evapotranspiration due to decreased forested area). However, comparing the 20th Century results to those of the 19th Century, it appears that a significant increase in precipitation has become the dominant mechanism, since the observed reforestation over that period should theoretically have led to decreased discharge. To test this theory we carried out further hydrological simulations to delineate the effects of land use and climatic change. For the period 4000-3000 BP we carried out a further simulation with STREAM, using one ECBilt-CLIO-VECODE ensemble member as climate input data, but using the land use and WHC maps of the 20th Century. Similarly, we ran a simulation with the 20th Century climate input data, but using the land use and WHC data for 4000-3000 BP. In this way the effects of changes in climate and land use were delineated. Similarly, we ran STREAM using climate data of the 19th Century with land use data for the 20th Century, and vice versa.

The results of these simulations (Table 3.5) show that the change in climatic conditions between 4000-3000 BP and the 20th Century had only a minor effect on discharge; almost all of the change on this timescale can be attributed to large-scale changes in land use (mainly a large decrease in forest at the expense of agricultural and urban land). The results of our sensitivity analysis show that changes in WHC have very little effect on either mean discharge or flood frequency, and hence we can attribute the increases to the significant reduction in AE which occurred as a direct result of deforestation. An examination of the changes in discharge characteristics between the 19th and 20th Centuries reveals the opposite pattern. As expected, the increased crop factor (due to reforestation) between these two time-periods means that the effect of land use change alone is to force

a slight reduction in mean discharge and high-flow magnitude. However, the increase in precipitation (mean and intensity) between these two time-periods has overwhelmed the land use forcing, leading to increased discharge magnitudes, especially in the winter half-year (due to a relatively large increase in winter half-year precipitation), and increased magnitude of high-flow events (due to increased precipitation intensity and increased winter half-year antecedent soil moisture).

Table 3.5: Percentage change in mean annual (Q_{ann}), summer (Q_{sum}), and winter (Q_{win}) discharge and various high-flow percentiles (Q_k, k = 75, 90, 95, 99) between 4000-3000 BP and the 20th Century (above), and between the 19th and 20th Centuries (below). The increases in discharge and high-flow magnitude between the period 4000-3000 BP and the 20th Century are mainly due to changes in land use. However, the increases in discharge and high-flow magnitude between the 19th and 20th Centuries are due to climatic change (mainly increased mean winter half-year precipitation and increased precipitation intensity).

	Q_{ann}	Q_{sum}	Q_{win}	Q_{75}	Q_{90}	Q_{95}	Q_{99}
Percentage change between 4000-3000 BP and 20th Century							
Climate and land use	+12.5	+28.8	+7.7	+11.3	+7.1	+5.6	+4.1
Climate only	-	+0.7	-0.1	-0.4	+0.6	+0.1	-0.6
Land use only	+12.4	+28.1	+7.8	+11.7	+6.6	+5.5	+4.8
Percentage change between 19th Century and 20th Century							
Climate and land use	+3.5	+0.3	+4.6	+4.3	+2.9	+3.2	+4.0
Climate only	+4.5	+2.2	+5.4	+5.5	+3.7	+3.7	+4.5
Land use only	-1.0	-1.9	-0.7	-1.2	-0.8	-0.5	-0.5

3.5 Discussion

3.5.1 Effects of land use change on discharge

Our results are in agreement with those of recent studies on the effects of land use change on Meuse discharge. Tu (2006) investigated the observed discharge characteristics of the Meuse for the period 1912-2000, and found the effects of land use change to be marginal or statistically undetectable. Ashagrie et al. (2006) used the HBV model to simulate changes in Meuse discharge over the 20th Century, and concluded that the observed change in land use did not have a significant effect on discharge. Although we did not simulate changes in land use within the 20th Century, we see that the effect of land use change in the 20th Century in relation to the 19th Century is minor. On this timescale the changes in land use were relatively small and worked in a compensatory fashion in terms of their effects on AE, since the crop factor associated with forest is high, whereas that associated with urban areas is low.

Whilst land use change has not greatly influenced discharge over the last century, our results show that on a longer timescale the large-scale deforestation of the basin has led to significant increases in mean discharge and flood frequency. It

is now widely accepted that forests can cause a reduction in mean discharge, especially during the summer half-year (Calder, 1993). The results of paired catchment studies in temperate zones have established strong links between deforestation and increasing mean discharge, and vice versa (Andréassian, 2004; Bosch and Hewlett, 1982; Hornbeck et al., 1993; Sahin and Hall, 1996). In single basin studies, large increases in discharge due to deforestation, or decreases due to reforestation, have been noted in Europe (Gallart and Llorens, 2004; Keesstra, 2006), Africa (Mahe et al., 2005; Scott et al., 2005), North America (Trimble et al., 1987), and South America (Costa et al., 2003; Iroumé et al., 2005). Various modelling studies of European streamflow have simulated significant changes in response to land use change (Bultot et al, 1990; Klöcking and Hamberlandt, 2002; Wegehenkel, 2002). Two of the most important factors affecting discharge via land use change are: (a) alterations in evapotranspiration totals (Calder, 1993; Hornbeck et al., 1993; Keesstra, 2006; Robinson et al., 2003) due to changes in leaf area, stomatal response, and interception; and (b) changes in soil water holding characteristics (Cosandey et al., 2005; Mahe et al., 2005); in our model the discharge effects of land use change can be mainly ascribed to changes in AE, since the model is fairly insensitive to changes in WHC.

The effect of deforestation on high-flow events is more debated (EEA, 2001). In a review of 113 paired catchments, Andréassian (2004) found that flood volumes and peak-flows could increase after deforestation, but that the response was much more varied in time and space than for mean discharge. Nevertheless, large-scale deforestation has led to increased peak-flows around the globe (Brown et al., 2005; Gentry and Parody, 1980; Jones, 2000; Mahe et al., 2005), whilst reforestation has led to significant reductions in flood peaks (Fahey, 1994; Robinson et al., 1991). In our simulations, large-scale deforestation led to increased flood frequency due to significant decreases in AE; this decrease in AE has both a direct effect due to increased surplus water availability, and an indirect effect due to earlier soil saturation.

3.5.2 Comparison of simulation results with proxy and historical data

In order to verify the results of our model for the late Holocene, we compared our findings with results based on multi-proxy data. The results of most of these studies are qualitative only, and hence we can only compare the signal of change with that of our model results. Simulated mean summer and winter half-year temperatures are in reasonable agreement with multi-proxy reconstructions of regional temperature for the late Holocene, which show a gradual decrease in temperature (especially in summer) (Bohncke et al., 1987; Goosse et al., 2006; Zagwijn, 1994). For example, Zagwijn (1994) produced temperature curves for Amsterdam (Netherlands) based on distribution maps of the first pollen occurrences of four indicator plant species. According to these curves, summer temperatures were approximately 0.5°C higher in the period 4000-3000 BP than in the period 1000-2000 AD, whilst winter temperatures were broadly similar. Our results for the

Meuse basin show a decrease in summer half-year temperature between those periods of ca. 0.58°C in the summer half-year, and ca. 0.26°C in the winter half-year. Proxy data on late Holocene precipitation change in the region are scarce, but suggest a slight increase in precipitation in the last millennium compared to the period 4000-3000 BP (Bohncke and Vandenberghe, 1991; Van Geel et al., 1996), though they give no qualitative assessment of the magnitude of change, nor indications of seasonal changes. Whilst these proxy data are very limited in detail, their main trends are in agreement with our results.

The qualitative results of multi-proxy studies on late Holocene Meuse discharge are in agreement with our conclusion of increasing mean discharge and high-flows. Berendsen and Stouthamer (2001) suggest that an increase in meander wavelengths in the Rhine-Meuse delta after ca. 2800 BP may be indicative of increased bankfull discharge in both rivers. Furthermore, they postulate that an increase in flood frequency may have occurred somewhere between 3000-2000 BP, as attested by an increase in avulsion frequency and the reoccupation of residual channels by floodwaters (e.g. Hofstede et al., 1989). De Moor (2007) states that the increasing thickness of fining-up sequences in the fluvial deposits of the Geul (Meuse tributary) could represent an increase in bankfull discharge due to deforestation since Roman times. Zagwijn (1986) suggests that a reduction of forested area in the Netherlands, especially since Roman times, led to a reduction in evapotranspiration, and consequently increased discharge. Similarly, Bohncke and Vandenberghe (1991) derived qualitative estimates of changes in evapotranspiration, precipitation, and temperature in the Mark Basin (southern Netherlands) to suggest that discharge was higher at 1000-2000 AD than at 4000-3000 BP. Based on an examination of historically documented floods over the period 1000-2000 AD, WL (1994a) conclude that the frequency of high-flow events since 1911 appears to have been greater than in the preceding centuries. However, it should be stressed that the frequency of floods in the historical record may be underestimated due to the lack of systematic measurements.

3.5.3 Uncertainties and limitations

Our model experiment includes a number of limitations, the most important being those associated with database uncertainties: (1) the climate model has a low spatial resolution and simplified physics compared to GCMs. This makes it impossible to correctly simulate the regional details and variability of daily precipitation; (2) the downscaling of precipitation is carried out using a simple linear correction technique based on monthly correction factors. Leander and Buishand (2007) found it to be advantageous to correct also for the variability of 10-day precipitation amounts. However, given the long timescales involved in the palaeodischarge approach a more sophisticated downscaling method was found to be unfeasible; (3) the land use data represent only a generalised pattern of land use change over the last millennium; (4) the resolution used in STREAM means that only larger river networks can be delineated. The chosen resolution does, however, allow for the assessment of changes in long-term discharge trends at

the basin scale (see Appendix 1); and those associated with physical process uncertainties: (1) the Thornthwaite and Mather equation (1957) for AE is highly simplified; (2) the impact of anthropogenic water extraction and canalisation is not fully accounted for; (3) STREAM (and indeed any hydrological model), cannot fully describe the hydrological processes within the basin, and especially the groundwater and soil water processes are overly simplified. Hence it is difficult to assess the effects of changing soil characteristics on Meuse discharge, although changes in soil water holding capacity have been estimated.

These limitations inevitably introduce uncertainties in our results, and hence they should be used with caution. The discharge results should not be taken as exact figures for each period studied, but rather they give an indication of the main trends in mean discharge and flood frequency over the late Holocene, and can be used to examine relative changes between the time-slices studied. Similarly, the land use data do not represent the exact situation per century, but give an indication of the trend in land use change over the last millennium, and hence allow for an investigation of the sensitivity of the hydrological system to those changes.

Despite these limitations, the calibration and validation of the model was successful for annual, monthly, and daily discharge characteristics. Furthermore, the climate and discharge results are in agreement with the general trends inferred from the limited local and regional multi-proxy data. One of the major advantages of our approach is that we were able to perform millennial scale simulations in ensemble mode, with multiple land use scenarios, which would not have been feasible with a full GCM.

3.6 Conclusions

According to our simulations the mean discharge, flood frequency, and flood magnitudes of the Meuse river were significantly greater in the last millennium than in the period 4000-3000 BP, as was the variability of mean annual discharge. The mean annual discharge increased by 6.6% between these time-slices; the most marked increase occurred in the summer half-year (+21.6%). The recurrence time of large high-flow events ($Q > 3000\ m^3\ s^{-1}$) decreased from 77 years in the period 4000-3000 BP, to 65 years in 1000-2000 AD. On this timescale the increases in mean discharge and flood frequency can be almost fully attributed to changes in land use, and namely decreased evapotranspiration as a result of the large-scale deforestation of the basin. On a millennial timescale climatic change has had a minor effect on late Holocene Meuse discharge.

However, between the 19th and 20th Centuries climate change has overwhelmed land use change as the most important mechanism. Although evapotranspiration was higher in the 20th Century than in the 19th Century (due to reforestation and increased temperature), the mean discharge was greater in the 20th Century than during any preceding century, and 2.5% greater than in the 19th Century. The occurrence of large high-flows ($Q > 3000\ m^3\ s^{-1}$) was almost twice as frequent

during the 20th Century as during the natural reference period 4000-3000 BP. Mean discharge and flood frequency were also greater in the 20th Century than in the period 1000-1900 AD, although the discharge and flood frequency in the latter period were still greater than in the natural reference period 4000-3000 BP. The increases in mean discharge and flood frequency in the 20th Century are the result of a strong increase in annual and winter half-year precipitation compared to the preceding centuries, probably related to anthropogenic climate change. The effect of land use change alone between the 19th and 20th Centuries was to force a slight decrease in mean discharge and flood frequency, but these decreases were more than compensated for by increased precipitation in the 20th Century.

Many basins in western Europe have experienced similar changes in land use as a result of human activities during the late Holocene, and similar land use changes have occurred at different times throughout the mid-latitudes. The results of this study suggest that more research is needed to examine the potential contribution of land use management to flood mitigation in these regions. Theoretically, large-scale reforestation may offer protection against increased flooding in basins with a similar hydrological setting to the Meuse. However, in many basins space is at a premium, and large-scale reforestation is not a viable option. Therefore, further experiments are needed to assess the relative effects of limited reforestation in the coming century, in combination with projected climate change scenarios. Since our model has been validated against (limited) multi-proxy data on a millennial timescale, and for large environmental changes, it forms a useful tool for such assessments.

Chapter 4

Sensitivity of discharge and flood frequency to 21st Century and late Holocene changes in climate and land use (River Meuse, northwest Europe)

Abstract

We used a coupled climate-hydrological model to simulate River Meuse discharge over the late Holocene (4000-3000 BP and 1000-2000 AD). We then used this model to simulate discharge in the 21st Century under SRES emission scenarios A2 and B1, with and without future land use change. Mean discharge and high-flow frequency increased significantly between 4000-3000 BP and 1000-2000 AD; almost all of this increase can be attributed to the conversion of forest to agriculture. Between the 19th and 20th Centuries, further increases in discharge and high-flow frequency occurred due to increased (winter half-year) precipitation. Between the 20th and 21st Centuries discharge and high-flow frequency may increase further still by an order of magnitude similar to, or greater than, that of the last 4000 years. Over the 21st Century, climatic change dominates the impacts on hydrology; the effects of the future land use change scenarios used are statistically insignificant. The magnitude of extreme flood events (return period 1250-yrs) is significantly greater in the 21st Century under scenario A2 than in the 20th Century. In contrast to the long-term influence of deforestation on mean discharge, changes in forest cover have had little effect on these extreme floods, even on the millennial timescale.

This chapter is based on the paper: Ward, P.J., Renssen, H., Aerts, J.C.J.H., Verburg, P.H., 2008. Sensitivity of discharge and flood frequency to 21st Century and late Holocene changes in climate and land use (River Meuse, northwest Europe). Submitted to Climatic Change.

4.1 Introduction

The relatively large number of high-flow events on the River Meuse (Fig. 4.1) in recent years, compared to the rest of the 20th Century (De Wit et al., 2007b), has led to widespread public, academic, and political interest. Future climate change is expected to have major impacts on river discharge (Kundzewicz et al., 2007), hence many modelling studies have been carried out to assess the potential changes in Meuse discharge and flood frequency in the 21st Century (e.g. Booij, 2005; Bultot et al., 1988, 1990; De Wit et al., 2001, 2007a; Gellens, 1991; Gellens and Roulin, 1998; Middelkoop et al., 2004; Van Deursen and Middelkoop, 2001, 2002).

To date, these studies have used models calibrated and validated against observed discharge data of the last century, and have compared projected discharge and flood frequencies in the 21st Century with those of the last 100 years. However, simulations of long-term changes (centuries to millennia) could help to understand the characteristics of natural decadal-centennial scale variability in discharge (Arnell et al., 2001), and to assess future changes in the context of natural variability. Ward et al. (2007; Chapter 2) simulated the discharge of 19 river basins around the world on a monthly time-step for three periods during the Holocene, and Aerts et al. (2006) extended these simulations for the period 9000 BP until 2100 AD for 15 of the basins. The results of the latter study showed that river discharges in the majority of the basins are more sensitive to future climate change than to natural climate variability over the last 9000 years. These simulations were carried out with a monthly time-step, and only considered natural changes in land use in response to long-term climatic change. Ward et al. (2008a; Chapter 3) simulated the daily discharge of the Meuse over the periods 4000-3000 BP and 1000-2000 AD. The period 4000-3000 BP was selected as a natural reference period since the natural climatic forcings at that time were broadly similar to those of today (Goudie, 1992), whilst human influence on land use was minimal (Bunnik, 1995; Gotjé et al., 1990; RWS Limburg/IWACO, 2000). The basin was heavily influenced by human activities in the period 1000-2000 AD, namely changes in land use throughout the period, and greenhouse gas and sulphate aerosol emissions since the industrial revolution. The results showed that the discharge and frequency of high-flows increased over the course of the last millennium, mainly as a result of decreased evapotranspiration due to the large-scale conversion of forest to agricultural land. However, despite reforestation over the last 100 years, discharge and high-flow frequency increased between the 19th and 20th Centuries. Almost all of this increase can be explained by the simulated increase in precipitation, particularly in the winter half-year (November-April). Hence, climate and land use have both had major effects on late Holocene Meuse discharge on different timescales. Assessments of the future effects of these factors would allow us to assess future change in the context of millennial scale natural and human-induced environmental change. Furthermore, as the results of Ward et al. (2008a; Chapter 3) are in good agreement with the limited multi-proxy evidence available, the model's performance has been verified to some extent for a period when environmental conditions were different to those of today.

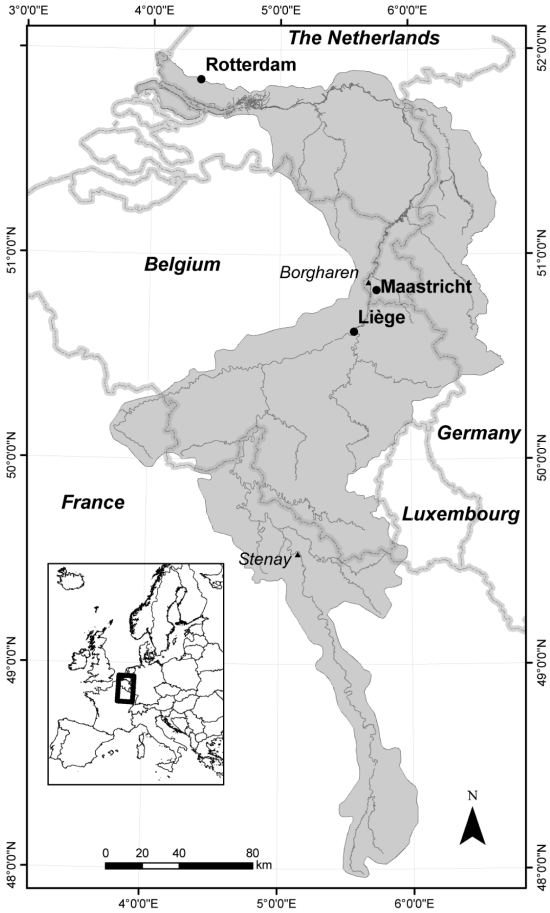

Fig. 4.1: Map showing the location of the Meuse Basin (after RWS Limburg/IWACO, 2000). For this study the model was set up upstream from Borgharen. The inset shows the location of the Meuse basin in Europe.

The aim of the present study is to simulate the daily discharge of the Meuse in the 21st Century, in order to assess the effects of projected climate and land use change on discharge and flood frequency. These effects will be analysed against those caused by natural and anthropogenic environmental changes over the course of the late Holocene, as simulated by Ward et al. (2008a; Chapter 3). This will allow us to assess the nature and scale of future changes in discharge and flood frequency in the context of long-term (millennial) changes; such analyses are currently lacking around the globe.

4.2 Study area

The Meuse is a predominantly rain-fed river with a total length of ca. 875 km. For this study the basin has been modelled upstream from Borgharen (Fig. 4.1).

The model was set up upstream from this point for a number of reasons. Firstly, discharge measurements at Borgharen, corrected for canal extractions between Liège and Borgharen, are available since 1911, which is the longest observed discharge time-series in the basin, and allows for model calibration and validation. Secondly, current water management practice in the Netherlands uses daily discharge observations at Borgharen in the estimation of flood return periods. Thirdly, we did not model the basin as far downstream as the current Rhine-Meuse confluence, since its location has changed over the course of the Holocene (Berendsen and Stouthamer, 2001). Mean annual precipitation over the basin is ca. 950 mm a^{-1}, and is reasonably evenly distributed throughout the year. The spatial distribution of precipitation is to a large extent a reflection of elevation and distance from the coast. Mean temperatures show marked seasonal variations, and annual potential evapotranspiration is much greater in the summer half-year (May-October) than in the winter half-year (November-April) (76% and 24% of the total respectively). The mean annual discharge of the Meuse and its associated canals at the border of Belgium and the Netherlands is ca. 276 m^3 s^{-1}; summer and winter half-year mean discharge are 146 m^3 s^{-1} and 406 m^3 s^{-1} respectively (Ashagrie et al., 2006).

4.3 Methods

Initially, the climate model ECBilt-CLIO-VECODE (Brovkin et al., 2002; Goosse and Fichefet, 1999; Opsteegh et al., 1998) was coupled with the hydrological model STREAM (Aerts et al., 1999) to simulate Meuse palaeodischarge at a spatial resolution of 2’ x 2’ with a daily time-step, for the periods 4000-3000 BP and 1000-2000 AD (Ward et al., 2008a; Chapter 3). Climate change was modelled in a transient manner, whilst land use configurations were stationary for periods of one century. The model was calibrated against observed data. In the present study the experiment was subsequently continued until 2100 AD.

ECBilt-CLIO-VECODE is a three-dimensional coupled climate model consisting of three components describing the atmosphere, ocean, and vegetation (Brovkin et al., 2002; Goosse and Fichefet, 1999; Opsteegh et al., 1998). The output used in this study were forced by annually varying orbital parameters (Renssen et al., 2005a); atmospheric volcanic aerosol content and fluctuations in solar activity following Goosse et al. (2005); and atmospheric greenhouse gas and sulphate aerosol concentrations following Renssen et al. (2005a) for 4000-3000 BP and 1000-1750 AD, and Goosse et al. (2005) for 1750-2000 AD. For the 21st Century, atmospheric volcanic aerosol content and fluctuations in solar activity were assumed to have the same values as for the 20th Century (Goosse et al., 2005) in order to facilitate comparisons between the 20th and 21st Centuries, and atmospheric greenhouse gas and sulphate aerosol concentrations were prescribed according to the Special Report on Emission Scenarios (SRES) of the Intergovernmental Panel on Climate Change (IPCC, 2000). We used SRES emission scenarios A2 and B1 since these lie towards the upper and lower end of the full spectrum of IPCC scenarios respectively in terms of projected temperature

change by the end of the 21st Century, and can therefore be used to assess the response of the system to a broad range of possible future changes. Compared to the baseline concentration of atmospheric CO_2 in 1990 AD (ca. 354 ppm), the A2 and B1 scenarios prescribe increases to 836 ppm and 540 ppm respectively by 2100 AD.

The climate model experiments were run in ensemble mode, with four ensemble members. Each ensemble member represents a single model run. The ensemble members are forced using the same climatic parameters, but with slightly different initial climatic conditions to account for the chaotic behaviour of the atmospheric system. Hence, the difference between the ensemble members gives an idea of the natural variability, whereas an ensemble mean can be used to evaluate long-term trends.

Land use configurations for the 20th and 21st Centuries were obtained from the EURURALIS 2.0 project (WUR/MNP, 2007; www.eururalis.eu). For the 20th Century the land use configuration was based on the situation in 2000 AD. For the 21st Century the land use configuration was based on the projected situation following the scenarios 'Continental Market' and 'Global Cooperation', which correspond with the storylines of the climate emission (SRES) scenarios A2 and B1 respectively. Throughout the rest of this paper we therefore refer to these land use scenarios as A2 and B1. However, since the focus of the SRES scenarios (IPCC, 2000) is completely outside land use, agriculture, and rural development, and lacks the regional disaggregation needed for high resolution land use modelling (Verburg et al., 2006), the EURURALIS scenarios were elaborated for land use issues and agricultural policies typical for Europe (Westhoek et al., 2006). Future land use change was simulated with an extended version of the global economic model (GTAP) and an integrated assessment model (IMAGE) to calculate changes in demand for agricultural area at the country level, whilst a spatially explicit land use change model (CLUE-s) was used to translate these land claims into land use patterns at a 1 km x 1 km resolution (Verburg et al., 2006, 2008). Since land use change is dependent on physical, socio-economic, and political processes (such as changes in the common agricultural policy, oil prices, etc.) (Van Rompaey et al., 2002; Verburg, 2006), it is difficult to simulate meaningful scenario changes for long timeframes, and therefore the results for the 21st Century are highly sensitive to future socio-economic and political decisions and preferences. Therefore, the land use simulations of the EURURALIS project were made only up to 2030 AD, thereby indicating the possible long-term trend relative to that of the last millennium. The projected land use for 2030 AD was used for the entire 21st Century. The use of a stationary land use scenario per century allows for a direct comparison with the results for 4000-3000 BP and 1000-2000 AD, for which the same method was used.

The land use maps were reclassed to crop factor maps. A crop factor map is used in STREAM to calculate potential evapotranspiration (*PE*). The crop factor is a

dimensionless factor by which the reference *PE* is multiplied in order to account for the difference in *PE* over different land use types. The land use maps were reclassed to crop factors based on values in Kwadijk (1993) and Aerts and Bouwer (2002): urban (0.8); forests (1.1); agriculture and grasslands (0.9); wetlands (1.1); and water bodies (1.5). Hence, the effects of land use change as simulated in this study only pertain to changes in the coverage of each land use type, and not to future changes in factors such as land use intensity (e.g. changes in crop types, irrigation etc.) or changes in water management measures (e.g. water retention basins). The examination of such measures would require the use of a higher resolution and more complex hydrological model. However, the use of such a model would prohibit the examination of future changes with respect to long-term millennial changes (due to prohibitive computational time), which is the main aim of this study.

STREAM is a grid-based spatially distributed water balance model that describes the hydrological cycle of a drainage basin as a series of storage compartments and flows (Aerts et al., 1999). The STREAM hydrological model was run for the 21st Century for climate scenarios A2 and B1, both with and without land use change, in order to assess the relative effects of these factors on discharge and high-flow events.

4.4 Results

4.4.1 Land use change

The relative change in basin-averaged land use (upstream from Borgharen) between the 20th and 21st Centuries is shown in Table 4.1. In Appendix 2, maps showing the changes in the spatial distribution of land use can be found. The overall change in land use in the A2 scenario is small. This scenario depicts a world of divided regional blocks in which each block strives for self sufficiency so as to be less reliant on other blocks. Agricultural trade barriers and support mechanisms continue to exist. In combination with high economic growth in the region, claims on land resources are high for both urbanisation and agriculture. As a result, agricultural abandonment is limited. In spite of the low net changes there are some shifts in land use patterns: marginal, low intensity grasslands on the steep slopes of the Belgian Ardennes are reforested, whilst some patches of forest in the areas more suitable for agriculture (on the plateaus and the margins of the region) are reclaimed for agriculture.

Under the B1 scenario the forested area increases by ca. 2%, whilst the area under agriculture and grassland decreases by about the same amount. The B1 scenario depicts a world of successful international cooperation aimed at poverty reduction and environmental protection. Trade barriers are removed and governance aims at protecting cultural and natural heritage values. Increased global trade in agricultural commodities, in combination with increased productivity, leads to lower claims on agricultural lands in marginal areas, such as large parts

of the Meuse basin. As crops can be produced much more efficiently in other regions of Europe (and the rest of the world), large areas of arable land in the Meuse catchment could potentially be abandoned or reforested. However, under this scenario subsidies for farmers in less suitable areas are maintained, and since most of the Meuse basin is eligible for such subsidies, land abandonment is reduced to a large extent.

In both scenarios the rate of urbanisation is rather low. This is mainly due to the limited number of major cities located in the catchment, and the catchment's location outside the core economic regions of the riparian countries. Large areas of agricultural land in western Belgium (outside the Meuse basin) are converted to urban area; this loss of prime agricultural land provides another incentive for farmers in the eastern part of the country (where the Meuse catchment is situated) to continue farming.

Table 4.1: Land use upstream from Borgharen for the 20th and 21st Centuries, reclassed to the land use classes shown in the table.

	Time-period		
Land use class	20th Century	21st Century (A2)	21st Century (B1)
Urban	9.7%	10.3%	10.3%
Forests	34.7%	34.6%	36.6%
Agriculture and grasslands	54.7%	54.6%	52.6%
Other	0.9%	0.5%	0.5%

4.4.2 Long-term trends in climate and discharge

The long-term changes in mean 50-yr discharge at Borgharen, and basin-averaged mean annual temperature and precipitation per 50-yr period, are shown in Fig. 4.2; in these simulations the 21st Century experiments are carried out using the A2 and B1 climate and land use configurations.

Over the course of the late Holocene, mean 50-yr temperature shows a statistically significant long-term decreasing trend (Fig. 4.2). This trend is also evident over the period 1000-1900 AD (Mann-Kendall (MK) test, $p < 0.001$). However, since the period 1800-1850 AD, the curve of mean temperature (Fig. 4.2) shows a sustained increasing trend, with large increases in the 21st Century under both the A2 and B1 scenarios, to temperatures far higher than those in any other period studied. By 2050-2100 AD the simulated mean annual temperatures are 1.70˚C (A2) and 1.13˚C (B1) higher than during the period 1950-2000 AD.

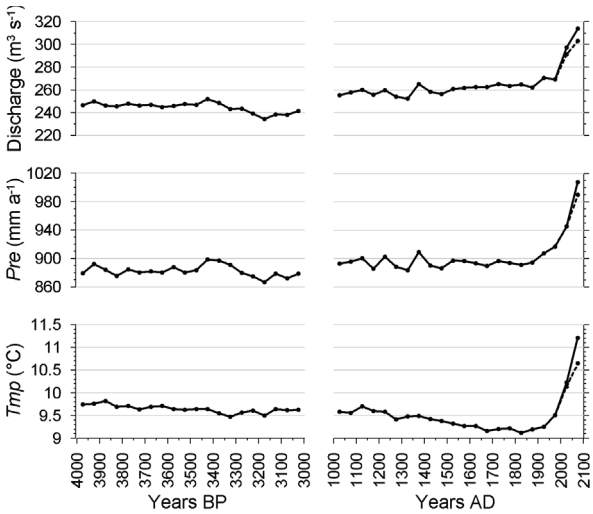

Fig. 4.2: Long-term changes in mean annual discharge at Borgharen, basin-averaged precipitation (pre), and basin-averaged temperature (tmp). The means of the four ensemble members are shown for each 50-yr period. For the 21st Century the A2 scenario is shown as an unbroken line (upper), and the B1 scenario as a dotted line (lower).

Whilst mean 50-yr precipitation shows no significant monotonic trend in either the period 4000-3000 BP or 1000-2000 AD (MK-test, p = -0.1048 and p = -0.2176 respectively), mean annual precipitation is significantly greater in 1000-2000 AD than in 4000-3000 BP (Fig. 4.2). Despite there being no significant monotonic trend over the last millennium, the simulations again show a sustained increase after the period 1800-1850 AD (Fig. 4.2). The simulated mean precipitation in the period 1950-2000 AD (917.2 mm a^{-1}) is higher than in any preceding 50-yr period, with even stronger increases simulated for the 21st Century, reaching ca. 1008.1 mm a^{-1} and 989.9 mm a^{-1} by 2050-2100 AD under scenarios A2 and B1 respectively.

The effects of long-term changes in climate and land use on discharge are also shown in Fig. 4.2. The mean 50-yr discharge increased significantly (t-test, $p < 0.001$) from ca. 244.8 m^3 s^{-1} in 4000-3000 BP to ca. 261.0 m^3 s^{-1} in 1000-2000 AD, and mean annual discharge shows a significant increasing trend over the period 1000-2000 AD (MK-test, $p < 0.001$). Moreover, the mean annual discharge in the 20th Century (270.0 m^3 s^{-1}) is significantly higher than during the rest of the last millennium (t-test, $p < 0.001$). This long-term trend of increasing mean 50-yr discharge continues and strengthens in the 21st Century; the modelled discharges for the period 2050-2100 AD of 314.0 m^3 s^{-1} (A2) and 303.3 m^3 s^{-1} (B1) are much higher than during any other 50-yr period in the time-slices studied (Fig. 4.2).

4.4.3 Changes in climate and discharge between the 20th and 21st Centuries

The long-term simulations of temperature, precipitation, and discharge all suggest large increases over the coming century, resulting in values far greater than those seen over the last 4000 years. In this section we examine the changes in climate and discharge in the 20th and 21st Centuries in more detail. In Figs. 4.3 (scenario A2) & 4.4 (scenario B1), the 10-yr running means of the four ensemble runs are given for temperature, precipitation, actual evapotranspiration (*AE*), and discharge, in the period 1900-2100 AD; the results are shown per season, i.e. winter (December, January, February), spring (March, April, May), summer (June, July, August), and autumn (September, October, November).

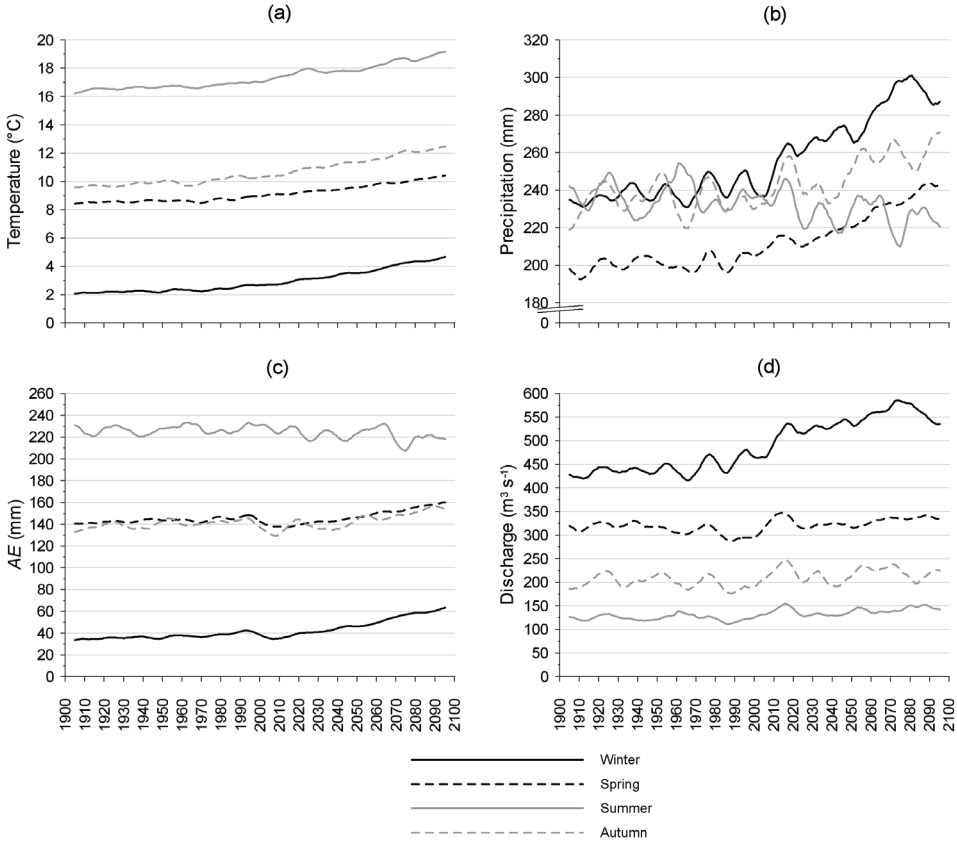

Fig. 4.3: 10-yr running means (scenario A2) of the four ensemble members for basin-averaged (a) temperature, (b) precipitation, and (c) actual evapotranspiration (AE), and for (d) mean discharge at Borgharen. The results are shown for winter (December, January, February), spring (March, April, May), summer (June, July, August), and autumn (September, October, November).

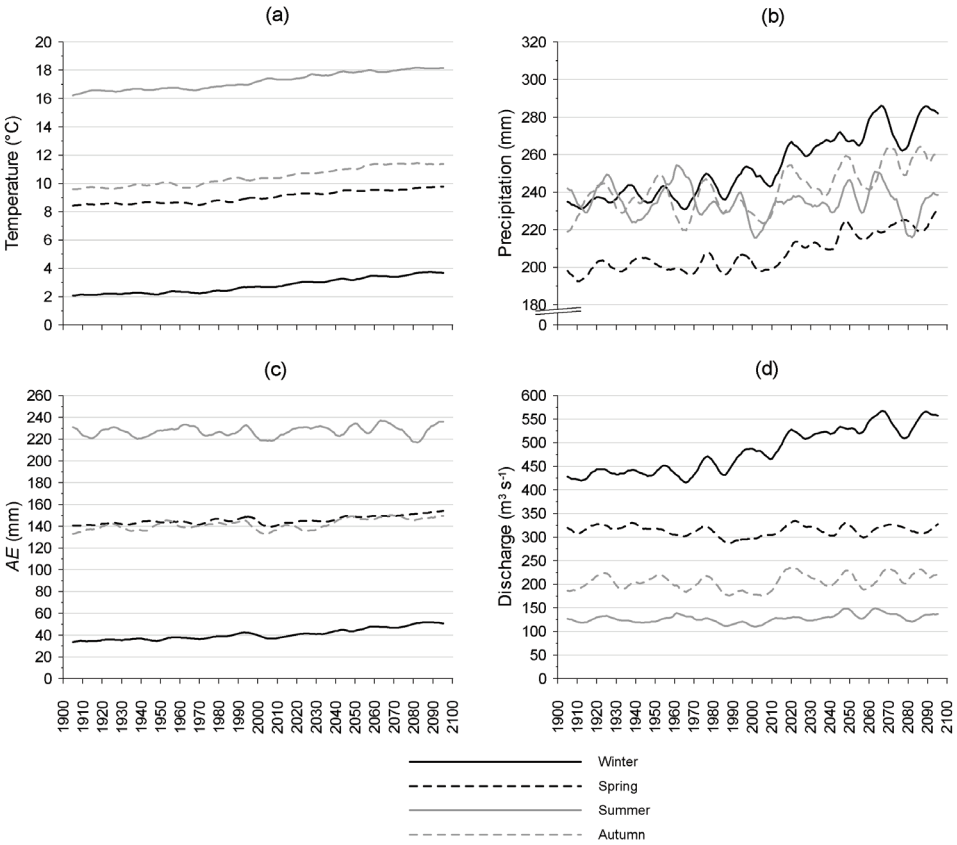

Fig. 4.4: 10-yr running means (scenario B1) of the four ensemble members for basin-averaged (a) temperature, (b) precipitation, and (c) actual evapotranspiration (AE), and for (d) mean discharge at Borgharen. The results are shown for winter (December, January, February), spring (March, April, May), summer (June, July, August), and autumn (September, October, November).

Over the course of the 20th Century, annual mean, summer half-year, and winter half-year temperature all show significant upward trends (MK-test, $p < 0.001$). For the 21st Century, the results of the MK-test to detect monotonic trends (Table 4.2) reveal significant positive trends in mean annual temperature under both scenarios. Moreover, highly significant positive trends are simulated for all seasons, with the trends in the 21st Century being stronger than those during the 20th Century. Mean annual temperature in the period 2050-2100 AD is projected to be 1.70˚C (A2) or 1.13˚C (B1) higher than in the period 1950-2000 AD. The resulting mean annual temperature for the period 2050-2100 AD under the A2 scenario (ca. 11.21˚C) is significantly higher than that under scenario B1 (10.65˚C) (t-test, $p < 0.001$). The difference in mean annual temperature in the first half of the 21st Century (2000-2050 AD) between A2 and B1 (0.09˚C) is already significant (t-test, $p = 0.034$).

Table 4.2: Results of the Mann-Kendall (MK) test to assess the presence or absence of a monotonic trend (in temperature (tmp), precipitation (pre), actual evapotranspiration (AE), and discharge) over the course of the 21st Century. A positive MK statistic represents a positive trend, whilst a negative MK statistic represents a negative trend. Probabilities with statistical significance (α = 0.05) are shown in bold. The results are shown for mean annual values, as well as values for winter (December, January, February), spring (March, April, May), summer (June, July, August), and autumn (September, October, November).

	Period									
	Annual		Winter		Spring		Summer		Autumn	
	MK	p	MK	p	MK	p	MK	p	MK	p
A2 Scenario										
Tmp	11.92	**<0.001**	12.23	**<0.001**	10.43	**<0.001**	8.71	**<0.001**	10.67	**<0.001**
Pre	4.96	**<0.001**	6.53	**<0.001**	7.61	**<0.001**	-1.83	0.067	5.84	**<0.001**
AE	5.81	**<0.001**	12.24	**<0.001**	10.33	**<0.001**	-1.60	0.109	4.75	**<0.001**
Discharge	2.91	**0.004**	4.34	**<0.001**	1.96	**0.049**	1.96	**0.049**	0.42	0.671
B1 Scenario										
Tmp	9.30	**<0.001**	9.13	**<0.001**	7.29	**<0.001**	5.69	**<0.001**	7.43	**<0.001**
Pre	4.8	**<0.001**	4.14	**<0.001**	5.68	**<0.001**	1.07	0.284	3.19	**0.001**
AE	6.02	**<0.001**	9.12	**<0.001**	7.65	**<0.001**	1.643	0.100	4.55	**<0.001**
Discharge	3.20	**0.001**	3.82	**<0.001**	1.02	0.306	1.99	**0.047**	1.51	0.130

During the 21st Century, significant positive trends are simulated for mean annual precipitation under both scenarios (Table 4.2). These significant increasing trends are expected over the 21st Century in winter, spring, and autumn under both scenarios, with the greatest increase in winter (Figs. 4.3b & 4.4b and Table 4.2). Summer precipitation decreases somewhat between the periods 1950-2000 (238.2 mm a^{-1}) and 2050-2100 for both scenario A2 (226.2 mm a^{-1}) and B1 (236.3 mm a^{-1}), although this decrease is not statistically significant in either case (t-test, p = 0.070 and p = 0.752 for A2 and B1 respectively). In relation to the mean annual precipitation of 917 mm a^{-1} in the period 1950-2000 AD, increases of 91 mm a^{-1} and 73 mm a^{-1} are expected by 2050-2100 AD under scenarios A2 and B1 respectively. Hardly any difference in mean annual precipitation is simulated between scenarios A2 (945.9 mm a^{-1}) and B1 (945.7 mm a^{-1}) during the first half of the 21st Century (t-test, p = 0.989). For both scenarios, no changes in the interannual variability of precipitation are projected for any season (F-test, α = 0.05), except for an increased variability during the spring under scenario A2.

The interactions of changes in temperature and precipitation, as well as soil moisture content, have an effect on the simulated values of actual evapotranspiration (*AE*). Due to increasing trends in temperature over the course of the 20th Century, mean annual and winter half-year *AE* also increased significantly over that time-

period. Mean annual *AE* shows a strong and significant increasing trend over the course of the 21st Century under both scenarios A2 and B1 (Table 4.2), with the greatest increase under the former scenario. Reference to Figs. 4.3c & 4.4c and Table 4.2 shows significant increasing trends in *AE* for all seasons under both scenarios, except for in the summer, for which no significant trend is simulated under either scenario. The absence of trends in summer *AE*, despite the increased temperature, can be explained by two factors: (a) slightly decreased summer season precipitation between the periods 1950-2000 and 2050-2100, and (b) less soil moisture availability in the summer season due to increased *AE* in the preceding months.

No significant trends in either annual, summer half-year, or winter half-year discharge were simulated over the course of the 20th Century. However, for the 21st Century the results of the present study show clear increasing trends in mean annual discharge (Table 4.2) under both scenarios. For the first half of the 21st Century, the mean annual discharges for scenarios A2 (297.4 $m^3 s^{-1}$) and B1 (291.4 $m^3 s^{-1}$) are both significantly higher than that of the period 1950-2000 AD (269.2 $m^3 s^{-1}$) (t-test, $p < 0.001$), although the difference between the two scenarios is not significant (t-test, $p = 0.232$). During the second half of the 21st Century these mean discharges are even greater (A2 = 314.0 $m^3 s^{-1}$, B1 = 303.3 $m^3 s^{-1}$), and the difference between the scenarios is significant (t-test, $p = 0.027$).

The vast majority of the increase in discharge under both scenarios is derived from the increase in winter season discharge (Figs. 4.3d & 4.4d). Nevertheless, between the periods 1950-2000 AD and 2050-2100 AD, mean discharge increases significantly for all seasons under both the A2 and B1 scenarios (t-test, $\alpha = 0.05$). Summer season discharge increases from 125.2 $m^3 s^{-1}$ in 1950-2000, to 142.9 $m^3 s^{-1}$ (A2) and 135.6 $m^3 s^{-1}$ (B1) in the period 2050-2100. This is despite statistically insignificant decreases in mean summer precipitation of ca. 12 mm (A2) and ca. 2 mm (B1) between 1950-2000 and 2050-2100, and no significant changes in *AE* between those periods. Hence, the changes in discharge cannot be accounted for by precipitation change alone. The modelled values of monthly groundwater storage shed light on these results; significant increases during the summer months occur under both scenarios as a result of the strong increase in precipitation during the preceding autumn, winter, and spring. Hence, the modelled reduction in surface flow due to slightly decreased summer precipitation is more than compensated for by increasing baseflow.

4.4.4 High-flow events

The frequency of high-flow events increased significantly between the natural reference period (4000-3000 BP) and 1000-2000 AD (Kolmogorov-Smirnov (KS) test, $p < 0.001$), with a further increase in the 20th Century. In Fig. 4.5 these results can be seen alongside those for the 21st Century. A clear increase in the frequency of high-flow events can be seen for both scenarios, even compared to the already augmented high-flow frequencies of the 20th Century (KS-test, $p < 0.001$).

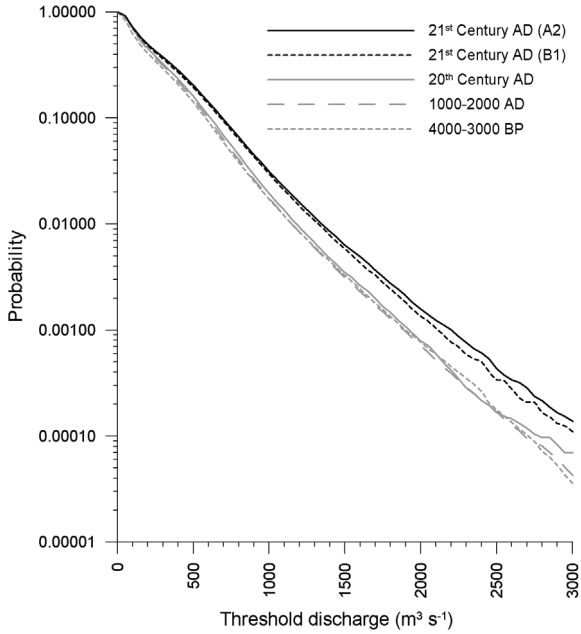

Fig. 4.5: Probability of daily discharge over a threshold. High-flow events of Q > 3000 $m^3 s^{-1}$ (similar in magnitude to the major floods of 1926 and 1993) are predicted more frequently in the 21st Century than in any of the preceding time-periods shown, with the greatest increase under scenario A2.

Based on these daily frequency distributions, we examined the changes in the simulated recurrence times of high-flow events of the following magnitudes: Q > 800 $m^3 s^{-1}$, 1300 $m^3 s^{-1}$, 1950 $m^3 s^{-1}$, and 3000 $m^3 s^{-1}$ (Table 4.3). These correspond approximately to the discharge percentiles Q_{95}, Q_{99}, $Q_{99.9}$, and $Q_{99.995}$ in the observed record at Borgharen (1912-2000 AD). For the 21st Century, large increases are expected for all of these discharge percentiles under both scenarios. For example, high-flows with a magnitude of 3000 $m^3 s^{-1}$ (similar in magnitude to the major floods of 1926 and 1993) are expected to occur under scenario A2 twice as frequently as in the 20th Century, and almost four times as frequently as during the natural reference period 4000-3000 BP.

In order to assess the change in the frequency of extreme flood events over the late Holocene, and under the two future change scenarios, we applied extreme value statistics to the simulated annual maximum discharges; for each time-period we lumped the results of the four ensemble members. We first assessed the quality of fit of several extreme value distributions (Gamma, GEV, Gumbel, Johnson, Lognormal, Pareto, Weibull) against the simulated values for the periods 4000-3000 BP, 1000-2000 AD, and the 21st Century, using the KS and χ^2 tests; we found that the Gumbel distribution gave the best overall fit.

Table 4.3: Simulated recurrence times of daily discharge (Q) in excess of 800, 1300, 1950, and 3000 $m^3 s^{-1}$; these discharge magnitudes correspond approximately to discharge percentiles Q_{95}, Q_{99}, $Q_{99.9}$, and $Q_{99.995}$ respectively, in the observed time-series for Borgharen between 1912-2000 AD.

	Discharge ($m^3 s^{-1}$)			
Time-period	> 800	> 1300	> 1950	> 3000
4000-3000 BP	26 days	165 days	3.2 years	77 years
1000-2000 AD	25 days	168 days	3.4 years	65 years
20th Century	22 days	150 days	3.0 years	40 years
21st Century (A2 scenario)	15 days	86 days	1.5 years	20 years
21st Century (B1 scenario)	16 days	92 days	1.8 years	25 years

We then fit Gumbel distributions to each of the time-periods studied, and used these to estimate the magnitude of flood events with long return periods. In Table 4.4 the discharge magnitudes associated with flood events with a recurrence time of 1250 years are shown. The changes in these discharge magnitudes are small between the periods 4000-3000 BP, 1000-2000 AD, and the 20th Century. For the 21st Century, relatively large increases in the discharge magnitude can be seen, especially for scenario A2, which falls outside the upper 95% confidence limit of the 20th Century simulation. The results in Table 4.4 also show that the effects of land use change on the magnitude of such extreme events is small, with little change simulated between the periods 4000-3000 BP and 1000-2000 AD, despite a reduction in forest cover of more than 50%.

Table 4.4: Discharge magnitude associated with a high-flow event with return period 1250 years. These magnitudes are obtained by fitting a Gumbel distribution to the values of annual maximum discharge. The values presented in the table are based on the simulation results for all four ensemble members. The value for observed discharge is based on the observed annual maximum discharges at Borgharen for the period 1912-2000 AD. For the 20th Century simulations, the discharge magnitude associated with the upper and lower 95% confidence limits of the Gumbel distribution are also shown; for the 21st Century the discharge magnitude falls outside these limits under the A2 scenario.

Simulation	Discharge ($m^3 s^{-1}$)
Observed discharge (1912-2000 AD)	4112
20th Century	4137
20th Century (lower/upper 95% confidence limits)	3857/4416
4000-3000 BP	4093
1000-2000 AD	4073
21st Century (A2: climate and land use)	4615
21st Century (A2: climate only)	4617
21st Century (B1: climate and land use)	4350
21st Century (B1: climate only)	4357

4.4.5 Relative contributions of climate and land use change to changes in discharge

Our results show significant increases in the mean discharge and frequency of high-flows on the Meuse in the 21st Century compared to the 20th Century. In Table 4.5 it can be seen that the combined effects of climate and land use change on mean annual, summer half-year, and winter half-year discharge, as well as a number of high-flow percentiles, are statistically significant (t-test, $\alpha = 0.05$); the signal of increased discharges is therefore greater than the associated noise. In order to assess the relative contribution of changes in climate and land use to these increases, we carried out further simulations with STREAM, but using the land use configuration of the 20th Century in combination with the 21st Century climate data, and vice versa. In this way the effects of changes in climate and land use were delineated; the results are also shown in Table 4.5. For both scenarios, the effects of land use change alone on mean annual discharge are small (< 0.1% (A2) and -0.6% (B1)), and statistically insignificant (t-test, $\alpha = 0.05$). Under scenario B1, land use change does force a decrease in mean summer discharge of ca. 1.5%, but this effect is still much smaller (and with the opposite sign) than that of projected climate change. In all cases the effect of projected land use change on the magnitude of high-flow events is small and statistically insignificant; almost all of the increase in the magnitude of discharge percentiles Q_{90}, Q_{95}, Q_{99}, and $Q_{99.9}$ can be explained by the projected changes in climate. The effects of land use change as simulated in this study, only pertain to changes in the crop factor and in the water holding capacity of the soil resulting from changes in land use. Changes in land use intensity or water management measures (e.g. water retention areas) may have a greater influence on discharge. However, the results are indicative of the long-term (millennial) changes in discharge characteristics due to the effects of land use conversion on evapotranspiration and soil water storage.

Table 4.5: Percentage change in absolute values of mean annual (Q_{ann}), summer half-year (May-October) (Q_{sum}), and winter half-year (November-April) (Q_{win}) discharge and various high-flow percentiles (Q_k, k = 90, 95, 99, 99.9) between the 20th and 21st Centuries under scenario A2 (above) and B1 (below). Changes with statistical significance (t-test, α = 0.05, n = 400) (100 years x four ensemble members) are shown in bold type; the t-test was carried out on the annual values for each parameter.

	Q_{ann}	Q_{sum}	Q_{win}	Q_{90}	Q_{95}	Q_{99}	$Q_{99.9}$
Percentage change between 20th Century and 21st Century (A2 scenario)							
Climate and land use	**+13.2**	**+10.3**	**+14.2**	**+12.8**	**+12.9**	**+13.8**	**+14.4**
Climate only	**+13.2**	**+10.5**	**+14.1**	**+12.6**	**+12.7**	**+13.7**	**+14.4**
Land use only	-	-0.2	+0.1	+0.2	+0.2	+0.1	-
Percentage change between 20th Century and 21st Century (B1 scenario)							
Climate and land use	**+10.1**	+4.6	**+12.0**	**+11.2**	**+11.3**	**+12.2**	**+9.6**
Climate only	**+10.7**	**+6.1**	**+12.3**	**+11.4**	**+11.5**	**+12.3**	**+9.8**
Land use only	-0.6	-1.5	-0.3	-0.2	-0.2	-0.1	-0.2

We also carried out a similar exercise to assess the relative effects of changes in climate and land use change on discharge between the natural reference period 4000-3000 BP and the 21st Century; the results are shown in Table 4.6. For both scenarios, the effects of climate and land use change on mean annual discharge have been of a similar order of magnitude on this timescale; the effects of land use change have been stronger in the summer half-year, whilst the effects of climate change have been stronger in the winter half-year. For all of the high-flow percentiles shown here, both changes in climate and land use have caused significant increases between the natural reference period and the 21st Century.

Table 4.6: Percentage change in mean annual (Q_{ann}), summer half-year (May-October) (Q_{sum}), and winter half-year (November-April) (Q_{win}) discharge and various high-flow percentiles (Q_k, k = 90, 95, 99, 99.9) between the period 4000-3000 BP and the 21st Century under scenario A2 (above) and B1 (below). On this timescale the effects of climate and land use change on mean annual discharge have been of a similar order of magnitude; the effects of land use change have been stronger in the summer half-year, whilst the effects of climate change have been stronger in the winter half-year. For all of the discharge percentiles shown here, both changes in climate and land use have caused changes with statistical significance (t-test, α = 0.05, n = 400) (100 years x four ensemble members).

	Q_{ann}	Q_{sum}	Q_{win}	Q_{90}	Q_{95}	Q_{99}	$Q_{99.9}$
Percentage change between 4000-3000 BP and 21st Century (A2 scenario)							
Climate and land use	+26.7	+41.3	+22.4	+20.8	+20.0	+18.9	+16.5
Climate only	+14.0	+13.7	+14.1	+13.9	+14.2	+14.3	+11.6
Land use only	+12.7	+27.6	+8.3	+6.9	+5.8	+4.6	+4.9
Percentage change between 4000-3000 BP and 21st Century (B1 scenario)							
Climate and land use	+23.2	+33.9	+20.1	+19.1	+18.3	+17.2	+11.6
Climate only	+11.3	+7.9	+12.4	+12.5	+13.0	+12.8	+7.8
Land use only	+11.9	+26.0	+7.7	+6.6	+5.3	+4.4	+3.8

4.5 Discussion

4.5.1 Effects of long-term changes in climate and land use on past and future Meuse discharge

The simulated discharge and high-flow frequency of the Meuse increased significantly between the periods 4000-3000 BP and 1000-2000 AD; on this millennial timescale almost all of the increase was the result of decreased evapotranspiration due to the conversion of forest to agricultural land. However, despite a significant increase in forested area between the 19th and 20th Centuries, a further increase in discharge occurred between these two periods; this increase is attributable to a large increase in (winter half-year) precipitation (Ward et al., 2008a; Chapter 3). The results of the present study suggest that this long-term trend of increasing mean discharge will continue and strengthen over the 21st Century. When comparing the mean annual discharge and magnitude of high-flow

events between the 20th and 21st Centuries, the effects of the projected changes in land use are small for both scenarios, and almost all of the increase is due to climatic change. Despite the theoretical potential of changes in forest cover to significantly alter mean discharge and flood magnitudes (as exemplified by the effects over the late Holocene), no major changes in land use are expected for the 21st Century. Modest land use changes such as those simulated here for the 21st Century appear to have little effect on discharge and flood frequency at the basin scale. Since increasing temperatures in the 21st Century will lead to augmented values of *AE*, the higher discharges simulated for the 21st Century are mainly in response to the large increases in precipitation. For the first half of the 21st Century there is no significant difference in the projected discharge of the Meuse for scenarios A2 and B1; the difference between the scenarios becomes greater and statistically significant in the second half of the 21st Century. This is logical since the expected emissions of greenhouse gases under SRES emission scenarios A2 and B1 diverge more greatly during the second half of the 21st Century. Furthermore, much of the warming expected in the first half of the 21st Century is due to so-called 'committed climate change', which will occur due to past emissions irrespective of the future emission pathway taken (IPCC, 2007).

Despite the fact that land use change in the 21st Century may have little effect on the mean discharge and high-flow frequency of the Meuse, the effects of climate and land use change on mean discharge have been of a similar order of magnitude if we compare the periods 4000-3000 BP and the 21st Century. The effects of land use change have been stronger in the summer half-year, and the effects of climate change stronger in the winter half-year. This difference can be explained by (a) the relatively strong increase in 21st Century winter half-year precipitation compared to summer half-year precipitation, and (b) the relatively large decrease in summer *AE* due to the large-scale conversion of forest to agricultural land between the natural reference period and the 21st Century. Nevertheless, even on the millennial timescale the deforestation of almost half of the basin has had little effect on extreme high-flow events (in this case operationalised by high-flow events with a return period of 1250 years). Whilst numerous studies of the effects of deforestation on flood events have shown increased peak-flows around the globe (e.g. Brown et al., 2005; Gentry and Parody, 1980; Jones, 2000; Mahe et al., 2005), reviews of paired catchment studies show that this is not always the case (Andréassian, 2004; EEA, 2001). Cosandey et al. (2005) state that the effects of deforestation on flood generation are less severe during large-scale, low intensity (frontal) rainfall events. The most severe flood events on the Meuse occur as a result of extended periods of frontal rainfall over large parts of the basin (Berger, 1992). Since the most extreme rainfall events of such a nature occur in the Meuse basin during the winter, we postulate that the combination of saturated soils associated with a long period of antecedent precipitation, and low evapotranspiration rates during the winter, combine to minimise the effects of changes in forest cover on the most extreme flood events.

4.5.2 Comparison with other studies

The results of hydrological modelling results for the future tend to agree that an increase in 21st Century mean Meuse discharge can be expected in the winter season (e.g. Booij, 2005; Bultot et al., 1988, 1990; De Wit et al., 2001; Gellens and Roulin, 1998; Middelkoop et al., 2004; Van Deursen and Middelkoop, 2001). This increase is the result of the modelled increase in winter precipitation in the vast majority of climate model simulations or 'perturbations' in the region (e.g. Booij, 2005; Bultot et al., 1988, 1990; De Wit et al., 2001, 2007a; Gellens and Roulin, 1998; Giorgi and Coppola, 2007; Kwadijk and Rotmans, 1995; Van den Hurk et al., 2006). For the summer half-year and summer season, hydrological modelling results show more inter-model and inter-scenario variation. Assuming a CO_2 doubling between the concentrations at 2000 AD and the end of the 21st Century, De Wit et al. (2001) simulated slight decreases (0-5%) in summer discharge. However, based on four climate change scenarios of Können (1999), Middelkoop et al. (2004) simulated a similarly small increase under three scenarios, with a 10% decrease under the other scenario (which assumes a drying of the climate of western Europe). Gellens and Roulin (1998) carried out simulations for eight Belgian subcatchments using seven general circulation models (GCMs), and found an increase in summer season discharge for about half of the runs, with a decrease for the other half (ranging from increases of ca. 20% to decreases of ca. 40% depending on the subcatchment and model). This inter-model variation can be explained to a large degree by differences between the climate scenarios and climate models used; for the summer period, climate modelling results still show a wide range of future possibilities. Although climate models agree on increasing summer temperatures, precipitation change in northwest Europe is highly sensitive to the model used. Whilst all of the regional climate model (RCM) simulations used by De Wit et al. (2007a) show decreases in summer season precipitation, those used by Gellens and Roulin (1998) show decreases in four cases, with increases in the remaining three cases. This uncertainty is reflected in the most recent KNMI (Royal Netherlands Meteorological Institute) scenarios for the coming century (Van den Hurk et al., 2006), which show no unequivocal picture for summer season precipitation in the Netherlands.

In terms of flood generation, the majority of high-flows on the Meuse occur in the winter as a result of prolonged zonal precipitation over large parts of the basin, especially on already saturated soils (Berger, 1992). As the simulation of increased winter precipitation across the region is robust, the inter-model agreement on the changes in high-flows is improved. An increased frequency of high-flows over the 21st Century is also simulated by Booij (2005) and Van Deursen and Middelkoop (2001, 2002). Using the HBV model, and synthetic series of precipitation and temperature assuming a doubling of CO_2 between the end of the 20th and 21st Centuries, Booij (2005) simulated an increase in the magnitude of discharge events with a return period of 100 years of ca. 9 to 13% (depending on which model resolution was used). In the present study we simulated similar increases in the magnitude of discharges with a return period of 100 years, namely +12% (A2) and

+6% (B1). Leander et al. (2008) used long synthetic sequences of precipitation and temperature derived from three RCMs to force the HBV model, and found either little change in the most extreme discharge quantiles, or a large increase, depending on the GCM used to force the RCM. Increases in flood frequency in the 21st Century have been simulated for a number of tributaries by Bultot et al. (1988, 1990), Gellens (1991), and Gellens and Roulin (1998).

Few modelling studies of the Meuse have looked specifically at the effects of changes in land use. Using the IRMB conceptual model for the Houille basin (a small tributary of the Meuse in Belgium with catchment size of ca. 113 km^2), Bultot et al. (1990) estimated that a hypothetical conversion of land use from 100% coniferous forest to 100% pasture would result in an increase in mean annual discharge of ca 13.5%. Ashagrie et al. (2006) and Tu et al. (2005) found no evidence in the observed record to suggest that land use change in the 20th Century had had a significant effect on Meuse discharge. However, modelling studies addressing the effects of projected 21st Century land use change scenarios on discharge are elusive. The current study indicates that in spite of the large land use changes expected in the 21st Century at the European level (Busch, 2006; Rounsevell et al., 2006; Verburg et al., 2006), the projected land use changes in the Meuse basin are relatively small, and as a result climate impacts dominate changes in hydrology.

Recent studies by Leander and Buishand (2007) and Leander et al. (2008) show that the estimation of extreme discharge percentiles from the results of hydrological models is highly dependent on the climate model used and the method used to correct the bias of those climate models. The climate model used in this study has a low spatial resolution and simplified atmospheric physics compared to GCMs (and RCMs), which makes it difficult to precisely simulate the regional details and variability of daily precipitation. Furthermore, the downscaling of precipitation is carried out using a simple linear correction technique (Bouwer et al., 2004). Nevertheless, the discharge results in this study are in general agreement with qualitative assessments of palaeodischarge derived from multi-proxy records of the late Holocene. Hence, the model is useful for assessing the main trends and changes over long time-scales, although the absolute values should be treated with caution. Future applications of this approach may benefit from using higher resolution RCMs nested into GCMs. This may lead to improved precipitation time-series, especially for the summer months when intense convective rainfall events can lead to localised extreme flows (Berger, 1992). However, the computational cost involved with such simulations on millennial time-scales in ensemble mode currently renders this approach prohibitive.

4.5.3 Implications for water management

Our results suggest that the increases in mean annual discharge and high-flow frequency of the Meuse in the 21st Century will be at least as great as the changes simulated over the last 4000 years. The emission scenarios used in this study lie

towards the upper (A2) and lower (B1) end of the full range of SRES emission scenarios (IPCC, 2000) in terms of the concentration of greenhouse gases in the atmosphere by the end of the 21st Century, and hence represent a broad spectrum of possible futures. For the first half of the 21st Century the differences between the two scenarios are relatively small, but by the second half of the 21st Century the effects under scenario A2 become much more severe than those under scenario B1. At present it is not possible to say which of the future pathways is more likely to occur, as this is dependent on political, socioeconomic, and technical developments at the global scale. Nevertheless, even under the more optimistic B1 scenario the simulated changes are large. Hence, the model results suggest that increased discharges and high-flow frequencies may be unavoidable, even if a concerted and immediate effort were undertaken at the global scale to mitigate greenhouse gas emissions. This underscores the need for adaptation strategies to maintain current safety levels.

Current water management laws in the Netherlands state that water defences must safely withstand a design discharge, which is defined as the discharge with a given return period in years (TAW, 2000). At present this design discharge is estimated by fitting statistical distribution functions to observed annual discharge maxima, and then extrapolating to the required return period (Diermanse, 2004). The use of multi-scenario ensemble simulations of discharge in this study under a range of future climate and land use change scenarios shows that the discharge associated with such low frequency events will increase in the future. Hence, estimates of design discharge based on observed discharge measurements will be too low.

For the embanked sections of the Meuse in the Netherlands, the design discharge is currently 3800 $m^3 s^{-1}$. This is considerably lower than our simulated discharge magnitude for floods with a return period of once per 1250 years during the 20th Century of 4137 $m^3 s^{-1}$. However, reference to Table 4.4 shows that most of this discrepancy comes from the methods used to estimate these extreme return values. Applying only the Gumbel distribution (as was the case in this study) to the observed annual maxima at Borgharen for the period 1912-2000 results in a discharge magnitude of 4112 $m^3 s^{-1}$, whereas the design discharge is based on a combination of several extreme value statistic distributions. The steering committee ‘Integrale Verkenning Maas 2’ (IVM2), which was set up to assess which measures will be needed after 2020 AD to ensure that the Meuse continues to comply with flood defence laws, assumes a discharge of 4600 $m^3 s^{-1}$ in its water defence plans until 2100 AD (Ministry of Transport, Public Works and Water Management, 2006); this represents an increase compared to the current design discharge of ca. 21%. Our simulations show an increase in the discharge magnitude associated with a flood of return period of once per 1250 years of ca. 12% between the 20th Century and 21st Century under scenario A2, and ca. 5% under scenario B1. Our results therefore suggest that the 4600 $m^3 s^{-1}$ used in IVM2 provides a reasonable basis for the planning of future water management

measures. For the unembanked sections of the Meuse in the Netherlands, the design discharge is based on a high-flow event with a return period of once per 250 years. Our model results also suggest that the discharge associated with this return period will increase substantially by ca. 12% (A2) and 6% (B1) in the 21st Century compared to the 20th Century.

Whilst large-scale deforestation in the Meuse basin has had a major effect on discharge and high-flows over the course of the late Holocene, the effects of the land use changes projected for the coming century are relatively small. Although the B1 scenario indicates that some reforestation may occur in the 21st Century, large-scale reforestation is not expected to occur in the Meuse basin (WUR/MNP, 2007), due to the high economic demand on land and the attention to the preservation of cultural landscapes. Furthermore, our results suggest that changes in the percentage cover of forest have had little impact on the magnitude of the most extreme floods, even on a millennial timescale.

Whilst the effects of 21st Century land use change on high-flow frequencies may be small, this does not necessarily mean that the impacts of land use change on flood risk are small. Flood risk can be defined as the probability of flooding multiplied by the potential flood damage (e.g. Smith, 1994). Hence, assessments of flood risk must also examine potential flood damage, which is highly dependent on land use (Wind et al., 1999). Further studies should therefore be carried out to assess the combined effects of land use change and climate change on flood damage, as well as on high-flow frequencies.

In other basins around the world, the effects of land use change on discharge and high-flow frequency may be much larger, depending on the characteristic dominant changes in land use. In particular, urbanisation may have a large effect on runoff. Moreover, changes in the percentage cover of forest have been shown to have a great influence on soil erosion and the delivery of sediments to rivers in the Meuse basin (Stam, 2002; Ward et al., 2008c; Chapter 6).

4.6 Conclusions

Over the late Holocene, the Meuse river has experienced a long-term increase in both mean discharge and the frequency of high-flows similar in magnitude to those experienced during the major floods of 1926 and 1993. Between the periods 4000-3000 BP and the last millennium, most of this increase was the result of decreased evapotranspiration due to the conversion of forest to agricultural land. However, between the 19th and 20th Centuries mean discharge and high-flow frequency increased further; on this timescale increased (winter half-year) precipitation overwhelmed land use change as the most important mechanism. In the 21st Century the discharge and high-flow frequency is projected to increase further still, with climatic change being the dominant factor. The magnitude of extreme floods with a return period of 1250 years is significantly larger in the 21st Century under scenario A2 than in the 20th Century. Deforestation has had little

effect on such extreme floods, even on the millennial timescale.

One of the main values of the approach used in this study is that it allows us to delineate the effects of changes in climate and land use on long (centennial to millennial) timescales, and thereby identify mechanisms important to changes in discharge and high-flow frequency. The approach also allows us to examine the effects of anthropogenic activities against a natural reference period, which is not possible when only examining discharge records of the last century and the coming century. Furthermore, the results of the model are verified to some extent against geomorphological evidence from periods in which environmental conditions were different to those of the present day. The modelling approach used here can provide a useful tool for assessing the effects of long-term and future environmental change on discharge and high-flow frequency in other basins around the world. However, the simplified modelling approach used does not permit for an examination of the effects of human interference in the hydrological system in terms of adaptation strategies such as the building of dams and weirs; canalisation; the deepening or widening of river channels to increase discharge capacity; and the creation of retention areas for flood waters; etc. Over the past centuries, and in the 21st Century, such activities have had, or will have, major impacts on the Meuse. In future analyses of the effectiveness of these adaptation strategies, model structures must be employed that allow for the quantification of the effects of these measures on discharge. However, the aim of this project was to gain a better insight into the effects of long-term changes in climate and land use on discharge and flooding, and the sensitivity of hydrological systems to those changes.

Chapter 5

River Meuse suspended sediment yield: a new estimate and past estimates revisited

Abstract

Despite increasing research into changes in the discharge of the River Meuse, estimates of the river's sediment yield are less forthcoming. Three published studies (in 1883, 1982, and 1987) have estimated suspended sediment yield close to the Belgian-Dutch border; the latter two studies surmise that this increased substantially between the late 19th and 20th Centuries. In this paper a more recent and longer time-series of observed discharge and suspended sediment data (1995-2005) is used to estimate mean annual suspended sediment yield (ca. 386,000 Mg a^{-1}), and the results of the previous studies are revisited. New insights suggest that those studies do not in themselves provide evidence of increased sediment yield: the higher estimates in the late 20th Century could equally be due to interannual variability or methodological differences. There has been no significant increase in rainfall erosivity between the late 19th and 20th Centuries, and the effect of land use change over that time would have been to cause a decrease in suspended sediment yield, rather than an increase. On the other hand, the endikement and regulation of the Meuse between Namur and Liège between the late 19th and 20th Centuries may have caused an increase in sediment yield by preventing the deposition of sediments on the floodplain in all but the largest of floods.

This chapter is based on the paper: Ward, P.J., 2008. River Meuse suspended sediment yield: a new estimate and past estimates revisited. Netherlands Journal of Geosciences, 87(2) 189-193.

5.1 Introduction

Concerns surrounding the effects of anthropogenic climate and land use change have stimulated increasing research into River Meuse hydrology in recent years. Suspended sediment yield (*SY*) (the total mass of suspended sediment passing a specific location in a given time interval) is also sensitive to changes in climate and land use, but has received little attention, partly due to the lack of systematic measurements of suspended sediment concentration (*SC*). Nevertheless, an understanding of *SY* is essential as sediments from agricultural areas are responsible for the supply of nutrients, pesticides, and heavy metal contaminants to river channels (e.g. Boers, 1996; De Wit and Behrendt, 1999), which can have an impact on the water quality of rivers and coastal areas. Furthermore, sediment delivery impacts on channel and floodplain morphology; the ecological functioning of floodplains (e.g. Richards et al., 2002); and sediment deposition rates in reservoirs and ponds (e.g. Verstraeten and Poesen, 1999). Currently, the only estimates of *SY* at the scale of the Meuse basin are those of Spring and Prost (1883), Close-Lecocq et al. (1982), and Lemin et al. (1987). The latter two studies suggest that a large increase in *SY* occurred between the late 19th and 20th Centuries. However, the estimates of *SY* in these studies are based on measurements made over short time-periods (maximum one year). Daily measurements of Meuse discharge (*Q*) and *SC* at Eijsden (Netherlands) are now available for 1995-2005, thus providing a longer time-series. In this paper we use these observations to examine the following research questions:

- What is the recent mean annual *SY* of the Meuse at Eijsden?;
- How does this estimate of *SY* compare to previous estimates?;
- Has the *SY* of the Meuse increased since the late 19th Century, as postulated by Close-Lecocq et al. (1982) and Lemin et al. (1987)?

5.2 Previous studies of Meuse *SY*

Spring and Prost (1883) measured daily *Q* and *SC* at Liège (Belgium) between November 1882 and November 1883. Daily *SC*s were estimated as the product of the instantaneous daily measurements of *Q* and *SC*, integrated over the entire day (e.g. Phillips et al., 1999; Robertson and Roerish, 1999), and were summed to estimate annual *SY*. Using this method they obtained an estimate of annual *SY* for that year of 238,191 Mg. Close-Lecocq et al. (1982) carried out a similar exercise one century later, taking measurements between December 1979 and April 1980, on a number of days in July 1980 (following a major high-flow), and between August 1980 and January 1981. Based on these measurements they developed the following rating curve:

$$\log Q_s = 1.9606 \cdot \log Q - 0.73234 \quad (r = 0.93) \qquad \text{(Eq. 5.1)}$$

where *Q* is discharge ($m^3 s^{-1}$), and Q_s is suspended sediment flux ($g s^{-1}$). Substitution of observed *Q* data for Ampsin-Neuville (ca. 10km upstream) for 1958-1977 into this regression model provided an estimate of mean annual *SY* of 388,458 Mg a^{-1}.

Based on this estimate they surmised that *SY* had increased significantly since the late 19th Century, and suggest that this may be due to industrial activities on the Sambre and the Meuse. Lemin et al. (1987) measured *Q* and *SC* at Liège on 62 days between January 1983 and February 1984, mainly during high-flows, and developed the following rating curve:

$$\log Q_s = 2.14 \cdot \log Q - 1.11 \quad (r = 0.93) \qquad \text{(Eq. 5.2)}$$

Using this regression equation with daily *Q* data for 1983, they calculated a *SY* for that year of 483,409 Mg ± 122,562 Mg, and state that this confirms the conclusion of Close-Lecocq et al. (1982), namely that Meuse *SY* increased strongly between the late 19th and 20th Centuries. However, they suggest that this increase may be related to the endikement and regulation of the Meuse between Namur and Liège over that period, which prevents the deposition of sediments on the floodplain in all but the largest floods.

In a recent publication, Doomen et al. (2008) developed a supply-based rating curve for the estimation of Meuse *SC* for given values of *Q*. The rating curve is based on an empirically derived power function of the form:

$$SC = aQ^b + c \qquad \text{(Eq. 5.3)}$$

where a, b, and c are empirically derived coefficients. However, the rating curve differs from traditional power functions in that the coefficient b varies depending on the presence or absence of sediment stock in the channel bed; when stock is present b is higher (i.e. steeper rating curve), and when stock is exhausted b is lower (i.e. less steep rating curve). Sediment stock is assumed to increase when discharge is below a given threshold, and decrease when discharge is above that threshold. This supply-based rating curve leads to an improvement in the prediction of *SC* when compared to rating curves which do not consider sediment depletion.

5.3 Data and materials

Data on daily *Q* and *SC* for 1995-2005 at Eijsden were obtained from the Waterbase website (http://www.waterbase.nl/). The measurements were taken continuously throughout the day, from which daily average values were obtained. In the present study, the mean daily values of *Q* and *SC* were multiplied to estimate daily *SY*, and these daily estimates were summed to provide annual estimates. This method of estimating annual *SY* is considered to be the most accurate method if sufficient data (at least daily) are available (Robertson and Roerish, 1999). Since these measurements are available daily, and are taken continuously throughout the day rather than once per day, it is assumed that they give a reasonably accurate estimate of *SY*, approaching the true value. Hence, in the present study, I refer to these estimates as ‘observed’. *SC* data were missing for 50 days, the days being spread throughout the year and the time-period: for these days the concentration was estimated using the rating curve of Doomen et al. (2008).

5.4 Results and discussion

The mean annual observed *SY* for 1995-2005 at Eijsden, as calculated from daily observations of *Q* and *SC*, is 386,000 Mg; interannual variability is high (σ = 231,000 Mg), as is the range (maximum = 725,000 Mg; minimum = 73,000 Mg). The estimates of the three previous studies fall within the variability of these observed values. This immediately casts doubt on the conclusion of Close-Lecocq et al. (1982) and Lemin et al. (1987) that their results provide evidence of an increase in *SY*.

Furthermore, the different methodologies used in the previous three studies can themselves lead to large variations in estimates of *SY*. Close-Lecocq et al. (1982) and Lemin et al. (1987) used log linear sediment rating curves to estimate Q_s as a function of *Q*. Such a log linear rating curve for 1995-2005 at Eijsden (Fig. 5.1) has the form:

$$\log Q_s = 1.5855 \cdot \log Q - 0.3237 \quad (r = 0.91) \qquad \text{(Eq. 5.4)}$$

Despite the high correlation coefficient, Fig. 5.1 shows that the relationship is not truly log linear, since the gradient steepens at ca. log *Q* = 2.5. Since Close-Lecocq et al. (1982) and Lemin et al. (1987) used a limited numbers of observations biased towards high-flows, such a change in gradient would not have been visible. For example, Lemin et al. (1987) based their rating curve on measurements of 62 days, and the minimum measurement of *Q* on which their estimation was based is ca. 170 $m^3 s^{-1}$ (i.e. log *Q* = ca. 2.23 $m^3 s^{-1}$). Reference to Fig. 5.1 shows that a rating curve based on Eijsden observations only for days on which log *Q* > 2.23, would indeed be steeper.

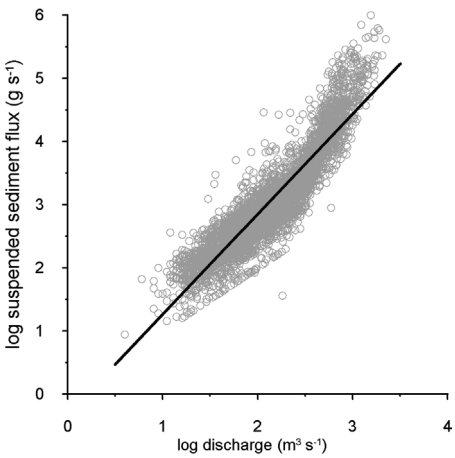

Fig. 5.1: Scatter plot of the logarithms of daily discharge and suspended sediment flux at Eijsden for 1995-2005. The black line indicates the log linear sediment rating curve between log discharge and log suspended sediment flux. Despite the high correlation coefficient (r = 0.91), the relationship is clearly not truly log linear; the gradient becomes more steep after log discharge = ca. 2.5 $m^3 s^{-1}$.

To illustrate the sensitivity of log linear rating curves to the length of the measuring period used in their estimation, log linear curves for each individual year of the Eijsden observations are plotted against the rating curve based on the entire

period 1995-2005 (Fig. 5.2). For comparison purposes, the curves of Close-Lecocq et al. (1982) and Lemin et al. (1987) are also shown. The rating curves of the individual years at Eijsden show a large spread around the mean curve for 1995-2005; hence a rating curve based on an individual year of observations cannot be applied to *Q* data of other years. Furthermore, Fig. 5.2 shows that the log linear rating curves of Close-Lecocq et al. (1982) and Lemin et al. (1987) are too steep since they are based on observations biased towards high-flows: the use of these curves will lead to an overestimation of *SY*.

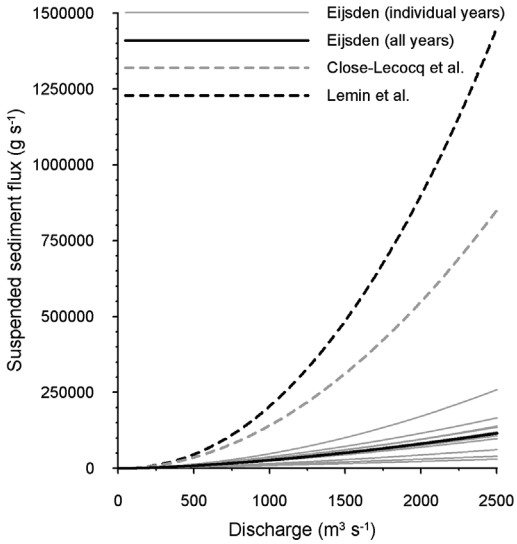

Fig. 5.2: Log linear sediment rating curves between discharge and suspended sediment flux. The curves based on individual years of observations at Eijsden (between 1995 and 2005) show a large spread around the curve based on observations for all of the years in the period 1995-2005 taken together. Furthermore, all of these curves were found to produce an underestimation of annual sediment yield (SY) of between 36.2% and 84.4%. The curves of Close-Lecocq et al. (1982) and Lemin et al. (1987) are much steeper since they are based on discharge observations biased towards high-flows, and hence lead to an overestimation of SY.

5.4.1 Predictive power of the regression curves

When substituting observed *Q* data into the individual annual log linear rating curves for Eijsden (Fig. 5.2), substantial underestimations of annual *SY* (compared to observed values for those years) were found in all cases (between 36.2% and 84.4%). This discrepancy occurs for a large part because log linear regression curves are obtained based on least squares regression on the logarithms of *Q* and Q_s. Hence, when the inverse logarithm is taken, the differences between observations and regression curve are greater for observations above the curve than for observations below the curve (Asselman, 1997; Ferguson, 1986; Phillips et al., 1999; Walling and Webb, 1982). On the other hand, the rating curves of

Close-Lecocq et al. (1982) and Lemin et al. (1987) would both lead to a substantial overestimation of mean annual *SY* (+83.0% and +158.1% respectively). The use of these *Q* observations biased towards high-flows to estimate sediment rating curves leads to severe overestimations of *SY*, despite the underestimation due to the use of log linear regression.

In order to assess the ability of the supply-based sediment rating curve of Doomen et al. (2008) to estimate annual *SY*, I used their method, in combination with the observed discharge data for Eijsden for 1995-2005, to estimate annual *SY* over that period. The agreement between observed annual *SY*, and *SY* estimated using this method, was reasonably good on a year to year basis (r = 0.87, Nash and Sutcliffe (1970) efficiency coefficient, N&S = 0.71). The estimate of mean annual *SY* for the entire period (ca. 337,000 Mg a^{-1}) was lower than that of the observed record (ca. 386,000 Mg a^{-1}), although the difference is not statistically significant (t-test: t = 0.512, p = 0.614). Furthermore, the interannual variability of *SY* calculated using the method of Doomen et al. (2008) (σ = 211,000) is similar to that of the observed record (F-test: F = 0.900, p = 0.354). Hence this physically based rating curve, whilst actually developed for predicting daily *SC*, gives a better estimation of annual *SY* than the previously discussed *SY* rating curves.

5.4.2 Preliminary assessment of 20th Century SY changes

On a long time-scale (i.e. centennial or longer), rating curves cannot be used to estimate *SY* as they are specific to the basin conditions during the period for which they are estimated. The most promising way to examine long-term changes would be through the use of models and proxy data. Whilst such a study is beyond the scope of this paper, the possible role that a number of factors may have had on *SY* over the course of the last century are discussed briefly.

The most widely used parameter representing the erosional impact of rain on soils is the R factor of the Revised Universal Soil Loss Equation (RUSLE) (Renard et al., 1997). Verstraeten et al. (2006a) made monthly estimates of the R factor at Ukkel (Belgium) for the period 1898-2002 based on observed 10-minute rainfall depth time-series, and found neither a significant trend nor any abrupt changes in the 105 year time-series. Hence, there was no significant increase in rainfall erosivity between the late 19th Century and the period in which the studies of Close-Lecocq et al. (1982) and Lemin et al. (1987) were carried out, and therefore no resultant significant increase in *SY* can be expected.

Land use is also an important factor controlling *SY*, with erosion in forests and urban areas generally very low, and erosion in agricultural areas higher. The percentage area of the Meuse basin (upstream from Eijsden) covered by forest was ca. 10 percentage points higher in the late 20th Century than in the late 19th Century, whilst the percentage of urban area increased from ca. 2% in the 19th Century to ca. 9% in the 20th Century. The area of the Meuse basin covered by agricultural land was ca. 16 percentage points lower in the late 20th Century than

in the late 19th Century (Ward et al., 2008a; Chapter 3). Hence, the land use changes which have occurred between the late 19th and 20th Centuries would have the effect of reducing *SY*.

The findings of the present study suggest that the higher values of *SY* obtained by Close-Lecocq et al. (1982) and Lemin et al. (1987), compared to Spring and Prost (1883), may result from interannual differences in *SY* or differences in methodologies, rather than be indicative of a structural increase in mean *SY*. Nevertheless, the endikement and regulation of the Meuse between Namur and Liège may indeed have caused an increase in the sediment yield of the river, as suggested by Lemin et al. (1987). It would be useful to carry out detailed geomorphological fieldwork in the floodplains to investigate what effect these measures have had on sediment yield over the last century.

5.5 Conclusions

- For the period 1995-2005, the mean annual estimated *SY* of the Meuse at Eijsden is approximately 386,000 Mg a^{-1}. Interannual variability is high (σ = 231,000 Mg), as is the range of observed *SY* for individual years (between 73,000 and 725,000 Mg a^{-1}).

- Sediment rating curves based on single year observations of *Q* and *SC* are highly sensitive to the year used to calculate the regression model, and can lead to highly erroneous estimates of *SY* when applied to other years. When discharge data biased towards high-flows are used to estimate rating curves, large overestimations of *SY* can occur.

- The *SY* estimates of Spring and Prost (1883), Close-Lecocq et al. (1982), and Lemin et al. (1987) fall within the range of observed annual values of Meuse *SY* at Eijsden for the period 1995-2005. Hence, it is not possible to conclude from the aforementioned studies that mean *SY* has increased since the late 19th Century. Rainfall erosivity at Ukkel shows no significant trend between the late 19th and 20th Centuries, and changes in land use in that period would have led to a reduction in *SY* due to reduced levels of soil erosion, rather than an increase. On the other hand, the endikement and regulation of the Meuse between Namur and Liège may indeed have caused an increase in the sediment yield of the river, as suggested by Lemin et al. (1987).

Chapter 6

The impact of land use and climate change on late Holocene and future suspended sediment yield of the Meuse catchment

Abstract

In this study we investigate the relative importance of changes in land use and climate on suspended sediment yield (*SY*) on millennial timescales in the Meuse basin. We use a spatially distributed soil erosion and sediment delivery model (WATEM/SEDEM) to simulate *SY* in three time-periods: 4000-3000 BP (minimal anthropogenic influence); 1000-2000 AD (includes land use and climate change); and 21st Century. Changes in climate are based on climate model output (ECBilt-CLIO-VECODE). For the 21st Century the model is forced according to two emission scenarios of the Intergovernmental Panel on Climate Change (IPCC), namely SRES scenarios A2 and B1. These scenarios lie towards the higher and lower end of the full IPCC scenario range respectively. For 4000-3000 BP the basin is assumed to be almost fully forested; for 1000-2000 AD land use is reconstructed using CORINE data, historical sources, and land use modelling; and for the 21st Century land use is based on the European land use change project EURURALIS. Whilst rainfall erosivity increases by only 3% between 4000-3000 BP and 1000-2000 AD, *SY* increases from ca. 92,000 Mg a^{-1} to ca. 306,000 Mg a^{-1}. This model prediction is in agreement with the limited regional multi-proxy data available. Our simulations show that almost all of this increase is due to the conversion of forest to agriculture. Over the period 1000-1900 AD, *SY* shows a significant increasing trend, with a peak of ca. 388,000 Mg a^{-1} in the 19th Century (due to continuing deforestation). In the 20th Century, reforestation and rapid urbanisation result in a decrease to ca. 281,000 Mg a^{-1}. Sensitivity analyses show that although land use change acts as the primary control on long-term changes in *SY*, the sensitivity of *SY* to changes in climate increases as the percentage of deforested land increases. For the 21st Century the results are highly sensitive to the scenarios used. Due to relatively large increases in rainfall erosivity, *SY* increases by 12% compared to the 20th Century according to scenario A2, or by 8% according to B1. However, the associated land use change scenarios cause decreases in *SY* of 26% (A2) and 46% (B1). The net effect is thus a decrease of *SY*. This study highlights the potentially significant efficacy of land use planning as a tool to mitigate the negative effects of soil erosion and sediment delivery to rivers.

This chapter is based on the paper: Ward, P.J., Van Balen, R.T., Verstraeten, G., Renssen, H., Vandenberghe, J. The impact of land use and climate change on late Holocene and future suspended sediment yield of the Meuse catchment. Geomorphology, in press, doi:10.1016/j.geomorph.2008.07.006.

6.1 Introduction

Soil erosion and the delivery of eroded sediments to river channels cause many environmental problems and can pose substantial financial burdens on society. Soil erosion on arable land has numerous detrimental on-site impacts, including the loss of topsoil and fertilisers, decreased crop yield and accessibility (due to the formation of gullies) in the short-term, and decreased soil productivity in the long-term (Verstraeten et al., 2002). The delivery of sediments eroded from agricultural areas is also responsible for the supply of nutrients, pesticides, and heavy metal contaminants to river channels (e.g. Boers, 1996; De Wit and Behrendt, 1999; Verstraeten and Poesen, 2002), which can have an impact on the water quality of rivers and coastal areas. Sediment delivery also impacts on channel and floodplain morphology (e.g. Asselman and Middelkoop, 1995; De Moor et al., 2008); the ecological functioning of floodplains (Richards et al., 2002); and sediment deposition rates in reservoirs and ponds (Verstraeten and Poesen, 1999).

Two important factors affecting soil erosion and sediment delivery to river channels are changes in land use and climate (e.g. Houben et al., 2006; Toy et al., 2002; Van Rompaey et al., 2002). Given that climate and land use are expected to change as a result of human activities in the future (IPCC, 2007), it is important to examine the potential effects of these changes on soil erosion and sediment delivery to river channels. A number of studies have been carried out to estimate the potential effects of future climate change on soil erosion at the scale of small watersheds (e.g. Boardman and Favis-Mortlock, 1993; Favis-Mortlock and Boardman, 1995; Nearing et al., 2005; Pruski and Nearing, 2002). At a global scale, attempts have been made to quantify the effects of future changes in climate and land use on sediment delivery by rivers to the oceans (e.g. Ito, 2007; Yang et al., 2003), and have found that the conversion of forests to cropland has led to an increase in the global potential for soil erosion over the last century, with a further increase in potential in the future due to the expected changes in climate. However, these studies only examine soil erosion and do not examine the effects on sediment delivery (and hence sediment yield). In Europe, both soil erosion and sediment delivery are now important topics on the political agendas of local, national, and European policy makers (Van Rompaey et al., 2005). In western Europe this is given added impetus by the fact that future climatic changes there are expected to be relatively large (Giorgi and Coppola, 2007).

In order to assess the potential effects of land use and climate change on future soil erosion and sediment delivery, calculations can be based on modern measurements. A more robust approach is, however, to gain an understanding of these processes over a much longer timescale. This enables us to gain an understanding of past processes prior to human influence, to examine the relative impacts of climate and land use change through time, and to validate the performance of predictive models (Lang and Bork, 2006).

In the Meuse basin, as in most medium to large catchments, little research has been carried out on soil erosion and sediment delivery at the catchment scale. However, long-term changes in land use and climate have had large impacts on the discharge and flood frequency of this river over the late Holocene and 20th Century respectively (Ward et al., 2008a; Chapter 3), and therefore effects on sediment delivery can also be expected. The results of a recent study by De Moor and Verstraeten (2008), based on detailed geomorphological reconstructions and sediment delivery modelling, suggest that the sediment yield of the Geul River (a tributary which enters the Meuse a few kilometres north of Maastricht in the Netherlands; Fig. 6.1) increased greatly between the Early-Mid Holocene (ca. 6000 Mg a^{-1}) and the period 1000-2000 AD (ca. 48,000 Mg a^{-1}), due to the conversion of forest to arable land. Whilst not a tributary of the Meuse, geomorphological studies in the Nethen catchment (55 km^2), which drains into the Scheldt basin via the Dijle in Belgium, suggest that large increases in sediment delivery have occurred since Medieval times (Rommens et al., 2006). Since few studies have been carried out to assess the impacts of climate and land use change on soil erosion and sediment delivery in medium to large basins, we will use a spatially distributed soil erosion and sediment delivery model (WATEM/SEDEM) of the Meuse basin to:

- estimate the background level of suspended sediment yield prior to significant human influence (4000-3000 BP);
- estimate the long-term changes in suspended sediment yield in the periods 4000-3000 BP and 1000-2000 AD;
- delineate the effects of land use and climate change on suspended sediment yield;
- simulate suspended sediment yield under 21st Century climate and land use change scenarios.

6.2 Regional setting

The Meuse basin covers an area of ca. 33,000 km^2, extending over parts of Belgium, France, Germany, the Netherlands, and Luxembourg. The Meuse basin can be split into three main sections: (a) the upper reaches (Lotharingian Meuse); (b) the central reaches (Ardennes Meuse); and (c) the lower reaches (Dutch Meuse). The Lotharingian Meuse extends from the source at Pouilly-en-Bassigny (France) to the confluence with the Chiers (ca. 25 km downstream from Stenay), and is characterised by a lengthy and narrow catchment of low gradient through mainly sedimentary Mesozoic rocks; along this section there are no major tributaries. The Ardennes Meuse extends from the confluence of the Meuse and the Chiers to the Dutch border near Eijsden; along this reach the major tributaries Viroin, Semois, Lesse, Sambre, and Ourthe join the Meuse. The Ardennes Meuse transects mainly Palaeozoic rocks of the Ardennes Massif and the river is narrow and steep. The Dutch Meuse extends from Eijsden to the confluence with the Rhine in the Hollandsche Diep (Berger, 1992). The Meuse is a predominantly rain-fed river; mean annual precipitation over the basin is ca. 950 mm, and is reasonably evenly distributed throughout the year. The spatial distribution of

precipitation is to a large extent a reflection of elevation and distance from the coast. The mean annual discharge of the Meuse and its associated canals at the border of Belgium and the Netherlands is ca. 276 $m^3 s^{-1}$ (Ashagrie et al., 2006). The maximum altitude in the basin is ca. 700 m.a.s.l.

For this project the model was set up upstream from Eijsden (Fig. 6.1), i.e. the Ardennes Meuse and the Lotharingian Meuse. Hence, the majority of the Dutch and German sections of the basin are not included since these tributaries mainly drain into the Meuse downstream from this point. The model was set up upstream from this point as daily measurements of discharge and sediment concentration are available for Eijsden for the period 1995-2005, which allow for model calibration. Furthermore, we did not model the basin as far downstream as the current Rhine-Meuse confluence, since its location has changed over the course of the Holocene (Berendsen and Stouthamer, 2001).

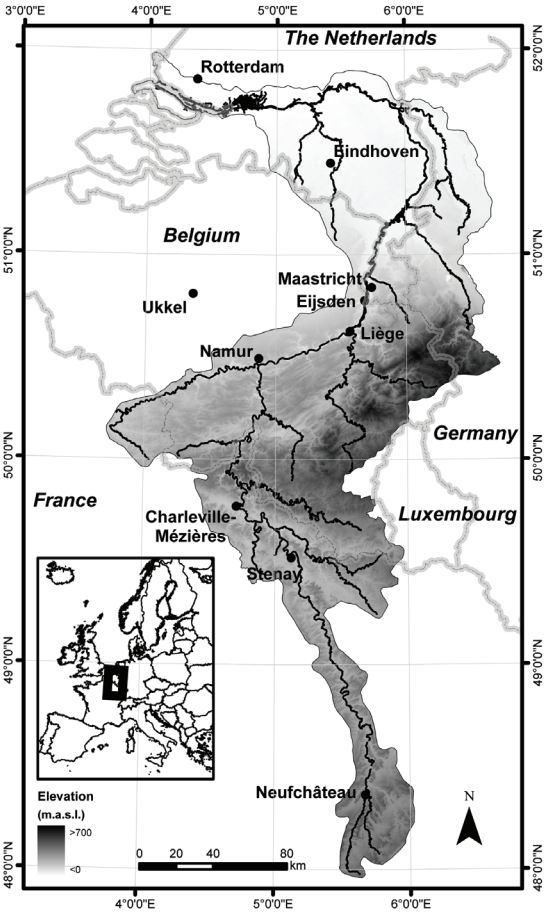

Fig. 6.1: Digital elevation model (DEM) showing the location of the Meuse Basin in northwest Europe. For this study the model was set up for the area upstream from Eijsden (DEM after Jarvis et al. (2006); boundaries after RWS Limburg/IWACO (2000)).

6.3 Materials and methods

In this study we use the WATEM/SEDEM model to simulate changes in the long-term annual suspended sediment yield (*SY*) of the Meuse per half-century for three time-slices: 4000-3000 BP, 1000-2000 AD, and the 21st Century. The period 4000-3000 BP was selected as it represents the most recent time-period in which the natural orbital forcings on climate were broadly similar to those of today (Goudie, 1992), whilst human influence on land use was minimal (Bunnik, 1995; Gotjé et al., 1990; RWS Limburg/IWACO, 2000). The period 1000-2000 AD was heavily influenced by human activities, namely changes in land use throughout the period, and greenhouse gas and sulphate aerosol emissions since the industrial revolution. For the 21st Century, our climate configurations are in line with the Special Report on Emission Scenarios (SRES) A2 and B1 of the IPCC (2000) (see Section 6.3.2.3), and the land use configurations are derived from the associated scenarios of the EURURALIS project (Verburg et al., 2006, 2008; WUR/MNP, 2007) (see Section 6.3.2.4).

6.3.1 Sediment delivery model

WATEM/SEDEM is a spatially distributed soil erosion and sediment delivery model, which we used to estimate the flux of sediment from the hillslopes to the Meuse basin river network. Detailed descriptions of the model are provided in Van Oost et al. (2000), Van Rompaey et al. (2001a), and Verstraeten et al. (2002); in this section only the main principles are summarised.

WATEM/SEDEM is a grid-based model that uses IDRISI raster layers as input, and calculates total annual sediment production, deposition, and export (i.e. *SY*). The model firstly calculates the mean annual soil loss per grid cell based on a 2D application of the Revised Universal Soil Loss Equation (RUSLE) (Renard et al., 1991):

$$E = R \cdot K \cdot LS_{2D} \cdot C \cdot P \qquad \text{(Eq. 6.1)}$$

where E is the mean annual soil loss (kg m^{-2} a^{-1}); R is the rainfall erosivity factor (MJ mm m^{-2} h^{-1} a^{-1}); K is the soil erodibility factor (kg h MJ^{-1} mm^{-1}); LS_{2D} is the slope-length factor according to Desmet and Govers (1996) to account for flow convergence in a 2D landscape; C is the crop factor; and P is the erosion control practice factor.

In the next step the eroded sediment is routed through the basin to a permanent river channel based on the transport capacities of overland flow. From the river channel the sediment is delivered directly to the pre-specified catchment outlet. WATEM/SEDEM does not simulate riverbank erosion, floodplain sedimentation, or channel storage, and hence the simulated sediment delivery values should be interpreted as sediment delivery towards the entire river network of the catchment.

The transport capacity of the overland flow (which is proportional to the potential for concentrated flow erosion) determines the sediment transport rates on hillslopes (Van Rompaey et al., 2001a), such that:

$$TC = \text{ktc} \cdot R \cdot K(LS_{2D} - 4.1\text{s}^{0.8}) \qquad \text{(Eq. 6.2)}$$

where *TC* is the transport capacity (kg m^{-1} a^{-1}), ktc is the transport capacity coefficient (m), and *s* is the slope gradient (m m^{-1}). For each grid cell the sediment input is either routed downslope (if the sediment input is lower than the transport capacity), or deposited (if the transport capacity is lower than sediment input). The transport capacity coefficient is the only model parameter that needs to be calibrated. The calibration of the model is described in Section 6.4.

6.3.2 Model input

The input data required to run the model are supplied in the form of IDRISI raster layers, each with identical resolution and spatial coverage. For this study we used a spatial resolution of 100 m x 100 m. This resolution was used by Verstraeten (2006) to simulate the *SY* of the Scheldt river basin at Rupelmonde (Belgium), upstream from which the area of the basin is approximately 19,000 km^2; this is similar to the size of the Meuse basin upstream from Eijsden (ca. 20,750 km^2) which will be modelled in this study. The input data layers are described in the following paragraphs.

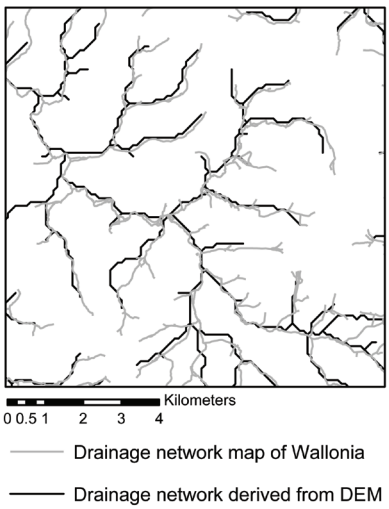

Fig. 6.2: Comparison of the drainage network according to the Wallonia dataset Réseau hydrographique 1:10,000, and the drainage network derived from the DEM. The area shown here covers 10 km x 10 km.

6.3.2.1 Digital elevation model (DEM)

A digital elevation model (DEM) is used in WATEM/SEDEM to calculate slope gradient and the length-slope factor (LS_{2D}), and to route sediment downstream. For this study we used the DEM of SRTM (Shuttle Radar Topography Mission; Jarvis et al., 2006) which is available online from http://srtm.csi.cgiar.org, with a spatial resolution of 3'' x 3'' (corresponding to roughly 60 m x 90 m). We reprojected this data onto a UTM grid (zone 31N) with a resolution of 100 m x 100 m. The DEM was also used to construct a river channel network using the RUNOFF module in IDRISI, and a 50 ha. catchment area threshold value to differentiate channels from hillslopes (e.g. Verstraeten, 2006). This value resulted in a river channel network which corresponds well with the drainage network map of Wallonia (Réseau hydrographique 1:10,000; Fig. 6.2), which was provided by the Direction de la Coordination Informatique - Cellule SIG, DGRNE, and is available online at http://environnement.wallonie.be/cartosig/Inventaire_Donnees/usage/HYDRO.html.

6.3.2.2 Soil erodibility factor (K)

The soil erodibility factor (*K*) describes the susceptibility of soil to erosion by rainfall. Due to a lack of detailed field data on changes in *K* over the late Holocene, we assume this factor to have remained constant over the periods 4000-3000 BP and 1000-2100 AD. This is an oversimplification, as soil erosion following deforestation will have led to thinner soil profiles in some regions (especially in loess areas) (e.g. De Moor and Verstraeten, 2008; Rommens et al., 2006). For this study, *K* was estimated based on soil texture and stoniness according to the European Soil Database (ESDB v.2 Raster Library; Van Liedekerke et al., 2006). The database is available online at http://eusoils.jrc.it/data.html, and has a spatial resolution of 1 km x 1 km. For the Meuse basin the soil texture database makes a distinction between four textures, which were reclassed to soil erodibility factors (K_{text}) after Verstraeten (2006) (Table 6.1).

Table 6.1: Reclassification of soil texture from the European Soil Database (Van Liedekerke et al., 2006) to soil erodibility factors (K_{text}) following Verstraeten (2006).

Soil texture	K_{text} (kg h MJ^{-1} mm)
Coarse (<18% clay and >65% sand)	20
Medium (18-35% clay and >15% sand, or <18% clay and 15-65% sand)	35
Medium fine (<35% clay and <15% sand)	42
Fine (35-65% clay)	40

These soil erodibility factors were then corrected to reflect the effect of stones in the soil profile on soil erodibility (Box Jr., 1981):

$$K = K_{text} \cdot \exp^{(-0.0278St)} \qquad \text{(Eq. 6.3)}$$

where *St* is the weight of stones in the topsoil expressed as a percentage of total weight of the topsoil. The soils on the steeper slopes of the Ardennes Meuse are relatively shallow, and hence the potential for erosion there is lower. Little field data is available to estimate the exact effects of this on soil erodibility, and therefore in this study we made a conservative 'best-estimate' of these effects by reducing *K* on slopes exceeding 20%, by 50% (Fig. 6.3). This *K* map represents a rather conservative estimate, as many of the steeper slopes of the Ardennes Meuse are almost devoid of topsoil, and hence erosion is minimal, and moreover the steepest slopes often consist of bare rock. Therefore, we also created a *K* map representing an extreme case scenario, whereby the stoniness of slopes with a gradient greater than 15% was increased to 50%, and all slopes steeper than 30% were regarded as bare rock (i.e. *K* = 0).

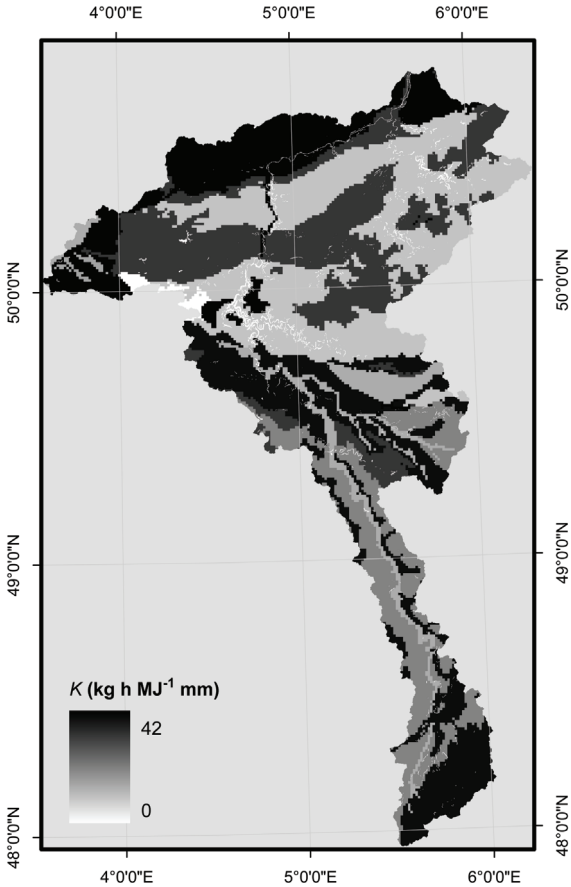

Fig. 6.3: Map showing the 'best-estimate' of the spatial distribution of the soil erodibility factor (K) (kg h MJ^{-1} mm) upstream from Eijsden, based on soil texture, stoniness, and slope.

6.3.2.3 Rainfall erosivity factor (R)

The rainfall erosivity factor (*R*) is used to represent the erosional impact of rain on soils, and is based on both annual rainfall and rainfall intensity. Maps of spatially distributed rainfall erosivity were used to simulate the effects of long-term changes in precipitation. The values of *R* were calculated for each grid cell per half century, based on a regression equation describing the annual value of *R* as a function of daily precipitation totals. Daily precipitation data were derived from the climate model ECBilt-CLIO-VECODE (Brovkin et al., 2002; Goosse and Fichefet, 1999; Opsteegh et al., 1998). The output used in this study were derived from a transient run forced by annually varying orbital parameters following Renssen et al. (2005a); atmospheric volcanic aerosol content and fluctuations in solar activity following Goosse et al. (2005); and atmospheric greenhouse gas and sulphate aerosol concentrations following Renssen et al. (2005a) for 4000-3000 BP and 1000-1750 AD, and Goosse et al., (2005) for 1750-2000 AD. For the 21st Century, atmospheric greenhouse gas emissions and sulphate aerosols were based on scenarios A2 and B1 of the SRES emission scenarios (IPCC, 2000). These represent two possible future scenarios of greenhouse gas and sulphate aerosol emissions in the 21st Century. The A2 and B1 scenarios lie towards the upper and lower end of the full spectrum of IPCC scenarios respectively in terms of the concentration of atmospheric CO_2 by 2100 AD, and can therefore be used to assess the response of the system to a broad range of possible future changes. The climate model results were spatially and statistically downscaled for the Meuse basin at a spatial resolution of 2' x 2' by Ward et al. (2008a; Chapter 3).

The simulated daily precipitation depths were used to empirically derive a regression equation which describes the annual value of *R* at Ukkel (Belgium) as a function of daily simulated precipitation at Ukkel. In order to estimate the regression equation we used estimates of *R* at Ukkel based on 10-minute observations of rainfall total made by Verstraeten et al. (2006a). The following regression equation was obtained:

$$R = \sum_{d=1}^{d=360} a \cdot pre_d^{\,1.8067} \qquad \text{(Eq. 6.4)}$$

where *R* is the annual rainfall erosivity factor (MJ mm m^{-2} h^{-1} a^{-1}), a is an empirically derived monthly calibration factor, and *pre* is the precipitation depth (mm) on day, *d*. This regression equation was then used to estimate *R* for each grid cell within the basin, resulting in the map shown in Fig. 6.4. This spatial distribution of *R* shows a good similarity to estimates based on precipitation measurements, as described in the study of Bollinne et al. (1979).

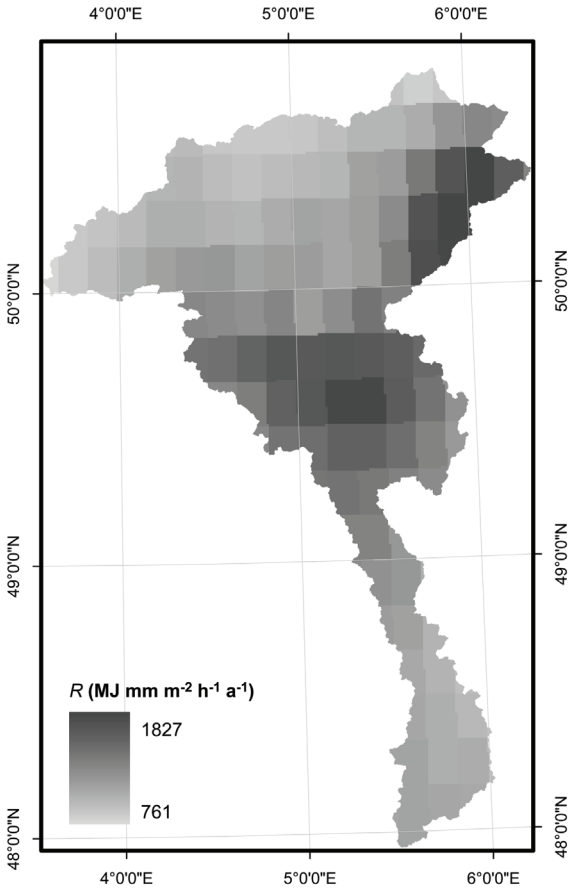

Fig. 6.4: Map showing the spatially distributed rainfall erosivity factor (R) (MJ mm m^{-2} h^{-1} a^{-1}) upstream from Eijsden for the period 1950-2000 AD, based on climate model output.

6.3.2.4 Crop factor (C) and erosion control practice factor (P)

A crop factor (*C*) is used to define the susceptibility of different land use types to water erosion. Different land use categories were assigned different values of *C* based on RUSLE standard calculation methods (Verstraeten et al., 2003), namely: 0 for water and urban land use (i.e. no erosion); 0.001 for forests and wetlands; 0.005 for pasture; and 0.370 for arable land. In this study we created a *C* map for each century by reclassing the land use maps (as shown in Appendix 3) to *C*, in order to simulate the effects of long-term changes in land use. The model is relatively insensitive to changes in these values. We carried out sensitivity analysis by running the calibrated model for the period 1950-2000 with the *C* values adjusted by ±50% (which represent extreme values, see Bakker et al., 2008), and this resulted in a change in *SY* of just ±7%.

For the 20th Century we used the CORINE Land Cover 2000 database (CLC2000 100 m version 8/2005 (V2) © EEA, Copenhagen, 2005, http://dataservice.eea.eu.int/dataservice), and reclassed the land use categories of CORINE to those required in WATEM/SEDEM (i.e. water, urban, forest, pasture, arable).

For the 21st Century we used data from the EURURALIS 2.0 project (WUR/MNP, 2007; www.eururalis.eu), pertaining to land use in 2030 at a spatial resolution of 1 km x 1 km. In the EURURALIS project an extended version of the global economic model (GTAP) and an integrated assessment model (IMAGE) were used to calculate changes in demand for agricultural areas at the country level while a spatially explicit land use change model (CLUE-s) was used to translate these demands into land use patterns at a 1 km x 1 km resolution (Verburg et al., 2006, 2008). In order to develop plausible developments in European land use a scenario-based approach was employed, whereby the scenarios followed the concept storylines of the SRES (IPCC, 2000). However, since the focus of these scenarios is completely outside land use, agriculture, and rural development, and lacks the regional disaggregation needed for high resolution land use modelling (Verburg et al., 2006), they were elaborated for land use issues and agricultural policies typical for Europe (Westhoek et al., 2006). The resulting scenarios are therefore complementary to those of IPCC (2000). Hence, we used the land use change scenarios 'Continental Market' and 'Global Cooperation', which correspond to SRES A2 and B1 respectively. Throughout the rest of this paper we refer to both the climate and land use scenarios as A2 and B1.

For the period 1000-1900 AD we reconstructed land use based on the maps of Ward et al. (2008a; Chapter 3). These give an overview of Meuse basin land use per century from the 11th to 19th Centuries at a spatial resolution of 2' x 2' (ca. 2.4 km x 3.7 km) based on census data, historical records, and palaeovegetation reconstructions. These maps were constructed by estimating the percentage cover of five land use classes (urban, forest, agriculture and grasslands, wetlands, and water bodies) per century for 39 Meuse subcatchments. Since our WATEM/SEDEM model has a higher spatial resolution than the land use maps of Ward et al. (2008a; Chapter 3), it was necessary to increase the spatial resolution. Furthermore, since those land use maps were constructed for use in hydrological modelling, they make no distinction between pasture and arable land, which is required in the present study. Hence, the construction of the land use maps for the period 1000-1900 AD involved two main steps: (a) estimating the percentage cover of each land use class for each subcatchment used by Ward et al. (2008a; Chapter 3), and (b) using the land use change simulation approach of Van Rompaey et al. (2001b) to backcast land use change from the reference state in the 20th Century to the situation in the 11th Century, thereby spatially distributing the land use covers to the desired resolution.

Concerning step a, the percentage cover of urban area, wetlands, water bodies, and forests per subcatchment was based directly on Ward et al. (2008a; Chapter

3). In order to estimate the ratio of agricultural land devoted to pasture and arable farming, we first established the present day ratio at the basin scale based on CORINE data, namely arable (59%) and pasture (41%). Then, we estimated the relative change in this ratio at the basin scale for each century based on the Meuse cells in the global maps of Pongratz et al. (2007). We then estimated the ratio of pasture to arable land per century for each subcatchment of Ward et al. (2008a; Chapter 3).

Step b involved spatially distributing these percentage covers per subcatchment onto the WATEM/SEDEM grid. Firstly, the areal coverages of urban area, water bodies, and wetlands from the land use maps of Ward et al. (2008a; Chapter 3) were simply resampled onto the higher resolution grid of WATEM/SEDEM. Then, the percentage covers of forests, pasture, and arable land per subcatchment (as calculated in step a) were used to backcast land use changes from the 20th to the 11th Century, based on the method of Van Rompaey et al. (2001b). Based on the present day spatial distribution of land use, the probability of each grid cell belonging to each land use class is calculated (based on the soil texture and slope of that cell); these probability maps are then used to perform stochastic simulations of land use change through time. We used the map of the 20th Century as a reference situation. Then, a land use map of the 19th Century was developed as follows. The grid cells pertaining to urban areas, water bodies, and wetlands in the 19th Century were already known from the maps of Ward et al. (2008a; Chapter 3), and were simply resampled onto the WATEM/SEDEM grid. Then, we calculated the change in the number of grid cells of forest, pasture, and arable land between the 20th Century and the 19th Century, based on the percentage covers estimated in step a. For example, if there were 100 arable grid cells in the 20th Century, and 150 arable grid cells were required in the 19th Century, then 50 extra arable grid cells would be needed in the 19th Century compared to the 20th Century. Hence, the 100 arable grid cells of the 20th Century were ‘fixed’ as arable cells on the 19th Century map. Then, the 20th Century forest and pasture grid cells were allowed to be converted to arable cells in the land use change simulations. Such a simulation works by first selecting a forest or pasture cell at random from the 20th Century map. Next, a random number is generated between 0 and 1, and compared with the probability of that cell having the land use ‘arable’. If the random number is less than this probability, the land use of the grid cell is altered to arable and subsequently ‘fixed’; if not, the grid cell retains its original land use. This procedure is re-iterated until the desired number of forest or pasture cells have been converted to arable (in this case 50). The arable cells are then ‘fixed’ and the simulations carried out for the next land use category. The simulations were carried out for each subcatchment individually, starting from the 20th Century, and then backcasting one century at a time until the 11th Century.

The method requires the estimation of the probability of a given grid cell having a given land use category. In the present day the probability of a grid cell having the category forest, pasture, or arable, is significantly related to the slope gradient

and soil texture class of that cell. The mean slope gradient of cells pertaining to forest, pasture, and arable land are 4.27%, 2.91%, and 2.65% respectively (based on the DEM and CORINE land use data); these slope gradients differ significantly from each other according to the Kruskall Wallis test (KW, $\chi^2 = 6601$, $p < 0.001$). We used CORINE land use data and soil texture data from the EDSB dataset (Van Liedekerke et al., 2006) to examine the relationship between land use and soil texture, based on the statistical Chi-square test (χ^2). The null-hypothesis of the χ^2-test states that 'the land use categories forest, pasture, and arable have the same distribution over different soil textures as over the total distribution'. Reference to Table 6.2 shows that this hypothesis can be rejected for all three land use types ($p < 0.001$).

Table 6.2: Results of χ^2-test between land use categories and soil texture classes, showing the observed number of cells of each soil texture class per land use category, and the expected number of cells assuming that there is no relationship between soil texture class and land use. For all land use categories the null hypothesis is rejected ($p < 0.001$), meaning that soil texture has a significant effect on the spatial distribution of forests, pasture, and arable land.

	Forest		Pasture		Arable	
Soil texture class	Observed	Expected	Observed	Expected	Observed	Expected
Coarse	1577	1820	1629	1093	1294	1587
Medium	18,540	15,223	7673	9146	11,429	13,274
Medium fine	6417	8095	3855	4863	9744	7058
Fine	4314	5803	5457	3486	4578	5060
Organic soil	171	79	22	48	3	69
Total cells	31,019	31,019	18,636	18,636	27,048	27,048
χ^2	1591.2		1836.3		1441.5	
p	< 0.001		< 0.001		< 0.001	

Given the significant relationship between land use and both slope gradient and soil texture, we used these two factors to estimate the probability that a given cell has a given land use category. For a single variable (i.e. slope category or soil texture) this probability is estimated as the relative frequency of a given land use (i.e. forest, pasture, or arable land) within that variable. For example, for slope class 0-2%, 22.1% of the cells pertain to forest. Therefore, the probability of a cell with slope 0-2% being forest is 0.221. Such a single variable land use probability can be calculated for each slope or texture class and for each land use type. However, in this case two variables are used (slope and texture class), and hence the overall probability is calculated as:

$$P(\text{land use} | A_i \cap B_i) = \frac{P(\text{land use} | A_i) \cdot P(\text{land use} | B_i)}{P(\text{land use})} \qquad \text{(Eq. 6.5)}$$

where A_i is the *i*th class of variable *A* (e.g. the class '*0-2%*' of the variable '*slope*'), and B_i is the *i*th class of variable *B* (e.g. the class '*coarse*' of the variable '*soil texture class*'). For example, the probability of a cell with slope class '*0-2%*' and texture class '*fine*', being forest, can be calculated as:

$$P(\text{forest}|slope\ '0-2\%' \cap texture\ 'fine') = \frac{P(\text{forest}|slope\ '0-2\%') \cdot P(\text{forest}|texture\ 'fine')}{P(\text{forest})}$$

(Eq. 6.6)

Using Eq. 6.5 the spatial pattern of land use probabilities was calculated for each land use category (forest, pasture, arable).

It should be noted that the probabilities calculated here for the occurrence of each land use class based on slope and soil texture are related to current land use practice. Since different practices would have been employed in the past (e.g. different agricultural methods), these probabilities will have changed to some extent over time. Nevertheless, given the lack of knowledge of these probabilities in the past, the method does allow us to spatially distribute the land use within each subcatchment based on a logical preference for particular soil textures and slopes on agricultural land, rather than via a purely random technique. In this study the erosion control practice factor (*P*) assumes a constant value of unity, as little information on past erosion control practices is available.

6.4 Calibration and validation

The WATEM/SEDEM model requires the calibration of only one parameter, namely the ktc (transport capacity) coefficient. Whilst a large dataset of observed and estimated *SY* is available for 26 small catchments in Belgium (Verstraeten and Poesen, 2001), these data are mainly for catchments in Flanders, and generally in the Belgian loess belt. For the Meuse basin very few studies have been carried out to assess the *SY* of the river. Spring and Prost (1883), Close-Lecocq et al. (1982), and Lemin et al. (1987) measured discharge and suspended sediment load at Liège to estimate *SY* based on observed data for a single year or less. However, Ward (2008a; Chapter 5) showed that these findings are highly dependent on both the time-periods and methods used, and that these estimates are therefore not per se representative of long-term mean annual *SY*.

Recently, Doomen et al. (2008) developed a supply-based sediment rating curve for the estimation of Meuse suspended sediment concentration (*SC*) for given values of discharge (*Q*):

$$SC = aQ^b + c \qquad \text{(Eq. 6.7)}$$

where a, b, and c are empirically derived coefficients. The coefficient b varies depending with the presence or absence of sediment stock in the channel bed; when stock is present b is higher, and when stock is exhausted b is lower. Sediment

stock is assumed to increase when discharge is below a given threshold, and decrease when discharge is above that threshold. Ward (2008a; Chapter 5) substituted discharge values observed at Eijsden between 1995 and 2005 into this sediment rating function, and found that the resultant estimates of annual *SY* agreed well with observed *SY* over that period. Hence, in the present study we used the sediment rating curve of Doomen et al. (2008), in combination with observed discharge data for 1950-2000 at Eijsden, to derive an estimated mean annual *SY* over that period of 283,000 Mg a^{-1}. The observed discharge data were taken from the Waterbase website of RWS Waterdienst (http://www.waterbase.nl/).

The model was then calibrated against this estimate of mean annual *SY* by changing the ktc coefficients for land use types with a low transport capacity coefficient, ktc_{low} (i.e. forests and pastures), and those with a high transport coefficient, ktc_{high} (i.e. arable land). The calibration run was carried out using the mean observed rainfall erosivity factor (*R*) for 1950-2000. Since there are not enough observed data of *SY* to calibrate ktc_{low} and ktc_{high} separately, we altered only the values of ktc_{low} and estimated the other using a fixed ratio of 3.3, which has been found to reflect the relative difference in transport capacity between the different land use types in central Belgium (Verstraeten, 2006; Verstraeten et al., 2006b). The combination of ktc_{low} and ktc_{high} which provided the best match between simulated and observed *SY* was 0.80 and 2.64 respectively, giving a simulated *SY* of 282,927 Mg a^{-1} (compared to the observed *SY* of ca. 283,000 Mg a^{-1}). Since the soil erodibility factors (*K*) for slopes used in the calibration run were based on a best-estimate, and are subject to much uncertainty, we also carried out a simulation with the extreme-case scenario for *K*, as described in Section 6.3.2.2. Using the values for the calibration parameters stated above, this resulted in a *SY* of 265,368 Mg a^{-1}, i.e. just 6% lower than with the best-estimate. Since the extreme-case scenario only forces a relatively small change in *SY*, the uncertainty associated with the value of *K* on slopes will not affect the usefulness of the model results vis-à-vis the assessment of relative changes in long-term *SY*.

As the calibration was carried out for only one measuring station, validation was carried out in three steps. Firstly, mean basin-wide rainfall erosivity factors (*R*) were calculated for each individual decade between 1950-2000, and subsequently used to force the model using the calibrated values of ktc_{low} and ktc_{high}. The output were found to have a reasonable agreement with observed values of mean annual *SY*, as shown in Fig. 6.5 (r = 0.76 and N&S = 0.51). Whilst the model somewhat underestimates the interdecadal variability in *SY*, this level of correlation is encouraging given that: land use has been assumed constant over the period 1950-2000; other human impacts including dredging, changes in agricultural practice, and sediment conservation practices have been ignored; actual *SY* is also dependent on the availability of sediment stock from preceding years; and the model does not account for within channel deposition or erosion. The second step of the validation made use of estimates of *SY* for the Ourthe

(Meuse tributary) and Meuse rivers at Liège, made by Lemin et al. (1987). They found that the *SY* of the Ourthe at Liège was ca. 20.4% of the magnitude of the *SY* of the Meuse at Liège, just upstream from the confluence with the Ourthe (with a range of uncertainty from 12.4% to 33.9%). In our simulations the *SY* of the Ourthe was ca. 23.9% of the magnitude of the *SY* of the Meuse at the same point. Hence, the relative contributions of these two river sections to total *SY* appear to be well simulated. This is especially promising since the percentage cover of arable land (where most soil erosion occurs) upstream from Liège on the Ourthe (19.4%) differs greatly from that upstream from Liège on the Meuse (32.3%). Thirdly, the mean annual value of soil erosion per hectare (irrespective of soil delivery) as simulated by WATEM/SEDEM (0.26 Mg ha^{-1} a^{-1}) was compared to two estimates based on maps of erosion estimates at the European scale, namely the USLE estimates of Van der Knijff et al. (2000) and estimates from the PESERA project (Kirkby et al., 2004; S.P.I.04.73., 2004; website: http://eusoils.jrc.it/ESDB_Archive/pesera/pesera_cd/index.htm). Our estimate of soil erosion is similar to that of Van der Knijff et al. (2000) (0.18 Mg ha^{-1} a^{-1}), though much lower than that of PESERA (0.91 Mg ha^{-1} a^{-1}). However, as both of these estimates are based on models at the European scale, Van Rompaey et al. (2003) have shown that neither is capable of accurately estimating soil erosion at the local scale across all European environments. For the upstream Meuse basin, very few estimates of alluvial sediment storage are available, and hence no direct calibration was carried out based on observed sediment storage estimates. However, alluvial sediment storage in these areas is very low compared to that in lowland systems (Notebaert and Verstraeten, 2008), and hence the effects on *SY* are small. Moreover, if these stored sediment volumes were taken into account during the calibration, this would simply lead to higher values of the ktc coefficients, and would not affect the relative changes in *SY* between the time-periods studied.

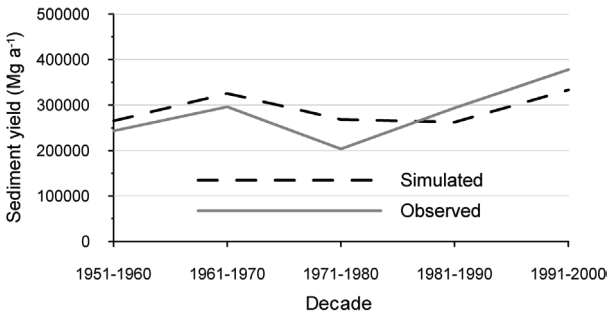

Fig. 6.5: Observed and simulated mean annual sediment yield per decade at Eijsden for the period 1950-2000 AD (r = 0.76, N&S efficiency = 0.51).

6.5 Results and discussion

6.5.1 Land use change

The land use of the Meuse basin has changed significantly over the course of the

late Holocene; these changes have had a profound effect on the susceptibility of the underlying soil to erosion, as expressed by the crop factor (*C*) (Fig. 6.6). In the period 4000-3000 BP the mean basin-wide value of *C* was extremely low (0.001), since the basin was almost fully forested (98%) at that time (e.g. Bunnik, 1995; Gotjé et al., 1990; Lefevre et al., 1993; Tallis, 1990), with a few small areas covered by wetlands and water bodies. By the 11th Century, *C* had increased to 0.090, in response to the reduction of forest area (to ca. 54%) in the intervening years; the forest had been replaced by pasture and arable land. The conversion of forest to pasture and arable land continued until the end of the 19th Century, at which point *C* shows a peak value of 0.147. It should be noted that the changes assumed here are based partly on linear extrapolation between the 11th and 18th Centuries due to the lack of detailed information for that period (Ward et al., 2008a; Chapter 3). In reality some centuries will have seen faster/slower rates of land use change, and the long-term deforestation may at times even have been checked by external influences such as the bubonic plague (e.g. Lang et al., 2003; Ruddiman, 2003). However, since this study mainly aims to assess the long-term trends in *SY*, rather than to reconstruct exact estimates of *SY* per century, more accurate centennial land use maps are not required. Reforestation and rapid urbanisation in the 20th Century led to a decrease in *C* compared to the peak value of the 19th Century. For the 21st Century, both the A2 and B1 scenarios of EURURALIS lead to a further decrease in *C*, with the strongest decline in the latter. These reductions are mainly caused by the expected reduction in arable land; the expected changes in forest and urban area are small.

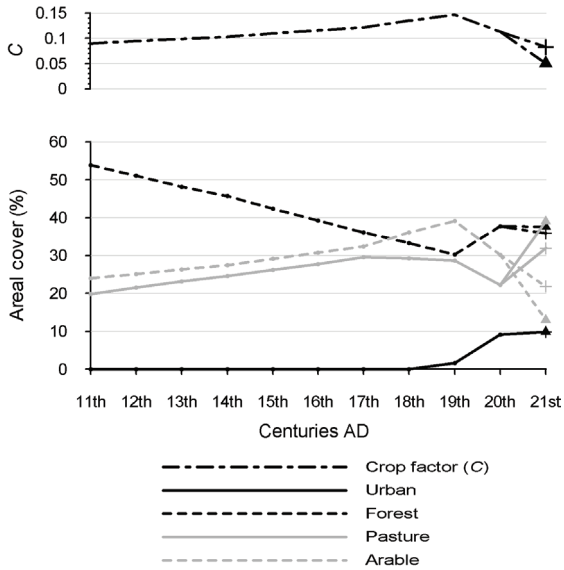

Fig. 6.6: Areal coverage (%) of urban area, forest, pasture, and arable land, and the mean basin-wide crop factor (C) upstream from Eijsden for the period 1000-2100 AD. For the 21st Century, land use is based on future scenarios A2 (shown by '+' symbol), and B1 (shown by triangle symbol) derived from the EURURALIS dataset (WUR/MNP, 2007).

6.5.2 Long-term changes in late Holocene sediment yield

The results of our long-term simulations of Meuse basin *SY* show a striking increase between the period 4000-3000 BP (ca. 92,000 Mg a^{-1}) and the last millennium (ca. 306,000 Mg a^{-1}), despite an increase in *R* of just 3% between those periods (Fig. 6.7). Over the period 4000-3000 BP, *SY* and *R* show little change, and in neither case can a linear trend be identified (MK-test = 0.454, p = 0.650 in both cases). However, between the 11th and 19th Centuries inclusive, Fig. 6.7 suggests a strong increasing trend in *SY* from ca. 258,000 Mg a^{-1} in the 11th Century to ca. 388,000 Mg a^{-1} in the 19th Century. The trend is highly significant (MK = 5.265, $p < 0.001$; Spearman's rank = 0.983, $p < 0.001$); for the same period no significant trend in *R* is noted (MK = 0.568, p = 0.570; Spearman's rank = 0.185, p = 0.463).

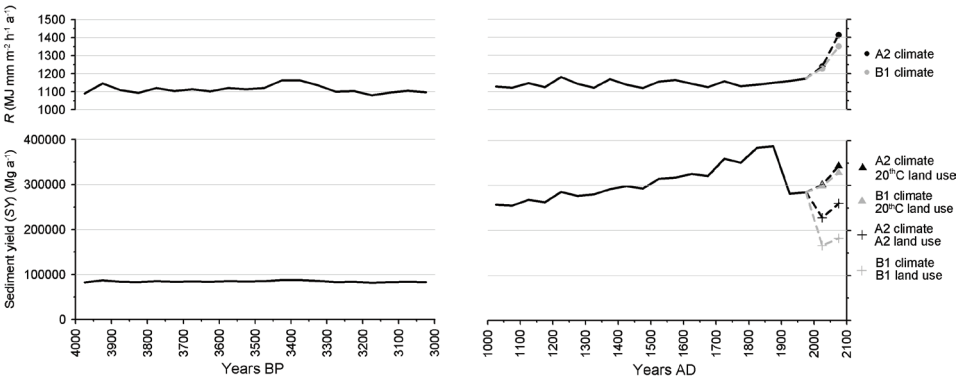

Fig. 6.7: Long-term (50-yr) changes in mean annual sediment yield and rainfall erosivity factor (R) over the periods 4000-3000 BP and 1000-2000 AD, and projected changes for the 21st Century according to climate model results forced by SRES emission scenarios A2 and B1. For the 21st Century, the model runs have been carried out with estimates of future land use according to the A2 and B1 scenarios of EURURALIS (shown by '+' symbols), and with land use held constant to that of the 20th Century (shown by triangle symbols). Note that land use changes are prescribed per century, whilst R is prescribed per 50-yr period.

Within the framework of increasing *SY* over the last millennium, the 20th Century is anomalous, since the average *SY* in this period is ca. 281,000 Mg a^{-1}, some 28% lower than the 19th Century peak value. Studies carried out in the late 20th Century by Close-Lecocq et al. (1982) and Lemin et al. (1987) conclude that the *SY* of the Meuse increased significantly between the late 19th and late 20th Centuries. These studies were based on estimates of *SY* derived from daily measurements of Meuse discharge and suspended sediment load at Liège, compared to similar estimates by Spring and Prost (1883) a century earlier. However, the results of Close-Lecocq et al. (1982) and Lemin et al. (1987) are based on observations carried out for periods of less than a year, and in the case of Lemin et al. (1987) mainly during high-flows. The results of Spring and Prost (1883) are based on observations taken during one year. Ward (2008a; Chapter 5) examined observed time-series of Meuse *SY* at Eijsden for the period 1995-2005, and found the

interannual variability to be greater than the differences between the three former studies. Hence, Ward (2008a; Chapter 5) argues that these studies do not provide evidence of increased *SY* over that time-period, since the discrepancy could easily be explained by methodological differences (e.g. the bias towards measurements during high-flows) and natural climatic variations alone (due to the (sub-)annual observation periods). Based on a conceptual assessment of the potential effects of climate and land use change on *SY*, Ward (2008a; Chapter 5) suggests that Meuse *SY* in the late 20th Century may have been lower than that of the late 19th Century as a result of changes in land use. On the other hand, Lemin et al. (1987) suggest that the increase in sediment yield which they described between the 19th and 20th Centuries may have resulted from the endikement and regulation of the Meuse river between Namur and Liège between those periods, which prevents the deposition of sediments on the floodplain in all but the largest floods. It would be useful to carry out detailed geomorphological fieldwork in the floodplains to investigate what effect this has had on sediment yield over the last century, and to what extent this compensates for the decreases simulated in the present paper in response to land use change.

Since the change in *R* has been very small over the course of the late Holocene, it can be assumed that the large increase in *SY* can be mainly ascribed to the effects of land use change. In order to delineate the effects of climate variability (*R*) and land use change on the *SY* of the last century we carried out a further simulation whereby the climate data for the period 4000-3000 BP were used in combination with the 20th Century land use map, and the 20th Century climate data were used in combination with the Holocene land use map. The results of these simulations (Table 6.3) show that the increase in *R* between these two time-periods forced an increase in *SY* of ca. 9%, whilst the changes in land use forced an increase in *SY* of some 198%. Thus, on this timescale almost all of the increase in *SY* can be ascribed to the effects of land use change.

Table 6.3: Absolute and percentage change in sediment yield (SY) between 4000-3000 BP and the 20th Century as a result of climate change only, land use change only, and climate and land use change together. On this timescale the large increase in SY can mainly be attributed to the effects of land use change (and mainly the conversion of forest to arable land).

	Change in *SY* between 4000-3000 BP and 20th Century	
	δ*SY* (Mg a^{-1})	δ*SY* (%)
Climate change only	+8000	+9%
Land use change only	+181,000	+198%
Climate and land use change	+190,000	+207%

In order to further investigate the relative effects of climate and land use change on *SY*, two sensitivity analyses were carried out to examine the relative effects

of: (a) changes in *R* and the conversion of forest to arable land, and (b) changes in *R* and the conversion of forest to pasture. This was achieved by individually varying the input maps of *R* and land use. A synthetic range for values of *R* was chosen to cover the full range of basin-wide values of *R* simulated in the periods 4000-3000 BP and 1000-2000 AD (1000-1225 MJ mm m^{-2} h^{-1} a^{-1}), with simulations being carried out for increments of 25 MJ mm m^{-2} h^{-1} a^{-1} within this range. Land use maps were created to show incremental decreases in forest cover from 100% to 0%, with the remaining land being assigned as either arable (Fig. 6.8a), or pasture (Fig. 6.8b). The land use maps were created by assuming a reference situation of 100% forest cover, and then simulating land use changes according to the methods described in Section 6.3.2.4. Within the range of climate variability simulated over the late Holocene, changes in land use clearly have a much greater effect than changes in *R*. Moreover, conversion of forest to arable land has a much larger impact on *SY* than conversion to pasture. Interestingly, the results in Fig. 6.8 show that as the percentage cover of forest decreases, the effect of an incremental increase in *R* increases. Therefore, whilst land use change (and namely the conversion of forests to arable land) acts as the primary control on long-term changes in *SY*, the sensitivity of *SY* to changes in climate increases as the amount of deforested land increases.

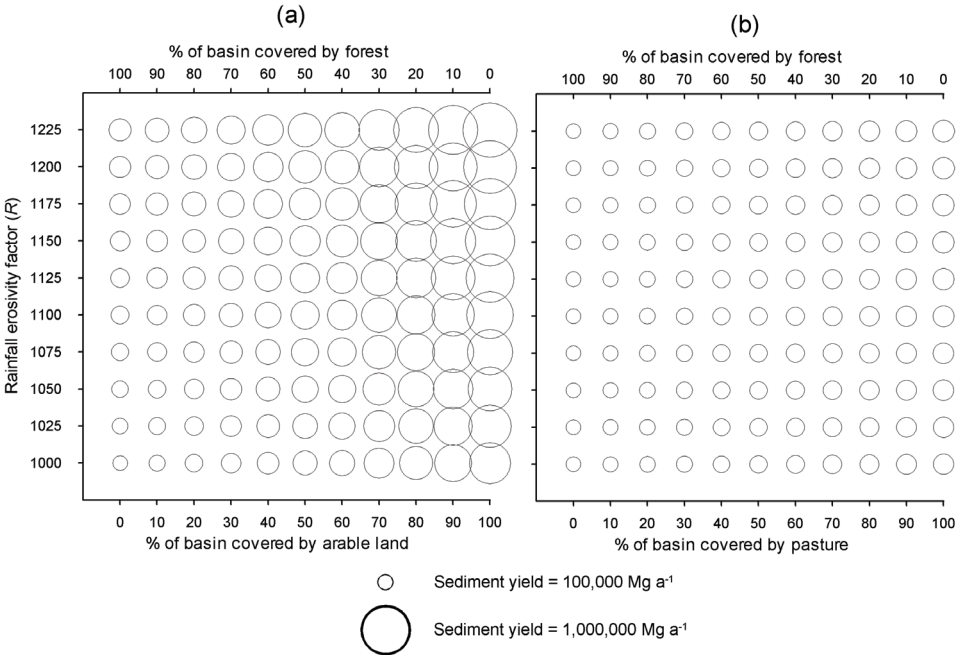

Fig. 6.8: Bubble plots showing the individual effects of changes in land use and rainfall erosivity factor (R) (MJ mm m^{-2} h^{-1} a^{-1}). In Fig. 8a the effects of forest conversion to arable land are shown, and in Fig. 8b the effects of forest conversion to pasture. Sediment yields show a greater response to changes in land use than changes in rainfall erosivity, although the relative influence of changes in rainfall erosivity increases as the total forest coverage decreases, especially when converted to arable land.

6.5.3 Comparison with multi-proxy evidence

Our findings of a large increase in Meuse basin *SY* between the last millennium and the more or less natural situation at 4000-3000 BP are in line with the findings of a number of field studies carried out in the Rhine-Meuse delta. Beets and Van der Spek (2000) examined the amount of bed load deposited in the main branch of the Rhine between 4000 BP and 1700 BP, and the evolution of channel morphology in the Rhine-Meuse delta during the Holocene. Based on these findings they postulate that the supply of fluvial sediments was low at that time. Erkens et al. (2006) reconstructed the long-term sediment delivery to the Rhine delta between 9000 and 1000 BP (with increments of 1000 years) by establishing the volume of stored sediments in the delta area based on DEMs and over 200,000 corings. For the period 9000-1000 BP they estimate that the mean suspended sediment delivery rate to the delta was ca. 1,000,000 Mg a^{-1}, compared to ca. 3,400,000 Mg a^{-1} in the period 1970-2000 AD. Whilst these results refer to the Rhine delta only, which has different characteristics to the neighbouring Meuse, the increase between long-term mean Holocene and present-day sediment delivery rate is of the same order of magnitude as our simulated increase in *SY*.

Based on detailed geomorphological reconstructions and sediment delivery modelling, De Moor and Verstraeten (2008) conclude that the *SY* of the Geul River (a small Meuse tributary which enters the Meuse a few kilometres north of Maastricht in the Netherlands) increased more than eight-fold between the mid Holocene and the period 1000-1500 AD. This increase is even greater than that simulated in the present study, but this can be explained by the higher erodibility of the mainly loess soils of the Geul basin, and the fact that ca. 86% of the basin is estimated to have been cultivated by 1000 AD, as opposed to 44% of the Meuse basin.

The importance of land use change on *SY* has also been noted in numerous other basins around the world (e.g. Keesstra et al., 2005; Kettner et al., 2007; Lang and Bork, 2006; Nearing et al., 2005; Trimble, 1999). A permanent vegetation cover protects soils from direct rainfall impact, crusting, and sealing, and can reduce the amount of surface runoff significantly. Furthermore, since areas under forests have a high sediment trapping efficiency, forested areas cause higher rates of deposition on the flow path between erosional areas and river channels (Van Rompaey et al., 2002).

6.5.4 Potential changes in sediment yield under future scenario conditions

For the 21st Century our simulation results are highly sensitive to the scenario (both land use and climate) used (Fig. 6.7), with decreased *SY* in the 21st Century compared to the 20th Century when both climate and land use change are considered, and increased *SY* when only climate change is considered. The effects of land use and climate change have been delineated and are shown

for each scenario in Table 6.4. The simulated increase in *R* (due to an increase in both mean annual precipitation and intense rainfall events) is greater under the more extreme A2 emission scenario than under the B1 scenario. As a result, the effects of climate change on *SY* are greater under the A2 climate change scenario. The effects of projected land use change under scenarios A2 and B1 are relatively large, forcing decreases in *SY* of 26% and 46% respectively (relative to the 20th Century). Since the changes in the percentage cover of forest and urban area are expected to be relatively modest in the 21st Century (Fig. 6.6), most of this land use change effect can be ascribed to the expected large decrease in arable land at the expense of pasture and grassland. The combined effects of climate and land use change force large decreases in *SY* in the coming century for both scenarios, particularly for the B1 scenario, since the increase as a result of augmented rainfall erosivity is less than the decrease as a result of land use change. It should be noted that land use pertaining to 2030 AD has been used in the simulations for the entire 21st Century, whilst separate values of *R* have been used for 2000-2050 AD and 2050-2100 AD. Since land use change is dependent on socio-economic and political decisions, and also on physical characteristics (Van Rompaey et al., 2002; Verburg, 2006), it is difficult to simulate meaningful scenario changes for a longer timeframe, and therefore the results shown here for the late 21st Century are highly sensitive to future socioeconomic and political decisions and preferences. However, the results are indicative of the possible long-term trend relative to that of the last millennium.

Table 6.4: Absolute and percentage change in sediment yield (SY) between the 20th and 21st Centuries as a result of climate change only, land use change only, and climate and land use change together, according to the A2 and B1 emission scenarios of the IPCC, and the associated land use change scenarios of EURURALIS.

	Change in *SY* between the 20th and 21st Centuries			
	A2 scenario		B1 scenario	
	δ*SY* (Mg a^{-1})	δ*SY* (%)	δ*SY* (Mg a^{-1})	δ*SY* (%)
Climate change only	+34,000	+12%	+23,000	+8%
Land use change only	-73,000	-26%	-130,000	-46%
Climate and land use change	-39,000	-14%	-106,000	-38%

For the Rhine basin, Asselman (1997) used a model of soil loss based on the Universal Soil Loss Equation (USLE) to investigate the effects of future climate change (by 2050 AD) on *SY* under the Business as Usual (BaU) scenario of the IPCC (1992). She found that climate and land use may force a small decrease (ca. 3%) in *SY*, with an 18% decrease and 15% increase associated with land use and climate change respectively. Whilst these figures cannot be directly compared to our estimates for the Meuse, due to differences in basin characteristics, scenarios used, and methodologies, the signs of the changes are in agreement with our findings.

A reduction in Meuse *SY* could be beneficial for a number of existing and proposed Meuse flood defence measures. For example, an international flood action plan for the Meuse which was drawn up by riparian states in 1998 includes a number of measures to reduce the vulnerability of the basin to flooding, including the construction of retention basins, the recovery or construction of floodplains, and the increase of the discharge capacity through the widening of the river channel and floodplains (De Wit et al., 2007b). A reduction in *SY* could mean that less dredging would be needed in the future in order to maintain these measures.

6.6 Conclusions

According to the results of this study, the *SY* of the Meuse River has increased significantly over the course of the late Holocene. Prior to significant anthropogenic influence (4000-3000 BP) the mean annual *SY* was fairly constant, with a mean value of ca. 92,000 Mg a^{-1}. For the last millennium, mean annual *SY* increased more than three-fold to ca. 306,000 Mg a^{-1}. During this period the mean *SY* was far from constant, showing a very strong positive trend between the 11th and 19th Centuries inclusive, followed by a significant decrease in the 20th Century. The results are in agreement with the limited regional multi-proxy data available. On the millennial timescale almost all of the increase in *SY* can be ascribed to the effects of anthropogenic land use change. Sensitivity analyses show that although land use change acts as the primary control on long-term changes in *SY* (and especially the conversion of forest to arable land), the sensitivity of *SY* to changes in climate increases as the amount of deforested land increases.

The mean *SY* of the 20th Century is some 28% lower than that of the 19th Century, as a result of planned reforestation and rapid urbanisation. These findings are in contrast to those of two earlier works (Close-Lecocq et al., 1982; Lemin et al., 1987) which suggest an increase in *SY* between the late 19th and 20th Centuries. It is possible that the increase in *SY* observed in those studies was obtained due to natural climatic variations and methodological differences, rather than being indicative of a structural increase in *SY*. Nevertheless, the endikement and regulation of the Meuse between the late 19th and 20th Centuries may indeed have resulted in an increase in sediment yield between Namur and Liège, as suggested by Lemin et al. (1987).

For the near-future (21st Century), *SY* is highly sensitive to the scenario (both climate and land use) used. Relatively large increases in rainfall erosivity over the coming century, under both the A2 and B1 emission scenarios, force increases in *SY* compared to the 20th Century of ca. 12% and 8% respectively. However, the land use change scenarios associated with these two emission scenarios force decreases in *SY* of 26% and 46% respectively, especially due to the replacement of arable land with pasture and grassland. Although the scenarios used here do not represent the full range of possible future changes, they do lie towards the upper and lower end of the full range of IPCC scenarios respectively, and therefore give a good idea of the potential range of uncertainty in future *SY*. Given

this large uncertainty, robust management strategies should be employed for the future, although the potential reduction in *SY* compared to the 20th Century could be beneficial to the maintenance of existing and proposed flood defence measures. It is encouraging that in none of the combinations of future scenarios used here did the simulated *SY* of the 21st Century exceed the simulated peak value of the 19th Century. Since the majority of catchments around the world are expected to experience increasing rainfall erosivity over the coming century, this study highlights the potentially significant efficacy of sound land use planning as a tool to mitigate the negative effects of soil erosion and increased sediment delivery to rivers.

Chapter 7

Synthesis

7.1 Objectives and research questions

The main objectives of the research discussed in this thesis were to assess the long-term trends and changes in discharge, flood frequency, and sediment yield of the River Meuse during the late Holocene and the 21st Century in response to natural and anthropogenic changes in climate and land use, and to compare the relative impacts of these factors on different timescales. In order to address these objectives, the following four key research questions were formulated:

1. Can we develop a coupled climate-hydrological modelling approach to simulate long-term changes in palaeodischarge? To what extent can multi-proxy data be used to test the performance of such models as tools for palaeodischarge assessment?
2. How has the discharge and flood frequency of the River Meuse changed between a natural reference period when the natural climate forcings were similar to those of today and human influence on land use was minimal (4000-3000 BP), and a period influenced by anthropogenic changes in land use (1000-2000 AD) and greenhouse gas and sulphate aerosol emissions (post industrial revolution)? What mechanisms caused these changes in discharge and flood frequency?
3. What are the relative effects of climate change and land use change on the discharge and flood frequency of the Meuse during the 21st Century? How do these compare to the effects of long-term natural and anthropogenic change over the late Holocene?
4. What effects have changes in land use and climate had on soil erosion and sediment yield in the Meuse basin during the late Holocene? What effects can be expected in the 21st Century?

In this chapter a synthesis is provided of the answers to these research questions, based on the results described in Chapters 2 to 6. In addition, a number of implications of the results for water management are given, as well as a number of recommendations for future research.

7.2 The use of a coupled climate-hydrological model to assess palaeodischarge

Prior to this study, the coupling of a climate model with a spatially distributed hydrological model had not been used to assess changes in palaeodischarge over the Holocene. Hence, before setting up a detailed model for the Meuse, the first step in this thesis (Chapter 2; Ward et al., 2007) involved setting up a low resolution model (0.5° x 0.5°) with a monthly time-step to simulate the discharge of 19 rivers

around the globe (Amazon, Congo, Danube, Ganges, Krishna, Lena, Mackenzie, Mekong, Meuse, Mississippi, Murray-Darling, Nile, Oder, Rhine, Sacramento-San Joaquin, Syr Darya, Volga, Volta, Zambezi). This research served as a pilot study to examine the usefulness of such a coupled modelling approach in the assessment of long-term changes in (palaeo)discharge. The climate model ECBilt-CLIO-VECODE (Brovkin et al., 2002; Goosse and Fichefet, 1999; Opsteegh et al., 1998) was coupled offline with the hydrological model STREAM (Aerts et al., 1999) to simulate the discharge of these rivers in three time-slices, namely: Early Holocene (9000-8650 BP), Mid Holocene (6200-5850 BP), and Recent (1750-2000 AD). The model results were compared to palaeodischarge estimates based on multi-proxy records available in the literature in order to test the model's skill in retrodicting the changes over the Holocene. The quality of the proxy data for each basin, in terms of the confidence that they reflect the actual palaeodischarge situation of the river in question during the relevant time-slice, was classed as *good*, *reasonable*, or *low*. Of the model runs for which the proxy data were *good* or *reasonable*, 72% were in good agreement with the proxy data, and 92% were in at least reasonable agreement. The agreement between model and proxy data was especially good for sub-tropical basins influenced by northern hemisphere monsoons, and mid-latitude European basins with (varying degrees of) maritime influence.

Since the modelling approach proved useful in the retrodiction of monthly palaeodischarges, it was subsequently applied to the Meuse basin (Chapter 3; Ward et al., 2008a). The spatial resolution was increased to 2' x 2' (ca. 2.4 km x 3.7 km), and a daily time-step was implemented in order to assess long-term changes in flood frequency. In addition, more detailed estimates were made of the long-term changes in land use, compared to the pilot study. Again, the results of the simulations were in good agreement with qualitative long-term signals derived from various multi-proxy records.

These applications of the coupled climate-hydrological modelling approach show that the method forms a useful tool for the assessment of long-term changes in palaeodischarge. Multi-proxy data provide a means to verify model performance against periods in which environmental conditions were different to those during the period of instrumental measurements. As a result, our confidence in the ability of such models to simulate future changes in discharge and flood frequency is improved compared to models calibrated and validated only against instrumental records from the last century.

7.3 Late Holocene discharge and flood frequency of the River Meuse: effects of climate and land use change

The coupled climate-hydrological model was used to simulate the daily discharge of the Meuse river over two periods: 4000-3000 BP and 1000-2000 AD (Chapter 3; Ward et al., 2008a). The period 4000-3000 BP was selected as a 'natural reference period', as the natural climatic forcings at that time were broadly similar to those of today (Goudie, 1992), whilst human influence on land use was minimal

(Bunnik, 1995; Gotjé et al., 1990; RWS Limburg/IWACO, 2000). The period 1000-2000 AD was heavily influenced by human activities, namely changes in land use throughout the period, and greenhouse gas and sulphate aerosol emissions since the industrial revolution. By comparing the changes in discharge characteristics between these two periods it was therefore possible to examine the effects of anthropogenic changes in both climate and land use. It was assumed that the basin was almost fully forested during the period 4000-3000 BP. For 1000-2000 AD land use change was reconstructed based on historical sources.

The results presented in this thesis show that the mean discharge and flood frequency of the Meuse were significantly greater in the last millennium than in the natural reference period 4000-3000 BP. The mean annual discharge increased by 6.6% between 4000-3000 BP (244.8 $m^3 s^{-1}$) and 1000-2000 AD (260.9 $m^3 s^{-1}$); the most marked increase occurred in the summer half-year (May-October) (+21.6%). The recurrence time of high-flow events with a discharge in excess of 3000 $m^3 s^{-1}$ (i.e. similar in magnitude to during the floods of 1926 and 1993), decreased from 77 years in the period 4000-3000 BP, to 65 years in 1000-2000 AD. On this timescale the increases in mean discharge and flood frequency can be almost fully attributed to the effects of decreased evapotranspiration as a result of the large-scale deforestation of the basin. On this millennial timescale, climatic change had an insignificant effect on late Holocene Meuse discharge. However, between the 19th and 20th Centuries, climate change overwhelmed land use change as the most important mechanism forcing changes in discharge and flood frequency. This is in agreement with the results of Tu (2006), which show no evidence of a significant effect of land use change on observed 20th Century Meuse discharge time-series. Although evapotranspiration was higher in the 20th Century than in the 19th Century (due to reforestation and increased temperature), the mean discharge was greater in the 20th Century (270 $m^3 s^{-1}$) than during any preceding century, and 2.5% greater than in the 19th Century. Moreover, the occurrence of high-flow events greater than 3000 $m^3 s^{-1}$ was almost twice as frequent during the 20th Century than during the natural reference period 4000-3000 BP. The increases in mean discharge and flood frequency in the 20th Century (compared to the 19th Century) are the result of a strong increase in annual and winter precipitation, probably related to anthropogenic climate change.

A comparison of the discharge results for the Meuse derived from the detailed model (Chapter 3; Ward et al., 2008a), with the results derived from the global model (Chapter 2; Ward et al., 2007), further illustrates these conclusions. The results of the global model show that long-term changes in orbital forcing had little effect on Meuse discharge between the periods 9000-8650 BP, 6200-5850 BP, and 1750-2000 AD. The results of the detailed model show that the effects of long-term climatic change on discharge were small between 4000-3000 BP and the last millennium. Since anthropogenic changes in land use were not accounted for in the global model, the effects of large-scale deforestation between the Mid Holocene and last millennium were not simulated in that model configuration.

7.4 Projected changes in discharge and flood frequency of the Meuse in the 21st Century

Simulations of daily Meuse discharge were carried out for the 21st Century (Chapter 4; Ward et al., 2008b). The climate runs were based on forcings described in the Special Report on Emission Scenarios (SRES) of the Intergovernmental Panel on Climate Change (IPCC, 2000). SRES scenarios A2 and B1 were used as these lie towards the upper and lower end of the full spectrum of IPCC scenarios respectively (in terms of atmospheric concentrations of CO_2 by 2100 AD), and can therefore be used to assess the response of the system to a broad range of possible future changes. The 21st Century land use configurations were derived from the EURURALIS 2.0 project (WUR/MNP, 2007); the 'Continental Market' and 'Global Cooperation' scenarios were used. The concept storylines of these scenarios correspond to those of SRES scenarios A2 and B1 respectively (and are therefore referred to thusly in this thesis), although the storylines were elaborated for land use issues and agricultural policies typical for Europe (Westhoek et al., 2006). These scenarios show relatively small changes in land use between the 20th and 21st Centuries, the most significant change being an increase of forested area by ca. 2% in scenario B1 (and concurrently a decrease in agricultural area of ca. 2%) compared to the 20th Century.

The simulations for the 21st Century show increases in mean annual temperature, precipitation, and discharge, to values far greater than those simulated in either the period 4000-3000 BP or 1000-2000 AD. The simulated increases in mean discharge between the periods 1950-2000 AD and 2050-2100 AD (+16.6% for A2, and +12.7% for B1) are greater than the increase in mean discharge over the entire period 4000-3000 BP to 1950-2000 (+10.0%). Furthermore, the frequency of high-flows with a discharge in excess of 3000 $m^3 s^{-1}$ at Borgharen (similar in magnitude to the discharge during the major floods of 1926 and 1993) increases from once per 40 years in the 20th Century to once per 20 years in the 21st Century under scenario A2, and once per 25 years under scenario B1. For both mean discharge and flood frequency, the increases simulated under scenario A2 are significantly greater than those simulated under scenario B1, although the increases between the 20th and 21st Centuries under the more optimistic B1 scenario are also large and statistically significant. On this timescale the effects of the modest land use change projected for the 21st Century are small; almost all of the modelled increase in mean annual discharge and high-flow frequency is the result of climatic change. Between the period 4000-3000 BP and the 20th Century, there was little change in the frequency of extreme floods (return period 1250 years); the large-scale deforestation of the basin had only a minor effect on the magnitude of such events. However, for the 21st Century, increases are projected under both scenarios A2 and B1 due mainly to increased winter precipitation, with the increases under the former scenario being highly significant.

7.5 Meuse basin sediment yield: effects of climate and land use change over the late Holocene and 21st Century

In order to examine the effects of long-term changes in climate and land use on the sediment yield of the River Meuse, the spatially distributed soil erosion and sediment delivery model WATEM/SEDEM was used (Van Oost et al., 2000; Van Rompaey et al., 2001a; Verstraeten et al., 2002) to simulate changes in 50-yr mean sediment yield (Chapter 6; Ward et al., 2008c). The model was forced using the climate output of ECBilt-CLIO-VECODE (Brovkin et al., 2002; Goosse and Fichefet, 1999; Opsteegh et al., 1998), and land use configurations were determined from historical records and future projections of the EURURALIS project (WUR/MNP, 2007) The sediment yield of the Meuse River increased significantly over the course of the late Holocene. During the natural reference period 4000-3000 BP, the mean 50-yr sediment yield was fairly constant, with a mean value of ca. 92,000 Mg a^{-1}. For the last millennium, the mean 50-yr sediment yield increased more than three-fold to ca. 306,000 a^{-1}. Over the course of the last millennium the mean 50-yr sediment yield was far from constant, showing a very strong positive trend between the 11th and 19th Centuries inclusive, with a peak of ca. 388,000 Mg a^{-1} in the 19th Century. These results are in agreement with the limited regional multi-proxy data available. On a millennial timescale almost all of this increase in sediment yield can be ascribed to the effects of anthropogenic land use change, and mainly the conversion of forest to arable land. In the 20th Century, planned reforestation and rapid urbanisation led to a reduction in simulated mean annual sediment yield to ca. 281,000 Mg a^{-1}. This finding is in contrast to the results of two earlier works (Close-Lecocq et al., 1982; Lemin et al., 1987), which suggest that an increase in sediment yield occurred between the late 19th and 20th Centuries. In Chapter 5 (Ward, 2008a), it is shown that the increase in sediment yield noted in the aforementioned studies may be caused by either interannual differences, or by the methodologies used in those studies, rather than being indicative of a systematic increase. However, it is also possible that the endikement and regulation of the Meuse between Namur and Liège over the course of the 20th Century did indeed lead to an increase in sediment yield over that time period, as suggested by Lemin et al. (1987). It would be useful to carry out detailed geomorphological fieldwork in the floodplain to investigate what effects the endikement and regulation of the river have had on sediment yield, in relation to the decrease simulated in response to land use change.

For the 21st Century, sediment yield is highly sensitive to the scenario (both climate and land use) used. Relatively large increases in rainfall erosivity over the coming century, under both the A2 and B1 emission scenarios, force increases in sediment yield compared to the 20th Century of ca. 12% and 8% respectively. However, the associated land use change scenarios force decreases in sediment yield of 26% and 46% respectively, especially due to the replacement of arable land with pasture and grassland. The net effect is thus a decrease of sediment yield compared to the 20th Century.

The results of sensitivity analyses show that although land use change acts as the primary control on long-term changes in sediment yield, the sensitivity of sediment yield to changes in climate increases as the percentage of deforested land increases.

7.6 Final outcomes

Changes in both land use and climate have major impacts on the discharge, flood frequency, and sediment yield of the River Meuse. Over the course of the last 4000 years, the large-scale deforestation of the basin has been the dominant mechanism causing increases in these three parameters, whilst millennial scale (natural) changes in climate have played only a secondary role. Nevertheless, whilst deforestation has led to increased high-flow frequencies over the late Holocene, it has had little effect on the most extreme flood events (e.g. those with a return period of 1250 years and longer). In the 21st Century, simulated mean annual temperature and precipitation in the Meuse basin are far greater than the values simulated for the last 4000 years. As a result, further and large increases in discharge and high-flow frequency are simulated, even for the most extreme flood events. The effects of the modest changes in 21st Century land use on discharge and flood frequency are small. Nevertheless, land use change continues to be the dominant factor controlling changes in sediment yield in the 21st Century. Despite a relatively large increase in the erosivity of rainfall, sediment yield is expected to fall in relation to that of the 20th Century. This is because the increases in soil erosion and sediment yield attributable to enhanced rainfall erosivity are more than compensated for by the decreases attributable to 21st Century land use change (mainly the replacement of arable land with pasture). In terms of sediment yield, even modest changes in land use have a great impact, especially conversions of arable land to either forest, pasture, or urban area). Moreover, the sensitivity of sediment yield to changes in climate increases as the proportion of the basin covered by forest decreases.

The differences in the responses of discharge and sediment yield in the 21st Century, despite long-term increasing trends in both parameters over the late Holocene, can be explained by the different physical processes causing those changes.

For discharge, the simulated long-term Holocene increase between 3000 BP and the 19th Century can be attributed mainly to the effects of deforestation on evapotranspiration. The replacement of forested land with agriculture and grasslands leads to a significant decrease in actual evapotranspiration totals due to changes in leaf area, stomatal response, interception, and soil water holding characteristics (Calder, 1993; Hornbeck et al., 1993; Mahe et al., 2005, Robinson et al., 2003). In our experiments the effects of changes in soil water holding capacity were minor since the model is fairly insensitive to changes in this parameter. With regards to evapotranspiration, the rates over pasture and arable land in the Meuse basin are similar, and hence the expected replacement of large

areas of arable land with pasture in the coming century (Chapter 6; Ward et al., 2008c) have little effect on discharge (and is therefore not simulated).

However, over the same period (3000 BP to 19th Century AD) the large increase in sediment yield has been invoked by different physical process, even though this increase can also mainly be attributed to deforestation. This increase is related to the protective effect of forest cover on the soil. A permanent forest cover provides protection against direct rainfall impact as interception by the canopy and leaf litter reduces the kinetic energy of rainfall impact; permanent vegetation cover protects against crusting and sealing; and strong root systems can help to bind and restrain soil particles (e.g. De Ploey, 1989; Van Rompaey et al., 2002). When forests are converted to agricultural areas, these protective properties are greatly reduced. However, unlike discharge, sediment yield is highly dependent on the type of agriculture (arable or pasture) since soil erosion on the former is greater than on the latter. Furthermore, land use change also has a great effect on the transportation of eroded sediments. In forests and pastures the transport capacity of overland flow is much lower than on arable land, meaning that eroded sediments are more easily redeposited in the former areas, thus reducing the total amount of sediment transported to the river (e.g. Van Oost et al., 2000).

Projections of land use change in the 21st Century suggest that the change in forest cover compared to the 21st Century will be relatively small, whereas the area covered by pasture is expected to increase significantly, with concomitant reductions in arable land. Hence, whilst these changes will not have a great effect on discharge, the effects on soil erosion and sediment transportation (and therefore sediment yield) will be much greater, because soil erosion and sediment transportation are both significantly higher on arable land than under pasture. Furthermore, the increase in sediment yield between 3000 BP and the 19th Century is of a much greater magnitude than the increase in discharge between these two periods, suggesting that sediment yield in the Meuse basin is more sensitive to land use change than is the case for discharge.

7.7 Implications for water management

Large-scale changes in the percentage forest cover of the basin can have significant impacts on discharge, flood frequency, soil erosion, and sediment yield. However, in the Meuse basin large-scale reforestation is not expected to occur in the 21st Century (WUR/MNP, 2007), due to the high economic demand on land and the attention to the preservation of cultural landscapes. Whilst the potential for reforestation to help reduce flood frequency in the Meuse basin by increasing evapotranspiration is therefore limited, the benefits of converting even a few percent of agricultural land to forest are great in terms of the effects on soil erosion and sediment yield. The effects of reforestation on the timing of peak flows (due to the reduction of runoff velocities and buffering) has not been examined in this study.

Although the effects of 21st Century land use change on high-flow frequencies may be small, this does not necessarily mean that the effects of land use change on flood risk are small. Assessments of flood risk must also examine potential flood damage, which may be highly dependent on land use change, particularly urbanisation. Future studies should be carried out to assess the effects of land use change (and climate change) on flood risk, as well as on high-flow frequencies.

Changes in discharge, flood frequency, and sediment yield in the 21st Century are all highly sensitive to the future climate scenario used. Even under the relatively optimistic B1 scenario, the simulated increases in discharge and flood frequency over the coming century are large. Hence, these effects may be unavoidable, even if a concerted and immediate effort were undertaken at the global scale to mitigate greenhouse gas emissions. This highlights the need for adaptation strategies to reduce the possibility of flooding in the future. Such strategies must be robust in terms of their flexibility towards the future, being able to deal explicitly with uncertainties, and providing a range of benefits under a whole range of future scenarios. Examples of such measures include multifunctional land use planning options whereby the land use in risk-prone areas is harmonious with intermittent inundation. For example, along the section of the Meuse between the Dutch and Belgian borders (Grensmaas), gravel is currently being extracted from an area of ca. 1100 ha., in order to enlarge the river channel and create a more appealing landscape. Aside from the benefits for nature conservation and tourism, such projects increase the flow capacity of the channel during high-flows, and provide additional areas for flood retention. The results of the present study underscore the need for adaptation measures of this nature, since they provide increased protection against flooding under all future scenarios.

The simulated reduction in the sediment yield of the Meuse in the 21st Century compared to the 20th Century could be beneficial for a number of existing and proposed Meuse flood defence measures. For example, an international flood action plan which was drawn up by the riparian states in 1998 includes measures to reduce the vulnerability of the basin to flooding, including the construction of retention basins, the recovery or construction of floodplains, and the increase of the discharge capacity through the widening of the river channel and floodplains. A reduction in sediment yield could mean that less dredging would be needed in the future in order to maintain these measures.

At present, water management laws in the Netherlands state that water defences must safely withstand a design water level, which is defined as the water level with a given return period in years. Currently, the return period for embanked river sections of the Netherlands is once per 1250 years, and once per 250 years for unembanked sections (Ministry of Transport, Public Works and Water Management, 2005, 2006). Since the introduction of the Water Defence Act in 1995, this water level must be reassessed every five years. At present this occurs based on the so-called design discharge, i.e. the discharge which occurs

at Borgharen once per 1250 years. At present this design discharge is estimated by fitting statistical distribution functions to observed annual discharge maxima, and then extrapolating to the required return period. However, the results of this study show that the discharge associated with such low frequency events will increase in the future, and hence estimates of design discharge based on observations from the past will be too low. The use of multi-scenario ensemble simulations of discharge, such as those performed in this study, could assist in the estimation of design discharges under a range of future climate and land use change scenarios.

Not only are the implications great for water management in the Meuse basin, but also in basins around the world, as major changes in discharge characteristics can also be expected elsewhere over the coming century. For example, Aerts et al. (2006) (using the model described in Chapter 2; Ward et al., 2007) simulated the discharge of 15 rivers around the globe, and found that for the majority of these rivers the projected change in mean discharge between the 20th and 21st Centuries due to climate change alone would be greater than, or of similar magnitude to, the change between the period 9000-8650 BP and 1750-2000 AD. The sensitivity of sediment yield to relatively small changes in land use in the Meuse basin highlights the importance of carrying out basin scale studies of this parameter around the world. In order to provide meaningful assessments of 21st Century sediment yield, detailed research on future land use change at the basin scale is a prerequisite.

One of the main values of using coupled models to simulate changes in discharge, flood frequency, and sediment yield over millennial timescales is that it facilitates a delineation of the effects of changes in climate and land use, thereby assisting in the identification of important causal mechanisms. The approach allows for the examination of the effects of anthropogenic activities against a natural reference period, which is not possible when only examining observed records or simulations of the last century and the coming century. Furthermore, the results of the coupled palaeodischarge models can be verified against multi-proxy evidence for periods in which environmental conditions were different to those of the present day. For these reasons the methodologies presented in this thesis form promising approaches for assessing the effects of past and future changes in climate and land use on hydrology and sediment yield in other basins around the world. However, the simplified modelling approaches used do not permit for an examination of the effects of human interference in the hydrological system in terms of adaptation strategies such as the building of dams and weirs; canalisation; the deepening or widening of river channels to increase discharge capacity; and the creation of retention areas for flood waters; etc. Over the past centuries, and in the 21st Century, such activities have had, or will have, major impacts on the Meuse. In future analyses of the effectiveness of these adaptation strategies, model structures must be employed that allow for the quantification of the effects of these measures on discharge and sediment yield. However, the aim

of this project was to gain a better insight into the effects of long-term changes in climate and land use on discharge, flood frequency, and sediment yield, and the sensitivity of hydrological systems to those changes.

7.8 Future research and recommendations

This thesis has provided valuable answers to the key research questions posed in the introduction, and the approach used forms a useful tool for the assessment of long-term changes in discharge, flood frequency, and sediment yield. Still, improvements can always be made. In this section, the final section of the thesis, a number of these improvements are discussed, as well as a number of recommendations for future research avenues and applications of the modelling approach.

- The climate model (ECBilt-CLIO-VECODE) used in this thesis has a relatively low spatial resolution and simplified physics compared to regional circulation models (RCMs). This makes it difficult to correctly simulate the regional details and variability of daily precipitation, especially for convective rainfall events. It would therefore be useful to use an RCM nested in a general circulation model (GCM) to obtain a more realistic series of spatial and temporal precipitation. However, at the present day it is not feasible to carry out such a study in ensemble mode for the long time-periods used here, as the computational time associated with these runs would be prohibitive. Any study of such a nature would necessarily involve the use of shorter time-slices (e.g. centuries), which would hinder the examination of long-term trends. As computational efficiency increases, the use of nested RCMs in palaeodischarge modelling should become more feasible.

- The statistical downscaling of precipitation was carried out according to a simple linear correction technique based on monthly correction factors. It would be useful to assess the results of this downscaling against a number of more sophisticated methods. For example, Leander and Buishand (2007) found it to be advantageous to correct also for the variability of 10-day precipitation amounts. Nevertheless, the precipitation results from the simple downscaling techniques were found to be in good agreement with observed records.

- Given the relatively low resolution of ECBilt-CLIO-VECODE, values for potential evapotranspiration were not taken directly from the climate model, but were calculated within STREAM based on the Thornthwaite (1948) equation for potential evapotranspiration and the Thornthwaite & Mather equation (1957) for actual evapotranspiration. If an RCM were used to simulate the climatic parameters, the results obtained directly from the model could be analysed against those of the Thornthwaite & Mather approach, to compare the skill of these methods.

- In this study the models are coupled offline; an online coupling of ECBilt-CLIO-VECODE with STREAM and WATEM/SEDEM would be an interesting challenge. This would allow for a more rapid simulation of palaeodischarge and sediment yield, and provide a more integrated tool for basin analysis.

- Specifically for the Meuse basin, the resolution used in this study for the STREAM model (2' x 2') means that only larger river networks can be delineated, and therefore the model cannot be used to assess the effects of climate and land use change in small headwater catchments. Given the resolution of the climate model used in the present study this is acceptable, since the precipitation data are in any case too coarse to carry out detailed assessments of discharge in small upstream catchments. However, in possible future applications using higher resolution RCMs, it would be essential to use a higher resolution for the hydrological model if the purpose of the research were to assess discharge in upstream tributaries.

- In terms of the validation of the results against palaeodischarge proxy data, the proxy evidence available for the Meuse basin at present are generally of a highly qualitative nature. Attempts to quantify the signals of change in discharge and sediment yield, though difficult, provide an interesting scientific challenge. Work is currently being carried out (within the same project as this research) to develop new proxy methods for reconstructing palaeodischarge using freshwater mussels (Versteegh et al., 2008) and changes in precipitation using sphagnum mosses (Brader et al., 2008). The results of these studies may provide more quantitative evidence for model verification.

- Since the methods used in this thesis have proved valuable for assessing the discharge, flood frequency, and sediment yield of the Meuse basin over the late Holocene and the 21st Century, it would be beneficial to apply the method to other basins around the world in order to assess regional effects of climate and land use change. Aerts et al. (2006) applied the low resolution model, described in Chapter 2 (Ward et al., 2007), to 15 river basins around the world, but an application of the daily model would also allow for an assessment of the changes in flood frequency in those (and other) basins, and the application of WATEM/SEDEM would allow for an assessment of the changes in soil erosion and sediment yield, which are expected to be major issues in many basins in the future.

- Water defences are often designed to withstand a discharge with a given return period. Currently, such estimates are usually carried out by extrapolating discharge observations of the last century to the desired return period. However, as this study has shown, these flood frequencies are variable through time and therefore assessments based on past discharge observations may not be valid for the future. Multi-scenario

climate-hydrological models such as the one used in this thesis can provide a powerful tool in the assessment of the return periods of extreme floods under altered environmental conditions, and their use could be more widely implemented in flood risk assessment.

- In this project we have not examined the effects of human interference in the hydrological system in terms of adaptation strategies such as the building of dams and weirs; canalisation; the deepening or widening of river channels to increase discharge capacity; the creation of retention areas for flood waters; etc. The results of our study highlight the need for continuing improvement of such measures in the future, and hence further research is required to quantify the effects of these measures in terms of their effects on hydrology and sediment yield.

References

Adam, D.P., Sims, J.D., Throckmorton, C.K., 1981. 130,000-yr continuous pollen record from Clear Lake, Lake County, California. Geology, 9(8), 373-377.

Adamson, D.A., Gasse, F., Street, F.A., Williams, M.A.J., 1980. Late Quaternary History of the Nile. Nature, 288, 50-55, doi:10.1038/288050a0.

Aerts, J.C.J.H., Bouwer, L.M., 2002. STREAM Krishna. A hydrological model for the Krishna River in India. RIKZ/Coastal Zone Management Centre, The Hague, The Netherlands, 34 pp., www.geo.vu.nl/users/ivmstream/public/aerts&bouwer2002a.pdf.

Aerts, J.C.J.H., Droogers, P., 2004. Climate change in contrasting river basins. Adaptation strategies for water, food and environment. CABI, Wallingford, U.K., 264 pp.

Aerts, J.C.J.H., Kriek, M., Schepel, M., 1999. STREAM (Spatial Tools for River Basins and Environment and Analysis of Management Options): 'Set Up and Requirements'. Physics and Chemistry of the Earth, Part B: Hydrology, Oceans and Atmosphere, 24(6), 591-595, doi:10.1016/S1464-1909(99)00049-0.

Aerts, J.C.J.H., Renssen, H., Ward, P.J., De Moel, H., Odada, E., Bouwer, L.M., Goosse, H., 2006. Sensitivity of global river discharges under Holocene and future climate conditions. Geophysical Research Letters, 33, L19401, doi:10.1029/2006GL027493.

Alcamo, J., Henrichs, T., Rösch, T., 2000. World Water in 2025: Global modeling and scenario analysis for the World Commission on Water for the 21st Century. Kassel World Water Series Report No. 2, University of Kassel, Kassel, Germany, 47 pp., http://www.usf.uni-kassel.de/usf/archiv/dokumente/kwws/kwws.2.pdf.

Alcamo, J., Döll, P., Henrichs, T., Kaspar, F., Lehner, B., Rösch, T., Siebert, S., 2003. Development and testing of the WaterGAP 2 global model of water use and availability. Hydrological Sciences Journal, 48(3), 317-337, doi:10.1623/hysj.48.3.317.45290.

Andréassian, V., 2004. Waters and forests: from historical controversy to scientific debate. Journal of Hydrology, 291(1-2), 1-27, doi:10.1016/j.jhydrol.2003.12.015.

Andreev, A., Tarasov, P., Schwamborn, G., Ilyashuk, B., Ilyashuk, E., Bobrov, A., Klimanov, V., Rachold, V., Hubberten, H.W., 2004. Holocene paleoenvironmental records from Nikolay Lake, Lena River Delta, Arctic Russia. Palaeogeography, Palaeoclimatology, Palaeoecology, 209(1-4), 197-217, doi:10.1016/j.palaeo.2004.02.010.

Arnell, N.W., 1999. A simple water balance model for the simulation of streamflow over a large geographic domain. Journal of Hydrology, 217(3-4), 314-335, doi:10.1016/S0022-1694(99)00023-2.

Arnell, N.W., Bates, B., Lang, H., Magnuson, J.J., Mulholland, P., Fisher, S., Liu, C., McKnight, D., Starosolszky, O., Taylor, M., Aquize, E., Arnott, S., Brakke, D., Braun, L., Chalise, S., Chen, C., Folt, C.L., Gafny, S., Hanaki, K., Hecky, R., Leavesley, G.H., Lins, H., Nemec, J., Ramasastri, K.S., Somlyódy, L., Stakhiv, E., 1996. Hydrology and freshwater ecology. In: Watson, R.T., Zinyowera, M.C., Moss, R.H. (Eds.), Climate Change 1995: Impacts, Adaptations and Mitigation of Climate Change: Scientific-Technical Analyses. Contribution of Working Group II to the Second Assessment Report of the Intergovernmental Panel on Climate Change. Cambridge University Press, Cambridge, U.K., pp. 325-363.

Arnell, N., Liu, C., Compagnucci, R., Da Cunha, L., Hanaki, K., Howe, C., Mailu, G., Shiklomanov, I., Stakhiv, E., 2001. Hydrology and water resources. In: Houghton, J.T., Ding, Y., Griggs, D.J., Noguer, M., Van der Linden, P.J., Dai, X., Maskell, K., Johnson, C.A. (Eds.), Climate Change 2001: Impacts, Adaptation and Vulnerability. Contribution of Working Group II to the Third Assessment Report of the Intergovernmental Panel on Climate Change. Cambridge University Press, Cambridge, U.K., pp. 193-233.

Ashagrie, A.G., De Laat, P.J.M., De Wit, M.J.M., Tu, M., Uhlenbrook, S., 2006. Detecting the influence of land use changes on discharges and floods in the Meuse River Basin - the predictive power of a ninety-year rainfall-runoff relation? Hydrology and Earth System Sciences, 10, 691-701, www.hydrol-earth-syst-sci.net/10/691/2006/.

Asselman, N.E.M., 1997. Suspended sediment in the River Rhine. The impact of climate change on erosion, transport, and deposition. Ph.D. Thesis, Universiteit Utrecht, Utrecht, The Netherlands, 257 pp.

Asselman, N.E.M., Middelkoop, H., 1995. Floodplain sedimentation: quantities, patterns, and processes. Earth Surface Processes and Landforms, 20(6), 481-499, doi:10.1002/esp.3290200602.

Bakker, M.M., Govers, G., Van Doorn, A., Quetier, F., Chouvardas, D., Rounsevell, M., 2008. The response of soil erosion and sediment export to land-use change in four areas of Europe: The importance of landscape pattern. Geomorphology, 98(3-4), 213-226, doi:10.1016/j.geomorph.2006.12.027.

Becker, B., Schirmer, W., 1977. Palaeoecological study on the Holocene valley development of the River Main, southern Germany. Boreas, 6(4), 303-321, doi:10.1111/j.1502-3885.1977.tb00296.x.

Beets, D.J., Van der Spek, A.J.F., 2000. The Holocene evolution of the barrier and the back-barrier basins of Belgium and the Netherlands as a function of late Weichselian morphology, relative sea-level rise and sediment supply. Geologie en Mijnbouw, 79(1), 3-16.

Berendsen, H.J.A., Stouthamer, E., 2001. Palaeogeographic development of the Rhine-Meuse delta, The Netherlands. Koninklijke Van Gorcum, Assen, The Netherlands, 268 pp.

Berger, A.L., 1978. Long-term variations of daily insolation and Quaternary Climatic Changes. Journal of the Atmospheric Sciences, 35(12), 2362-2367, doi:10.1175/1520-0469(1978)035<2362:LTVODI>2.0.CO;2.

Berger, H.E.J., 1992. Flow forecasting for the River Meuse. Ph.D. Thesis, TU Delft, Delft, The Netherlands, 356 pp.

Beven, K., 1985. Distributed models. In: Anderson, M.G., Burt, T.P. (Eds.), Hydrological Forecasting. John Wiley & Sons, Chichester, U.K., pp. 405-435.

Beven, K., 1989. Changing ideas in hydrology - The case of physically-based models. Journal of Hydrology, 105(1-2), 157-172.

Blouet, V., Lansival, R., Paitier, H., 1993. Aux origins de la Lorraine rurale, de 6000 avant notre ère à l'an mil. Images de Patrimoine no.127. Editions Serpenoise, Metz, France, 80 pp.

Boardman, J., Favis-Mortlock, D.T., 1993. Climate change and soil erosion in Britain. The Geographical Journal, 159(2), 179-183.

Boer, M.M., De Groot, R.S., 1990. Landscape-ecological impact of climatic change. Proceedings of a European conference, Lunteren, The Netherlands, 3-7 December 1989. IOS Press, Amsterdam, The Netherlands, 429 pp.

Boers, P.C.M., 1996. Nutrient emissions from agriculture in the Netherlands: causes and remedies. Water, Science and Technology, 33(4), 183-189, doi:10.1016/0273-1223(96)00229-6.

Bogaart, P.W., Van Balen, R.T., Kasse, C., Vandenberghe, J., 2003. Process-based modelling of fluvial system response to rapid climate change II. Application to the River Maas (The Netherlands) during the Last Glacial-Interglacial Transition. Quaternary Science Reviews, 22(20), 2097-2110, doi:10.1016/S0277-3791(03)00144-6.

Bohncke, S.J.P., Vandenberghe, J., 1991. Palaeohydrological development in the Southern Netherlands during the last 15000 years. In: Starkel, L., Gregory, K.J., Thornes, J.B. (Eds.), Temperate Palaeohydrology. John Wiley & Sons, Chichester, U.K., pp. 253-281.

Bohncke, S.J.P., Vandenberghe, J., Coope, R., Reiling, R., 1987. Geomorphology and palaeoecology of the Mark valley (southern Netherlands): palaeoecology, palaeohydrology and climate during the Weichselian Late Glacial. Boreas, 16(1), 69-85, doi:10.1111/j.1502-3885.1987.tb00756.x.

Bollinne, A., Laurant, A., Boon, W., 1979. L'érosivité des précipitations à Florennes. Révision de la carte des isohyètes et de la carte d'érosivité de la Belgique. Bulletin de la Société Géographique de Liège, 15, 77-99.

Booij, M.J., 2002. Appropriate modelling of climate change impacts on river flooding. Ph.D. Thesis, University of Twente, The Netherlands, 206 pp.

Booij, M.J., 2003. Determination and integration of appropriate spatial scales for river basin modelling. Hydrological Processes, 17(13), 2581-2598, doi:10.1002/hyp.1268.

Booij, M.J., 2005. Impact of climate change on river flooding assessed with different spatial model resolutions. Journal of Hydrology, 303(1-4), 176-198, doi:10.1016/j.jhydrol.2004.07.013.

Boomer, I., Aladin, N., Plotnikov, I., Whatley, R., 2000. The palaeolimnology of the Aral Sea: a review. Quaternary Science Reviews, 19(13), 1259-1278, doi:10.1016/S0277-3791(00)00002-0.

Bork, H.R., Lang, A., 2003. Quantification of past soil erosion and land use/land cover changes in Germany. In: Lang, A., Hennrich, K., Dikau, R. (Eds.), Long Term Hillslope and Fluvial System Modelling - Concepts and Case Studies from the Rhine River Catchment. Springer, Heidelberg, Germany, pp. 232-239.

Bosch, J.M., Hewlett, J.D., 1982. A review of catchment experiments to determine the effect of vegetation changes on water yield evaporation. Journal of Hydrology, 55, 3-23.

Boucsein, B., Fahl, K., Stein, R., 2000. Variability of river discharge and Atlantic-water inflow at the Laptev Sea continental margin during the past 15,000 years: implications from maceral and biomarker records. International Journal of Earth Sciences, 89(3), 578-591, doi:10.1007/s005310000111.

Bouwer, L.M., Aerts, J.C.J.H., Van de Coterlet, G.M., Van de Giesen, N., Gieske, A., Mannaerts, C., 2004. Evaluating downscaling methods for preparing Global Circulation Model (GCM) data for hydrological impact modelling. In: Aerts, J.C.J.H., Droogers, P. (Eds.), Climate Change in Contrasting River Basins. Adaptation Strategies for Water, Food and Environment. CABI Publishing, Wallingford, U.K., pp. 25-47.

Bouwer, L.M., Vermaat, J.E., Aerts, J.C.J.H., 2006. Winter atmospheric circulation and river discharge in northwest Europe. Geophysical Research Letters, 33, L06403, doi.1029/2005GL025548.

Bowler, J.M., 1981. Australian salt lakes. A palaeohydrologic approach. Hydrobiologia, 82, 431-444.

Box Jr., J.E., 1981. The effects of surface slaty fragments on soil erosion by water. Soil Science Society of America Journal, 45, 111-116.

Brader, A.V., Bohncke, S.J.P., Beets, C.J., Reichart, G.J., 2008. Deducing climate signals from hydrogen isotopes in Sphagnum. 9th NAC conference, 18-19 March 2008, Veldhoven, The Netherlands.

Brovkin, V., Ganopolski, A., Claussen, M., Kubatzki, C., Petoukhov, V., 1999. Modelling climate response to historical land cover change. Global Ecology and Biogeography, 8(6), 509-517.

Brovkin, V., Bendtsen, J., Claussen, M., Ganopolski, A., Kubatzki, C., Petoukhov, V., Andreev, A., 2002. Carbon cycle, vegetation, and climate dynamics in the Holocene: Experiments with the CLIMBER-2 model. Global Biogeochemical Cycles, 16(4), 1139, doi:10.1029/2001GB001662, 2002.

Brovkin, V., Claussen, M., Driesschaert, E., Fichefet, T., Kicklighter, D., Loutre, M.-F., Matthews, H.D., Ramankutty, N., Schaeffer, M., Sokolov, A., 2006. Biogeophysical effects of historical land cover changes simulated by six Earth system models of intermediate complexity. Climate Dynamics, 26, 587-600, doi 10.1007/s00382-005-0092-6.

Brown, A.E., Zhang, L., McMahon, T.A., Western, A.W., Vertessy, R., 2005. A review of paired catchment studies for determining changes in water yield resulting from alterations in vegetation. Journal of Hydrology, 310, 28-61, doi:10.1016/j.jhydrol.2004.12.010.

Buisman, J., Van Engelen, A.F.V., 1995. Duizend jaar weer, wind en water in de Lage Landen I: tot 1300. Van Wijnen, Franeker, The Netherlands, 656 pp.

Bultot, F., Coppens, A., Dupriez, G.L., Gellens, D., Meulenberghs, F., 1988. Repercussions of a CO2 doubling on the water cycle and on the water balance - A case study for Belgium. Journal of Hydrology, 99(3-4), 319-347.

Bultot, F., Dupriez, G.L., Gellens, G., 1990. Simulation of land use changes and impacts on the water balance - case study for Belgium. Journal of Hydrology, 114(3-4), 327-348.

Bunnik, F.P.M., 1995. Pollenanalytische Ergebnisse zur Vegetations- und Land-wirtschaftsgeschichte der Jülicher Lößbörde von der Bronzezeit bis in die frühe Neuzeit. Bonner Jahrbücher, 195, 313-349.

Busch, G., 2006. Future European agricultural landscapes - What can we learn from existing quantitative land use scenario studies? Agriculture, Ecosystems & Environment, 114(1), 121-140, doi:10.1016/j.agee.2005.11.007.

Calder, I.R., 1993. Hydrologic effects of land use change. In: Maidment, D.R. (Ed.), Handbook of hydrology. McGraw-Hill, Inc., New York, U.S.A., pp. 13.1-13.50.

Chatters, J.C., Hoover, K.A., 1986. Changing late Holocene flooding frequencies on the Columbia River, Washington. Quaternary Research, 26(3), 309-320.

Christensen, N.S., Wood, A.W., Voisin, N., Lettenmaier, D.P., Palmer, R.N., 2004. The effects of climate change on the hydrology and water resources of the Colorado River basin. Climatic Change, 62(1-3), 337-363, doi:10.1023/B:CLIM.0000013684.13621.1f.

Claussen, M., Mysak, L.A., Weaver, A.J., Crucifix, M., Fichefet, T., Loutre, M.-F., Weber, S.L., Alcamo, J., Alexeev, V.A., Berger, A., Calov, R., Ganopolski, A., Goosse, H., Lohmann, G., Lunkeit, F., Mokhov, I.I., Petoukhov, V., Stone, P., Wang, Z., 2002. Earth system models of intermediate complexity: closing the gap in the spectrum of climate system models. Climate Dynamics, 18(7), 579-586, doi:10.1007/s00382-001-0200-1.

Close-Lecocq, J.F., Pissart, A., Koch, G., 1982. Les transports en suspension et en solution de la Meuse à Liege et à Tailfer (amont de Namur). Bulletin de la Société Géographique de Liège, 18, 5-18.

Cocke, S., LaRow, T.E., 2000. Seasonal predictions using a regional spectral model embedded within a coupled ocean-atmosphere model. Monthly Weather Review, 128(3), 689-708.

Coe, M.T., Harrison, S.P., 2002. The water balance of northern Africa during the Mid-Holocene: an evaluation of the 6 ka BP PMIP simulations. Climate Dynamics, 19(2), 155-166, doi:10.1007/s00382-001-0219-3.

Cosandey, C., Andréassian, V., Martin, C., Didon-Lescot, J.F., Lavabre, J., Folton, N., Mathys, N., Richard, D., 2005. The hydrological impact of the mediterranean forest: a review of French research. Journal of Hydrology, 301(1-4), 235-249, doi:10.1016/j.jhydrol.2004.06.040.

Costa, M.H., Botta, A., Cardille, J.A., 2003. Effects of large-scale changes in land cover on the discharge of the Tocantins River, Southeastern Amazonia. Journal of Hydrology, 283(1-4), 206-217, doi:10.1016/S0022-1694(03)00267-1.

Damblon, F., 1992. Palaeobotanical analyses of Eriophorum and Molinia tussocks as a means of reconstructing recent history of disturbed mires in the Haute-Ardenne, Belgium. Review of Palaeobotany and Palynology, 75(3-4), 273-288.

Davis, O.K., 1999. Pollen analysis of Tulare Lake, California: Great Basin-like vegetation in Central California during the full-glacial and early Holocene. Review of Palaeobotany and Palynology, 107(3-4), 249-257, doi:10.1016/S0034-6667(99)00020-2.

De Moor, J.J.W., 2007. Human impact on Holocene catchment development and fluvial processes - the Geul River catchment, SE Netherlands. Ph.D. Thesis, VU University Amsterdam, Amsterdam, The Netherlands, 141 pp.

De Moor, J.J.W., Verstraeten, G., 2008. Alluvial and colluvial sediment storage in the Geul River catchment (The Netherlands) - Combining field and modelling data to construct a Late Holocene sediment budget. Geomorphology, 95(3-4), 487-503, doi:10.1016/j.geomorph.2007.07.012.

De Moor, J.J.W., Kasse, C., Van Balen, R.T., Vandenberghe, J., Wallinga, J., 2008. Human and climate impact on catchment development during the Holocene - Geul River, the Netherlands. Geomorphology, 98(3-4), 316-339, doi:10.1016/j.geomorph.2006.12.033.

De Ploey, J., 1989. Erosional systems and perspectives for erosion control in European löss areas. Soil Technology Series,1, 93-102.

Desmet, P.J.J., Govers, G., 1996. A GIS procedure for automatically calculating the USLE LS factor on topographically complex landscape units. Journal of Soil and Water Conservation, 51(5), 427-433.

De Wit, M.J.M., Behrendt, H., 1999. Nitrogen and Phosphorus emissions from soil to surface water in the Rhine and Elbe basins. Water Science and Technology, 39(12), 109-116, doi:10.1016/S0273-1223(99)00325-X.

De Wit, M., Warmerdam, P., Torfs, P., Uijlenhout, R., Roulin, E., Cheymol, A., Van Deursen, W., Van Walsum, P., Ververs, M., Kwadijk, J., Buiteveld, H., 2001. Effect of climate change on the hydrology of the river Meuse. Dutch National Research Programme on Global Air Pollution and Climate Change. Report number 410.200.090, RIVM, Bilthoven, The Netherlands, 143 pp.

De Wit, M.J.M., Van den Hurk, B., Warmerdam, P.M.M., Torfs, P.J.J.F., Roulin, E., Van Deursen, W.P.A., 2007a. Impact of climate change on low-flows in the river Meuse. Climatic Change, 82(3-4), 1573-1480, doi:10.1007/s10584-006-9195-2.

De Wit, M.J.M., Peeters, H., Gastaud, P.H., Dewil, P., Maeghe, K., Baumgart, J., 2007b. Floods in the Meuse basin: Event descriptions and an international view on ongoing measures. International Journal of River Basin Management, 5(4), 279-292.

DGRNE, 2000. L'Environnement wallon à l'aube du XXIe Siècle. Approche évolutive. DGRNE, Namur, Belgium, http://environnement.wallonie.be/eew2000/gen/framegen.htm.

Dierkens, A., Plumier-Torfs, J., 1999. Mosa Nostra: de Maasvallei van Verdun tot Maastricht in de Merovingische periode (5e-8e eeuw). Carnets du Patrimoine. Ministère de la Région Wallonne, Namur, Belgium, 64 pp.

Diermanse, F.L.M., 2004. HR2006 herberekening werklijn Maas. Report Q3623. WL Delft Hydraulics, Delft, The Netherlands.

Döll, P., Kaspar, F., Lehner, B., 2003. A global hydrological model for deriving water availability indicators: model tuning and validation. Journal of Hydrology, 270(1-2), 105-134, doi:10.1016/S0022-1694(02)00283-4.

Doomen, A.M.C., Wijma, E., Zwolsman, J.J.G., Middelkoop, H., 2008. Predicting suspended sediment concentrations in the Meuse River using a supply-based sediment rating curve. Hydrological Processes, 22(12), 1846-1856, doi:10.1002/hyp.6767.

Dornbusch, J., 1997. Großer Atlas zur Weltgeschichte. Westermann Verlag, Braunschweig, Germany, 245 pp.

Dutoo, D., 1994. Onderzoeksproject Watersnood Maas. Het areaal onder bos in het Franse maasbekken van 1908 tot 1988, Universiteit Gent, Gent, Belgium, 26 pp.

Dyke, A.S., Prest, V.K., 1987. Late Wisconsin and Holocene history of the Laurentide Ice Sheet. Géographie Physique et Quaternaire, 41(2), 237-263.

Dyke, A.S., Dale, J.E., McNeely, R.N., 1996. Marine molluscs as indicators of environmental change in glaciated North America and Greenland during the last 18000 years. Géographie Physique et Quaternaire, 50(2), 125-184.

EEA, 2001. Sustainable water use in Europe. Part 3: Extreme hydrological events: floods and droughts. Environmental issue report No. 21, EEA, Copenhagen, Denmark, 84 pp., http://environnement.wallonie.be/eew2000/gen/framegen.htm.

Ely, L.L., Enzel, Y., Baker, V.R., Cayan, D.R., 1993. A 5000-year record of extreme floods and climate change in the southwestern United States. Science, 262(5132), 410-412, doi:10.1126/science.262.5132.410.

Erkens, G., Cohen, K.M., Gouw, M.J.P., Middelkoop, H., Hoek, W.Z., 2006. Holocene sediment budgets of the Rhine Delta (The Netherlands): a record of changing sediment delivery. In: Rowan, J.S., Duck, R.W. (Eds.), Symposium Sediment Dynamics and the Hydromorphology of Fluvial Systems, Dundee, Scotland. IAHS Press, Wallingford, U.K., pp. 406-415.

ESRI, 1992. Global topographic database ArcWorld 1:3M on CD-ROM. Environmental Systems Research Institute, Inc. (ESRI), Redlands, U.S.A.

Fahey, B., 1994. The effect of plantation forestry on water yield in New Zealand. New Zealand Forestry, 39(3), 18-23.

FAO, 2003. Digital Soil Map of the World (DSMW) Version 3.6. CD-ROM. FAO, Rome, Italy.

Favis-Mortlock, D., Boardman, J., 1995. Nonlinear responses of soil erosion to climate change: a modelling study on the UK South Downs. Catena, 25(1-4), 365-387, doi:10.1016/0341-8162(95)00018-N.

Ferguson, R.I., 1986. River loads underestimated by rating curves. Water Resources Research, 22(1), 74-76.

Froment, A., 1975. Les premiers stades de la succession végétale après incendie de tourbe dans la reserve naturelle des Hautes-Fagnes. Vegetatio, 29(3), 209-214, doi:10.1007/BF02390012.

Gallart, F., Llorens, P., 2004. Observations on land cover changes and water resources in the headwaters of the Ebro catchment, Iberian Peninsula. Physics and Chemistry of the Earth A/B/C, 29(11-12), 769-773, doi:10.1016/j.pce.2004.05.004.

Gellens, D., 1991. Impact of a CO2-induced climatic change on river flow variability in three rivers in Belgium. Earth Surface Processes and Landforms, 16(7), 619-625, doi:10.1002/esp.3290160706.

Gellens, D., Roulin, E., 1998. Streamflow response of Belgian catchments to IPCC climate change scenarios. Journal of Hydrology, 210(1-4), 242-258, doi:10.1016/S0022-1694(98)00192-9.

Gentry, A.H., Parody, J.L., 1980. Deforestation and increased flooding of the Upper Amazon. Science, 210(4476), 1354-1356, doi:10.1126/science.210.4476.1354.

Giorgi, F., 2006. Climate change hot-spots. Geophysical Research Letters, 33, L08707, doi:10.1029/2006GL025734.

Giorgi, F., Coppola, E., 2007. European climate-change oscillation (ECO). Geophysical Research Letters, 34, L21703, doi:10.1029/2007GL031223.

Giresse, P., Lanfranchi, R., 1984. Les climats et les océans de la région Congolaise pendant l'Holocène-Bilans selon les échelles et les méthodes de l'observation. In: Coetzee, J.A., Van Zinderen Bakker Sr., E.M. (Eds.), Palaeoecology of Africa Volume 16. A.A. Balkema, Rotterdam, The Netherlands, pp. 77-88.

Giresse, P., Bongo-Passi, G., Delibrias, G., Duplessy, J.C., 1982. La lithostratigraphie des sédiments hémipélagiques du delta profond du fleuve Congo et ses indications sur les paléoclimats de la fin du Quaternaire. Bulletin de la Société Géologique de France, 7(4), 803-815.

Goman, M., Wells, L., 2000. Trends in river flow affecting the northeastern reach of the San Francisco Bay estuary over the past 7000 years. Quaternary Research, 54(2), 206-217, doi:10.1006/qres.2000.2165.

Goodbred, S.L., Kuehl, S.A., 2000. Enormous Ganges-Brahmaputra sediment discharge during strengthened early Holocene monsoon. Geology, 28(12), 1083-1086, doi:10.1130/0091-7613(2000)28<1083:EGSDDS>2.0.CO;2.

Goosse, H., Fichefet, T., 1999. Importance of ice-ocean interactions for the global ocean circulation: a model study. Journal of Geophysical Research - Oceans, 104(C10), 23337-23355.

Goosse, H., Renssen, H., Timmermann, A., Bradley, R.S., 2005. Internal and forced climate variability during the last millennium: a model-data comparison using ensemble simulations. Quaternary Science Reviews, 24(12-13), 1345-1360, doi:10.1016/j.quascirev.2004.12.009.

Goosse, H., Arzel, O., Luterbacher, J., Mann, M.E., Renssen, H., Riedwyl, N., Timmermann, A., Xoplaki, E., Wanner, H., 2006. The origin of the European Medieval Warm Period. Climate of the Past, 2, 99-113, www.clim-past.net/2/99/2006/.

Gotjé, W., Van Wayjen, M.C.A., Van Geel, B., 1990. A palynological study of a Holocene deposit from Grand-Bongard (Hautes-Fagnes, Belgium). Geologie en Mijnbouw, 69, 227-241.

Goudie, A., 1992. Environmental change: Contemporary problems in Geography. Clarendon Press, Oxford, U.K., 329 pp.

Gregory, K.J., 1996. Introduction. In: Branson, J., Brown, A.G., Gregory, K.J. (Eds.), Global Continental Changes: the Context of Palaeohydrology. Geological Society Special Publication No. 115. The Geological Society, London, U.K., pp. 1-8.

Hall, A.M., Thomas, M.F., Thorp, M.B., 1985. Late Quaternary alluvial placer development in the humid tropics: the case of the Birim Diamond Placer, Ghana. Journal of the Geological Society, 142, 777-787.

Harrison, S.P., Dodson, J., 1993. Climates of Australia and New Guinea since 18,000 yr B.P. In: Wright Jr., H.E., Kutzbach, J.E., Webb III, T., Ruddiman, W.F., Street-Perrott, F.A., Bartlein, P.J. (Eds.), Global Climates Since the Last Glacial Maximum. University of Minnesota Press, Minneapolis, pp. 265-293.

Henderson-Sellers, A., McGuffie, K., Pitman, A.J., 1996. The Project for Intercomparison of Land-surface Parametrization Schemes (PILPS): 1992 to 1995. Climate Dynamics, 12(12), 849-859, doi:10.1007/s003820050147.

Henrard, D., 2003. The Mesolithic of the Ourthe Basin: Landscape settlement and Neolithisation. L'anthropologie, 107(5), 615-644.

Heusser, L., 1978. Pollen in Santa Barbara Basin, California: A 12,000-yr record. Geological Society of America Bulletin, 89(5), 673-678.

Hipel, K.W., McLeod, A.I., 1994. Time Series Modelling of Water Resources and Environmental Systems. Elsevier, Amsterdam, The Netherlands, 399 pp.

Hofstede, J.L.A., Berendsen, H.J.A., Janssen, C.R., 1989. Holocene palaeogeography and palaeoecology of the fluvial area near Maurik (Neder-Betuwe, The Netherlands). Geologie en Mijnbouw, 68, 409-419.

Hornbeck, J.W., Adams, M.B., Corbett, E.S., Verry, E.S., Lynch, J.A., 1993. Long-term impacts of forest treatment on water yield: a summary for Northeastern USA. Journal of Hydrology, 150(2-4), 323-343.

Houben, P., Hoffmann, T., Zimmermann, A., Dikau, R., 2006. Land use and climatic impacts on the Rhine system (RheinLUCIFS): Quantifying sediment fluxes and human impact with available data. Catena, 66(1-2), 42-52, doi:10.1016/j.catena.2005.07.009.

Howard, A.J., Macklin, M.G., Bailey, D.W., Mills, S., Andreescu, R., 2004. Late-glacial and Holocene river development in the Teleorman Valley on the southern Romanian Plain. Journal of Quaternary Science, 19(3), 271-280, doi:10.1002/jqs.805.

Hurst, H.E., Black, R.M., Simaika, Y.P., 1946. The Nile Basin: The Future conservation of the Nile. Vol. VII. Ministry of Public Works, Physical Department, Cairo, Egypt.

Ingram, B.L., Ingle, J.C., Conrad, M.E., 1996. Stable isotope record of late Holocene salinity and river discharge in San Francisco Bay, California. Earth and Planetary Science Letters, 141(1), 237-247, doi:10.1016/0012-821X(96)00060-X.

IPCC, 1992. Climate Change 1992: The supplementary report to the IPCC Scientific Assessment. Cambridge University Press, Cambridge, U.K., 116 pp.

IPCC, 2000. Special Report on Emission Scenarios. Cambridge University Press, New York, U.S.A., 599 pp.

IPCC, 2001. Climate Change 2001: The Scientific Basis. Contribution of Working Group I to the Third Assessment Report of the Intergovernmental Panel on Climate Change. Cambridge University Press, Cambridge, U.K., 881 pp.

IPCC, 2007. Climate Change 2007. The Physical Science Basis. Contribution of Working Group I to the Fourth Assessment Report of the Intergovernmental Panel on Climate Change. Cambridge University Press., Cambridge, U.K., 996 pp.

Iroumé, A., Huber, A., Schulz, K., 2005. Summer flows in experimental catchments with different forest covers, Chile. Journal of Hydrology, 300(1-4), 300-313, doi:10.1016/j.jhydrol.2004.06.014.

Ito, A., 2007. Simulated impacts of climate and land-cover change on soil erosion and implication for the carbon cycle, 1901 to 2100. Geophysical Research Letters, 34, L09403, doi:10.1029/2007GL029342.

Jakeman, A.J., Hornberger, G.M., 1993. How Much Complexity is Warranted in a Rainfall-Runoff Model? Water Resources Research, 29(8), 2637-2649.

Jarvis, A., Reuter, H.I., Nelson, A., Guevara, E., 2006. Hole-filled seamless SRTM data V3. International Centre for Tropical Agriculture (CIAT), Cali, Colombia, http://environnement.wallonie.be/eew2000/gen/framegen.htm.

Jolly, D., Harrison, S.P., Damnati, B., Bonnefille, R., 1998. Simulated climate and biomes of Africa during the Late Quaternary: comparison with pollen and lake status data. Quaternary Science Reviews, 17(6-7), 629-657.

Jones, J.A., 2000. Hydrologic processes and peak discharge response to forest removal, regrowth, and roads in 10 small experimental basins, western Cascades, Oregon. Water Resources Research, 36(9), 2621-2642.

Kale, V.S., Rajaguru, S.N., 1987. Late Quaternary alluvial history of the northwestern Deccan upland region. Nature, 325(12), 612-614, doi:10.1038/325612a0.

Kale, V.S., Gupta, A., Singhvi, A.K., 2003. Late Pleistocene-Holocene palaeohydrology of Monsoon Asia. In: Gregory, K.J., Benito, G. (Eds.), Palaeohydrology: Understanding Global Change. John Wiley & Sons, Chichester, U.K., pp. 213-232.

Keesstra, S.D., 2006. The effects of natural reforestation on the hydrology, river morphology and sediment budget of the Dragonja River catchment, SW Slovenia. Ph.D. Thesis, VU University Amsterdam, Amsterdam, The Netherlands, 188 pp.

Keesstra, S.D., Van Huissteden, J., Vandenberghe, J., Van Dam, O., De Gier, J., Pleizier, I.D., 2005. Evolution of the morphology of the river Dragonja (SW Slovenia) due to land-use changes. Geomorphology, 69(1-4), 191-207, doi:10.1016/j.geomorph.2005.01.004.

Kettner, A.J., Gomez, B., Syvitski, J.P.M., 2007. Modeling suspended sediment discharge from the Waipaoa River system, New Zealand: The last 3000 years. Water Resources Research, 43, W07411, doi:10.1029/2006WR005570.

Kim, J., Miller, N.L., Farrara, J.D., Hong, S.-Y., 2000. A seasonal precipitation and stream flow hindcast and prediction study in the western United States during the 1997/98 winter season using a dynamic downscaling system. Journal of Hydrometeorology, 1(4), 311-329, doi:10.1175/1525-7541(2000)001<0311:ASPASF>2.0.CO;2.

Kirchner, J.W., 2006. Getting the right answers for the right reasons: Linking measurements, analyses, and models to advance the science of hydrology. Water Resources Research, 42, W03S04, doi:10.1029/2005WR004362.

Kirkby, M.J., Jones, R.J.A., Irvine, B., Gobin, A., Govers, G., Cerdan, O., Van Rompaey, A.J.J., Le Bissonnais, Y., Daroussin, J., King, D., Montanarella, L., Grimm, M., Vieillefont, V., Puigdefabregas, J., Boer, M., Kosmas, C., Yassoglou, N., Tsara, M., Mantel, S., Van Lynden, G.J., Huting, J., 2004. Pan-European Soil Erosion Risk Assessment: The PESERA Map, Version 1 October 2003. Explanation of Special Publication Ispra 2004 No.73 (S.P.I.04.73). European Soil Bureau Research Report No.16, EUR21176, Office for Official Publications of the European Communities, Luxembourg, 18 pp.

Kleinn, J., Frei, C., Gurtz, J., Lüthi, D., Vidale, P.L., Schär, C., 2005. Hydrologic simulations in the Rhine basin driven by a regional climate model. Journal of Geophysical Research, 110, D04102, doi:10.1029/2004JD005143.

Klein Tank, A.M.G., Wijngaard, J.B., Können, G.P., Böhm, R., Demarée, G., Gocheva, A., Mileta, M., Pashiardis, S., Hejkrlik, L., Kern-Hansen, C., Heino, R., Bessemoulin, P., Müller-Westermeier, G., Tzanakou, M., Szalai, S., Pálsdóttir, T., Fitzgerald, D., Rubin, S., Capaldo, M., Maugeri, M., Leitass, A., Bukantis, A., Aberfeld, R., Van Engelen, A.F.V., Forland, E., Mietus, M., Coelho, F., Mares, C., Razuvaev, V., Nieplova, E., Cegnar, T., Antonio López, J., Dahlström, B., Moberg, A., Kirchhofer, W., Ceylan, A., Pachaliuk, O., Alexander, O.V., Petrovic, P., 2002. Daily dataset of 20th-century surface air temperature and precipitation series for the European Climate Assessment. International Journal of Climatology, 22(12), 1441-1453, doi:10.1002/joc.773.

Klemeŝ, V., 1986. Operational testing of hydrological simulation models. Hydrological Sciences Journal, 31(1), 13-24.

Klepper, O., Van Drecht, G., 1998. Waribas, water assessment on a river basin scale: a computer program for calculating water demand and water satisfaction on a catchment basin level for global-scale analysis of water stress. Report 402.001.009, RIVM, Bilthoven, The Netherlands, 124 pp.

Klöcking, B., Haberlandt, U., 2002. Impact of land use changes on water dynamics - a case study in temperate meso and macro scale river basins. Physics and Chemistry of the Earth, Parts A/B/C, 27(9-10), 619-629, doi:10.1016/S1474-7065(02)00046-3.

Knol, W.C., Kramer, H., Gijsbertse, H., 2004. Historisch grondgebruik Nederland: een landelijke reconstructie van het grondgebruik rond 1900. Alterra-rapport 573, Alterra, Wageningen, The Netherlands, 89 pp., http://environnement.wallonie.be/eew2000/gen/framegen.htm.

Knox, J.C., 1983. Responses of River Systems to Holocene Climates. In: Wright Jr., H.E. (Ed.), Late-Quaternary Environments of the United States. Volume 2. The Holocene. Longman, London, U.K., pp. 26-41.

Knox, J.C., 1984. Fluvial responses to small scale climate changes. In: Costa, J.E., Jay Fleisher, P. (Eds.), Developments and Applications of Geomorphology. Springer-Verlag, Berlin, Germany, pp. 318-342.

Knox, J.C., 1985. Responses of floods to Holocene climatic change in the upper Mississippi Valley. Quaternary Research, 23(3), 287-300.

Knox, J.C., 2000. Sensitivity of modern and Holocene floods to climate change. Quaternary Science Reviews, 19(1-5), 439-457.

Knox, J.C., 2003. North American palaeofloods and future floods: Responses to climatic change. In: Gregory, K.J., Benito, G. (Eds.), Palaeohydrology. Understanding Global Change. John Wiley & Sons, Chichester, U.K., pp. 143-164.

Koehler, P.A., Scott Anderson, R., 1994. The paleoecology and stratigraphy of Nichols Meadow, Sierra National Forest, California, USA. Palaeogeography, Palaeoclimatology, Palaeoecology, 112(1-2), 1-17.

Können, G.P., 1999. De toekomst van het Nederlandse klimaat. KNMI, De Bilt, The Netherlands, 65 pp.

Krajewski, W.F., Lakshmi, V., Georgakakos, K.P., Jain, S.C., 1991. A Monte Carlo study of rainfall sampling effect on a distributed catchment model. Water Resources Research, 27(1), 119-128.

Krom, M.D., Stanley, J.D., Cliff, R.A., Woodward, J.C., 2002. Nile River sediment fluctuations over the past 7000 yr and their key role in sapropel development. Geology, 30(1), 71-74, doi:10.1130/0091-7613(2002)030<0071:NRSFOT>2.0.CO;2.

Kundzewicz, Z.W., Mata, L.J., Arnell, N.W., Döll, P., Kabat, P., Jiménez, B., Miller, K.A., Oki, T., Sen, Z., Shiklomanov, I.A., 2007. Freshwater resources and their management. In: Parry, M.L., Canziani, O.F., Palutikof, J.P., Van der Linden, P.J., Hanson, C.E. (Eds.), Climate Change 2007: Impacts, Adaptation and Vulnerability. Contribution of the Working Group II to the Fourth Assessment Report of the Intergovernmental Panel on Climate Change. Cambridge University Press, Cambridge, U.K., pp. 173-210.

Kutzbach, J.E., Street-Perrott, F.A., 1985. Milankovitch forcing of fluctuations in the level of tropical lakes from 18 to 0 kyr BP. Nature, 317(6033), 130-134, doi:10.1038/317130a0.

Kwadijk, J.C.J., 1991. Sensitivity of the River Rhine discharge to environmental change, a first tentative assessment. Earth Surface Processes and Landforms, 16(7), 627-637, doi:10.1002/esp.3290160707.

Kwadijk, J.C.J., 1993. The impact of climate change on the discharge of the River Rhine. Ph.D. Thesis, Universiteit Utrecht, Utrecht, The Netherlands, 201 pp.

Kwadijk, J., Rotmans, J., 1995. The impact of climate change on the River Rhine: a scenario study. Climatic Change, 30(4), 397-425, doi:10.1007/BF01093854.

Lang, A., Bork, H.R., 2006. Past soil erosion in Europe. In: Boardman, J., Poesen, J. (Eds.), Soil Erosion in Europe. John Wiley & Sons Ltd, Chichester, U.K., pp. 465-476.

Lang, A., Bork, H.R., Mäckel, R., Preston, N., Wunderlich, J., Dikau, R., 2003. Changes in sediment flux and storage within a fluvial system: some examples from the Rhine catchment. Hydrological Processes, 17(16), 3321-3334, doi:10.1002/hyp.1389.

Leander, R., Buishand, T.A., 2007. Resampling of regional climate model output for the simulation of extreme river flows. Journal of Hydrology, 332(3-4), 487-496, doi:10.1016/j.jhydrol.2006.08.006.

Leander, R., Buishand, A., Aalders, P., De Wit, M., 2005. Estimation of extreme floods of the river Meuse using a stochastic weather generator and a rainfall-runoff model. Hydrological Sciences Journal, 50(6), 1089-1103.

Leander, R., Buishand, T.A., Van den Hurk, B.J.J.M., De Wit, M.J.M., 2008. Estimated changes in flood quantiles of the river Meuse from resampling of regional climate model output. Journal of Hydrology, 351, 331-343, doi:10.1016/j.jhydrol.2007.12.020.

Leavesley, G.H., 1994. Modeling the effects of climate change on water resources - A review. Climatic Change, 28(1-2), 159-177, doi:10.1007/BF01094105.

Lefevre, D., Heim, J., Gilot, E., Mouthon, J., 1993. Evolution des environnements sedimentaires et biologiques a l'Holocene dans la plaine alluviale de la Meuse (Ardennes, France): premiers resultats. Quaternaire, 4(1), 17-30.

Legates, D.R., McCabe Jr., G.J., 1999. Evaluating the use of "goodness-of-fit" measures in hydrologic and hydroclimatic model validation. Water Resources Research, 35(1), 233-241.

Lemin, G., Koch, G., Hurtgen, C., Pissart, A., 1987. Les transports en suspension de la Meuse, l'Ourthe et la Höegne. Bulletin de la Société Géographique de Liège, 22-23, 39-61.

Loague, K.M., Freeze, R.A., 1985. A comparison of rainfall-runoff modelling techniques on small upland catchments. Water Resources Research, 21(2), 229-248.

Mahe, G., Paturel, J.-E., Servat, E., Conway, D., Dezetter, A., 2005. The impact of land use change on soil water holding capacity and river flow modelling in the Nakambe River, Burkina-Faso. Journal of Hydrology, 300(1-4), 33-43, doi:10.1016/j.jhydrol.2004.04.028.

Maizels, J.K., 1995. Palaeohydrology of polar and subpolar regions over the past 20.000 years. In: Gregory, K.J., Starkel, L., Baker, V.R. (Eds.), Global Continental Palaeohydrology. John Wiley & Sons, Chichester, U.K., pp. 259-299.

Mamedov, E.D., Trofimov, G.N., 1986. On the problem of long-term oscillations of the Central Asian rivers. Problemy osvoyeniya pustyn, 1, 12-16 (in Russian).

Maslin, M.A., Burns, S.J., 2000. Reconstruction of the Amazon basin effective moisture availability over the past 14,000 years. Science, 290(5500), 2285-2287, doi:10.1126/science.290.5500.2285.

Matthews, H.D., Weaver, A.J., Eby, M., Meissner, K.J., 2003. Radiative forcing of climate by historical land cover change. Geophysical Research Letters, 30(2), 1055, doi:10.1029/2002GL016098.

Meybeck, M., 2003. Global analysis of river systems: from Earth system controls to Anthropocene syndromes. Philosophical Transactions of the Royal Society of London: Biological Sciences, 358(1440), 1935-1955, doi:10.1098/rstb.2003.1379.

Middelkoop, H., Parmet, B., 1998. Assessment of the impact of climate change on peak flows in the Netherlands - a matter of scale. In: Lemellä, R., Helenius, N. (Eds.), Proceedings of the second international conference on climate and water. Helsinki University of Technology, Espoo, Finland, pp. 20-33.

Middelkoop, H., Daamen, K., Gellens, D., Grabs, W., Kwadijk, J.C.J., Lang, H., Parmet, B.W.A.H., Schädler, B., Schulla, J., Wilke, K., 2001. Impact of climate change on hydrological regimes and water resources management in the Rhine Basin. Climatic Change, 49(1-2), 105-128, doi:10.1023/A:1010784727448.

Middelkoop, H., Van Asselt, M.B.A., Van 't Klooster, S.A., Van Deursen, W.P.A., Kwadijk, J.C.J., Buiteveld, H., 2004. Perspectives on flood management in the Rhine and Meuse Rivers. River Research and Applications, 20(3), 327-342.

Ministry of Transport, Public Works and Water Management, 2005. Flood risks and safety in the Netherlands (Floris). Full report DWW-2006-014. Ministry of Transport, Public Works and Water Management, The Hague, The Netherlands, 94 pp.

Ministry of Transport, Public Works and Water Management, 2006. Integrale Verkenning Maas, Advies, Hoofdrapport en Achtergronddocumenten IVM2. Rijkswaterstaat Dienst Limburg, Maastricht, The Netherlands, 50 pp.

Mitchell, T.D., Jones, P.D., 2005. An improved method of constructing a database of monthly climate observations and associated high-resolution grids. International Journal of Climatology, 25, 693-712, doi:10.1002/joc.1181.

Mitchell, T.D., Carter, T.R., Hulme, M., New, M., 2003. A comprehensive set of high-resolution grids of monthly climate for Europe and the globe: the observed record (1901-2000) and 16 scenarios (2001-2100). Tyndall Centre Working Paper 55, Tyndall Centre for Climate Change Research, Norwich, U.K., 30 pp.

Moy, C.M., Seltzer, G.O., Rodbell, D.T., Anderson, D.M., 2002. Variability of El Niño/Southern Oscillation activity at millennial timescales during the Holocene epoch. Nature, 420, 162-165, doi:10.1038/nature01194.

Murphy, J., 2000. Predictions of climate change over Europe using statistical and dynamical downscaling techniques. International Journal of Climatology, 20(5), 489-501, doi:10.1002/(SICI)1097-0088(200004)20:5<489::AID-JOC484>3.0.CO;2-6.

Nash, J.E., Sutcliffe, J.V., 1970. River flow forecasting through conceptual models part I - A discussion of principles. Journal of Hydrology, 10(3), 282-290, doi:10.1016/0022-1694(70)90255-6.

Nearing, M.A., Jetten, V., Baffaut, C., Cerdan, O., Couturier, A., Hernandez, M., Le Bissonnais, Y., Nicholas, M.H., Nunes, J.P., Renscler, C.S., Souchère, V., Van Oost, K., 2005. Modelling response of soil erosion and runoff to changes in precipitation and cover. Catena, 61(2-3), 131-154, doi:10.1016/j.catena.2005.03.007.

NGDC, 1997. Terrain Base: Global 5. min elevation database. National Geophysical Data Center, Washington D.C., U.S.A., www.ngdc.noaa.gov.

Notebaert, B., Verstraeten, G., 2008. Holocene alluvial sediment deposition in contrasting environments in northwestern Europe. Sediment dynamics in a changing environment. IAHS Publication 325. Wallingford, U.K., *in press*.

Ntegeka, V., Willems, P., 2008. Trends and multidecadal oscillations in rainfall extremes, based on a more than 100-year time series of 10 min rainfall intensities at Uccle, Belgium. Water Resources Research, 44, W07402, doi:10.1029/2007WR006471.

Opsteegh, J.D., Haarsma, R.J., Selten, F.M., Kattenberg, A., 1998. ECBILT: a dynamic alternative to mixed boundary conditions in ocean models. Tellus, 50A(3), 348-367, doi:10.1034/j.1600-0870.1998.t01-1-00007.x.

Overeem, I., Veldkamp, A., Tebbens, L., Kroonenberg, S.B., 2003. Modelling Holocene stratigraphy and depocentre migration of the Volga delta due to Caspian Sea-level change. Sedimentary Geology, 159(3-4), 159-175, doi:10.1016/S0037-0738(02)00257-9.

Overpeck, J., Anderson, D., Trumbore, S., Prell, W., 1996. The southwest Indian Monsoon over the last 18000 years. Climate Dynamics, 12(3), 213-225, doi:10.1007/BF00211619.

Owen, R.B., Barthelme, J.W., Renaut, R.W., Vincens, A., 1982. Paleolimnology and archaeology of Holocene deposits northeast of Lake Turkana, Kenya. Nature, 298, 523-529, doi:10.1038/298523a0.

Petit, C.C., Lambin, E.F., 2002. Long-term land-cover changes in the Belgian Ardennes (1775-1929): model-based reconstruction vs. historical maps. Global Change Biology, 8(7), 616-630, doi:10.1046/j.1365-2486.2002.00500.x.

Pfister, L., Humbert, J., Hoffmann, L., 2000. Recent trends in rainfall-runoff characteristics in the Alzette river basin, Luxembourg. Climatic Change, 45(2), 323-337, doi:10.1023/A:1005567808533.

Pfister, L., Kwadijk, J., Musy, A., Bronstert, A., Hoffmann, L., 2004. Climate change, land use change and runoff prediction in the Rhine-Meuse basins. River Research and Applications, 20(3), 229-241, doi:10.1002/rra.775.

Phadtare, N.R., 2000. Sharp decrease in summer monsoon strength 4000-3500 cal yr B.P. in the Central Higher Himalaya of India based on pollen evidence from Alpine peat. Quaternary Research, 53(1), 122-129, doi:10.1006/qres.1999.2108.

Phillips, J.M., Webb, B.W., Walling, D.E., Leeks, G.J.L., 1999. Estimating the suspended sediment loads of rivers in the LOIS study area using infrequent samples. Hydrological Processes, 13(7), 1035-1050.

Pilling, C., Jones, J.A.A., 1999. High resolution climate change scenarios: implications for British runoff. Hydrological Processes, 13(17), 2877-2895.

Pongratz, J., Reick, C., Raddatz, T., Claussen, M., 2007. Reconstruction of global land use and land cover AD 800 to 1992. WDCC, Hamburg, Germany, http://environnement.wallonie.be/eew2000/gen/framegen.htm.

Preuss, J., 1990. L'évolution des paysages du basin intérieur du Zaïre pendant les quarante derniers millénaires. In: Lanfranchi, R., Schwartz, D. (Eds.), Paysages Quaternaires de l'Afrique Centrale Atlantique. Editions de l'Ostrom, Paris, France, pp. 260-270.

Pruski, F.F., Nearing, M.A., 2002. Runoff and soil loss responses to changes in precipitation: a computer simulation study. Journal of Soil and Water Conservation, 57(1), 7-16.

Renard, K.G., Foster, G.R., Weesies, G.A., Porter, J.P., 1991. RUSLE-revised universal soil loss equation. Journal of Soil and Water Conservation, 46(1), 30-33.

Renard, K.G., Foster, G.R., Weesies, G.A., McCool, D.K., Yoder, D.C., 1997. Predicting soil erosion by water: A guide to conservation planning with the Revised Universal Soil Loss Equation (RUSLE). Agriculture Handbook vol. 703. U.S. Department of Agriculture, Washington D.C., U.S.A., 384 pp.

Renssen, H., Knoop, J.M., 2000. A global river routing network for use in hydrological modeling. Journal of Hydrology, 230(3-4), 230-243.

Renssen, H., Brovkin, V., Fichefet, T., Goosse, H., 2003. Holocene climate instability during the termination of the African Humid Period. Geophysical Research Letters, 30(4), 1184, doi:10.1029/2002GL016636.

Renssen, H., Goosse, H., Fichefet, T., Brovkin, V., Driesschaert, E., Wolk, F., 2005a. Simulating the Holocene climate evolution at northern high latitudes using a coupled atmosphere-sea-ice-ocean-vegetation model. Climate Dynamics, 24(1), 23-43, doi:10.1007/s00382-004-0485-y.

Renssen, H., Goosse, H., Fichefet, T., Masson-Delmotte, V., Koç, N., 2005b. Holocene climate evolution in the high-latitude Southern Hemisphere simulated by a coupled atmosphere-sea ice-ocean-vegetation model. The Holocene, 15(7), 951-964, doi:10.1191/0959683605hl869ra.

Renssen, H., Lougheed, B.C., Aerts, J.C.J.H., De Moel, H., Ward, P.J., Kwadijk, J.C.J., 2007. Simulating long-term Caspian Sea level changes: The impact of Holocene and future climate conditions. Earth and Planetary Science Letters, 261, 685-693, doi:10.1016/j.epsl.2007.07.037.

Richards, K., Brasington, J., Hughes, F., 2002. Geomorphic dynamics of floodplains: ecological implications and a potential modelling strategy. Freshwater Biology, 47(4), 559-579, doi:10.1046/j.1365-2427.2002.00920.x.

Roberts, N., 2002. The Holocene - an environmental history. Blackwell, Oxford, U.K., 316 pp.

Robertson, D.M., Roerish, E.D., 1999. Influence of various water quality sampling strategies on load estimates for small streams. Water Resources Research, 35(12), 3747-3759.

Robinson, M., Gannon, B., Schuch, M., 1991. A comparison of the hydrology of moorland under natural conditions, agricultural use and forestry. Hydrological Sciences Journal, 36(6), 565-577.

Robinson, M., Cognard-Plancq, A.-L., Cosandey, C., David, J., Durand, P., Fürhrer, H.-W., Hall, R., Hendriques, M.O., Marc, V., McCarthy, R., McDonnell, M., Martin, C., Nisbet, T., O'Dea, P., Rodgers, M., Zollner, A., 2003. Studies of the impact of forests on peak flows and baseflows: a European perspective. Forest Ecology and Management, 186, 85-97(1), doi:10.1016/S0378-1127(03)00238-X.

Rodionov, S.G., 1994. Global and Regional Climate Interaction: The Caspian Sea Experience. Kluwer Academic Publishing, Dordrecht, The Netherlands, 241 pp.

Rommens, T., Verstraeten, G., Bogman, P., Peeters, I., Poesen, J., Govers, G., Van Rompaey, A., Lang, A., 2006. Holocene alluvial sediment storage in a small river catchment in the loess area of central Belgium. Geomorphology, 77(1-2), 187-201, doi:10.1016/j.geomorph.2006.01.028.

Rotnicki, K., 1991. Retrodiction of palaeodischarges of meandering and sinuous alluvial rivers and its palaeoclimatic implications. In: Starkel, L., Gregory, K.J., Thornes, J.B. (Eds.), Temperate Palaeohydrology. Fluvial Processes in the Temperate Zone during the last 15000 years. John Wiley & Sons, Chichester, U.K., pp. 431-471.

Rounsevell, M.D.A., Reginster, I., Araújo, M.B., Carter, T.R., Dendoncker, N., Ewert, F., House, J.I., Kankaanpää, S., Leemans, R., Metzger, M.J., Schmit, C., Smith, P., Tuck, G., 2006. A coherent set of land use change scenarios for Europe. Agriculture, Ecosystems and Environment, 114(1), 57-68, doi:10.1016/j.agee.2005.11.027.

Ruddiman, W.F., 2003. The anthropogenic greenhouse era began thousands of years ago. Climatic Change, 61(3), 261-293, doi:10.1023/B:CLIM.0000004577.17928.fa.

RWS Limburg/IWACO, 2000. Internationale ecologische verkenning Maas (EVIM). Historisch ecologische oriëntatie op het stroomgebied (fase 2a). Rijkswaterstaat Directie Limburg, Afdeling Integraal Waterbeleid, Maastricht, The Netherlands, 124 pp.

Sahin, V., Hall, M.J., 1996. The effects of afforestation and deforestation on water yields. Journal of Hydrology, 178(1-4), 293-309.

Scott, D.F., Bruijnzeel, L.A., Mackensen, J., 2005. The hydrological and soil impacts of forestation in the tropics. In: Bonell, M., Bruijnzeel, L.A. (Eds.), Forests, water and people in the humid tropics. Cambridge University Press, Cambridge, U.K., pp. 622-651.

Sefton, C.E.M., Boorman, D.B., 1997. A regional investigation of climate change impacts on UK streamflows. Journal of Hydrology, 195(1-4), 26-44.

Seltzer, G., Rodbell, D., Burns, S.J., 2000. Isotopic evidence for late Quaternary climatic change in tropical South America. Geology, 28(1), 35-38, doi:10.1130/0091-7613(2000)28<35:IEFLQC>2.0.CO;2.

Shabalova, M.V., Van Deursen, W.P.A., Buishand, T.A., 2003. Assessing future discharge of the river Rhine using regional climate model integrations and a hydrological model. Climate Research, 23, 233-246.

Sidorchuk, A., Panin, A., Borisova, O., 2003. The Lateglacial and Holocene palaeohydrology of Northern Eurasia. In: Gregory, K.J., Benito, G. (Eds.), Palaeohydrology: Understanding Global Change. Palaeohydrology. John Wiley & Sons, Chichester, U.K., pp. 61-76.

Smith, D.I., 1994. Flood damage estimation - A review of urban stage-damage curves and loss functions. Water SA, 20(3), 231-238.

S.P.I.04.73, 2004. The PESERA Map: Pan-European Soil Erosion Risk Assessment. Special Publication Ispra 2004 No. 73, Office for Official Publications of the European Communities, Luxembourg, map in ISO B1 format.

Spring, W., Prost, E., 1883. Étude sur les eaux de la Meuse. Annales de la Société Géologique de la Belgique, 11, 123-220.

Stager, J.C., Cumming, B., Meeker, L., 1997. A high-resolution 11,400-yr diatom record from Lake Victoria, East Africa. Quaternary Research, 47(1), 81-89, doi:10.1006/qres.1996.1863.

Stam, M.H., 1999. The dating of fluvial deposits with heavy metals, ^{210}Pb and ^{137}Cs in the Geul catchment (The Netherlands). Physics and Chemistry of the Earth Part B: Hydrology, Oceans and Atmosphere, 24(1), 155-160, doi:10.1016/S1464-1909(98)00028-8.

Stam, M.H., 2002. Effects of land-use and precipitation changes on floodplain sedimentation in the nineteenth and twentieth centuries (Geul River, The Netherlands). In: Martini, I.P., Baker, V.R., Garzón, G. (Eds.), Flood and megaflood processes and deposits: recent and ancient examples. Blackwell Science, Oxford, U.K., pp. 251-267.

Stanley, J.D., 1978. Ionian Sea sapropel distribution and late Quaternary palaeoceanography in the eastern Mediterranean. Nature, 274, 149-152, doi:10.1038/274149a0.

Stanley, J.D., Maldonado, A., 1977. Nile Cone: Late Quaternary stratigraphy and sediment dispersal. Nature, 266, 129-135, doi:10.1038/266129a0.

Talbot, M.R., Delibrias, G., 1980. A new late Pleistocene-Holocene water-level curve for Lake Bosumtwi, Ghana. Earth and Planetary Science Letters, 47(3), 336-344.

Talbot, M.R., Johannessen, T., 1992. A high resolution palaeoclimatic record for the last 27,500 years in tropical West Africa from the carbon and nitrogen isotopic composition of lacustrine organic matter. Earth and Planetary Science Letters, 110(1-4), 23-37.

Talbot, M.R., Livingstone, D.A., Palmer, P.G., Maley, J.M., Delibrias, G., Gulliksen, S., 1984. Preliminary results from sediment cores from Lake Bosumtwi, Ghana. In: Coetzee, J.A., Van Zinderen Bakker Sr., E.M. (Eds.), Palaeoecology of Africa Volume 16. A.A. Balkema, Rotterdam, The Netherlands, pp. 173-192.

Tallis, J., 1990. Climate change and plant communities. Academic Press, London, U.K.

TAW, 2000. From probability of exceedance to probability of flooding. Towards a new safety approach. Technische Adviescommissie voor de Waterkeringen, Directorate-General for Public Works and Water Management, Delft, The Netherlands, 24 pp.

Tebbens, L.A., Veldkamp, A., Van Dijke, J.J., Schoorl, J.M., 2000. Modeling longitudinal-profile development in response to Late Quaternary tectonics, climate and sea-level changes: the River Meuse. Global and Planetary Change, 27(1-4), 165-186, doi:10.1016/S0921-8181(01)00065-0.

Thornthwaite, C.W., 1948. An approach toward a rational classification of climate. Geographical Review, 38(1), 55-94.

Thornthwaite, C.W., Mather, J.R., 1955. The Water Balance. Publications in Climatology, vol. 8, nr. 1. Drexel Institute of Technology, Philadelphia, U.S.A., 86 pp.

Thornthwaite, C.W., Mather, J.R., 1957. Instructions and tables for computing potential evapotranspiration and the water balance. Publications in Climatology, 10, 183-243.

Toy, J.T., Foster, G.R., Renard, K.G., 2002. Soil erosion. Processes, prediction, measurement, and control. John Wiley, Hoboken, U.S.A., 338 pp.

Trimble, S.W., 1999. Decreased rates of alluvial sediment storage in the Coon Creek Basin, Wisconsin, 1975-93. Science, 285, 1244-1246.

Trimble, S.W., Weirich, F.H., Hoag, B.L., 1987. Reforestation and the reduction of water yield on the southern Piedmont since circa 1940. Water Resources Research, 23(3), 425-437.

Tu, M., 2006. Assessment of the effects of climate variability and land use change on the hydrology of the Meuse river basin. Ph.D. Thesis, VU University Amsterdam, Amsterdam, The Netherlands & UNESCO-IHE, Delft, The Netherlands, 190 pp.

Tu, M., Hall, M.J., De Laat, P.J.M., De Wit, M.J.M., 2005. Extreme floods in the Meuse river over the past century: aggravated by land-use changes? Physics and Chemistry of the Earth, Parts A/B/C, 30(4-5), 267-276, doi:10.1016/j.pce.2004.10.001.

Uliana, E., Lange, C.B., Wefer, G., 2002. Evidence for Congo River freshwater load in Late Quaternary sediments of ODP Site 1077 (5˚S, 10˚E). Palaeogeography, Palaeoclimatology, Palaeoecology, 187(1-2), 137-150, doi:10.1016/S0031-0182(02)00514-X.

Vandenberghe, J., Paris, P., Kasse, C., Gouman, M., Beyens, L., 1984. Paleomorphological and botanical evolution of small lowland valleys. A case study of the Mark Valley in Northern Belgium. CATENA, 11, 229-238.

Van den Hurk, B., Klein Tank, A., Lenderink, G., Van Ulden, A., Van Oldenborgh, G.J., Katsman, C., Van den Brink, H., Keller, F., Bessembinder, J., Burgers, G., Komen, G., Hazeleger, W., Drijfhout, S., 2006. KNMI Climate change scenarios 2006 for the Netherlands. KNMI Scientific Report WR 2006-01, KNMI, De Bilt, The Netherlands, 82 pp.

Van der Hammen, T., Urrego, L.E., Espejo, N., Duivenvoorden, J.F., Lips, J.M., 1992. Late-glacial and Holocene sedimentation and fluctuations of river water level in the Caquetá River area (Colombian Amazonia). Journal of Quaternary Science, 7(1), 57-67, doi:10.1002/jqs.3390070106.

Van der Knijff, J., Jones, R.J.A., Montanarella, L., 2000. Soil erosion risk assessment in Europe. EUR 19044 EN, Office for Official Publications of the European Communities, Luxembourg, 34 pp.

Van Deursen, W.P.A., 1995. Geographical Information Systems and Dynamic Models. Ph.D. Thesis, Universiteit Utrecht, The Netherlands, 198 pp.

Van Deursen, W., 2000. MEUSEFLOW 2.1, Laagwaterstudies Maasstroomgebied. Report number RI-2988A, RIZA, Arnhem, The Netherlands, 42 pp., www.carthago.nl/Publications/MeuseLaagwater.PDF.

Van Deursen, W.P.A., Middelkoop, H., 2001. Development of flood management strategies for the Rhine and Meuse basins in the context of integrated river management. Executive summary of the IRMA-SPONGE Project 3/NL/1/164/99 15 183 01, Netherlands Centre for River Studies, Rotterdam/Utrecht, The Netherlands, 38 pp.

Van Deursen, W.P.A., Middelkoop, H., 2002. Development of flood management strategies for the Rhine and Meuse basins in the context of integrated river management. Executive summary of the IRMA-SPONGE Project 2. In: Hooijer, A., Van Os, A. (Eds.), Towards Sustainable Flood Risk Management in the Rhine and Meuse River Basins. NCR, Delft.

Van Es, W.A., Sarfatij, H., Woltering, P.J., 1988. Archeologie in Nederland; rijkdommen van het bodemarchief. Rijksdienst voor Oudheidkundig Bodemonderzoek, Meulenhof-Informatief, Amsterdam, The Netherlands.

Van Geel, B., Buurman, J., Waterbolk, H.T., 1996. Archaeological and palaeoecological indications of an abrupt climate change in The Netherlands, and evidence for climatological teleconnections around 2650 BP. Journal of Quaternary Science, 11(6), 451-460, doi:10.1002/(SICI)1099-1417(199611/12)11:6<451::AID-JQS275>3.0.CO;2-9.

Van Liedekerke, M., Jones, A., Panagos, P., 2006. European Soil Database (ESDB) v2.0, 1km x 1km Raster Library. European Commission and the Soil Bureau Network, 19945 EN, CD-ROM, http://eusoils.jrc.it/data.html.

Van Oost, K., Govers, G., Desmet, P., 2000. Evaluating the effects of changes in landscape structure on soil erosion by water and tillage. Landscape Ecology, 15(6), 577-589, doi:10.1023/A:1008198215674.

Van Rompaey, A.J.J., Verstraeten, G., Van Oost, K., Govers, G., Poesen, J., 2001a. Modelling mean annual sediment yield using a distributed approach. Earth Surface Processes and Landforms, 26(11), 1221-1236, doi:10.1002/esp.275.

Van Rompaey, A.J.J., Govers, G., Van Hecke, E., Jacobs, K., 2001b. The impacts of land use policy on the soil erosion risk: a case study in central Belgium. Agriculture, Ecosystems and Environment, 83(1-2), 83-94, doi:10.1016/S0167-8809(00)00173-0.

Van Rompaey, A.J.J., Govers, G., Puttemans, C., 2002. Modelling land use changes and their impact on soil erosion and sediment supply to rivers. Earth Surface Processes and Landforms, 27(5), 481-494, doi:10.1002/esp.335.

Van Rompaey, A.J.J., Vieillefont, V., Jones, R.J.A., Montanarella, L., Verstraeten, G., Bazzoffi, P., Dostal, T., Krasa, J., De Vente, J., Poesen, J., 2003. Validation of soil erosion estimates at European scale. European Soil Bureau Research Report No.13, EUR 20827 EN, Office for Official Publications of the European Communities, Luxembourg, 26 pp.

Van Rompaey, A., Bazzoffi, P., Jones, R.J.A., Montanarella, L., 2005. Modeling sediment yields in Italian catchments. Geomorphology, 65, 157-169, doi:10.1016/j.geomorph.2004.08.006.

Verburg, P.H., 2006. Simulating feedbacks in land use and land cover models. Landscape Ecology, 21(8), 1171-1183, doi:10.1007/s10980-006-0029-4.

Verburg, P.H., Schulp, C.J.E., Witte, N., Veldkamp, A., 2006. Downscaling of land use change scenarios to assess the dynamics of European landscapes. Agriculture, Ecosystems and Environment, 114(1), 39-56, doi:10.1016/j.agee.2005.11.024.

Verburg, P.H., Eickhout, B., Van Meijl, H., 2008. A multi-scale, multi-model approach for analyzing the future dynamics of European land use. The Annals of Regional Science, 42(1), 57-77, doi:10.1007/s00168-007-0136-4.

Versteegh, E.A.A., Troelstra, S.R., Vonhof, H.B., 2008. Stable oxygen isotopes in freshwater mussels (Unionidae) as a proxy for late Holocene floods and droughts of Rhine and Meuse. Geophysical Research Abstracts Vol. 10, EGU-2008-A-02561, EGU General Assembly, 13-18 April 2008, Vienna, Austria.

Verstraeten, G., 2006. Regional scale modelling of hillslope sediment delivery with SRTM elevation data. Geomorphology, 81(1-2), 128-140, doi:10.1016/j.geomorph.2006.04.005.

Verstraeten, G., Poesen, J., 1999. The nature of small-scale flooding, muddy floods and retention pond sedimentation in central Belgium. Geomorphology, 29(3-4), 275-292, doi:10.1016/S0169-555X(99)00020-3.

Verstraeten, G., Poesen, J., 2001. Factors controlling sediment yield from small intensively cultivated catchments in a temperate humid climate. Geomorphology, 40(1-2), 123-144, doi:10.1016/S0169-555X(01)00040-X.

Verstraeten, G., Poesen, J., 2002. Regional scale variability in sediment and nutrient delivery from small agricultural watersheds. Journal of Environmental Quality, 31, 870-879.

Verstraeten, G., Van Oost, K., Van Rompaey, A., Poesen, J., Govers, G., 2002. Evaluating an integrated approach to catchment management to reduce soil loss and sediment pollution through modelling. Soil Use and Management, 19, 386-394, doi:10.1079/SUM2002150.

Verstraeten, G., Van Rompaey, A., Poesen, J., Van Oost, K., Govers, G., Stalpaert, L., 2003. Thema 2.20 kwaliteit bodem: erosie. In: Van Steertegem, M. (Ed.), MIRA-T 2003. Milieu- en natuurrapport Vlaanderen thema's. Vlaamse Milieumaatschappij, Mechelen, pp. 345-355.

Verstraeten, G., Poesen, J., Demarée, G., Salles, C., 2006a. Long-term (105 years) variability in rain erosivity as derived from 10-min rainfall depth data for Ukkel (Brussels, Belgium): Implications for assessing soil erosion rates. Journal of Geophysical Research, 111, D22109, doi:10.1029/2006JD007169.

Verstraeten, G., Poesen, J., Gillijns, K., Govers, G., 2006b. The use of riparian vegetated filter strips to reduce river sediment loads: an overestimated control measure? Hydrological Processes, 20(14), 2797-2819, doi:10.1002/hyp.6155.

Vörösmarty, C.J., Fekete, B.M., Tucker, B.A., 1998. Global River Discharge, 1807-1991, V[ersion] 1.1 (RivDis). Oak Ridge National Laboratory Distributed Active Archive Center, Oak Ridge, U.S.A., http://www.daac.ornl.gov.

Walling, D.E., Webb, B.W., 1982. Sediment availability and the prediction of storm-period sediment yields. In: Walling, D.E. (Ed.), Recent Developments in the Explanation and Prediction of Erosion and Sediment Yields. IAHS Publication number 137, Wallingford, U.K., pp. 327-337.

Wang, L., Sarnthein, M., Erlenkeuser, H., Grootes, P., Grimalt, J.O., Pelejero, C., Linck, G., 1999a. Holocene Variations in Asian Monsoon Moisture: A Bidecadal Sediment Record from the South China Sea. Geophysical Research Letters, 26(18), 2889-2892.

Wang, L., Sarnthein, M., Erlenkeuser, H., Grimalt, J., Grootes, P., Heilig, S., Ivanova, E., Kienast, M., Pelejero, C., Pflaumann, U., 1999b. East Asian monsoon climate during the Late Pleistocene: high-resolution sediment records from the South China Sea. Marine Geology, 156, 245-284.

Ward, P.J., 2007a. A coupled climate-hydrological model for Meuse palaeodischarge modelling: set-up and calibration. Technical Report: July 2007, VU University Amsterdam, Amsterdam, The Netherlands, 41 pp.

Ward, P.J., 2007b. Grote toename in de overstromingsfrequentie van de Maas door grootschalige ontbossingen. Climate changes Spatial Planning Newsletter, 9, p.6, http://www.klimaatvoorruimte.nl/pro1/general/start.asp?i=2&j=1&k=0&p=0&itemid=35.

Ward, P.J., 2008a. River Meuse suspended sediment yield: a new estimate and past estimates revisited. Netherlands Journal of Geosciences, 89(2), 189-193.

Ward, P.J., 2008b. Zicht op Maasafvoer door de eeuwen heen. Land en Water, 8, 30-31.

Ward, P.J., Aerts, J.C.J.H., De Moel, H., Renssen, H., 2007. Verification of a coupled climate-hydrological model against Holocene palaeohydrological records. Global and Planetary Change, 57(3-4), 283-300, doi:10.1016/j.gloplacha.2006.12.002.

Ward, P.J., Renssen, H., Aerts, J.C.J.H., Van Balen, R.T., Vandenberghe, J., 2008a. Strong increases in flood frequency and discharge of the River Meuse over the late Holocene: impacts of long-term anthropogenic land use change and climate variability. Hydrology and Earth System Sciences, 12, 159-175, www.hydrol-earth-syst-sci.net/12/159/2008/.

Ward, P.J., Renssen, H., Aerts, J.C.J.H., Verburg, P.H., 2008b. Sensitivity of discharge and flood frequency to 21st Century changes in climate and land use (River Meuse, northwest Europe). Submitted to Climatic Change.

Ward, P.J., Van Balen, R.T., Verstraeten, G., Renssen, H., Vandenberghe, J., 2008c. The impact of land use and climate change on late Holocene and future suspended sediment yield of the Meuse catchment. Geomorphology, *in press*, doi:10.1016/j.geomorph.2008.07.006.

Ward, R.C., Robinson, M., 1990. Principles of hydrology. McGraw-Hill Book Company, London, U.K., 365 pp.

Wegehenkel, M., 2002. Estimating of impact of land use changes using the conceptual model THESEUS - a case study. Physics and Chemistry of the Earth, 27(9-10), 631-640, doi:10.1016/S1474-7065(02)00047-5.

Westhoek, H.J., Van den Berg, M., Bakkes, J.A., 2006. Scenario development to explore the future of Europe's rural areas. Agriculture, Ecosystems & Environment, 114(1), 7-20, doi:10.1016/j.agee.2005.11.005.

Wilby, R.L., Wigley, T.M.L., 1997. Downscaling general circulation model output: a review of methods and limitations. Progress in Physical Geography, 21(4), 530-548, doi:10.1177/030913339702100403.

Wilby, R.L., Wigley, T.M.L., Conway, D., Jones, P.D., Hewitson, B.C., Main, J., Wilks, D.S., 1998. Statistical downscaling of general circulation model output: A comparison of methods. Water Resources Research, 34(11), 2995-3008.

Wilby, R.L., Hay, L.E., Gutowski Jr., W.J., Arritt, R.W., Takle, E.S., Pan, Z., Leavesley, G.H., Clark, M.P., 2000. Hydrological responses to dynamically and statistically downscaled climate model output. Geophysical Research Letters, 27(8), 1199-1202.

Williams, M.A.J., Clarke, M.F., 1984. Late Quaternary environments in north-central India. Nature, 308(12), 633-635, doi:10.1038/308633a0.

Wind, H.G., Nieron, T.M., De Blois, C.J., De Kok, J.L., 1999. Analysis of flood damages from the 1993 and 1995 Meuse floods. Water Resources Research, 35(11), 3459-3465, doi:10.1029/1999WR900192.

Wirrmann, D., Bertaux, J., Kossoni, A., 2001. Late Holocene paleoclimatic changes in Western Central Africa inferred from mineral abundance in dated sediments from Lake Ossa (Southwest Cameroon). Quaternary Research, 56(2), 275-287, doi:10.1006/qres.2001.2240.

WL, 1994a. Onderzoek Watersnood Maas. Deelrapport 4. Hydrologische aspecten. Waterloopkundig Laboratorium, Emmeloord, The Netherlands.

WL, 1994b. Onderzoek Watersnood Maas. Achtergrondrapport 1. Hydrolgie, Deel A + B. Onderzoeksproject Watersnood Maas, Het Belgische stroombekken. Waterloopkundig Laboratorium, Delft, The Netherlands.

Wood, A.W., Maurer, E.P., Kumar, A., Lettenmaier, D.P., 2002. Long-range experimental hydrologic forecasting for the eastern United States. Journal of Geophysical Research, 107(D20), 4429, doi:10.1029/2001JD000659.

Wood, A.W., Leung, L.R., Sridhar, V., Lettenmaier, D.P., 2004. Hydrologic implications of dynamical and statistical approaches to downscaling climate model outputs. Climatic Change, 62(1-3), 189-216, doi:10.1023/B:CLIM.0000013685.99609.9e.

WUR/MNP, 2007. Eururalis 2.0 CD-ROM. Wageningen UR, Wageningen, The Netherlands.

Yang, D., Kanae, S., Oki, T., Koike, T., Musiake, K., 2003. Global potential soil erosion with reference to land use and climate changes. Hydrological Processes, 17(14), 2913-2928, doi:10.1002/hyp.1441.

Yarnal, B., Lakhtakia, M.N., Yu, Z., White, R.A., Pollard, D., Miller, D.A., Lapenta, W.M., 2000. A linked meteorological and hydrological model system: The Susquehanna River Basin Experiment (SRBEX). Global and Planetary Change, 25(1-2), 149-161, doi:10.1016/S0921-8181(00)00026-6.

Yates, D.N., 1997. Approaches to continental scale runoff for integrated assessment models. Journal of Hydrology, 201(1-4), 289-310.

Zagwijn, W.H., 1986. Nederland in het Holoceen. Rijks Geologische Dienst, Haarlem, The Netherlands, 46 pp.

Zagwijn, W.H., 1994. Reconstruction of climate change during the Holocene in western and central Europe based on pollen records of indicator species. Vegetation History and Archaeobotany, 3(2), 65-88, doi:10.1007/BF00189928.

Zheng, Y., Keller, A.A., 2006. Understanding parameter sensitivity and its management implications in watershed-scale water quality modeling. Water Resources Research, 42, W05402, doi:10.1029/2005WR004539, 2006.

Appendices

Appendix 1

Selection of hydrological model and model resolution

There exists a plethora of models to simulate the hydrological cycle at a range of temporal and spatial resolutions. The concepts employed in hydrological models reflect the application for which the model will be used, and since the range of applications is large, so too is the range of modelling concepts. However, in their simplest form all hydrological models are governed by the water balance equation:

$$Q = P - ET \pm \Delta S \qquad \text{(Eq. A1.1)}$$

where Q is discharge, P is precipitation, ET is evapotranspiration, and ΔS is the change in storage in the system.

Hydrological models can be classified according to many different criteria, including: model application (e.g. within hydrology as exploratory or research tools for the understanding of hydrological processes, or outside hydrology in planning, design and prediction); model structure (from simple lumped black-box models to complex distributed physical and mathematical models); spatial disaggregation (lumped or distributed parameters); computational demand; temporal scale (e.g. hourly, daily, monthly, annual); and spatial scale (e.g. point, sub-basin, basin, regional, global) (Booij, 2005; Klemeš, 1986; Leavesley, 1994). Hereunder follows a brief description of the main modelling approaches based on model structure, after Leavesley (1994).

Empirical models: Such models are based on statistical relationships between components of the water balance equation, and convert input to output via a transform function statistically derived from empirical research. Hence they give no consideration to the physical laws governing the processes involved in the hydrological cycle (Leavesley, 1994). Whilst these models may be of use in the rapid assessment of contemporary rainfall-runoff relationships their application to long-term studies, or studies involving changes in major parameters (i.e. climate and land use), is therefore questionable (Kirchner, 2006).

Water balance models: Water balance models are based on the concepts and works of Thornthwaite (1948) and Thornthwaite and Mather (1955), and use a series of storage compartments and flows to account for the movement of water throughout a basin. Most models of this type consider total discharge to be a function of a delayed runoff component (baseflow) plus a direct runoff component. They are based on simple representations of hydrological processes, and given their quasi-physical basis these models can be used to simulate average discharge for a range of basin conditions, since they allow for the parameterisation of changes

in variables such as precipitation, evapotranspiration, land use, and soil type. Parameter estimation is often difficult given the lack of empirical observations on such variables as groundwater and soil water storage. However, only a limited number of parameters are considered in these models, which is advantageous over process-based distributed-parameter models (see below). Whilst the equations used can offer a robust tool for assessing long-term discharge patterns, they are too primitive to be able to model hydrological responses on timescales shorter than a day (Leavesley, 1994).

Conceptual lumped-parameter models: Similar to water balance models, conceptual lumped-parameter models attempt to account for the flow of water through a basin from the moment it enters as precipitation until the moment it is discharged at the outlet. They are also based on approximations and simplifications of physical laws, although flow paths and residence times in the storage compartments are considered in far greater detail. Hence, they tend to be applied with much shorter time-steps, for example minutes, hours, or a day (Leavesley, 1994). Process parameterisation usually takes place at the basin scale, and heterogeneous factors such as soil type and land use tend to be lumped at this scale. Therefore it is difficult to use these models for spatial planning, for which the alteration of local conditions needs to be represented.

Process-based distributed-parameter models: These models have a firm grounding in physical processes and in the processes involved in the hydrological cycle at the individual basin scale. The process equations have the ability of forecasting the spatial pattern of hydrological conditions as well as basin-wide storage and flows (Beven, 1985). Unlike conceptual lumped-parameter models, spatial distribution is applied using a raster approach whereby the process equations are carried out for each individual grid cell. However, as the physical reality of a model increases, so too does the number of parameters which must be estimated. Since empirical data on which to base such parameter estimations are usually scarce, and sometimes non-existent, over-parameterisation introduces many uncertainties into these models (Jakeman and Hornberger, 1993; Krajewski et al., 1991; Loague and Freeze, 1985). When the purpose of a model is to simulate the detailed processes of the hydrological cycle, such as in models for water quality management (Zheng and Keller, 2006), this high number of parameters may be necessary. However, unnecessary over-parameterisation often leads to little (if any) improvement in model performance (Beven, 1989; Booij, 2005; Jakeman and Hornberger, 1993; Loague and Freeze, 1985).

Desired characteristics of palaeodischarge model

Given the issues discussed above, the following points were considered during the selection of the hydrological model to be used in this thesis:

- the model should be spatially distributed in order to simulate changes in land use;
- the model must be able to deal with altered climatic conditions, hence a

purely empirical model is inappropriate. Furthermore, our goal is to better understand the main mechanisms which govern the response of discharge to climate change;
- the Meuse model must be capable of modelling processes on a daily basis in order to simulate individual high-flow events;
- the spatial disaggregation and resolution of the Meuse model must be high enough to allow effective daily discharge modelling at the basin scale and for the main tributaries;
- the model should contain as few calibration parameters as possible, whilst still retaining a physical grounding, given that parameter uncertainty in the palaeodischarge runs adds to overall model uncertainty;
- the Meuse model must be efficient to run in terms of computational time, given that a single 1000 year run involves 360,000 iterations.

Based on these considerations, the most appropriate model structure for this project is one combining elements of the water balance models and the process-based distributed-parameter models. The STREAM model (Aerts et al., 1999) fits these criteria well, and was therefore selected for use in this project.

Selection of resolution for the STREAM model

The STREAM Meuse model was set up with a daily time-step and at a spatial resolution of 2’ x 2’ (ca. 2.4 km x 3.7 km). The considerations for the choice of these time and spatial resolutions are discussed in this section.

As this research project aims to examine changes in both mean discharge and extreme events over the Holocene, a daily time-step is appropriate (Booij, 2002). In terms of modelling the response of the Meuse to long-term climatic and land use changes, a higher time resolution (e.g. hourly) is unnecessary since we are interested in the change in the number of extreme events and average discharge, rather than the detailed response of the hydrograph to single events.

The choice of spatial scale should allow a model to capture the dominant processes, yet not be so complex that excessive computational time is demanded (Booij, 2003). Based on this notion, Booij (2002) calculated the ‘appropriate’ model scale for assessing the impact of climate change on flooding in the Meuse by firstly establishing the appropriate spatial scales of key variables, assuming these to be equal to a fraction of the spatial correlation length of those variables. These appropriate variable scales were then weighted, and the results multiplied to establish an appropriate model scale of 10 km x 10 km.

Given the choice of a daily time-step, it was important to select a pragmatic spatial resolution in terms of computational time and disk storage space. Therefore, a pilot model was set-up in order to assess the feasibility of three spatial resolutions at least as high as the 10 km x 10 km proposed by Booij (2002), namely 30” x 30”, 1’ x 1’, and 2’ x 2’. For each resolution the total disk space and time which

would be needed to carry out all of the simulations required in this project was estimated (Table A1.1). These times exclude the time taken to run the climate model itself, since this is not affected by the resolution chosen for the hydrological model. Based on this pilot study, pragmatic considerations concerning time and disk space dictated that the resolution of 2' x 2' be chosen.

Table A1.1: Disk space and calculation time requirements to run the hydrological model in ensemble mode (four ensemble members) with a daily time-step for the periods 4000-3000 BP, 1000-2000 AD, and the 21st Century AD, and with multiple land use scenarios.

Resolution	Disk space	Calculation time
30" x 30"	ca. 6451 GB	ca. 28,896 hours (1204 days)
1' x 1'	ca. 1613 GB	ca. 5936 hours (248 days)
2' x 2'	ca. 403 GB	ca. 2352 hours (98 days)

For the model used to simulate the discharge of 19 rivers around the globe (Chapter 2; Ward et al., 2007), the STREAM model was also used since this project serves as a pilot study to test the approach prior to its application to the Meuse. Given the global scale of this model, a lower resolution was used (as discussed in Chapter 2; Ward et al., 2007), and a monthly time-step was used since the aim was to simulate long-term trends in mean annual palaeodischarge, rather than to analyse changes in flood frequency.

Appendix 2

Land use maps used in STREAM

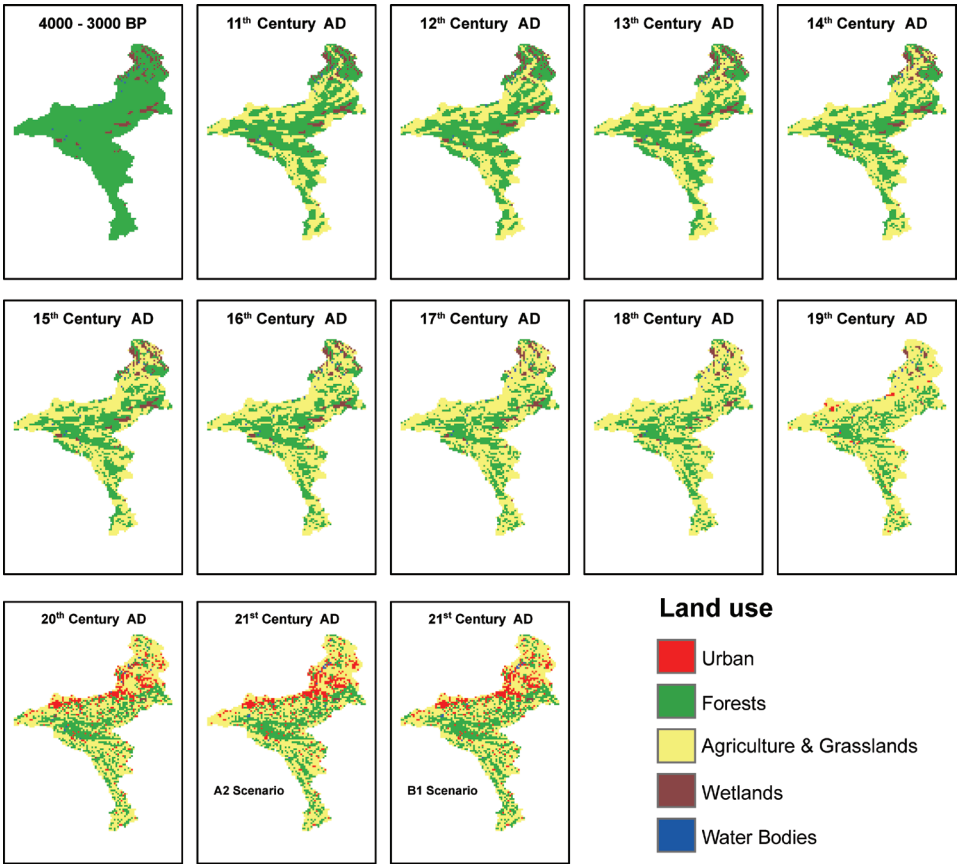

Fig. A2.1: Reconstructed Meuse basin land use maps for use in STREAM for the periods 4000-3000 BP, 1000-2000 AD, and the 21st Century. The 20th Century land use map is based on CORINE data, and the maps for the 21st Century are based on the A2 (Continental Market) and B1 (Global Cooperation) scenarios of the EURURALIS project (Verburg et al., 2006, 2008). The land use maps for the period 4000-3000 BP and for the 11th to 19th Centuries are reconstructed based on census data, historical records, and pollen analysis.

Appendix 3

Land use maps used in WATEM/SEDEM

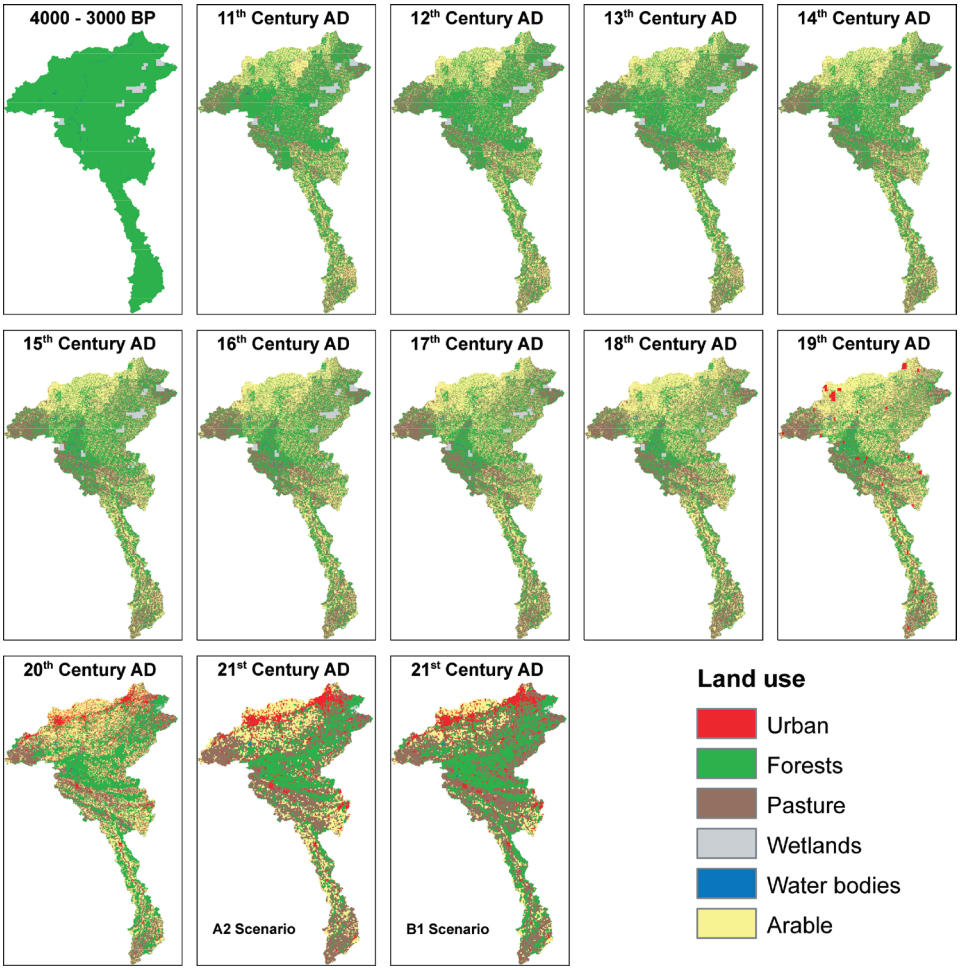

Fig. A3.1: Reconstructed Meuse basin land use maps for use in WATEM/SEDEM for the periods 4000-3000 BP, 1000-2000 AD, and the 21st Century. The 20th Century land use map is based on CORINE data, and the maps for the 21st Century are based on the A2 (Continental Market) and B1 (Global Cooperation) scenarios of the EURURALIS project (Verburg et al., 2006, 2008). The land use maps for the period 4000-3000 BP and for the 11th to 19th Centuries are reconstructed based on census data, historical records, and pollen analysis.